AUTOGENIC AND INTERMUSCULAR PATHWAYS IN CATS WITH PARTIAL SPINAL CORD LESIONS

A Dissertation
Presented to
The Academic Faculty

by

Elma Kajtaz

In Partial Fulfillment
of the Requirements for the Degree
Doctor of Philosophy in the
Biological Sciences

Georgia Institute of Technology
May 2019

COPYRIGHT © 2019 BY ELMA KAJTAZ

AUTOGENIC AND INTERMUSCULAR PATHWAYS IN CATS WITH PARTIAL SPINAL CORD LESIONS

Approved by:

Dr. T. Richard Nichols, Advisor
School of Biological Sciences
Georgia Institute of Technology

Dr. Boris I. Prilutsky
School of Biological Sciences
Georgia Institute of Technology

Dr. Simon Sponberg, Committee Chair
School of Physics,
School of Biological Sciences
Georgia Institute of Technology

Dr. Timothy Cope
School of Biological Sciences,
Department of Biomedical Engineering
Georgia Institute of Technology

Dr. Dena R. Howland
Kentucky Spinal Cord Injury Research
Center, Department of Neurological
Surgery, School of Medicine
University of Louisville
Rehabilitation, Research & Development
Robley Rex VA Medical Center

Date Approved: November 15, 2018

This dissertation is dedicated to all animals that made this research possible.

ACKNOWLEDGMENTS

I am so fortunate to walk through life along with many incredible people. As such, it is very challenging to thank everyone who has assisted my development as a person and as a scientist, but I would like to express my gratitude and appreciation of a few individuals.

My family, especially my father, instilled a passion for science in me since my early age, and for that, I am forever grateful. To my little brother and sister, who are following in my footsteps, I wish all the luck in the world. You are terrific, and I am so proud of you! Thank you for all your love and support. To my longest friend, Iskra, thank you for all the long soul-searching and purpose-of-life discussions, encouragement, and love. Thank you, Adrienne, Danny, and Zorana, my long-lost siblings, I am so glad I found you. I often feel we were made from the same mold. You complete me, and you make me a better person. You're a genuinely fantastic people, and this world needs more humans like you!

I've met incredible colleagues at Georgia Tech. Regan, thank you for being the perfect role model. I feel privileged to have been your peer! Matt, a.k.a. Mr. President, I am honored I had an opportunity to work with you in P.A.P.E.R. Your work ethic and attention to detail are remarkable, something I aspire to emulate. Ellenor, your wisdom and genuineness are praiseworthy – thank you for all your thoughtful advice. Shea, in many ways I feel you are my successor in Dr. Nichols' lab and P.A.P.E.R. I believe in you, and I am sure you will excel in grad school. Andy, Ricky, Josh, Ted, John, Audra, Nick, you all made a significant impact on my life, and you will always be my AP family! Thanks to all amazing undergrads we had in the lab throughout the years, Shushmita, Haley, Lee, Jessica and Mandy.

I have been fortunate to have two families during my grad school years. My young QBioS family invigorated me, rekindled my enthusiasm for science, and incited new ways of thinking and a new approach to my research. Ali, Bo, Shlomi, Hector, Joy, Nolan, Pedro, and Steven, I am so proud to be your peer in the inaugural QBioS program. Your unique and diverse scientific interests, incredible knowledge and admirable scholastic prowess, your desire to share expertise and to learn more, make the QBioS program so magnificent. Thank you all for enriching my life here at Tech, for supporting me and encouraging me to be the best I can possibly be.

I am beholden to Prof. T. Richard Nichols and Prof. Joshua Weitz for their support and guidance. They invested significant time teaching me new skills, discussing the nature of science, encouraging me to better myself, and attentively listening to all my hopes, dreams and fears. I will forever remember your lessons and mentorship. I would also like to thank Dr. Mark Lyle for helpful comments, advice, and invaluable help during the experiments. A special thanks to my committee members for all their support and advice. First, a particular thanks to Prof. Dena Howland who inspire me to excel and who makes me proud to be a woman in science. Thanks to Prof. Boris Prilutsky whose thoughtful suggestions made me appreciate biomechanics, to Prof. Simon Sponberg, who helped me gain new insights into my data, and Prof. Timothy Cope whose larger-than-life personality makes everything seem easier. Under their guidance, I have learned to think critically with the ‘big picture’ in mind. I would also like to thank Prof. Tom Burkholder, who had a significant impact on me as a young scientist. My only regret is not making him a part of my Ph.D. committee, but I live in hope I will have a privilege to work with him in the future. To all PRL staff who take care of our animals, thank you for all your compassion

and incredible care you provide to our little heroes. I would also like to acknowledge the exceptional contribution to this dissertation by Danny, Adrienne, Shea, Ali, Ellenor, and Matt. Thank you for all your comments and suggestions. You made this dissertation much better. Lastly, I would like to thank Lisa, Adrienne, Nykia, and Adrienne (W.) who made sure I was always on track with program requirements and liberated me from dreadful paperwork. Your hard work is much appreciated!

Thank you for all your help.

TABLE OF CONTENTS

ACKNOWLEDGMENTS **iv**

LIST OF TABLES **x**

LIST OF FIGURES **xii**

LIST OF SYMBOLS AND ABBREVIATIONS **xxiii**

SUMMARY **xxiv**

CHAPTER 1. Introduction **1**
1.1 Achieving postural equilibrium through joint stability **3**
1.2 Properties of the neuromuscular system **9**
1.2.1 Musculoskeletal system 10
1.2.2 Proprioception 16
1.2.3 Spinal cord circuitry 24
1.2.4 Modulation of spinal reflexes by the supraspinal areas 26
1.3 Impaired stability after spinal cord injury **29**
1.4 The purpose and specific aims **31**

CHAPTER 2. THE STRETCH REFLEX IS UPREGULATED IN THE MAIN KNEE AND ANKLE EXTENSORS IN CATS FOLLOWING LATERAL LESION OF THE SPINAL CORD **33**
2.1 Introduction **33**
2.2 Methods **38**
2.2.1 Animals 38
2.2.2 Survival surgery 38
2.2.3 Terminal experiments 39
2.2.4 Data acquisition 41
2.2.5 Data analysis 42
2.3 Results **46**
2.3.1 The comparison of weights and impulses of six muscles from spinally-intact and cats with lateral hemisection 46
2.3.2 The stiffness of VASTI muscles increases significantly, although transiently following lateral hemisection 47
2.3.3 The stiffness of GAS muscle increases following the lateral hemisection 50
2.3.4 The stiffness of PLANT shows little or no change following lateral hemisection 52
2.3.5 The stiffness of SOL does not significantly change following lateral hemisection 54
2.3.6 The FHL is the least affected muscle by the lesion in this study 56
2.3.7 The effect of lateral hemisection on TA was not significant, although it shows the opposite trend from those observed in extensor muscles 58
2.4 Discussion **60**

2.4.1 Potential biomechanical consequences of unregulated length feedback 64

CHAPTER 3. REDUCTION OF DEGREES OF FREEDOM IN CONTROL OF FORCE FEEDBACK PATHWAY AFTER PARTIAL SPINAL CORD INJURY: IMPLICATIONS FOR THE REGULATION OF LIMB STIFFNESS 69
3.1 Introduction 69
3.2 Methods 73
3.2.1 Animals 73
3.2.2 Survival surgery 74
3.2.3 Terminal experiments 74
3.2.4 Data acquisition 76
3.2.5 Data analysis 77
3.3 Results 83
3.3.1 The VASTI, a knee extensor muscles, strongly, consistently and chronically inhibits all distal muscles, following lateral hemisection, resulting in a strong proximal to distal bias in interactions involving VASTI 84
3.3.2 The FHL, which is primarily a toe flexor and ankle extensor, consistently and strongly inhibits all other ankle extensors, but not knee extensor, following lateral hemisection, resulting in a strong distal to proximal bias in interactions involving ankle extensors 96
3.3.3 The close ankle extensor synergists, GAS and PLANT, either exchange balanced strong inhibition or directional distal to proximal inhibition, resembling varying patterns observed in spinally-intact cats. 104
3.3.4 Interactions involving SOL muscle were more variable likely due to common excitatory length dependent linkage this muscle shares with other muscles 107
3.3.5 The magnitude of inhibition each muscle receives and donates suggests convergent force feedback bias 108
3.3.6 Reduction in degrees of freedom in regulation of force feedback following LHS, as potential explanation of consistently observed convergent bias 109
3.4 Discussion 113
3.4.1 Potential functional consequences of convergence of inhibition onto ankle extensors 115
3.4.2 Potential modulatory supraspinal tracts 117

CHAPTER 4. USING COMPUTATIONAL METHODS TO GENERATE FORWARD DYNAMIC SIMULATION OF STANCE PERTURBATION FROM MECHANOGRAPHIC DATA 119
4.1 Introduction 119
4.2 Methods 122
4.2.1 Muscles and their feedback features 123
4.2.2 From mechanographic measurements to joint angles and moments 125
4.2.3 Geometric limb model of an unloaded, standing limb configuration 128
4.2.4 Imposing vertical perturbations onto the limb with autogenic and the limb with autogenic and heterogenic feedback 132
4.3 Results 136
4.3.1 Responses to perturbation 136
4.4 Discussion 141

CHAPTER 5. DORSAL LESION OF THE SPINAL CORD RELEASES CLASP-KNIFE INHIBITION BUT DOES NOT AFFECT FORCE-DEPENDENT FEEDBACK **144**
5.1 Introduction **144**
5.2 Methods **147**
5.2.1 Animals 147
5.2.2 Survival surgery 147
5.2.3 Terminal experiments 148
5.2.4 Data acquisition 149
5.2.5 Data analysis 152
5.3 Results **155**
5.3.1 The VASTI exhibited significant autogenic CKI and exchanged heteronymous iFFB and CKI with ankle extensors. 155
5.3.2 The FHL donates the CKI and iFFB to other ankle extensors, but receives the CKI only from GAS, and varying magnitudes of iFFB from other muscles 161
5.3.3 A note on increased and decreased gain of the stretch reflex following dorsal hemisection 167
5.3.4 The latency of CKI and iFFB pathways 168
5.4 Discussion **171**
5.4.1 The CKI is apparent after dorsal lesions; sporadic autogenic, but abundant heterogenic CKI among knee and ankle extensors 171
5.4.2 Varied directional bias observed in cats with dorsal hemisection suggests that the organization of iFFB is not affected by dorsal hemisection 173
5.4.3 The supraspinal tracts affected by dorsal hemisection are unlikely to be modulators of the force-dependent pathway 174
5.4.4 The potential clinical implications of results presented in this chapter 176

CHAPTER 6. DISCUSSION **178**
6.1 Modulation of limb stiffness via integration of length and force feedback **179**
6.2 Potential benefits of variable joint stiffness **184**
6.3 Potential gait deficit in cats that cannot modulate force feedback bias **186**
6.4 Potential modulatory supraspinal tract(s) **190**
6.5 Implications for rehabilitation **194**
6.6 Methodological and prognostic limitations **194**
6.7 Conclusion **197**

REFERENCES **199**

LIST OF TABLES

Table 1-1	Table 1-1: Distribution of muscle spindles and Golgi tendon organs.	22
Table 2-1	Summary of relevant features; (i) weight (g), (ii) impulse (Ns), (iii) stiffness (N/mm), (iv) dynamic index (n.u.), and (v) reflex latency (ms	67
Table 3-1	VASTI↔GAS quiescent interactions across recovery time-points and limbs. Values of this interaction are presented as the mean ± standard deviation, for all three-recovery time-points, in both limbs, ipsilateral and contralateral to the lesion. For comparison purposes, presented are the mean ± standard deviation from CNT cats. Additionally, the number of muscle pairs evaluated and the net bias are given in the last column.	88
Table 3-2	VASTI↔PLANT quiescent interactions across recovery time-points and limbs. Values of this interaction are presented as the mean ± standard deviation, for all three-recovery time-points, in both limbs, ipsilateral and contralateral to the lesion. For comparison purposes, presented are the mean ± standard deviation from CNT cats. Additionally, the number of muscle pairs evaluated and the net bias are given in the last column.	92
Table 3-3	VASTI ↔FHL quiescent interactions across recovery time-points and limbs. Values of this interaction are presented as the mean ± standard deviation, for all three-recovery time-points, in both limbs, ipsilateral and contralateral to the lesion. For comparison purposes, presented are the mean ± standard deviation from CNT cats. Additionally, the number of muscle pairs evaluated and the net bias are given in the last column.	93
Table 3-4	FHL ↔ GAS quiescent interactions across recovery time-points and limbs. Details of this interaction are presented as the mean ± standard deviation, for all three-recovery time-points, in both limbs, ipsilateral and contralateral to the lesion. For comparison purposes, presented are the mean ± standard deviation from CNT cats. Additionally, the number of muscle pairs evaluated and the net bias are given in the last column.	97
Table 3-5	FHL ↔ PLANT quiescent interactions across recovery time-points and limbs. Details of this interaction are presented as the mean ± standard deviation, for all three-recovery time-points, in both limbs, ipsilateral and contralateral to the lesion. For comparison purposes, presented are the mean ± standard deviation from CNT cats.	104

Additionally, the number of muscle pairs and the net bias are given in the last column.

Table 3-6 PLANT ↔ GAS quiescent interactions across recovery time-points and limbs. Details of this interaction are presented as the mean ± standard deviation, for all three-recovery time-points, in both limbs, ipsilateral and contralateral to the lesion. For comparison purposes, presented are the mean ± standard deviation from CNT cats. Additionally, the number of muscle pairs evaluated and the net bias are given in the last column. 107

Table 4-1 Autogenic and heterogenic interactions in LHS cats' Ah (*left*) and AH (*right*) limbs. For presentation purposes only, autogenic feedback is a diagonal of the matrix, while heterogenic interactions are presented from donor (rows) to recipients (columns) off diagonally. 124

Table 4-3 Table showing muscles and joints characteristics when joints are in a configuration that makes muscles (in rows) slack. 125

Table 5-1 Table showing epochs and states of force response used to distinguish autogenic and heterogenic iFFB and CKI. The line and marker denote state and epoch (for example, the early epoch of state 2 is marked by blue circle marker and broken blue line in subsequent figures). 151

Table 5-2 Showing stiffness (N/mm) of knee and ankle extensors following dorsal hemisection. Values presented are an average ± standard deviation. These data were collected using the same approach described in Chapter II. Briefly, the slope of force rise during the last 1 mm of muscle elongation is assumed to be representative of muscular stiffness (equation 2.2). 168

Table 6-1 Summary of main findings from Aims I-IV 198

LIST OF FIGURES

Figure 1-1	Hierarchical organization of postural control. On the left side of the scheme are neural components, and on the right side are skeletal components of postural control organization. These two components meet at the level of the muscle, whereby the nervous system controls the skeletal system via efferent pathways.	2
Figure 1-2	Directional stability in the cat. Cats must maintain horizontal (longitudinal), lateral and vertical stability during any motor task.	5
Figure 1-3	Comparative views of a limb. A.) A limb with anatomical structures and stick figure superimposed, B.) A limb presented as a spring with a constant limb stiffness, C.) A limb presented as a series of variable stiffnesses, as some joints serve as springs while others may serve as dampeners, depending on a task.	6
Figure 1-4	Schematic representation of neural and musculoskeletal compartments acting in tandem in regulating stiffness of a limb as a whole. Adapted from Nichols & Houk (1976).	8
Figure 1-5	Lateral and medial view of cat hindlimb shows great complexity of muscular system. Acquired from 'Text-Atlas cat anatomy' by Crouch (1969), with permission (Permission/License ID: 4483740323443).	13
Figure 1-6	Maximal torques around ankle joint showing lines of action of muscles evaluated in this study. Adapted from Lawrence & Nichols (1993).	14
Figure 1-7	Muscle spindle. Acquired from anatomy digital library curated by Drs. Ronald A. Bergman.	17
Figure 1-8	Golgi tendon organ. Muscle spindle. Acquired from anatomy digital library curated by Drs. Ronald A. Bergman..	19
Figure 1-9	Muscle spindles and Golgi tendon organs respond to two distinct mechanical stimuli. Adequate stimulus for muscle spindle is length and rate of length change of a muscle (upper left), although new findings suggest that it incodes force stimuli as well (lower left). Adequate stimulus for GTO is an active force (lower right), although a class of GTO's respond to a passive stretch (upper right).	23
Figure 1-10	Afferent Ia and Ib spinal circuitries. Length feedback from muscle spindle monosynaptically connects to homonymous motoneuron,	24

while force feedback from GTO disynaptically connects onto motoneuron of another muscle via inhibitory Ib interneuron. This figure was used and edited to represent the correct view of the force-feedback pathway with permission (Permission/license ID: 4483341167284, (Norman L., Strominger R.J. et al. 2012)).

Figure 1-11 Cross-sectional view of a spinal cord showing the location of the local spinal cord circuitry and the location of the main descending and ascending tracts. 28

Figure 2-1 Force Response and its features. The force response (FR) is force generated by a muscle to resist a stretch. It can be characterized by (i) stiffness (k), which is change in force over change in length, (ii) peak of dynamic response (max(D)), (iii) dynamic index as difference between peak and steady state epoch (when the muscle is held isomerically during the last 50 ms of hold). Initial background force was subrtacted prior to the analysis. Early force response is characterized by mechanical response (Fm) for the first ~18 ms after the stretch onset. The time point when the slope drastically increases, as mechanical response becomes overwhelmingly neural response (Fd), is considered a reflex latency. 42

Figure 2-2 VASTI. The stiffness of VASTI in CNT (A), and LHS (B) group. In these, and subsequent figures, all data are pooled together (for LHS group that includes data from all recovery time-periods). The most pronounced changes in LHS (B) are an increase in slope, increase in peak, i.e., maximal dynamic response (distribution on the right side of A & B figures) and decrease in latency (distribution on the top of the A & B figures) in LHS group compared to CNT (A). The C represents dynamic index with static (steady state) and peak (maximal dynamic) on x and y axes, respectively. Identity (grey broken) line represents the border between adaptation and facilitation. The black circles are data from CNT group, while triangles are from LHS groups. Blue triangles are data from limb ipsilateral to the side of a lesion, while red triangles are from contralateral limb. Shift between linear fits (the black line is CNT fit and the blue line is LHS fit), suggests a change in sign of dynamic index as CNT force responses exhibit facilitation (positive dynamic index), whereas LHS force response adapt to the hold (negative dynamic index). 49

Figure 2-3 GAS. The data show an increase in gain of slope rise, peak, and no change in latency (A & B, and corresponding distributions). In C it shows that adaptation is evident in both CNT and LHS groups. This adaptation might be dependent on a peak of force response, as the 51

slope of LHS fit is larger than the slope of identity line. Legend details are described in Figure 2-2.

Figure 2-4 PLANT. Subtle and physiologically negligible differences between CNT (A) and LHS (B) groups, thoroughly explained in text. Notable is the slope of LHS fit (C), as it shows larger adaptations at high peak forces for LHS group. Legend details are described in Figure 2-2. 53

Figure 2-5 SOL. Subtle slope increase is evident in LHS (B), compared to CNT (A) group, and details are explained in the text. The slopes of CNT (black line) and LHS (blue line) group fits in the C panel are virtually indistinguishable, as these two groups do not exhibit any differences in the dynamic index. Legend details are described in Figure 2-2. 55

Figure 2-6 FHL. This muscle was least affected by lateral hemisection, as force response parameters showed very subtle and physiologically irrelevant changes. In A and B figures are CNT and LHS force response parameters supporting that claim. In C, slopes of CNT (black line) and LHS (blue line) fits are virtually identical. Legend details are described in Figure 2-2. 57

Figure 2-7 TA. The lateral lesion had no statistically significant effect on TA muscle, however the trend was opposite to that it had on extensor muscles. The TA slope of force response, i.e., its stiffness, and peak decreased, while latency increased (A & B, upper distributions), although physiologically not significant. In C, although CNT and LHS fits are identical, the LHS group was shifted forward as it had smaller peak. Legend details are described in Figure 2-2. 59

Figure 2-8 Potential moment changes following lateral hemisection. The moments that each muscle can develop are plotted in the sagittal (y-axis) and frontal planes (x-axis). Visual comparison of the stiffness of muscles from averaged CNT (left) responses to stiffness of muscles of an LHS cat from 3-wks recovery group (right) was accomplished by normalizing the diameter of circles to that of VASTI from LHS group (the largest stiffness). 64

Figure 3-1 Three levels of data analysis. Recorded raw data are first processed and outliers are eliminated (top). Next, both quiescent (left middle) and active (right middle) data are analyzed within cat. In quiescent trials, the force response of lone stretch is compared to the stretch in tandem with another muscle (left). Under active conditions, the same comparison is accomplished across varying background forces (right). The next step in analysis of active trials is fitting the state 1 and state 2 responses with polynomial fits, separately. 79

Following within cat analysis, under quiescent conditions, the data are pooled together as individual magnitudes in one direction plotted against magnitudes in the other direction within the pair of the muscles (left bottom). For active trials, the difference between polynomial curves are plotted against the common background force (right bottom). More detailed explanation can be found under quiescent and active condition sections.

Figure 3-2 VASTI ↔ GAS interactions in a representative cat. In A, quiescent GAS→VASTI interactions (left) from ipsilateral (dark red) and contralateral (light red) limb, and quiescent VASTI→GAS interaction (right) from ipsilateral (dark blue) and contralateral (light blue) were presented to show bilateral effect of unilateral lesion. In B, same interactions were presented across varying background forces. On the left, interaction from GAS to VASTI in ipsilateral (dark red) and contralateral (light red) limb, and on the right are interactions from VASTI to GAS from ipsilateral (dark blue) and contralateral (light blue) limb. Note: in the legend, i in front of the muscle name stands for ipsilateral, and c stands for contralateral. 86

Figure 3-3 VASTI ↔ GAS interactions across all cats. In A are quiescent data pooled across all cats. The averages of interaction from GAS to VASTI are plotted against the averages of interaction from VASTI to GAS across LHS (black markers) and CNT cats (grey markers). The pink filled trace is the distribution of GAS→VASTI magnitudes, and blue filled trace is the distribution of VASTI→GAS magnitudes, both from LHS cats. In the background are light grey filled distributions of magnitudes from CNT cats. In B are pooled active data magnitudes across LHS cats. The GAS→VASTI interactions are in red-pink color, while interaction VASTI→GAS interactions are blue-light blue color. The intensity of coloring corresponds to recovery time-points. The longer recovery period the darker the color. On the right, is a snapshot of interaction magnitudes at 10 N of recipient background force where each point is interaction from one limb. 87

Figure 3-4 VASTI ↔ PLANT interaction in representative cat. In A, quiescent PLANT→VASTI interactions (left) from ipsilateral (dark red) and contralateral (light red) limb, and quiescent VASTI→PLANT interaction (right) from ipsilateral (dark blue) and contralateral (light blue) were presented to show bilateral effect of unilateral lesion. In B, same interactions were presented across varying background forces. Left, interaction from PLANT to VASTI in ipsilateral (dark red) and contralateral (light red) limb, and on the 90

right are interactions from VASTI to PLANT from ipsilateral (dark blue) and contralateral (light blue) limb.

Figure 3-5 VASTI ↔ PLANT interaction across all cats. In A are quiescent data pooled across all cats. The averages of interaction from PLANT to VASTI are plotted against the averages of interaction from VASTI to PLANT across LHS (black markers) and CNT cats (grey markers). The pink filled trace is the distribution of PLANT→VASTI magnitudes, and blue filled trace is the distribution of VASTI→PLANT magnitudes from LHS cats. In the background are light grey filled distributions of magnitudes from CNT cats. In B are pooled active data across LHS cats. The PLANT→VASTI interactions are in red-pink color, while interaction VASTI→PLANT interactions are blue-light blue. The intensity of coloring corresponds to recovery time-points. The longer recovery period the darker the color. On the right, is a snapshot of interaction magnitude at 5 N of recipient background force. 91

Figure 3-6 VASTI ↔ FHL interaction in a representative cat. In A, quiescent FHL→VASTI interactions (left) from ipsilateral (dark red) and contralateral (light red) limb, and quiescent VASTI→FHL interaction (right) from ipsilateral (dark blue) and contralateral (light blue) were presented to show bilateral effect of unilateral lesion. In B, same interactions were presented across varying background forces. Left, interaction from FHL to VASTI in ipsilateral (dark red) and contralateral (light red) limb, and on the right are interactions from VASTI to FHL from ipsilateral (dark blue) and contralateral (light blue) limb. 94

Figure 3-7 VASTI ↔ FHL interaction across all cats. In A are quiescent data pooled across all cats. The averages of interaction from FHL to VASTI are plotted against the averages of interaction from VASTI to FHL across LHS (black markers) and CNT cats (grey markers). The pink filled trace is the distribution of FHL→VASTI magnitudes, and blue filled trace is the distribution of VASTI→FHL magnitudes from LHS cats. In the background are light grey filled distributions of magnitudes from CNT cats. In B are pooled active data across LHS cats. The FHL→VASTI interactions are in red-pink color, while interaction VASTI→FHL interactions are blue-light blue. The intensity of coloring corresponds to recovery time-points. The longer recovery period the darker the color. On the right, is a snapshot of interaction magnitude at 10 N of recipient background force. 95

Figure 3-8 FHL ↔ GAS interaction in a representative cat. In A, quiescent FHL→GAS interactions (left) from ipsilateral (dark red) and 99

contralateral (light red) limb, and quiescent GAS→FHL interaction (right) from ipsilateral (dark blue) and contralateral (light blue) were presented to show bilateral effect of unilateral lesion. In B, same interactions were presented across varying background forces. Left, interaction from FHL to GAS in ipsilateral (dark red) and contralateral (light red) limb, and on the right are interactions from GAS to FHL from ipsilateral (dark blue) and contralateral (light blue) limb.

Figure 3-9 FHL ↔ GAS interaction across all cats. In A are quiescent data pooled across all cats. The averages of interaction from FHL to GAS are plotted against the averages of interaction from GAS to FHL across LHS (black markers) and CNT cats (grey markers). The pink filled trace is the distribution of FHL→GAS magnitudes, and blue filled trace is the distribution of GAS→FHL magnitudes from LHS cats. In the background are light grey filled distributions of magnitudes from CNT cats. In B are pooled active data across LHS cats. The FHL→GAS interactions are in red-pink color, while interaction GAS→FHL interactions are blue-light blue. The intensity of coloring corresponds to recovery time-points. The longer recovery period the darker the color. On the right, is a snapshot of interaction magnitude at 10 N of recipient background force. 100

Figure 3-10 FHL ↔ PLANT interaction in a representative cat. In A, quiescent FHL→PLANT interactions (left) from ipsilateral (dark red) and contralateral (light red) limb, and quiescent PLANT→FHL interaction (right) from ipsilateral (dark blue) and contralateral (light blue) were presented to show bilateral effect of unilateral lesion. In B, same interactions were presented across varying background forces. Left, interaction from FHL to PLANT in ipsilateral (dark red) and contralateral (light red) limb, and on the right are interactions from PLANT to FHL from ipsilateral (dark blue) and contralateral (light blue) limb. 102

Figure 3-11 FHL ↔ PLANT interactions across all cats. In A are quiescent data pooled across all cats. The averages of interaction from FHL to PLANT are plotted against the averages of interaction from PLANT to FHL across LHS (black markers) and CNT cats (grey markers). The pink filled trace is the distribution of FHL→PLANT magnitudes, and blue filled trace is the distribution of PLANT→FHL magnitudes from LHS cats. In the background are light grey filled distributions of magnitudes from CNT cats. In B are pooled active data across LHS cats. The FHL→PLANT interactions are in red-pink color, while interaction PLANT→FHL interactions are blue-light blue. The intensity of coloring corresponds to recovery time-points. The longer recovery period 103

the darker the color. On the right, is a snapshot of interaction magnitude at 10 N of recipient background force.

Figure 3-12 PLANT ↔ GAS interaction in a representative cat. In A, quiescent PLANT→GAS interactions (left) from ipsilateral (dark red) and contralateral (light red) limb, and quiescent GAS→PLANT interaction (right) from ipsilateral (dark blue) and contralateral (light blue) were presented to show bilateral effect of unilateral lesion. In B, same interactions were presented across varying background forces. Left, interaction from PLANT to GAS in ipsilateral (dark red) and contralateral (light red) limb, and on the right are interactions from GAS to PLANT from ipsilateral (dark blue) and contralateral (light blue) limb. 105

Figure 3-13 PLANT ↔ GAS interaction across all cats. In A are quiescent data pooled across all cats. The averages of interaction from PLANT to GAS are plotted against the averages of interaction from GAS to PLANT across LHS (black markers) and CNT cats (grey markers). The pink filled trace is the distribution of PLANT→GAS magnitudes, and blue filled trace is the distribution of GAS→PLANT magnitudes from LHS cats. In the background are light grey filled distributions of magnitudes from CNT cats. In B are pooled active data across LHS cats. The PLANT→GAS interactions are in red-pink color, while interaction GAS→PLANT interactions are blue-light blue. The intensity of coloring corresponds to recovery time-points. The longer recovery period the darker the color. On the right, is a snapshot of interaction magnitude at 10 N of recipient background force (for GAS) and 5 N (for PLANT). 106

Figure 3-14 Average amount of inhibition each muscle receives and donates. As is evident VASTI and FHL donate the most inhibition, while GAS and PLANT receive the most of inhibition. This results in a convergent inhibitory force feedback bias targeting the main ankle extensors. 109

Figure 3-15 Reduction of degrees of freedom as potential explanation of observed data. All data lies on spectrum of proximal→distal to distal→proximal bias. However, data from LHS cats are limited to only one side of the spectrum, while CNT data are scattered and can assume several directional bias patterns. 112

Figure 3-16 Potential functional consequences of convergence of inhibition onto ankle extensors. Observed interactions in quiescent (left) and active (right) conditions were plotted between established maximal 116

torques of ankle extensors in the frontal (x-axis) and the sagittal (y-axis) plane.

Figure 4-1 The goal of this chapter is to estimate the kinematic and kinematic data (right) (joint angles and moments) from mechanographic data (left) (initial force, stiffness and length change). Data from VASTI (yellow), GAS (blue), PLANT (green) and FHL (red) was used for this purpose, because of their strong force-feedback interactions. 122

Figure 4-2 Unloaded (left) and loaded (right) limb configuration. Limb is loaded with 40% of individual cat's mass. The vector of this force is set to go through MTP joint (blue downward arrow), as to make moment produced at MTP joint zero ($r_{MTP} = 0$). Resisting ground reaction force is equal in amplitude but in the opposite direction. Moment required at knee and ankle joints to resist cat's mass will depend on the distance of force vector to position of those joints (i.e., rk and ra, respectively). If the moment at those joints does not match required moment imposed by perturbation, the limb will go through reconfiguration based on stiffness of those joints. Since the stiffness of a joint is dependent on stiffness of all muscles crossing that joint, autogenic and heterogenic state will greatly impact the stiffness developed at those joints. This is equivalent to having thicker or thinner coils of the spring. 135

Figure 4-3 Responses of knee (left) and ankle (right) joints of AH limb in autogenic (blue) and heterogenic (pink) state. Heterogenic state renders both joints more flexed. 137

Figure 4-4 Responses of knee (left) and ankle (right) joints of Ah limb in autogenic (blue) and heterogenic (pink) state**.** Heterogenic state makes both joints more flexed, however this depends on the strength of heterogenic feedback as weaker feedback had lesser effect onto joints. 138

Figure 4-5 Join angles of ankle and knee of AH (left) and Ah (right) limb in autogenic (blue) and heterogenic (pink) states. 139

Figure 4-6 Joint angles of knee (circle) and ankle (square) in autogenic (blue) and heterogenic (pink) state of AH (left) and Ah (right limb) across perturbation amplitudes. 140

Figure 5-1 Showing experimental set up (A) and raw force traces (B). The raw data (B - left) showing force responses of recipient (GAS) and donor (FHL) across varying background forces (active condition). The force responses show a strong CKI heteronymously exchanged from FHL onto GAS, and no apparent autogenic CKI in GAS. The pair of recipient stretches (right) stretched in tandem with donor 150

(state 2 - circle) and alone (state 1 - square). The stretch is broken down into an early (30-70 ms after the stretch onset - blue) and late epoch (110-150 ms after the stretch onset – red). Background force is marked with a black diamond.

Figure 5-2 VASTI↔GAS interaction in a representative cat. The VASTI muscle showed significant autogenic CKI in quiescent (A) and active (C) condition (separate early (blue) and late (red) regression lines in both S1 (full line) and S2 (dashed line). The force feedback arising from GAS to VASTI was insignificant. On the other hand, VASTI inhibited GAS strongly in both quiescent (B) and active (D) conditions. In active trials (D) there was insignificant CKI inhibition autogenically in GAS (red and blue full lines are overlapping). In state 2, there was medium force feedback inhibition in early epoch (blue full vs. blue dashed line), that strengthens in late epoch (red full vs red dashed line), presumably as a result of entangled CKI and iFFB. 157

Figure 5-3 VASTI↔GAS quiescent interactions across cats with dorsal hemisection. The magnitudes of interaction from GAS to VASTI were plotted against the magnitudes of interactions from VASTI to GAS (as described in detail in the Methods section). Overall, proximal to distal bias (red trace distribution) is prominent, presumably due to autogenic CKI that abolishes VASTI S1 force response, thus occluding the effect of heterogenic iFFB from GAS. 158

Figure 5-4 VASTI↔FHL interactions. The VASTI exhibits autogenic CKI in both quiescent (A), and active (C) trials (separate early (blue) and late (red) epoch S1 regression lines. Negligible force dependent inhibition was observed from FHL onto VASTI. On the other hand, VASTI donates medium force dependent inhibition onto FHL in quiescent (B) and active (D) trials, while FHL does not show signs of autogenic CKI in either conditions. 160

Figure 5-5 VASTI↔FHL quiescent interactions across cats with dorsal hemisection. The magnitudes of interaction from FHL onto VASTI were plotted against the magnitudes of interactions from VASTI onto FHL (as described in detail in Methods section). Overall, the prominent is proximal to distal bias (red trace distribution), presumably due to autogenic CKI that abolishes VASTI S1 force response, occluding the effect of heterogenic iFFB from FHL. 161

Figure 5-6 FHL↔GAS interaction. Balanced force feedback inhibition was exchanged between GAS and FHL and neither of them shows signs of autogenic CKI under quiescent conditions (A & B). Under active conditions, FHL inhibits GAS more strongly than the other way 162

around in both epochs (C & D), especially in the late epoch where inhibition is presumably arising from both iFFB and CKI pathways

Figure 5-7 FHL↔GAS quiescent interactions across cats with dorsal hemisection. The magnitudes of interaction from FHL onto GAS were plotted against the magnitudes of interactions from GAS onto FHL (as described in detail in Methods section). The bias varied from proximal to distal to distal to proximal (explained in text in detail), and magnitudes of FHL→GAS interactions were on average smaller compared to cats with lateral hemisection (Chapter II). Noteworthy is that these interactions probably include entangled iFFB and CKI in both directions. 163

Figure 5-8 FHL↔PLANT interaction. The most noticeable heterogenic effect is separation of two epochs of inhibition from FHL onto PLANT (A). Specifically, an early force dependent inhibition and superimposed on it, a clasp-knife inhibition in a late epoch. Similar heterogenic effect is observed in active trials (C). In early epoch we detect a strong force feedback inhibition (separated blue full and dashed regression line), and in late epoch in S2 we observed a clasp-knife inhibition superimposed onto force feedback inhibition, all resulting in a strong inhibitory heterogenic effect from FHL onto PLANT. Interaction from PLANT to FHL is characterized by a moderate force dependent inhibition in quiescent condition (B), and lack of clasp-knife inhibition in either condition or states (B & D). 164

Figure 5-9 FHL↔PLANT quiescent interaction across cats with dorsal hemisection. The magnitudes of interaction from FHL onto PLANT were plotted against the magnitudes of interactions from PLANT onto FHL (as described in detail in Methods section). The bias was distal to proximal, however, there were cases of proximal to distal bias (described in text). Noteworthy, interactions from FHL onto PLANT probably includes a compounded effect of iFFB and CKI, while interactions from PLANT onto FHL are presumably due to iFFB only. 165

Figure 5-10 FHL↔SOL interaction. The interaction from FHL onto SOL resembled those onto PLANT. In quiescent condition, one can discern two distinguished epochs of inhibition; early force dependent inhibition and late clasp-knife inhibition superimposed onto force dependent inhibition (A). Similar distinction between two kinds of inhibition can be made in active trials (C), as early (blue full (S1) vs dashed (S2)) regression lines are separate. These lines are even further apart in late epoch (red full (S1) and dashed (S2)). SOL did not significantly interact with FHL in either 166

quiescent (B) or active (D) trials. Neither FHL nor SOL showed autogenic clasp-knife inhibition in either conditions.

Figure 5-11 FHL↔SOL quiescent interactions across cats with dorsal hemisection. The magnitudes of interaction from FHL onto SOL were plotted against the magnitudes of interactions from SOL onto FHL (as described in detail in Methods section). The overall bias was distal to proximal and, in addition to iFFB, probably incorporated the strong heterogenic CKI from FHL onto SOL. 167

Figure 5-12 Latencies of heterogenic interactions between donor (column) and recipient (rows). Recipient muscles were held isometrically at high background forces, while donors were stretched. The black vertical line marks the stretch onset. The blue vertical lines mark earliest possible appearance of group I feedback (18 ms), and red lines mark the first possible appearance of group III feedback (80 ms). 170

Figure 5-13 Organization of the iFFB (left) and the CKI (right) following dorsal hemisection. In this chapter we presented data that points to varied inhibitory bias originating from the iFFB pathway. On the left, we presented two of three observed patterns of iFFB organization. On the right, we show organization of CKI compiled based on presence or absence of CKI in isometrically held recipient muscles 173

Figure 6-1 The ability of the nervous system to direct inhibitory bias toward the most distal joints (as in walking or running activity), an ankle (quiescent state following lateral hemisection) and to all limb joints (i.e., MTP, ankle and knee) in a quiescent and non-locomoting intact cat. 182

LIST OF SYMBOLS AND ABBREVIATIONS

c	Contralateral
CKI	Clasp-knife inhibition
CNT	Control
DSH	Dorsal Spinal Hemisection
FHL	Flexor Hallucis Longus
GAS	Gastrocnemius
GTO	Golgi Tendon Organs
i	Ipsilateral
iFFB	Inhibitory force feedback
LSH	Lateral Spinal Hemisection
mm	Millimeter
ms	Millisecond
MTU	Muscle-tendon unit
N	Newton
PLANT	Plantaris
s	Second
SCI	Spinal Cord Injury
SOL	Soleus
TA	Tibialis Anterior
VASTI	Vasti muscle group
XER	Crossed-extension reflex
%	Percentage

SUMMARY

Bipeds, like humans, stand with two-thirds of their body mass at about two-thirds of their body height above the ground, which, distributed within a relatively narrow base of support, makes us an inherently unstable system. It is not surprising that in the background of all motor control activities, such as standing or walking, are fundamental and dynamic processes that are aimed at maintaining and restoring the stability of the entire body. By exerting forces via their limbs against the ground, humans and animals can counteract both intrinsic and extrinsic perturbative forces and maintain their stability. The sensory feedback throughout the body contributes to the restorative forces developed by the limb muscles, with feedback from muscle mechanoreceptors being the most crucial. Briefly, length-dependent feedback from muscle spindle receptors increases joint stiffness locally, and intermuscular, widely-distributed inhibitory force-dependent feedback from Golgi tendon organs reduces limb stiffness, while excitatory force-feedback enhances joint coupling during locomotion. These pathways have shown remarkable task-dependent modulation by supraspinal tracts. Thus, the inability to modulate the gain and/or bias of these proprioceptive pathways properly after spinal cord injury could contribute to the crouched gait deficit often observed, even after functional recovery of stepping. Utilizing mechanographic method, in this study, we provided a comprehensive overview of changes in these pathways. This research ultimately contributes four major findings; i.) following lateral hemisection, the gain of length-feedback arising from knee and ankle extensors is selectively amplified, ii.) a strong, bilateral and chronic inhibitory force-feedback bias is directed toward ankle extensors, iii.) which likely contributes to the inability to maintain

static equilibrium and potentially to difficulty during the weight acceptance phase of a step cycle, and iv.) we provided evidence that supraspinal tract(s) that modulate force-feedback bias are likely located ventrally, whereas the dorsal tracts control the group III and IV pathways.

CHAPTER 1. INTRODUCTION

During the stance in humans and many non-human animals, two-thirds of the body mass is suspended at about two-thirds of the body height above the ground, which, combined with a relatively narrow base of support, makes us inherently unstable systems. It is not surprising that in the background of all motor control activities - both static (such as upright standing) and dynamic (such as walking) behaviors - are fundamental and dynamic processes that are aimed at maintaining and restoring the stability of the entire body. Although stability is maintained and/or restored as a whole-body response to intrinsic or extrinsic destabilizing perturbations, for the entire body to be stable, all limbs must be stable. In order for the limb to be stable, the constituent joints and muscles must be stable.

Unlike inanimate objects, animals have the capability to restore and maintain their stability. This capability is contingent on the cooperative interaction between the nervous and musculoskeletal systems. As with many complex systems, there are multiple levels of control organized in an orderly hierarchical structure (Bernstein 1967). The intersection of the nervous system and musculoskeletal system, where these controls are implemented is the muscle (Figure 1-1).

Information from many structures and levels is essential, as injuries to any of these (such as stroke, spinal cord injury, peripheral nerve injury, etc.) are detrimental to overall motor abilities. However, the relative contribution of these levels to the postural control has been intensely debated among scientists. Some argue that intrinsic properties of the muscle are sufficient to stabilize quiet standing in a human (Grillner 1972, Winter, Patla

et al. 1998), while others claim that the highest level of the hierarchy is required for adequate balance control (Hasan 2005). Many others have argued that various intermediate levels are crucial for posture, although they widely disagree on which particular pathway(s) are mainly responsible. Lyalka's research points to the importance of the ventral column in postural control, as T12 ventral hemisection drastically reduced postural response in rabbits, while rabbits with dorsal and lateral hemisection regained the postural response (Lyalka, Orlovsky et al. 2009). It is plausible that each unit in this hierarchical organization is responsible for the increasingly sophisticated integration of sensory and environmental information.

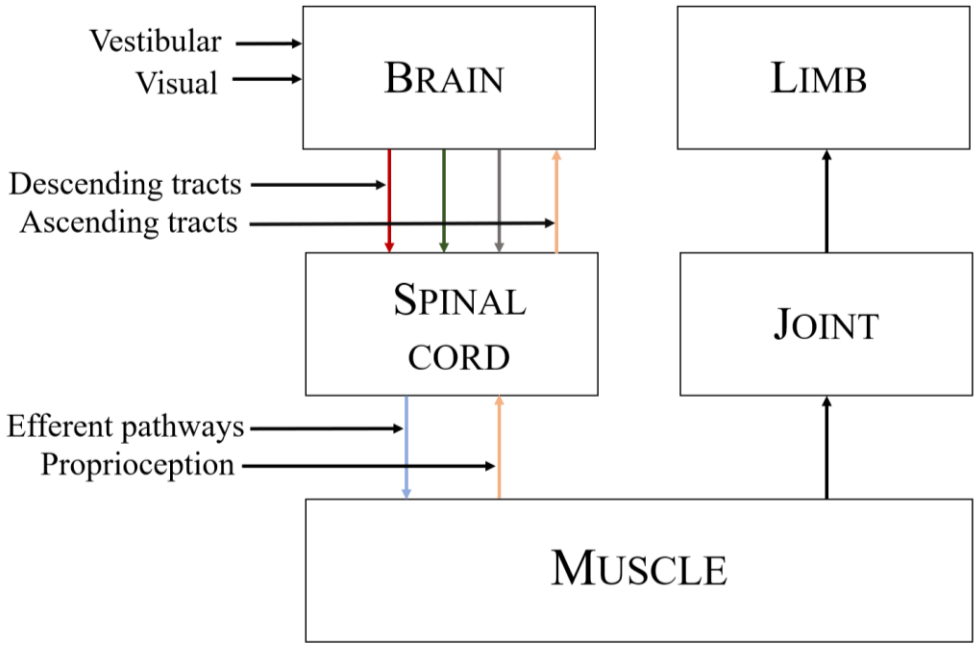

Figure 1-1: Hierarchical organization of postural control. On the left side of the scheme are neural components, and on the right side are skeletal components of postural control organization. These two components meet at the level of the muscle, whereby the nervous system controls the skeletal system via efferent pathways. Afferent pathways from sensory receptors from periphery provides feedback about the state of the skeletal system and enviroment back to the nervous system.

The focus of this dissertation is a relative contribution of proprioception and its regulatory supraspinal tract(s) to postural stability, although relevant structures will be discussed briefly and as pertinent. In the next sections, I will present contemporary and relevant past research on; i.) postural stability, ii.) neuromuscular system and its constituents, and iii.) spinal cord injury, as a framework, ultimately building towards the rationale and justification for this study, as the conclusion of this chapter.

1.1 Achieving postural equilibrium through joint stability

It would not be possible to discuss postural equilibrium without first touching on a hallmark of physiology; homeostasis. Homeostasis is defined as a crucial dynamic process by which an organism maintains its internal environment, upon which its survival depends, despite numerous and continuous disturbances. Both the internal and external environments of the organism change constantly, threatening fragile homeostatic balance. Therefore, maintaining homeostasis constitutes the dominant driving force underlying many physiological functions. The motor control system is no different. Much of its efforts involve maintaining the postural balance against destabilizing internal factors (breathing, heartbeat, muscle tremor, neural noise), external factors (gravity, environmental obstacles), and even collateral factors such as resultant movement and/or movements of other body parts. But why is controlling balance so crucial for the motor control system? Without postural balance, bipedal and quadrupedal organisms would not be able to perform any purposeful or voluntary motor activity beyond falling over.

Simply stated, balance is the state of an object when the net forces or moments acting upon it are zero (according to the Newton's First Law). The balance of an object is

related to the position of the center of its mass (CoM) and the area of its base of support. Any object is balanced if the line of gravity falls within the base of its support. Otherwise, it will fall. Thus, according to mechanical principles, the larger the base of support, the lower the center of mass, or both, the more stable the system. These Newtonian mechanics principles apply equally to humans and animals as they do to inanimate objects. Bipeds, like humans, stand with two-thirds of their body mass about two-thirds of their body height above the ground, distributed within a relatively small base of support, which makes us an inherently unstable system. Quadrupeds, stand on four limbs, which provides them with a broad base of support within which the horizontal projection of CoM can move significantly without loss of balance, hence making them relatively more stable. Unlike inanimate objects, humans and animals can sense perturbances, and exert forces via their limbs against the ground to counteract perturbative forces to prevent the fall. In this fashion, humans and animals can control their balance, while inanimate objects cannot.

Quadrupeds, such as cats have a broad base of support within which the horizontal projection of the center of mass can move significantly, seldom challenging the balance in the longitudinal plane (Figure 1-2). Furthermore, a cats' trunk is relatively stiff along the axis due to the structure of the vertebra, bolstering stability. However, the mobility of the vertebral column in the lateral direction, coupled with the much smaller base of support along the lateral axis, makes lateral stability more problematic. Vertical stability, i.e., ability to carry body weight against gravity, largely depends on the inherent limb stiffness and activity of anti-gravity muscles across all limb joints. Cats' hindlimbs are fairly flexed, requiring larger extensor muscle forces to maintain the relative extension against the flexing forces due to gravity.

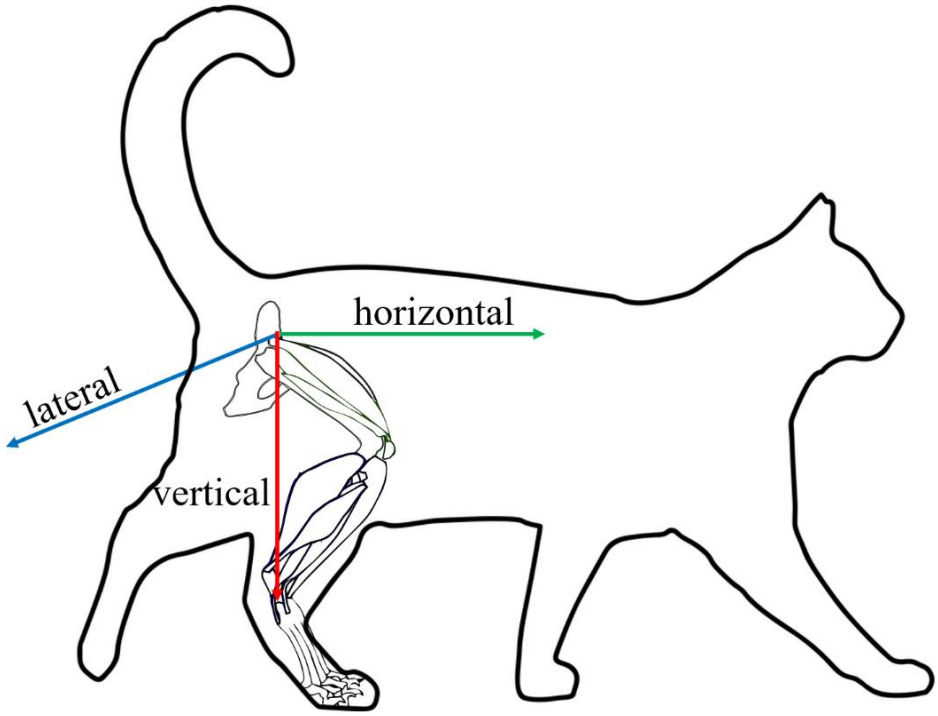

Figure 1-2: Directional stability in the cat. Cats must maintain horizontal (longitudinal), lateral and vertical stability during any motor task.

The apparent stiffness[1] (later on simply, stiffness (Latash and Zatsiorsky 1993)) of the limb arises from three groups of structural elements; (i) bones, joint capsule, cartilage (ii) ligaments, tendons, fascia and passive muscle properties, which comprise the static (passive) components, and (iii) neurally initiated muscle activity (net integration of supraspinal and proprioceptive pathways onto motoneurons). Bone segments, which provide a rigid, stiff framework, are linked via viscoelastic elements at joints. Joints possess inherent stability which arises from stiff structures surrounding it (ligaments, tendons, muscles, fascia, cartilage, joint capsule, skin) (Lew, Lewis et al. 1993). With the

[1] The mechanical properties of limbs can be summarized by the property of impedance that includes components related to elasticity, viscosity and inertia. The terms corresponding to elasticity and viscosity are generally nonlinearly related to position and velocity (Houk et al 2000), respectively, and frequently lumped together in the motor control literature as "stiffness" despite the fact that the term "stiffness" properly refers to the static mechanical properties of a system (Latash and Zatsiorsky 1993).

exception of muscles, all these structures provide a passive, relatively constant, and modest stiffness that is, by itself, insufficient for stability (Loram and Lakie 2002). The contribution of individual muscles to the stability is difficult to discern. Bergmark (1989) was the first to relate mechanical stability of the muscular system to the potential energy (Bergmark 1989). He reasoned that the musculoskeletal system could be considered stable if potential energy of the entire system is at a relative minimum. Muscle-tendon units (MTU) can contribute to the potential energy in the system by storing or releasing elastic energy related to their stiffness. A stiffer muscle stores more energy in relation to the distance it is stretched during a perturbation, thus stabilizing the limb (Potvin and Brown 2005).

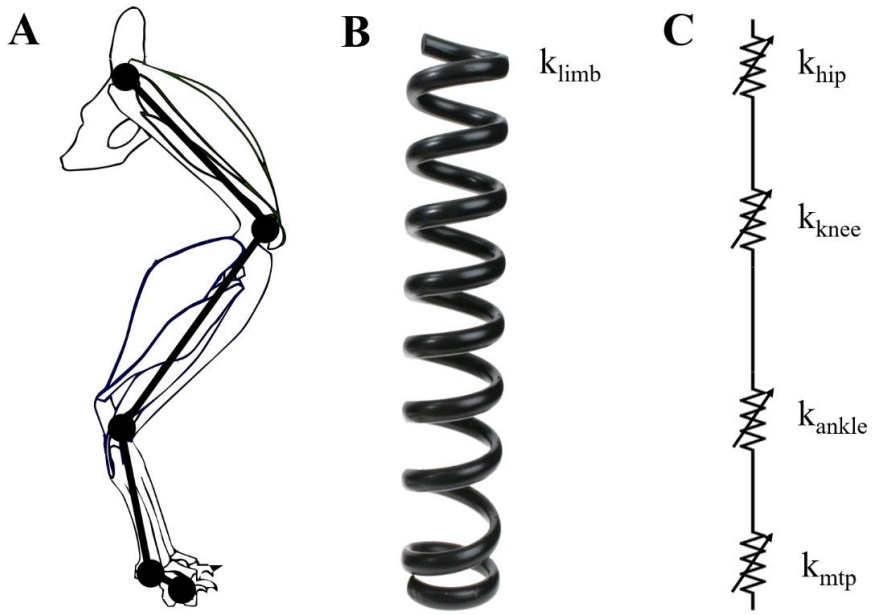

Figure 1-3: Comparative views of a limb. A.) A limb with anatomical structures and stick figure superimposed, B.) A limb presented as a spring with a constant limb stiffness, C.) A limb presented as a series of variable stiffnesses, as some joints serve as springs while others may serve as dampeners, depending on a task.

Physiologically and kinematically speaking, the concept of constant mechanical stiffness or compliance (Figure 1-3: B, k_{limb} = constant and uniform) may not be beneficial for different motor tasks (Rapoport, Mizrahi et al. 2003, Simon, Ingraham et al. 2014), as different dynamic tasks may require variable and/or joint-specific compliance (Figure 1-3: C). For instance, walking may require greater compliance of the ankle joint than standing would. The mechanism that the nervous system utilizes to modulate joint stiffness is by modulating stiffness of muscles traversing the particular joint.

Muscle stiffness is defined as the ratio of change in its force per change in its length (Johansson and Sjolander 1993). It is a function of intrinsic properties of the muscle (tendon, fascia, and passive contractile structures), and, to a greater extent, neural activation (Nichols and Houk 1976). The level of neural activation of a muscle at a given instant is the result of an integration of descending (efferent) inputs and segmental proprioceptive (afferent) feedback onto its motoneurons (Riemann and Lephart 2002, Riemann and Lephart 2002). It continually undergoes revisions and adjustments based on resultant movement, movement of other body parts, unexpected obstacles, etc. Thus accurate and timely sensory information about internal or external body conditions is critical for effective motor control and appropriate muscle stiffness. Although the source of this modulation is associated with visual perception (Sasaki, Usami et al. 2002), the vestibular system (Paloski, Wood et al. 2006), and tactile receptors (Kavounoudias, Roll et al. 2001), oftentimes proprioceptive feedback is the fastest and the most accurate (Ghez 1991). Furthermore, patients with impaired vision or vestibular function can maintain balance and posture quite well, but not without proprioceptive feedback (Sainburg, Ghilardi et al. 1995).

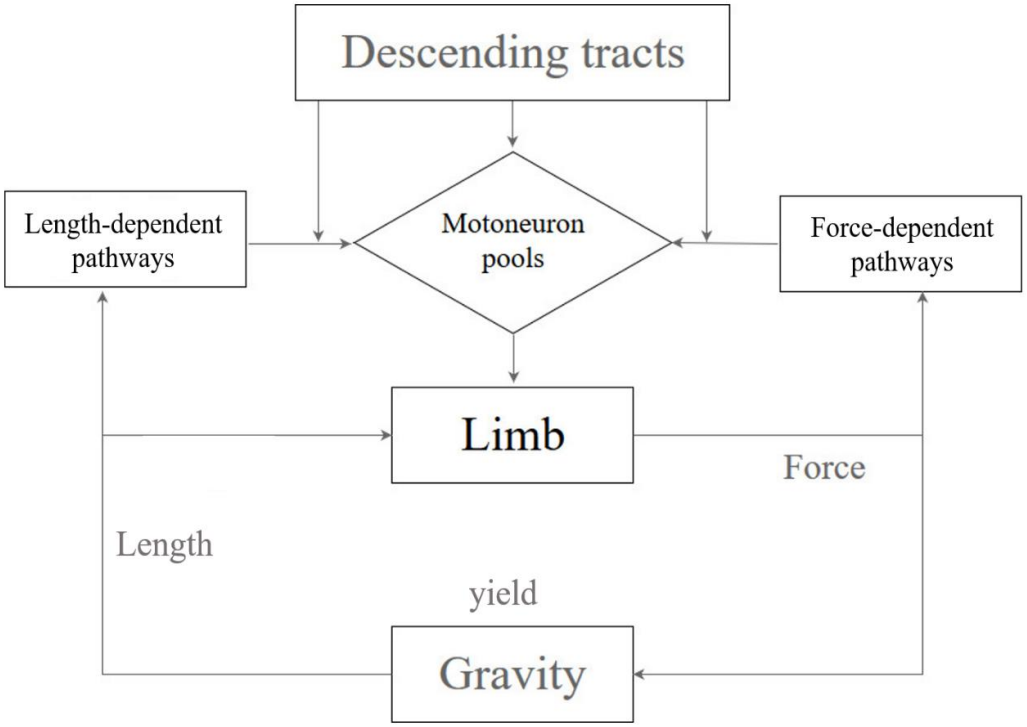

Figure 1-4: Schematic representation of neural and musculoskeletal compartments acting in tandem in regulating stiffness of a limb as a whole. Adapted from Nichols & Houk (1976), with author(s) permission.

The robust mechanical and neural coupling of bone segments and muscles by the nervous feedforward and feedback postural control systems render a limb a complete functional unit of posture and movement, and muscles and joints its constituents. Supraspinal motor centers issue an efferent (feedforward) command to selected muscles to execute a particular movement. The resultant movement changes the configuration of the limb, and the mechanical state of numerous muscles, directly or indirectly involved in that movement. Feedback from those muscles integrates with feedforward command in the nervous system, which in turn issues a correcting efferent command (if limb configuration does not result in the desired movement) or a new efferent command based on current limb configuration (Figure 1-4). This is a continuous, subtle process of commands and revisions involved in all motor tasks.

1.2 Properties of the neuromuscular system

A body is composed of numerous systems that operate tirelessly to maintain the homeostasis of the entire body (Guyton and Hall 2006). A system is an organized group of related components that collaborate to perform a common-goal action successfully (Taber & Thomas). Systems are organized hierarchically, but cross-talk and integration continuously happen on every level, both vertically, within the system across its components, and laterally, across the systems (Figure 1-1). The neuromuscular system is responsible for every single interaction with the environment we experience, all executed by motor control.

Motor control is a dynamical process by which animals and humans use their neuromuscular system to coordinate all the muscles during any interactive experience. In the background of all motor activities are fundamental and dynamic processes that are aimed at maintaining and restoring the stability of the entire body. It follows that a significant portion of motor control efforts is devoted to maintaining the stability of the body.

Postural control is dependent on coordination between motor control and the muscular system. The first line of defense against disturbances to postural control is the ‘short-range stiffness,’ which emerges from intrinsic mechanical properties of a muscle.

1.2.1 Musculoskeletal system

The intrinsic properties of the muscle arise from the viscoelasticity of the soft connective tissue components (Nichols and Houk 1976), existing actin-myosin cross-bridges (Edin and Johansson 1995), as well as properties of both single muscle fibers (i.e. sarcomere length-tension and force-velocity relationship) and whole muscles (arrangement of muscle fiber within a muscle). Two characterizing features of intrinsic muscle properties are the short-range stiffness (Hill 1968), i.e., the resistance to changes in length, and the yielding of a muscle to stretch (Grillner 1972). Stretching self-reinnervated muscle, which has permanently lost its stretch reflex (Cope, Bonasera et al. 1994), results in transient resistance, followed by a profound yield of a muscle, which is presumably due to the disruption of cross-bridges (Rack and Westbury 1970). Stretch reflex compensates for this non-linear property of a muscle by augmenting it in order to maintain a constant muscle stiffness (Nichols and Houk 1976).

The cat hindlimb has over 30 muscles (Figure 1-5), rich in a variety of fiber type compositions, fascicle length, physiological cross-sectional area, pennation angles, tendon length and thickness, architecture, and geometry, exerting various moments about different joints and axes of rotation (Ariano, Armstrong et al. 1973, Cutts 1989, Lawrence, Nichols et al. 1993). Many muscles cross one or more joints and one or more axes of rotation, regulating stiffness of the transversing joints. Muscles regulate the stiffness of joints by virtue of their resultant stiffness and their moment arm at the spanned joint (English and Weeks 1987, Carrasco, Lawrence et al. 1999). The massive proximal muscles regulate limb and body work, whereas the distal smaller muscles with longer tendons contribute to elastic energy saving (Biewener and Roberts 2000). Furthermore, the ‘force constrain

strategy' (Macpherson 1988) likely arises from the mechanical organization of the limb musculature (Honeycutt, Gottschall et al. 2009), as most muscles have small non-sagittal actions. Due to the complex interactions between the nervous system and diverse muscular system, there likely exists a link between muscle architecture (origin and insertion attachments, moment arms, etc.) and the neural control strategy used to control it. Thus, it is essential to understand the anatomy of a muscular system and to view the neural control organization within anatomical context. To explore this idea, a brief review of anatomy (per Text-Atlas cat anatomy (Crouch 1969)) and biomechanical actions of selected hip, knee, ankle, and toe extensors and flexors evaluated in this study is necessitated:

(i) The quadriceps muscles (QUADS) are comprised of four muscles: vastus lateralis muscle (VL), vastus medialis muscle (VM), vastus intermedius muscle (VI), and rectus femoris muscle (RF). Of these, RF is a biarticular muscle whereas the remaining are uniarticular; furthermore, VI is a homogeneous muscle comprised entirely of slow type muscle fibers, whereas the remaining muscles are heterogeneous (Ariano, Armstrong et al. 1973). Due to experimental set-up limitation, RF had to be transected to eliminate its action on the pelvis. Of the QUADS muscles, the ones that were tested as a group were the three vasti muscles (VASTI) freed from RF. The entire muscle group covers a significant portion of the femur and inserts onto the patella. Each of the individual VASTI muscles has a unique pulling direction about the patella (Abelew, Huyghues-Despointes et al. 1996), but as a group, they form a powerful knee extensor.

(ii) The two heads of the gastrocnemius (GAS), medial and lateral, originate at the medial and lateral sesamoid bones, lateral to the medial and lateral epicondyles of the femur, respectively. They insert via the Achilles tendon into the calcaneus. Thus, GAS

spans the knee and ankle joints and provides mechanical coupling between these two joints. However, it has a greater moment arm for plantarflexion at the ankle and therefore contributes preferentially to ankle joint stiffness, but still imparts a flexor moment to the knee. Its maximal plantarflexion and abduction moments are reported by Lawrence and Nichols (Lawrence, Nichols et al. 1993), and shown in Figure 1-6.

(iii) Soleus (SOL) originates at the fibula and inserts into the calcaneus through a long tendon functioning as an ankle extensor. In a cat, SOL is composed of solely slow twitch fibers. Its maximal moments at the ankle are shown in Figure 1-6.

(iv) Plantaris (PLANT) originates from the lateral part of the patella and forms a long tendon that passes above the GAS and SOL tendon and inserts into the tendon of flexor digitorum brevis. It is much more prominent in cats, compared to humans, probably due to their digitigrade walking. Its primary function is plantarflexion, but it also serves as a weak abductor, although it contributes very little to the off-sagittal movement of the ankle (Figure 1-6) (Lawrence and Nichols 1999).

(v) Flexor hallucis longus (FHL) originates from the upper part of fibular shaft and inserts into flexor digitorum longus (FDL) tendon in the foot through a long tendon that passes behind the medial malleolus. It contributes to ankle plantarflexion, adduction, toe flexion and claw protrusion (Goslow, Reinking et al. 1973). Although its moment arm is one-third that of the SOL (Young, Scott et al. 1993), it produces large forces (more than SOL and TA) (Sacks and Roy 1982) resulting in about two-thirds of the SOL moment (Figure 1-6) (Lawrence, Nichols et al. 1993).

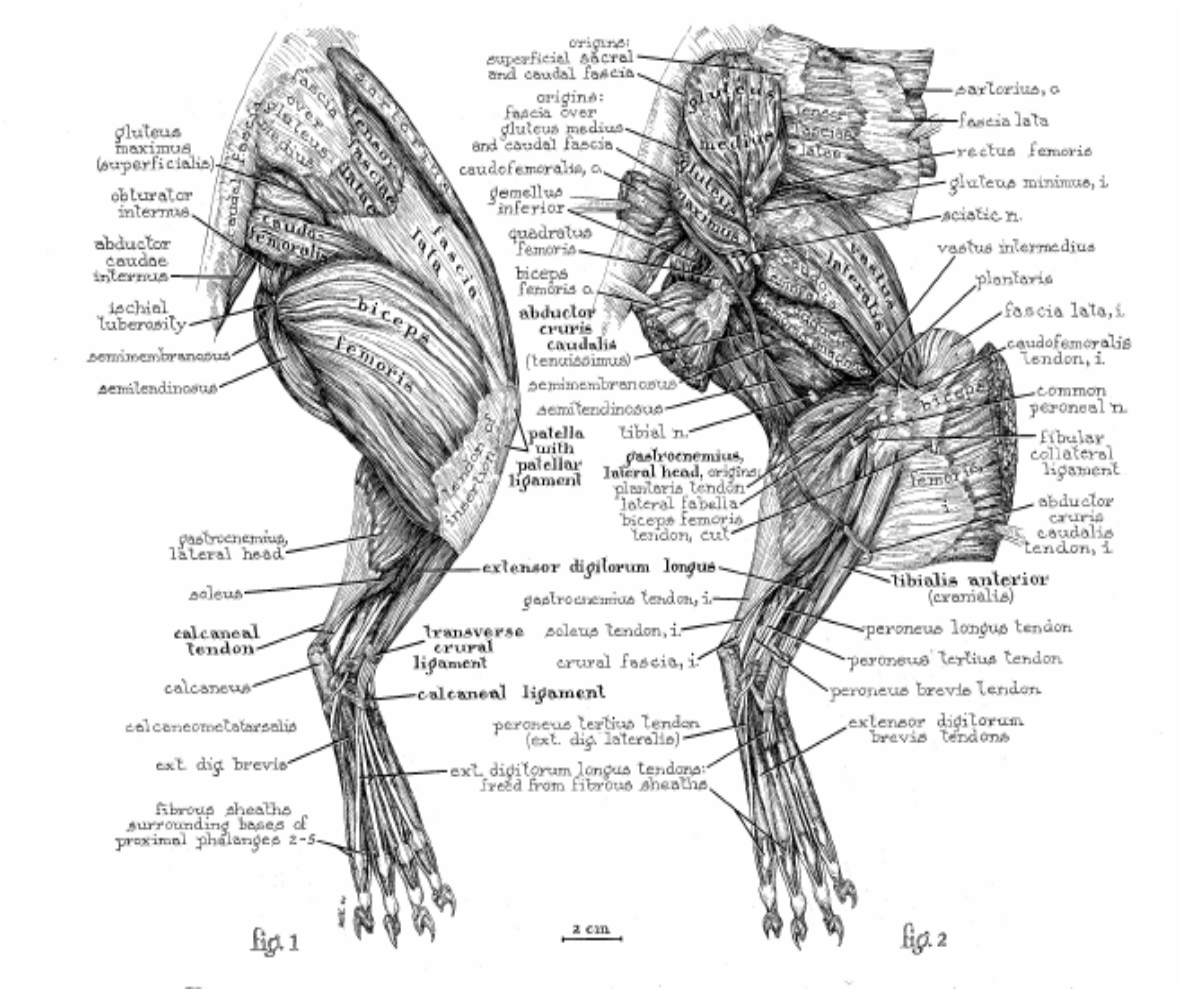

Figure 1-5: Lateral and medial view of cat hindlimb shows great complexity of muscular system. Acquired from 'Text-Atlas cat anatomy' by Crouch (1969), with permission (Permission/License ID: 4483740323443).

(vi) Tibialis anterior (TA) connects the lateral portions of the tibia to the medial foot at the base of the first metatarsal. Primarily, it dorsiflexes and inverts the foot. During the step cycle, it counteracts the forces causing the plantar flexion of the foot when the foot touches the ground, and during the swing, it dorsiflexes the foot and prepares it for landing.

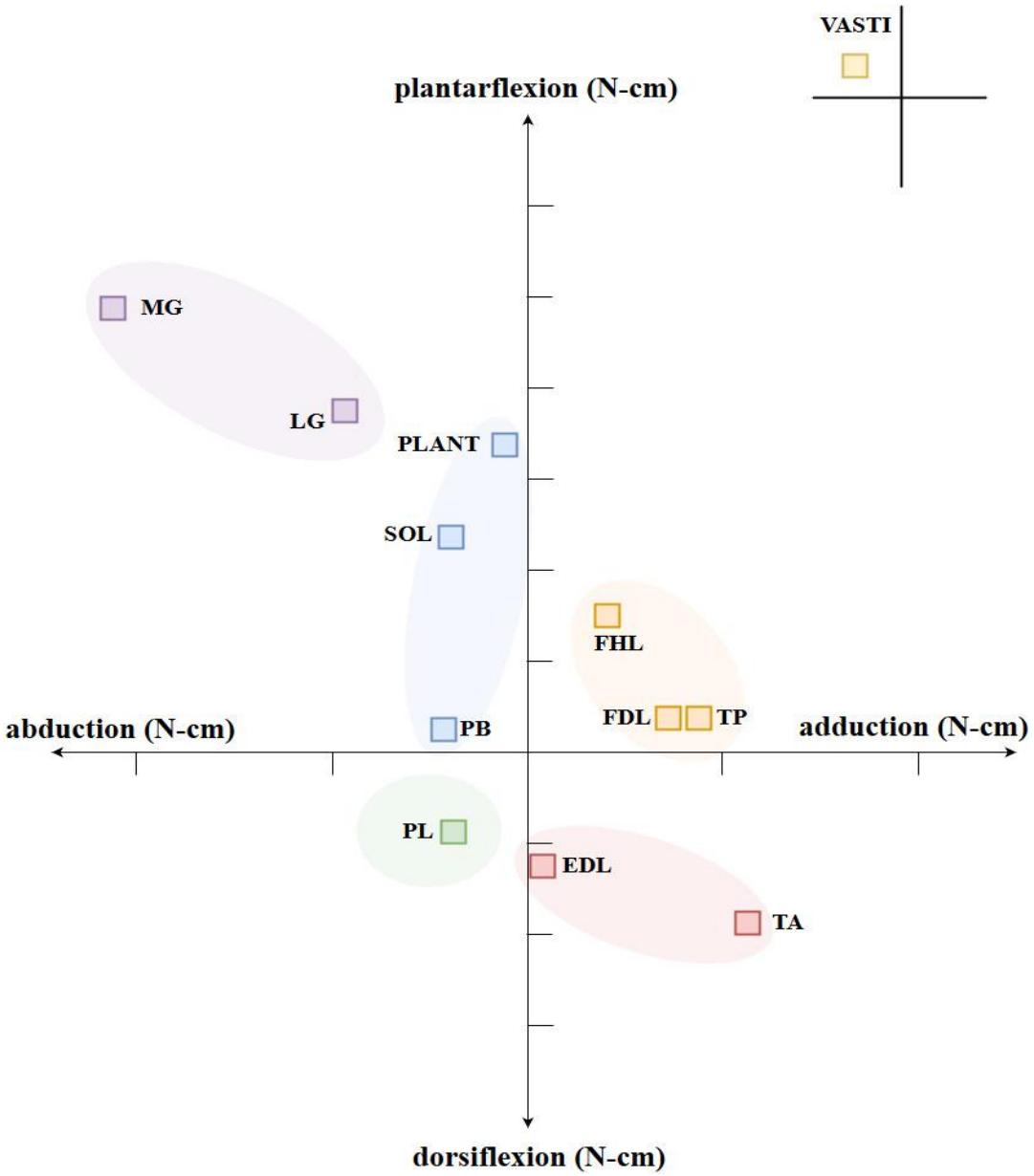

Figure 1-6: Maximal torques around ankle joint showing lines of action of muscles evaluated in this study**.** Adapted from Lawrence & Nichols (1993), with author(s) permission.

The connective tissues, such as fascia and tendons, are also important components of the muscular system and can influence limb mechanics. Together with activated muscles and bone, the connective tissue forms a complex mechanical network that has been described as a tensegrity structure (Silva, Fonseca et al. 2010). Tendons provide

mechanical buffering during locomotion (Roberts and Konow 2013). Due to the tendon compliance, eccentric contractions result in shortening of the muscle fibers while the whole muscle-tendon unit is lengthening (Hoffer, Caputi et al. 1989, Prilutsky, Herzog et al. 1996, Maas, Gregor et al. 2009, Konow, Azizi et al. 2012). This way, the tendon greatly enhances the mechanical efficacy of movement by storing and releasing energy (Alexander and Bennet-Clark 1977). The compliance of Achilles tendon, for example, is optimal for maximal muscle efficacy during locomotion (Lichtwark and Wilson 2007). Fascia provides an alternative route for force transmission (Maas, Meijer et al. 2005) to synergist muscles, presumably as a compensatory mechanism due to an injury (Maas and Sandercock 2010). Additionally, passive mechanical structures (such as the retinaculae at the ankle) are considered to act as mechanical stabilizers of the limb (Abu-Hijleh and Harris 2007). Muscles work within this complex mechanical infrastructure.

Idealized muscles transmit forces, as directed by the nervous system, onto the bones which translate them into moments. However, the transformation from motor command to the resultant movement is highly non-linear. First, activation of motoneurons follows the Henneman size principle (Henneman 1985, Henneman 1991), which is very non-linear. Second, tendon compliance (Griffiths 1991) and lateral force transmission ‘leak’ intended forces (Maas and Sandercock 2010) resulting in non-linear force transmission. Third, the large variety of attachments, pennation angles, and joint-angle-dependent moment arms challenges translation even further. One could state that the resultant movement is not necessarily the intended movement, even in the absence of perturbations. However, the nervous system must know the details about the resultant movement in order to formulate an adequate new command or correction response. The

solution to this conundrum is the continuously crowdsourced mechanical state of all muscles via proprioception.

1.2.2 Proprioception

Sherrington proposed that proprioception's primary purpose was the regulation of postural homeostasis and joint stability (Sherrington 1906). Many proprioceptors are specialized mechanoreceptors that respond to a specific flavor of the mechanical event, from which their function can be discerned. Although many of them contribute to effective postural control, in this section I will provide a brief review of muscle mechanoreceptors.

Ever since their discovery by Ruffini in 1889, muscle spindles are proprioceptors favored for study by motor control neuroscientists, and we know plenty about them (Matthews 1972, Grigg 1994). Muscle spindles (Figure 1-7) are specialized, encapsulated intrafusal muscle fibers innervated by both sensory (Ia and II afferents) and motor axons (γ-motoneurons). There are three classes of intrafusal fibers, bag_1, bag_2 and chain, each receiving Ia afferent terminal, while bag_2 and chain receive group II fibers as well. As they lie in parallel with extrafusal fibers, they are selectively sensitive to the length and rate of change of the length of those neighboring extrafusal fibers. Each spindle consists of a bundle of several intrafusal fibers enclosed within a capsule (for example, surface MG spindle has six intrafusal fibers, whereas deep units have about 10 per spindle, in range of 2-9 (Eldred, Bridgman et al. 1962)). The nervous system has the ability to modulate muscle spindle sensitivity via γ-motoneurons, thus influencing the way we 'perceive' external information, based on training, age, experience or situational circumstances.

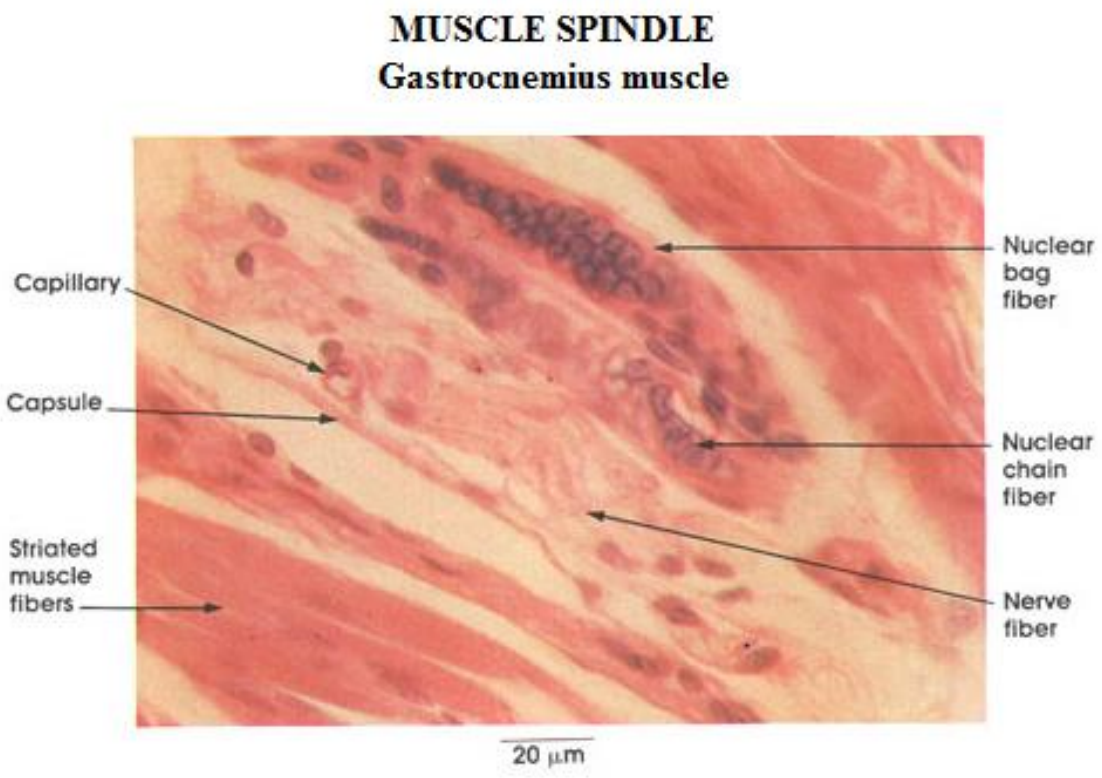

Figure 1-7: Muscle spindle. Acquired from anatomy digital library curated by Drs. Ronald A. Bergman and Michael P. D'Alessandro, with author(s) permission. (Bergman and D'Alessandro 2018)

Most of our knowledge about afferent pathways arising from muscle spindles comes from electrophysiological studies conducted by the Eccles and Jankowska group. Each motoneuron pool receives excitatory Ia connections from its homonymous muscle (Figure 1-10) (Eccles, Eccles et al. 1957, Eccles and Lundberg 1957), its synergists (Eccles, Eccles et al. 1957, Nichols 1999) and, in very rare instances, from heteronymous non-synergist muscles (Edgley, Jankowska et al. 1986), while antagonists receive appropriate reciprocal length-dependent inhibition (Kandel, Schwartz et al. 2000). The size of the Ia contribution, measured as the amplitude of excitatory postsynaptic potential (EPSP), is

larger in homonymous than in heteronymous motoneurons[2] (Mendell and Henneman 1968, Mendell and Henneman 1971), and most substantial in small/slow-twitch motor units (Eccles, Eccles et al. 1957). However, Ia afferents can form disynaptic and oligosynaptic connections with inhibitory interneurons and project inhibition to homonymous and synergistic muscles (Fetz, Jankowska et al. 1979, Jankowska, McCrea et al. 1981). The group II afferents also make monosynaptic connections to the alpha motoneurons (Kirkwood and Sears 1975), but EPSP amplitude is significantly smaller. Both inhibitory and excitatory signals from group II afferents transmit information about the length of a muscle when the muscle is static. Group II shares interneurons with group Ia (Edgley and Jankowska 1987) and group Ib afferents (Jankowska and Edgley 2010), but proportions of input from these two sources may vary. Interneurons receiving Ia, Ib and II inputs show co-localization in the deep dorsal horn of both the rat (Vincent, Gabriel et al. 2017) and cat (Brown and Culberson 1981) spinal cords.

The Golgi tendon organs (GTO's) are slow-adapting mechanoreceptors innervated by Ib afferents (Figure 1-8). About 8% of GTO's are located in the tendon proper (Barker 1967). The rest of the GTO's are situated at the transition from the muscle to the tendon or from the muscle to the aponeurosis in series with muscle fibers (Jami 1988, Jami 1992). Our understanding of the GTO feedback role in the neuromuscular system has been evolving over the past century. Initially, GTO feedback was considered to have a protective role against overloading of its autogenic muscle, as higher forces were required to activate it. This view was challenged by Houk's finding that adequate stimulus for GTO is not a

[2] Throughout this dissertation, *homonymous* and *autogenic* are used interchangeably to denote a feedback onto muscle from which that feedback originates, while *heteronymous*, *heterogenic* or *intermuscular* feedback refers to a sensory input from other muscles

passive stretch, but rather an active contraction of the muscle fibers connected in series with the GTO's (Houk and Henneman 1967). Nonetheless, there is evidence that the GTO responds to passive stretch to some extent (Jansen and Rudjord 1964, Schafer, Berkelmann et al. 1999). To reconcile these two findings, it has been proposed that sensitivity of GTO to either passive stretch or active contractile force is directly correlated to its structural stiffness (Fukami and Wilkinson 1977, Proske 1981); GTO's with more tendinous compartments are usually stiffer, which shields them from elongation and hinders activation by stretch (Zelená 1994). The simplest explanation for this observation is that the stiffness of the structure where the GTO is embedded will determine its primary sensitivity. The combined signals from both types of GTO provide an accurate estimate of muscle force, both active and passive (or total) (Schafer, Berkelmann et al. 1999).

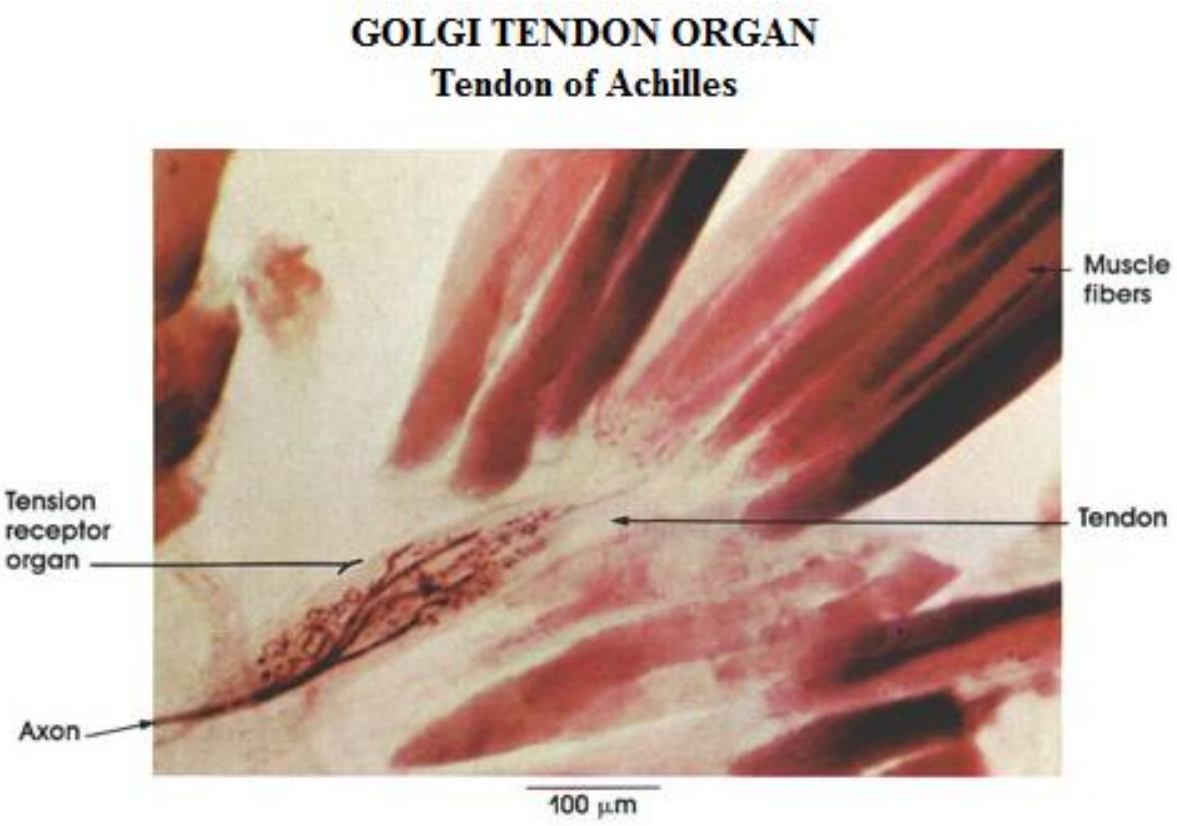

Figure 1-8: Golgi tendon organ. Acquired from anatomy digital library curated by Drs. Ronald A. Bergman and Michael P. D'Alessandro, with author(s) permission (Bergman and D'Alessandro 2018)

Eccles' work (Eccles, Eccles et al. 1957) points to GTO's as the origin of inhibitory interactions amongst muscles with similar action as well as non-synergist muscles, a conclusion that was subsequently upheld by Nichols (Bonasera and Nichols 1994, Wilmink and Nichols 2003). These two groups provided overwhelming evidence that the Ib pathways between extensor muscles are (i) inhibitory, (ii) widely distributed to heteronemyous and non-synergistic motoneurons, and (iii) force dependent. The force dependence arises from (i) recruitment of GTO's, (ii) interneuronal processing, and (iii) excitability of motoneurons (Bonasera and Nichols 1994, Wilmink and Nichols 2003). The Ib input onto homonymous muscle is not pronounced (Rymer and Hasan 1980). Instead, this feedback seems to converge mainly onto heteronomous motoneuron pools; in most cases onto those of muscles with different biomechanical actions (Eccles, Eccles et al. 1957, Wilmink and Nichols 2003). However, inhibitory interactions were also found amongst close synergies. For example, biarticular and monoarticular knee extensors (RF and VASTI), exchange significant inhibition (Prilutsky 2000, Wilmink and Nichols 2003). In the decerebrate cat, homonymous excitatory force feedback was observed only in specific muscles during locomotion, while the rest of heteronymous interactions were inhibitory (Ross 2006, Ross and Nichols 2009).

Intermuscular stimulation studies in intact and quietly standing cats have shown that twitch evoked feedback, presumably the GTO feedback is indeed widespread, but excitatory (Pratt 1995). The evidence for excitatory GTO feedback is stronger in a locomoting cat. A fictive locomotion study provided evidence that excitatory force feedback is widespread under these conditions (Guertin, Angel et al. 1995). Studies that employed electrical nerve stimulation and natural stimulation to evoke muscle feedback

have all shown excitatory and widespread feedback during locomotion (Pearson and Collins 1993, Donelan and Pearson 2004). This apparent discrepancy in results regarding the sign of force-dependent feedback was reconciled as a coexistence of both excitatory and inhibitory components (Ross 2006) in various combinations that are selectively employed or disengaged, depending on a particular motor task.

These two afferent pathways from muscle, length and force feedback, converge onto a complex interneuronal network, where integration, summation, and gating happen to a varying degree. In discerning specific contributions of length- and force-dependent pathways to the postural stability, we might examine; i.) the distribution of mechanoreceptors across muscles, ii.) receptor response to distinct mechanical events, and iii.) the convergence of afferent pathways onto a network of interneurons and motoneurons in the spinal cord.

i.) The mechanoreceptors are abundant throughout the body, but their distribution is not uniform. The human body has roughly 20,000 muscle spindles (Zelená 1994), and while some muscles are virtually void of spindles (such as the posterior head of M. digastricus and the mylohyoideus muscles), others contain an extraordinary number (like lumbrical muscles) (Voss 1971). Likewise, the number of GTO's in muscles is also uneven. In general, the number of GTO's per given muscle is smaller than the number of muscle spindles (Zelená 1994). These distributions (Table 1-1) are muscle- and species-specific, with no apparent connection between distribution and function. Banks and Stacy have found that muscle spindle correlates to muscle weight after logarithmic transformation (Banks, Hulliger et al. 2009), but no functional connection has been made for GTO's. My

personal speculation is that the more connective tissue a muscle is engulfed in, the more GTO's compared to spindles it has.

Table 1-1: Distribution of muscle spindles and Golgi tendon organs.

	Muscle spindles	**Golgi tendon organs**
VASTI	unknown	unknown
RF	77-132 [3]	unknown
ST	137 [1]	86 [1]
GAS	MG: 70 [1], 70 [2], 46-80 [3], LG: 25-45 [3]	MG :44 [1]
PLANT	41 [4]	unknown
SOL	53 [1], 40-70 [3], 56±7 [4]	45 [1]
FHL	75 [5]	unknown
TP	25 [1]	29 [1]
TA	52-89 [4]	43 [4]
EDL	71 [1]	unknown

Sources: [1](Banks, Barker et al. 1979), [2](Eldred, Bridgman et al. 1962), [3](Chin 1962), [4](Banks and Stacey 1988), [5](Boyd and Davey 1968)

ii.) Muscle spindles are almost universally characterized as length sensors, whereas there is evidence that two classes of GTO's coexist in a muscle; one sensitive to passive stretch and another kind to an active twitch. The former view has been updated recently, as new findings show muscle force encoded in muscle spindle firing (Blum, Lamotte D'Incamps et al. 2017). Muscle spindles and GTO's probably provide some complementary functions, in more ways than are obvious (Figure 1-9). Another exciting proposition about complementary role comes from Kistemaker's research. He proposes

that it is conceivable to derive the length of the whole MTU from combined feedback from muscle spindles and GTO's (Kistemaker, Van Soest et al. 2013).

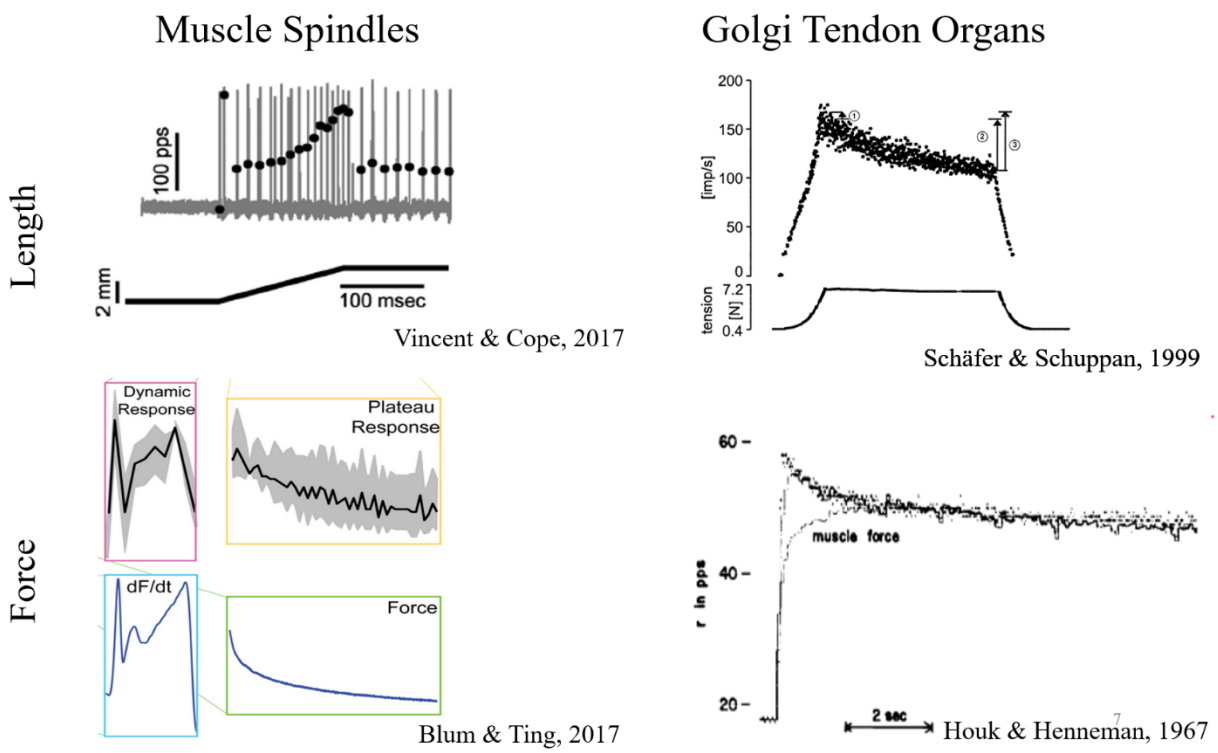

Figure 1-9: Muscle spindles and Golgi tendon organs respond to two distinct mechanical stimuli. Adequate stimulus for muscle spindle is length and rate of length change of a muscle (*upper left*), although new findings suggest that it incodes force stimuli as well (*lower left*). Adequate stimulus for GTO is an active force (*lower right*), although a class of GTO's respond to a passive stretch (*upper right*).

iii.) Locally focused length-feedback presumably transforms individual muscles into more spring-like actuators (Nichols and Houk 1976, Nichols, Gottschall et al. 2014). The nonhomogeneous and widespread distribution of force-feedback pathways throughout the limb, suggests that inhibitory force feedback helps regulate whole-limb compliance (Gottschall and Nichols 2007, Ross and Nichols 2009, Gottschall and Nichols 2011, Nichols, Gottschall et al. 2014), while excitatory force feedback heightens joint coupling

during locomotion (Pearson and Collins 1993, Prochazka, Gillard et al. 1997, Donelan and Pearson 2004). Taken together, at the limb-level, it is postulated that excitatory length-dependent feedback increases joint stiffness locally, while inhibitory force feedback decreases stiffness selectively, and in a task-dependent manner throughout the limb.

1.2.3 Spinal cord circuitry

The spinal cord plays a vital role in motor control, despite gross anatomy suggesting it is merely a conduit. It is the site of integration of proprioceptive feedback and descending control over motoneurons. Most of the incoming feedback converges onto interneurons scattered throughout the cord grey matter (Figure 1-10). Even the fibers involved in simple

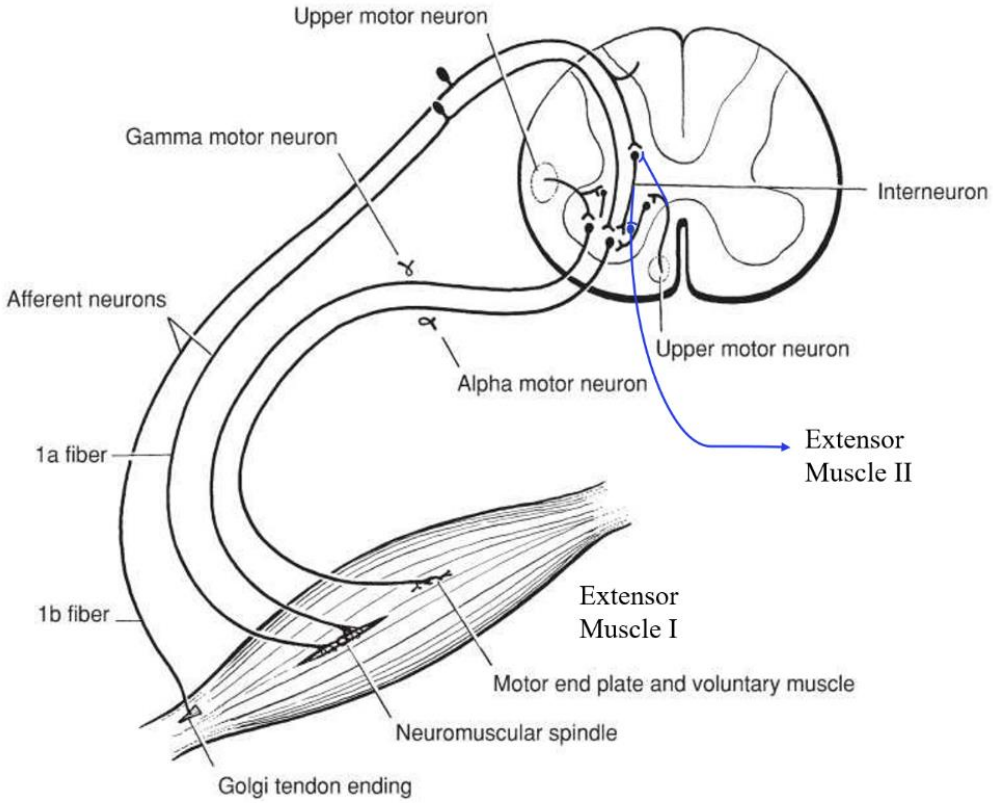

Figure 1-10: Afferent Ia and Ib spinal circuitries. Length feedback from muscle spindle monosynaptically connects to homonymous motoneuron, while force feedback from GTO disynaptically connects onto motoneuron of another muscle via inhibitory Ib interneuron. This figure was used and edited to represent the correct view of the force-feedback pathway with permission (Permission/license ID: 4483341167284, (Norman L., Strominger R.J. et al. 2012)).

monosynaptic stretch reflex bifurcates and may convey length information to a number of locations, including local interneurons, supraspinal centers or agonistic/antagonistic motoneurons (Leonard 1998). The bifurcations and interneuronal networks provide the anatomical basis for the spinal cord's integrative functions.

The spinal cord is capable of many self-sufficient motor activities. The interneuronal network in the spinal cord is incredibly complex and capable of numerous autonomic functions. The spinal central pattern generators can generate robust locomotor and other rhythmic patterns in spinalized mammals (Pearson and Rossignol 1991) and in an isolated spinal cord (Bonnot, Morin et al. 1998, Whelan, Bonnot et al. 2000, Bonnot, Whelan et al. 2002), even without feedback (Markin, Lemay et al. 2012). These ingrained and basic rhythmic motions are, from an evolutionary perspective, crucial for survival. For example, the sea turtle must rapidly locomote, immediately after hatching and leave the beach on which its egg incubated, or else quickly become food for a variety of predators. Built-in programs and spinal pattern generation mechanisms provide a motor infrastructure to support this rapid development (Grillner, Perret et al. 1976).

Because of the extensive interneuronal network, the spinal cord is capable of plasticity and learning. Numerous Durkovic's studies have shown that cutaneous afferents of a spinalized (spinal) cat are capable of being conditioned and modulated using Pavlov conditioning paradigm (Durkovic 1975, Durkovic and Light 1975, Durkovic 1983, Durkovic 1985, Durkovic and Damianopoulos 1986). Grau took this idea further, showing that the spinal cord is indeed capable of great plasticity, learning transiently and chronically, with or without supraspinal supervision (Grau, Salinas et al. 1990, Hoy, Huie et al. 2013, Huie, Stuck et al. 2015, Lee, Turtle et al. 2015). Even the stretch reflex is known

to be susceptible to conditioning, although it requires an intact corticospinal tract, which nonetheless attests to the plasticity of the spinal cord circuitry (Wolpaw and Carp 2006, Wolpaw 2010).

If proprioceptive feedback is indicative in postural deficit following spinal cord injury these studies offer hope that the same feedback can be modulated via training for rehabilitation.

1.2.4 Modulation of spinal reflexes by the supraspinal areas

Physical connectivity between afferent pathways and their interneuronal and motoneuronal targets provides merely a potential for a physiological influence. Many existing pathways simply do not have a physiological effect; they are dormant until summoned by descending tracts to meet a specific motor task requirement. Integration of proprioceptive input within the spinal cord involves summation, gating or modulation of its activity by descending tracts. This way supraspinal centers 'filter' and modulate sensory information that is to be conveyed to motoneurons (Riemann and Lephart 2002).

There are five mechanisms whereby supraspinal centers influence spinal reflexes; (i) direct input to α-motoneurons, (ii) excitation of segmental inhibitory interneurons, (iii) actions on afferent pathways that travel to other segmental levels (mostly heteronymous effect), (iv) input to γ-motoneurons thereby modulating receptor sensitivity, and (v) intersecting and modulating afferent feedback to segmental motoneurons (primarily homonymous effect). The supraspinal motor areas have different roles within the motor control hierarchy, described briefly below:

The motor cortex is responsible for planning, initiating, executing and controlling complex and discrete voluntary movements. It is divided into three distinct specialized areas, each of which projects directly and indirectly (via the brainstem) onto interneurons and motor neurons located in the spinal cord (Ghez 1991). The primary motor cortex is the origin point of neural efferent commands to muscles, which determines the amount of force generated and the direction of the movement. It receives substantial afferent input from several systems via different afferent pathways (Matthews 1997, Mihailoff and Hainses 1997). The premotor area, a second structure, also receives significant afferent input (Mihailoff and Hainses 1997). Its primary responsibilities are an organization, preparation, and possibly sensory guidance of movement. The third specialized structure, the supplementary motor area, has many proposed functions including the planning of sequences of movements, and the coordination between two sides of the body that involve groups of muscles (Ghez 1991, Mihailoff and Hainses 1997).

Phylogenetically speaking, the brainstem is a fairly primal structure (Matthews 1997), controlling more basic functions, such as postural equilibrium and automatic and stereotyped movements of the body (Matthews 1997, Mihailoff 1997). It is, however, under direct cortical control and acts as a relay station between the cortex and spinal cord. It is a site of significant integration of sensory information from vestibular, visual, and other somatosensory sources (Ghez 1991). The two main descending tracts, the medial and lateral tracts, project from the brainstem to the spinal cord where they regulate and modulate motoneuron activity, directly (Ghez 1991, Mihailoff 1997). The medial pathway influences the axial and proximal muscles, while the lateral pathway controls more distal limb muscles. Axons in this pathway make excitatory and inhibitory connections with the

interneurons and motoneurons involved with postural control, as disrupting the connection between the brainstem and spinal cord disrupts balance and response to perturbations (Deliagina, Orlovsky et al. 2006).

At the spinal cord level (Figure 1-11), corticospinal pathways affect distal muscle more strongly than proximal muscle (Brouwer and Ashby 1992, Lemon and Griffiths 2004). Conversely, reticular formation and the brainstem affect proximal muscles more than distal muscles (Hall and McCloskey 1983, Buford and Davidson 2004). Vestibulospinal tracts mediate postural adjustments and head movement by responding to the disturbances with counteracting muscle activation throughout the body (Kingma 2006). The lateral vestibulospinal tract engages antigravity muscles to compensate for tilts and body movements, whereas the medial vestibulospinal tract affects muscles bilaterally and mainly controls head position relative to the body.

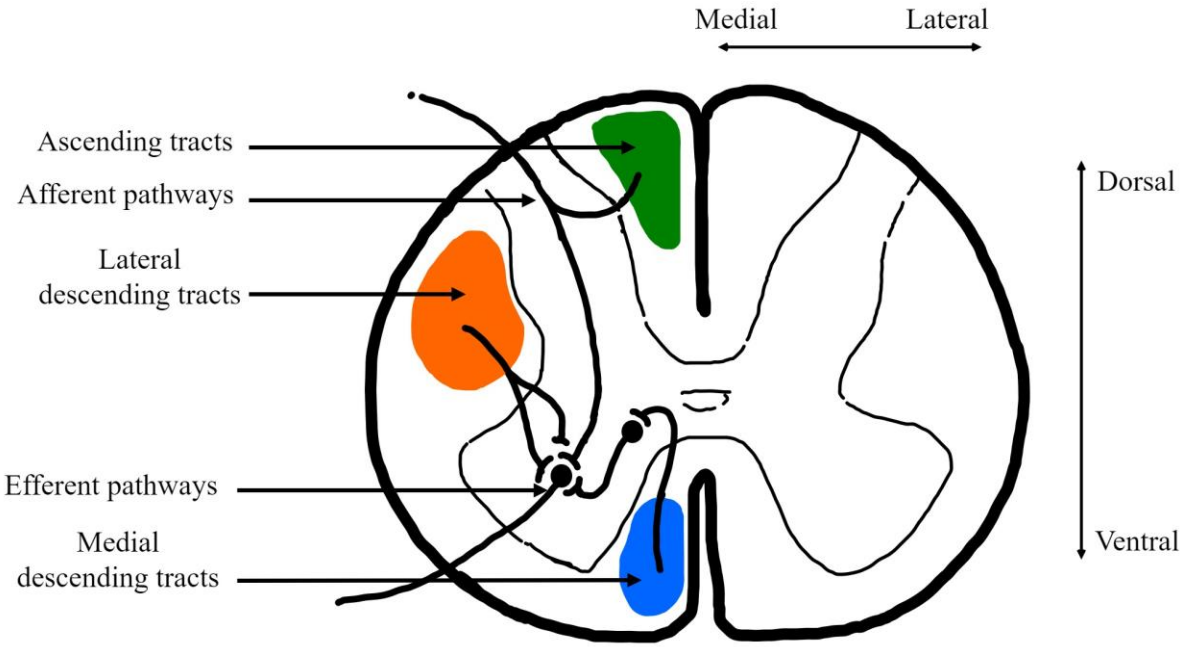

Figure 1-11: Cross-sectional view of a spinal cord showing the location of the local spinal cord circuitry and the location of the main descending and ascending tracts.

1.3 Impaired stability after spinal cord injury

A lesion in any of these tracts is accompanied by gait deficit. The magnitude of the deficit is contingent on i.) the location of the lesion, and ii.) the amount of damage. In a research setting, controlling the level and amount of damage with precise lesions to the spinal cord white matter enables us to determine functions of individual descending pathways, and elicit a specific and intended gait deficit.

There is consensus in the literature that cats, following immediate flaccid paresis after spinal cord injury (SCI), can regain the ability to stand (Macpherson and Fung 1999), and step (Grillner 1975, Barbeau and Rossignol 1987, Basso, Murray et al. 1994, Kuhtz-Buschbeck, Boczek-Funcke et al. 1996), and in some cases support weight during the quiet stance (Edgerton, Roy et al. 1991, De Leon, Hodgson et al. 1998, Macpherson and Fung 1999). Despite the locomotor recovery, the postural balance remains impaired (Lyalka, Orlovsky et al. 2009). The cats with spinal lesion often require external support at the tail to maintain mediolateral stability (Grillner and Rossignol 1978). However, although cats spinalized as adults have a poor balance control, kittens spinalized at a young age are reported to have a more complete recovery, including recovery of stability (Robinson and Goldberger 1986). The fact that lesions at a young age are not as detrimental as in older cats implies that the spinal cord might have the necessary circuits to compute appropriate responses to postural disturbances, or it can develop them. Furthermore, locomotion recovery implies that the spinal cord already has an internal model of limbs and body schema (Macpherson, Fung et al. 1997). It is entirely possible that the circuitry that is responsible for postural response is scattered across the caudal and rostral spinal segments, and that spared circuits might support balance control if adequately regulated.

Horizontal support surface perturbations have been traditionally used to evaluate postural stability (Macpherson 1988, Macpherson 1988). The findings from these studies were that, instead of directionally opposite restorative force responses, the exerted forces clustered into two diagonal XY populations toward and away from CoM (Macpherson 1988). Deemed the 'force constrain strategy,' this response involved directionally selective muscle activation (Macpherson 1988). However, the spinalized cat, although capable of producing tuned muscular responses to perturbations in some muscles, simply cannot develop appropriate force magnitude to indicate support of 'force constraint strategy.' It might be postulated that postural response requires coordination between limbs, but the same argument can be extended to stepping, which, as we have observed, recovers after spinalization. Injury to the ascending (sensory) tracts causes specific loss of sensory functions, most notable being a Brown-Séguard Syndrome, characterized by hypesthesia ipsilateral to the lesion side and contralateral analgesia (Taylor and Gleave 1957). The spinocerebellar tracts are rarely damaged in isolation, due to their lateral position, and result in an ipsilateral loss of muscle coordination. However, lesions to descending motor tracts often mask the loss of muscle co-ordination.

Disinhibition of spinal interneurons, following spinal lesions, has been proposed to underlie amplification of stretch reflex gain (Jankowska and Edgley 1993), and release of excitatory pathways (Aggelopoulos, Bawa et al. 1996, Aggelopoulos, Chakrabarty et al. 2008). Clinically, these circuit changes are observed as spasticity symptoms. Specifically, hyperactive stretch reflex, abnormal reciprocal inhibition, and hypertonia - hallmarks of spasticity - have all been labeled as significant contributors to gait deficit after injury of the spinal cord (Pepin, Norman et al. 2003). The length feedback abnormalities following

lateral lesion will be addressed in Chapter II. On the other hand, the effects of spinal lesions on force feedback have been neglected. Presuming that length and force feedback maintain limb stiffness and stability, it is inevitable that changes in length feedback would elicit force feedback changes, even if the force feedback is not modulated by descending tracts. However, force feedback has shown remarkable task-dependent modulation by supraspinal centers (Gottschall and Nichols 2007, Nichols, Gottschall et al. 2014), and preliminary study suggests that force feedback is affected by lateral lesion (Niazi 2015). The changes in force feedback organization are discussed in Chapter III. How length and force feedback integrate to control whole limb stiffness and contribute to instability after lateral hemisection is tackled in Chapter IV. Which descending tract(s) is responsible for regulation is more challenging to determine. The reticulospinal pathways have been shown to modulate both threshold (Feldman and Orlovsky 1972), and gain (Nichols and Steeves 1986) of stretch reflex and joint stiffness. The vestibulospinal tract carrying information from balance sensors might also be a potential candidate (Figure 1-11). These questions form the primary focus of Chapter V.

1.4 The purpose and specific aims

The purpose of this dissertation is to provide a more complete picture of proprioceptive pathways originating from many muscles crossing different joints in both spinally-intact, and lesion affected cats across three recovery-time points. Specifically:

I. In specific aim I, addressed in Chapter II, we evaluated changes in homonymous feedback, which is governed by length-dependent feedback, in spinally-

intact cats and cats with lateral hemisection across six knee, ankle, and toe extensors and flexors.

II. In specific aim II, addressed in Chapter III, we evaluated changes in heteronymous feedback, which arises from the interactions between muscles, across five knee and ankle extensors of spinally-intact cats and cats with lateral hemisection.

III. In specific aim III, addressed in Chapter IV, we integrated these two proprioceptive pathways in a simple geometric limb model, to estimate if unregulated force-dependent feedback contributes to postural imbalance after lateral hemisection.

IV. In specific aim IV, Chapter V, we have evaluated the effect of dorsal hemisection on force feedback and feedback arising from group III and IV afferents.

All data reported in this dissertation come from a decerebrate, non-locomoting, spinally-intact or selectively lesioned cat preparations. Classical literature illustrates that decerebrate cat can generate postural responses, such as rightening reflex (Magnus 1926), maintain posture (Mori 1987), exhibit attenuated 'force constrain strategy' (Honeycutt and Nichols 2014) and sustain locomotion (Whelan 1996). The decerebration procedure renders an animal comatose and insensate, removing the need for anesthetics to relieve the pain (and inhibit spinal excitability (Jinks, Martin et al. 2003)).

In Chapter VI, I briefly summarize the results and discuss them in the context of the nervous system and appropriate biomechanics.

CHAPTER 2. THE STRETCH REFLEX IS UPREGULATED IN THE MAIN KNEE AND ANKLE EXTENSORS IN CATS FOLLOWING LATERAL LESION OF THE SPINAL CORD

2.1 Introduction

The stretch reflex is the simplest and the fastest reflex arc in an animal (Pierrot-Deseiligny and Burke 2012). Despite its apparent simplicity, it is a significant contributor to all motor tasks. A stretch evokes feedback from many muscle mechanoreceptors. The Ia and II afferents originate from intrafusal muscle fibers responsible for monitoring length and rate of length change of neighboring extrafusal fibers. Liddell and Sherrington in 1924, were the first to describe the contribution of monosynaptic Ia response to static and dynamic components of a stretch within the stretch reflex. Each Ia afferent makes monosynaptic connections on all or nearly all of its homonymous motoneurons (Eccles, Eccles et al. 1957, Eccles and Lundberg 1957), onto some of its synergists (Eccles, Eccles et al. 1957, Nichols 1999) and rarely onto distant heteronemyous motoneuron pools (Edgley, Jankowska et al. 1986). The size of Ia contribution, measured as an amplitude of excitatory postsynaptic potential (EPSP), is more pronounced in homonymous than in heteronymous motoneurons (Mendell and Henneman 1968, Mendell and Henneman 1971), and largest in small/slow-twitch motor units (Eccles, Eccles et al. 1957). However, very rarely does afferent input directly synapse solely onto motoneurons. Instead, most of the afferents synapse onto interneurons throughout the grey matter of the spinal cord. Even in the case of monosynaptic stretch reflex, an incoming afferent bifurcates and relays afferent information to many other locations, such as interneurons, other motoneurons, or

supraspinal motor areas (Riemann and Lephart 2002). Those interneurons, in turn, bifurcate as well; excitatory interneurons bifurcate contralaterally, ipsilaterally or bilaterally, whereas inhibitory interneurons bifurcate ipsilaterally (Bannatyne, Liu et al. 2009). This forms a complex interneuronal network in the spinal cord where polysynaptic Ia circuits are very common. Superimposed onto this network is Ib afferent input from Golgi tendon organs (GTO). It was once believed that Ib pathway serves a protective role against the overloading of its homonymous muscle (Matthews 1933). This view has been challenged by Houk's finding that adequate stimulus for GTO is not a passive stretch, but rather an active contraction of the muscle fibers connected in series with GTO (Houk and Henneman 1967). Furthermore, Eccles' electrophysiological and Nichols' mechanographic studies have shown that GTO input onto homonymous muscle is negligible (Rymer and Hasan 1980), and instead, this feedback seems to converge mainly onto heteronomous motoneuron pools; in most cases onto those of muscles with different biomechanical actions (Eccles, Eccles et al. 1957, Bonasera and Nichols 1994, Wilmink and Nichols 2003, Lyle, Prilutsky et al. 2016). Another layer of complexity is group II afferents, the sensors for static muscle state. Although they make monosynaptic connections to motoneurons (Kirkwood and Sears 1975), to a lesser extent than Ia afferents, they more frequently form polysynaptic connections onto the interneuronal network (Cabaj, Stecina et al. 2006, Jankowska and Edgley 2010).

A stretch reflex increases the resistance of the muscle to stretch – is the most common definition found in the textbooks (Pierrot-Deseiligny and Burke 2012). Formerly, it was believed that the stretch reflex regulates a muscle length by compensating for changes in external load (Matthews 1972). However, evidence from decerebrate cat

strongly indicates that stretch reflex improves and augments non-linear intrinsic properties of the muscle, whereby keeping its stiffness constant (Nichols and Houk 1976).

The contribution of the short-latency stretch reflex (in conjunction with long latency pathways) to any motor task is undoubted. Its role during walking can be evaluated following self-reinnervation, which renders it permanently absent (Cope, Bonasera et al. 1994). Exaggerated ankle yielding during downslope walking following gastrocnemius self-reinnervation (Abelew, Miller et al. 2000, Maas, Prilutsky et al. 2007), and knee yield in all walking conditions following self-reinnervation of quadriceps (Mehta 2016) were the most pronounced walking deficits following recovery. Furthermore, studies in which the stretch reflex was absent or attenuated, such as studies involving experimental ischemia (Allum, Mauritz et al. 1982, Sinkjaer and Hayashi 1989), or vibration (Allum, Mauritz et al. 1982) have suggested that reflexes contribute about 30 – 50% of the net moment generated as a response to postural perturbations. The computational studies have yielded a similar conclusion (Zhang and Rymer 1997, Perreault, Crago et al. 2000). Thus, stretch reflex has been credited as a regulator of individual muscle stiffness, and, due to its focused and localized network, as a regulator of localized joint stiffness. Stiffer muscle appears to be beneficial for joint stability, as stiffer joint could potentially resist sudden perturbation more effectively or compensate for joint injury (McNair, Wood et al. 1992, Johansson and Sjolander 1993). However, different activities require a different level of compliance (Rapoport, Mizrahi et al. 2003); for example, walking may require more compliance of ankle joint than standing. Stretch reflex participates in both activities to a varying degree (Nashner 1976, Dietz, Mauritz et al. 1980).

The supraspinal centers via excitatory descending projections modulate this pathway in a task-specific manner. It has even been proposed that modulation of Ia afferents can be accomplished independently of the modulation of motoneuronal activity (Akazawa, Aldridge et al. 1982). This modulation of stretch reflex is achieved directly via monosynaptic excitatory connections to α-motoneurons (e.g., from the corticospinal or lateral vestibulospinal tracts), presynaptically onto afferent pathways, or indirectly by inhibiting or facilitating interneurons within spinal reflex pathways (Katz and Rymer 1989). Severing modulatory tracts inevitably disrupts this spinal circuit. Even following the recovery of stepping in the cats (Barbeau and Rossignol 1987, Basso, Murray et al. 1994, Kuhtz-Buschbeck, Boczek-Funcke et al. 1996), the gait deficit is persistent. Specifically, hyperactive stretch reflex, abnormal reciprocal inhibition, and hypertonia - hallmarks of spasticity - have all been labeled as significant contributors to the gait deficit in humans (Pepin, Norman et al. 2003).

Following removal of excitatory projections from the brain, disinhibition of spinal interneurons has been proposed to alter the gain of stretch reflex (Noga, Bras et al. 1992, Jankowska and Edgley 1993, Jankowska, Riddell et al. 1993). This is termed a ‘release phenomena,’ whereby unleashed and unfiltered proprioceptive afferents drive motoneuron activity. Particular tracts thought to be dominant regulators are reticulospinal pathways, as these pathways modulate both threshold (Feldman and Orlovsky 1972) and gain of stretch reflex (Kim and Partridge 1969, Nichols and Steeves 1986). Indeed, chronic spinal cats exhibited signs of clinical hyperreflexia and increased ventral root reflexes (Malmsten 1983). However, in medial gastrocnemius (MG) motoneurons, monosynaptic Ia excitatory postsynaptic potentials (EPSP) were either unchanged (Munson, Foehring et al. 1986) or

increased transiently (Nelson and Mendell 1979) in chronic spinal cats. Subsequent intracellular recordings in ankle extensor motoneurons of chronically spinalized cats showed that an amplitude of EPSP does not change in MG motoneurons, while amplification was observed in soleus, plantaris, and lateral gastrocnemius, the latter one significantly (Hochman and McCrea 1994). Following dorsolateral spinal injury, Taylor and Munson found stretch hyperreflexia in triceps surae muscles of awake cats (Taylor, Friedman et al. 1997). This increase in the gain of stretch reflex favoring one motoneuron species over the other is remarkable since spinalization removes modulation from the entire spinal region and all motoneurons. Considering that even the simplest movements involve activation of a large number of muscles, and engage their respective proprioceptive network, it is essential to evaluate stretch reflex changes in many muscles throughout a limb following spinal cord injury.

Using the mechanographic method, we evaluated stretch reflex arising from knee and ankle extensors, and ankle flexor in decerebrate spinally-intact cats and cats with lateral hemisection. Lateral hemisection has been traditionally used as an experimental method to elicit hyperreflexia (Hultborn and Malmsten 1983, Malmsten 1983). Although spinal lesions impair the normal physiological function of any circuit, it is still the best tool in elucidating what the default, unsuppressed stretch reflex circuitry entails. We observed a significant increase of the gain of stretch reflex in vastus and gastrocnemius muscle groups, but modest or no significant change in other extensor muscles. Lateral hemisection had no significant effect on the stiffness of ankle flexor. As primary knee and ankle anti-gravity muscles, the vastus and gastrocnemius muscles are essential for basic limb mechanics and posture, hence survival. Through evolutionary lenses, a substantial gain in stretch reflex

following an injury might be regarded as a compensatory mechanism for lack of descending drive, in an attempt to maintain the muscle tone of these most critical muscles.

2.2 Methods

2.2.1 Animals

The experiments were performed on ten purpose-bred female cats ranging from 3.3 - 4.1 kg and all data presented in this chapter were acquired during terminal experiments. Before the terminal experiment, cats received lateral hemisection at the University of Louisville and were allowed to recover for different time periods; 3 weeks (n = 2), 7 - 8 weeks (n = 3) and 12 - 13 weeks (n = 5). For comparison purposes only, data from 25 spinally-intact cats were opportunistically used to highlight any changes following the lateral spinal lesion. Data from a subset of these cats have been previously described (Lyle and Nichols 2018). All procedures in this study were completed by guidelines from the National Institute of Health and protocols approved by the Institutional Animal Care and Use Committee of Georgia Institute of Technology and the University of Louisville.

2.2.2 Survival surgery

Ten cats received the lateral T9-10 lesions at the University of Louisville. During the surgery, cats were initially anesthetized with isoflurane (5%) and oxygen mix in an induction chamber, then intubated and maintained on a mix of oxygen and isoflurane (1 - 4%) throughout the survival surgery. Blood pressure, EKG, heart rate, respiration rate, temperature, SpO_2 and expired CO_2 were monitored throughout the surgery to assure surgical depth of anesthesia. Laminectomies for lateral hemisections exposed spinal T9-10

segment. Next, following a dura split, dorsal columns and root entry zones were visualized to identify the midline. The intended area of the cord was cut with iridectomy scissors. The fibers adhering to dura were gently lifted with suction and cut. Dura was then sutured, durafilm and gelfoam placed on top and back of the dural sutures and closed in layers. The cats were allowed to recover for different periods before terminal experiments were performed at Georgia Tech.

2.2.3 Terminal experiments

In the terminal experiments, cats were anesthetized with isoflurane (5%) and oxygen gas mixture in an induction chamber. The tracheal intubation was performed, and isoflurane (2 - 4%) and oxygen mixture was used after that to maintain deep anesthesia. An IV was inserted into an external jugular vein for hydration and drug administration. Heart rate, EKG, respiratory rate, oxygen saturation, expired carbon dioxide, blood pressure, and core body temperature were monitored during all experiments. The core body temperature (37º C) was maintained by a heating pad or lamp. The head was rigidly fixed in a stereotaxic frame, the body was supported by a sling, and the hindlimbs were set with knee and ankle joint angles at approximately 110º and 90º, respectively. Hindlimb fixation was achieved using threaded rods inserted into the proximal (just distal to the greater trochanter) and distal femur (femoral condyle). The rods were connected by a bar and rigidly fixed to the stereotaxic frame. The proximal tibia was similarly stabilized by a separate threaded rod, while the distal tibia was secured with an ankle clamp.

The gastrocnemius (GAS), plantaris (PLANT), soleus (SOL), flexor hallicus longus (FHL), tibialis anterior (TA), and the vastus muscle group (VASTI) were dissected in both

hindlimbs. Muscles were released carefully from adjacent tissues and neighboring muscles to minimize mechanical coupling, while preserving their nerve and vascular supply. The PLANT tendons were separated from the GAS, released from its connection to the calcaneus, and cut distally near its insertion to the flexor digitorum brevis muscle. The GAS tendons were carefully separated from the SOL at their common insertion onto the calcaneus with small bone chips preserved. The tendons of FHL were cut proximal to the merger with the flexor digitorum longus tendon. The distal tendons of all muscles were attached to custom tendon clamps which were then connected to strain gauge myographs in series with the linear motors. The VASTI was carefully isolated by first releasing the sartorius muscle from its wide distal insertion, since the sartorius completely covers the quadriceps group. Then, blunt dissection was used to separate the VASTI from adjacent tissue along the medial and lateral femur, and the iliotibial band was transected proximally and distally around the patella. Additionally, blunt dissection was used to separate the vastus muscle group from the rectus femoris (RF). The RF was then transected using electrocautery mid-belly, to mitigate the need to stabilize the pelvis and eliminate RF action on it. The VASTI insertion was freed by cutting the patellar tendon. A small hole was drilled in the patella, through which a steel cable (0.9 mm diameter) was threaded. The other end of a cable was then connected to a tendon clamp in series with a myograph and linear motor via a pulley system.

A standard precollicular decerebration, which was completed in all cats (Silverman, Garnett et al. 2005), involved a vertical transection starting at the anterior margin of the superior colliculus. The brain matter rostral to the transection was removed. Following the decerebration, isoflurane anesthesia was titrated down over approximately 10 - 30 minutes

and then withdrawn. At the end of the experiment, heparin was injected in preparation for perfusion, and the animal was re-anesthetized using isoflurane. Euthanasia was accomplished by perfusing the animal through the heart, first with saline and then paraformaldehyde. Following euthanasia and perfusion, the hindlimb muscles were harvested.

2.2.4 Data acquisition

The details of a ramp-hold-release stretch protocol and the hardware and software used have been described previously in great detail (Nichols 1987, Lyle, Prilutsky et al. 2016). Briefly, the protocol involved 2-mm muscle stretches with a 50 ms ramp, 100 ms hold and 50 ms release (Figure 2-1) with a velocity of 0.04 m/s. This protocol involved stretching one muscle alone and in tandem with another muscle. Each trial had on average 20 – 40 stretch repetitions. Because the focus of this chapter was on examining homonymous feedback pathways, lone muscle stretches were used for this analysis. All lone repetitions of a muscle are averaged within a limb in an experiment. The muscle was held at constant background force of 2 - 3 N, to make it taut. The total force of the muscle is composed of background force (Figure 2-1: BGF) which was subtracted prior to the analysis (Ross and Nichols 2009, Lyle and Nichols 2018), and the force generated as the muscle resists a stretch, termed force response (FR). The force response is composed of mechanical (Figure 2-1, latency < 18 ms) and neural components. The neural component of the FR is a dependent variable.

2.2.5 Data analysis

All data were analyzed using custom-written MATLAB (2016b) programs.

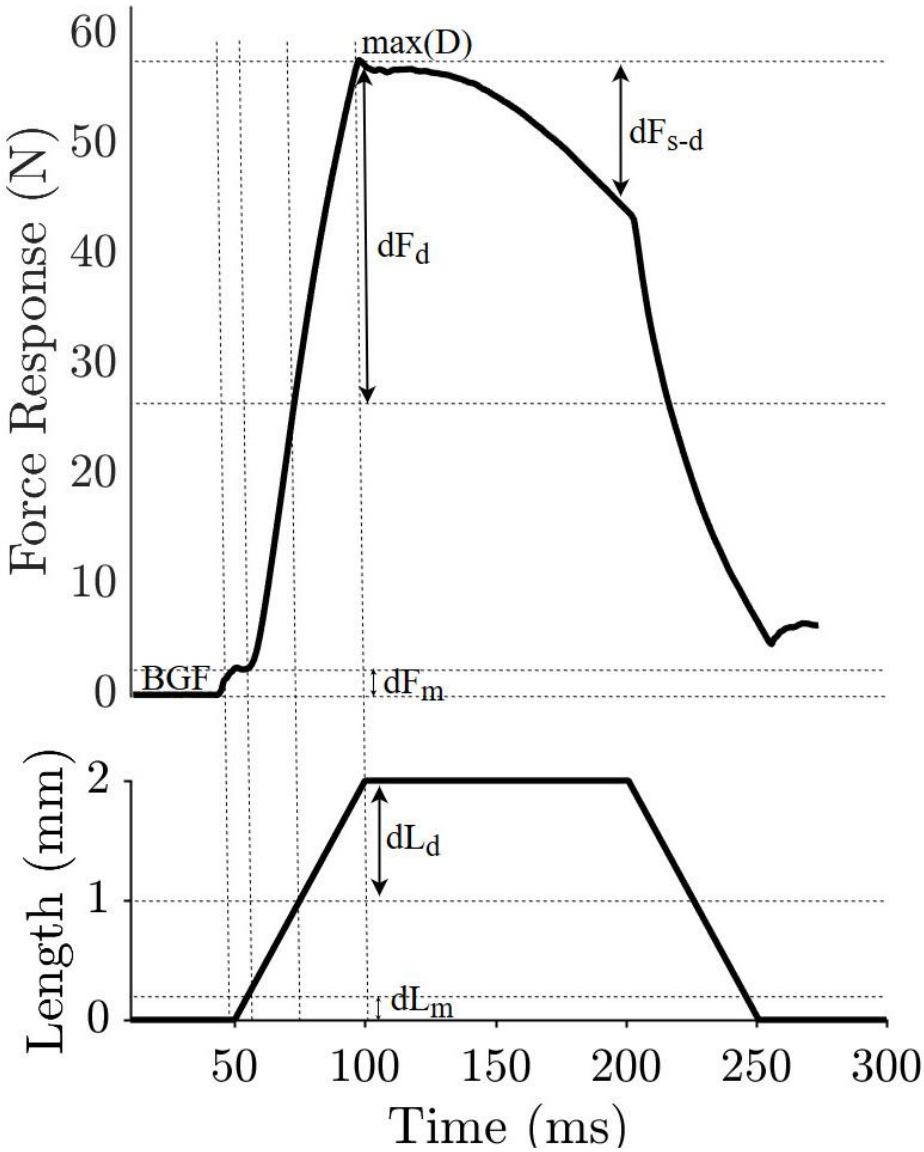

Figure 2-1: Force Response and its features. The force response (FR) is force generated by a muscle to resist a stretch. It can be characterized by (i) stiffness (*k*), which is change in force over change in length, (ii) peak of dynamic response *(max(D))*, (iii) dynamic index as difference between peak and steady state epoch (when the muscle is held isomerically during the last 50 ms of hold). Initial background force was subrtacted prior to the analysis. Early force response is characterized by mechanical response (F_m) for the first ~18 ms after the stretch onset. The time point when the slope drastically increases, as mechanical response becomes overwhelmingly neural response (F_d), is considered a reflex latency.

2.2.5.1 The features relevant to the force response

We chose five parameters to capture changes that may contribute to a muscle's force-generating capabilities; i.) muscle weights, ii.) impulse of force response, iii.) stiffness of force response, iv.) dynamic index of peak and static state, and v.) latency of divergence between mechanical and neural force response. The data points are obtained from each muscle of both limbs, which are treated independently. Relevant muscles from each experiment were harvested and weighed following euthanasia. All data are summarized in Table 2-1.

The impulse is simply an integral of force throughout ramp-hold-release duration:

$$I = \int FR \ (Ns) \qquad 2.1$$

The stiffness (k) is a slope of force rise during dynamic phase (change in muscle length during the last 25-ms of the ramp) (Figure 2-1).

$$k_d = \frac{dF_d}{dL_d} \ (N/mm) \qquad 2.2$$

This time cut-off was chosen to eliminate the influence of purely mechanical contribution to the stiffness. Stiffness was used as a proxy of gain of the stretch reflex. The stiffness of the mechanical force response component (k_m) is calculated in the same manner, as dF_m/dL_m, between 3 and 13 ms of stretch onset. Mechanical stiffness was not reported, but these values were used to estimate the first appearance of neural response (Figure 2-1), i.e., reflex latency.

The dynamic index is a normalized difference between the peak of force response (Figure 2-1: *max(D)*) at the end of the ramp, and an averaged static state, i.e., force response during the last 50 ms of hold (Figure 2-1):

$$D_{ind} = \frac{dF_{s-d}}{\max(D)} 100 \ (n.u.) \qquad 2.3$$

Physiologically, the dynamic index measures several components; (i) motoneuronal excitability due to persistent inward currents (PIC's), (ii) adaptation from muscle spindle response, (iii) recruitment (or derecruitment) of yet undefined interneuronal populations, and (iv) clasp-knife inhibition (that will be discussed in Chapter IV). Individual contribution of any of these is difficult to parse out, and in the context of this chapter, dynamic index is used to determine presence or absence of the clasp-knife inhibition following lateral hemisection.

The latency is operatively defined as the first detectable appearance of neural response. The time point where the slope of mechanical and neural force response diverge is taken as the first appearance of neural response. This divergence is determined as the increase in slope that supersedes an average and one standard deviation of the slope of a mechanical component. Most muscles had a distinct transition between mechanical and neural force response.

These features were evaluated in all muscles described in the Methods section, in both spinally-intact (CNT) and cats with lateral hemisection (LHS).

2.2.5.2 Statistical analysis

The lesion effect was estimated by comparing each of the above mentioned feature in CNT and LHS cats:

(i) If difference between ipsilateral and contralateral limb of LHS cats was not significant, according to the paired t-test, data from ipsilateral and contralateral limb are collapsed together.

(ii) Next, LHS (both ipsilateral and contralateral limbs across recovery time points) group is compared to CNT group using independent t-test. Levene's test for Equality of variances was used in determening the p-value. Should the sets have unequal variances, corrected p-value is reported. The significance was determined as $p \leq 0.05$.

The changes in these features in LHS cats across different recovery time points were of some interest, and these are evaluated using repeated measures analysis of variance test with bonferoni adjustments. The p-value is set to 0.05 for all statistical tests.

2.3 Results

We chose to evaluate five features of homonymous force response to best capture changes following lateral hemisection; i.) muscle weight, ii.) impulse response, iii.) stiffness, iv.) dynamic index, and v.) latency of response. The averages and standard deviations of these values throughout the three recovery time points (3, 7, and 12 weeks) from both ipsilateral and contralateral hindlimb, were reported in Table 2-1.

Subjectively evaluated, cats with lateral hemisection were clinically spastic, with significant clonus in vastus and gastrocnemius muscles (data not shown). They were all able to step (although accompanied by yielding at the weight-acceptance phase of a step) and stand. However, the response to perturbation was impaired. There was no significant difference in weight of CNT and LHS cats (3.80 ± 0.68 vs. 3.71 ± 0.34, respectively).

2.3.1 The comparison of weights and impulses of six muscles from spinally-intact and cats with lateral hemisection

As inadequate lower limb strength has been frequently attributed to crouched gait following incomplete spinal cord injury (Jayaraman, Thompson et al. 2013), we investigated force-generating capabilities of selected muscles in CNT and LHS animals, i.e., muscle weights and impulse.

The weight of VASTI was larger across all recovery time points following LHS compared to CNT group, although the gap was decreasing with time (Table 2-1: column 1, (i)). The GAS weights were smaller compared to CNT group, but despite that, its impulse was significantly larger across all recovery points compared to CNT group (Table 2-1:

column 2, (i, ii)). The weights of FHL, PLANT, SOL, and TA did not differ significantly, although extensors showed a negative, while TA more positive trend (Table 2-1: columns 3-6, (i)). Similar differential muscle atrophy following spinal cord injury has been reported previously in humans (Castro, Apple et al. 1999). Only PLANT did not exhibit an increase in impulse in extensor group, with VASTI and GAS exhibiting the most profound increase (Table 2-1: columns 1-5, (ii)), while the TA impulse was not affected (Table 2-1: column 6, (ii)). It seems that LHS impacts muscle weights negatively and impulse positively in extensors and has no effect on TA.

2.3.2 The stiffness of VASTI muscles increases significantly, although transiently following lateral hemisection

The VASTI muscles constitute the major knee extensor group. Therefore, following an injury, the inability to develop adequate anti-gravity force results in a knee joint yield. The self-reinnervation studies, mimicking a peripheral nerve injury, have shown that VASTI is heavily dependent on its length input, as its removal decreases VASTI force by 80% on average (Lyle, Prilutsky et al. 2016), and increases knee flexion during all walking slopes (Mehta 2016).

Conversely, immediately following lateral hemisection, the increased gain in length feedback of this muscle doubles on average, although transiently ($p < 0.05$ for 3 weeks post-LHS). The stiffness subsidies toward CNT values though recovery time-points and stabilizes at 23 - 24 N/mm after week 7 (Figure 2-2:[3] A & B; Table 2-1: column 1, (iii)).

[3] Please note that all subsequent data figures in this chapter follow the same convention. Specifically, in A are data from CNT group, while in B are data from LHS group (pooled together including both ipsilateral and contralateral limb across all recovery time points). To the right of these figures are maximal dynamic (max(D) or peak) distributions, while on the top are latency distributions (i.e., the time points of divergency

This change is accompanied by progressively increased adaptation during the hold phase, manifested as a flip in dynamic index sign compared to CNT group (Figure 2-2: C; Table 2-1: column 1, (iv), $p < 0.05$ for week 12). In spinally-intact cats, hold facilitates VASTI force output, as the difference between peak and static state (i.e., dynamic index) is positive. For the same peak amplitude, the static state of VASTI in LHS animals adapts to hold, as it fails to resist the hold. This can be quantified as a lateral, negative shift in peak-static state relationship (Figure 2-2: C & inserts). Despite showing substantial adaptation to stretch following lateral hemisection, the yield to hold in VASTI does not show signs of clasp-knife inhibition (described in detail in Chapter V).

Latency, estimated as the divergence between the slope of mechanical and neural response, decreased (although not significantly) and this effect was chronic and lesion side-dependent (Table 2-1: column 1, (v)).

---

between mechanical and neural stiffness of force response. The dynamic index is presented in C, as peak vs steady state plot. Least square regression lines are fit through CNT (black), and LHS (blue) data. LHS data are further divided by color; red triangles are data from contralateral, while blue triangles are from ipsilateral limb.

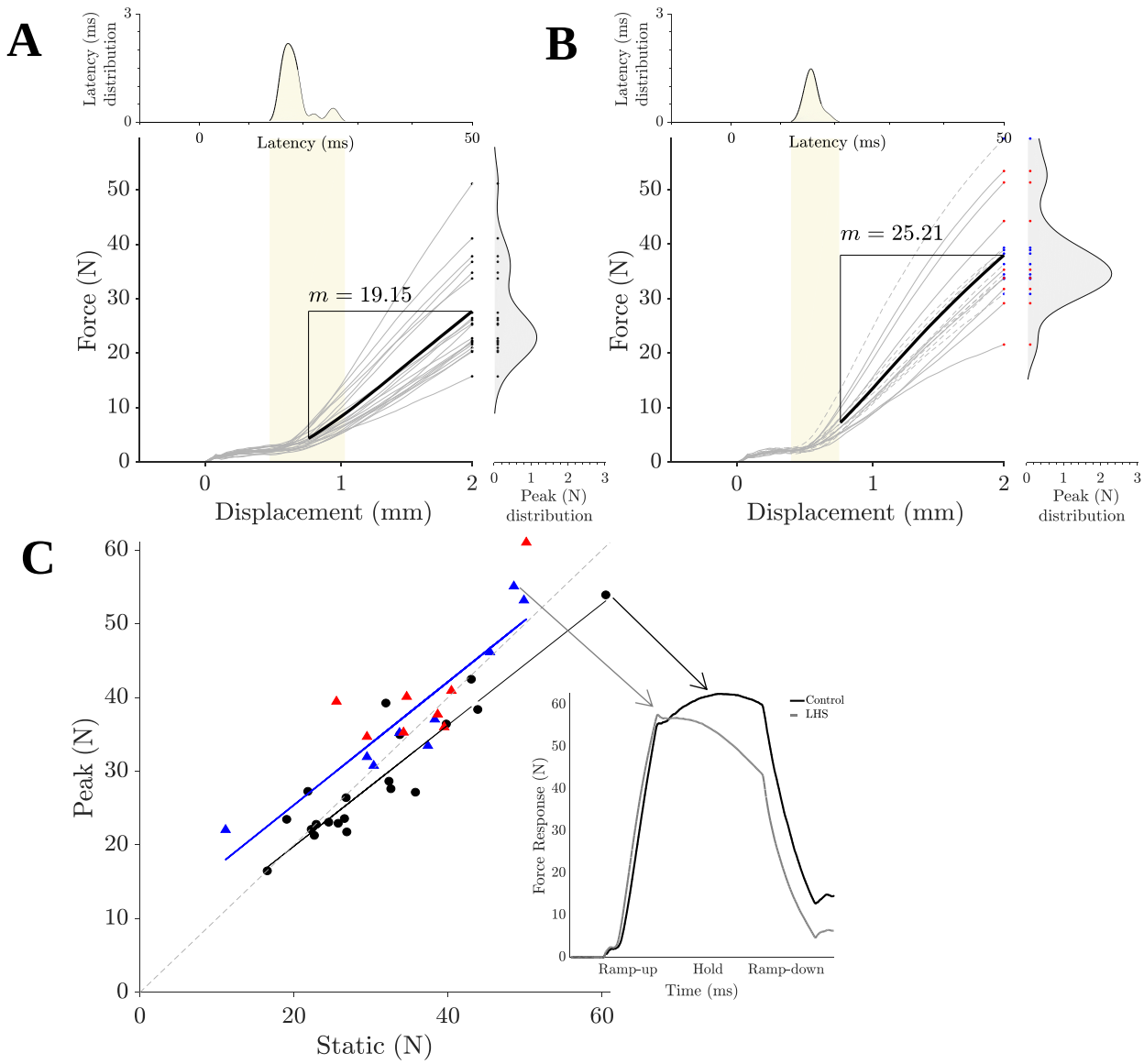

Figure 2-2: VASTI. The stiffness of VASTI in CNT (*A*), and LHS (*B*) group. In these, and subsequent figures, all data are pooled together (for LHS group that includes data from all recovery time-periods). The most pronounced changes in LHS (*B*) are an increase in slope, increase in peak, i.e., maximal dynamic response (distribution on the right side of A & B figures) and decrease in latency (distribution on the top of the A & B figures) in LHS group compared to CNT (*A*). The *C* represents dynamic index with static (steady state) and peak (maximal dynamic) on x and y axes, respectively. Identity (grey broken) line represents the border between adaptation and facilitation. The black circles are data from CNT group, while triangles are from LHS groups. Blue triangles are data from limb ipsilateral to the side of a lesion, while red triangles are from contralateral limb. Shift between linear fits (the black line is CNT fit and the blue line is LHS fit), suggests a change in sign of dynamic index as CNT force responses exhibit facilitation (positive dynamic index), whereas LHS force response adapt to the hold (negative dynamic index). Inserts are force responses belonging to CNT (black) and LHS (grey) cats to demonstrate facilitation (in CNT) and adaptation (in LHS). Note: All subsequent figures in this chapter follow the same convention.

2.3.3 The stiffness of GAS muscle increases following the lateral hemisection

As a biarticular muscle, GAS extends the ankle and flexes the knee. Self-reinnervation studies point to its role during the downslope walking, as removal of length-feedback causes excessing yield in the ankle joint (Maas, Prilutsky et al. 2007). Following the lateral hemisection, a gain of its length input more than doubles immediately after the lesion (Figure 2-3: A & B; Table 2-1: column 2, (iii), $p < 0.05$), depresses to almost control values in week 7, just to increase again in week 12 ($p < 0.05$). This increase, decrease and increase of feedback gain might represent cats' specific response in week seven, or plastic changes in the spinal cord, as it reorganizes its circuits.

Unlike the VASTI, the rest of the extensors in this study exhibited substantial adaptations to hold (negative dynamic index) even in CNT cats. Immediately after the injury, there was less adaptation to hold in GAS, meaning that the dynamic index was less negative compared to the CNT group (Figure 2-3: C). However, by the week 12 post-LHS it reached the CNT values (Figure 2-3: C; Table 2-1: column 2, (iv)).

Latency does not change significantly following lateral hemisection or throughout the recovery time-periods in either limb (Table 2-1: column 2, (v)).

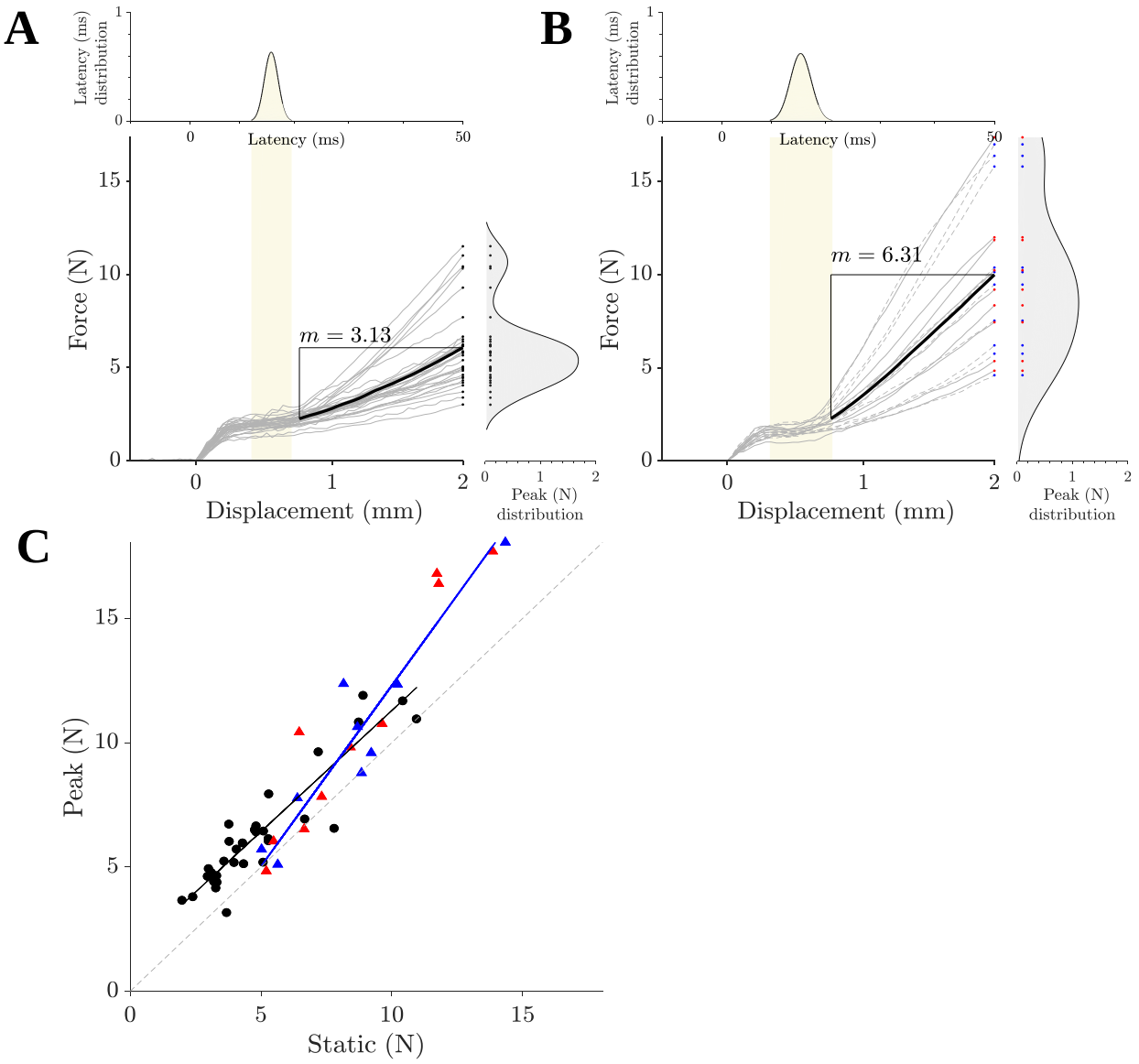

Figure 2-3: GAS. The data show an increase in gain of slope rise, peak, and no change in latency (*A* & *B*, and corresponding distributions). In *C* it shows that adaptation is evident in both CNT and LHS groups. This adaptation might be dependent on a peak of force response, as the slope of LHS fit is larger than the slope of identity line. Legend details are described in Figure 2-2.

2.3.4 The stiffness of PLANT shows little or no change following lateral hemisection

The stiffness of PLANT, a muscle with diverse action across three joints, does not show a significant change following the injury. Its length feedback maintains its stiffness at 3 - 4 N/mm in both spinally-intact and LHS cats throughout the recovery time-points (Figure 2-4: A & B; Table 2-1: column 3, (iii)). Dynamic index, on the other hand, increases significantly (Table 2-1: column 3, (iv), $p < 0.05$) immediately after the injury, although it shows a negative trend by decreasing toward the CNT values in week 12. There are notable bilateral differences (Figure 2-4, Table 2-1: column 3, (iv)). Latency increased, but not significantly early after the injury in ipsilateral limb, but throughout the recovery course, it decreases to CNT values (Table 2-1: column 3, (v)).

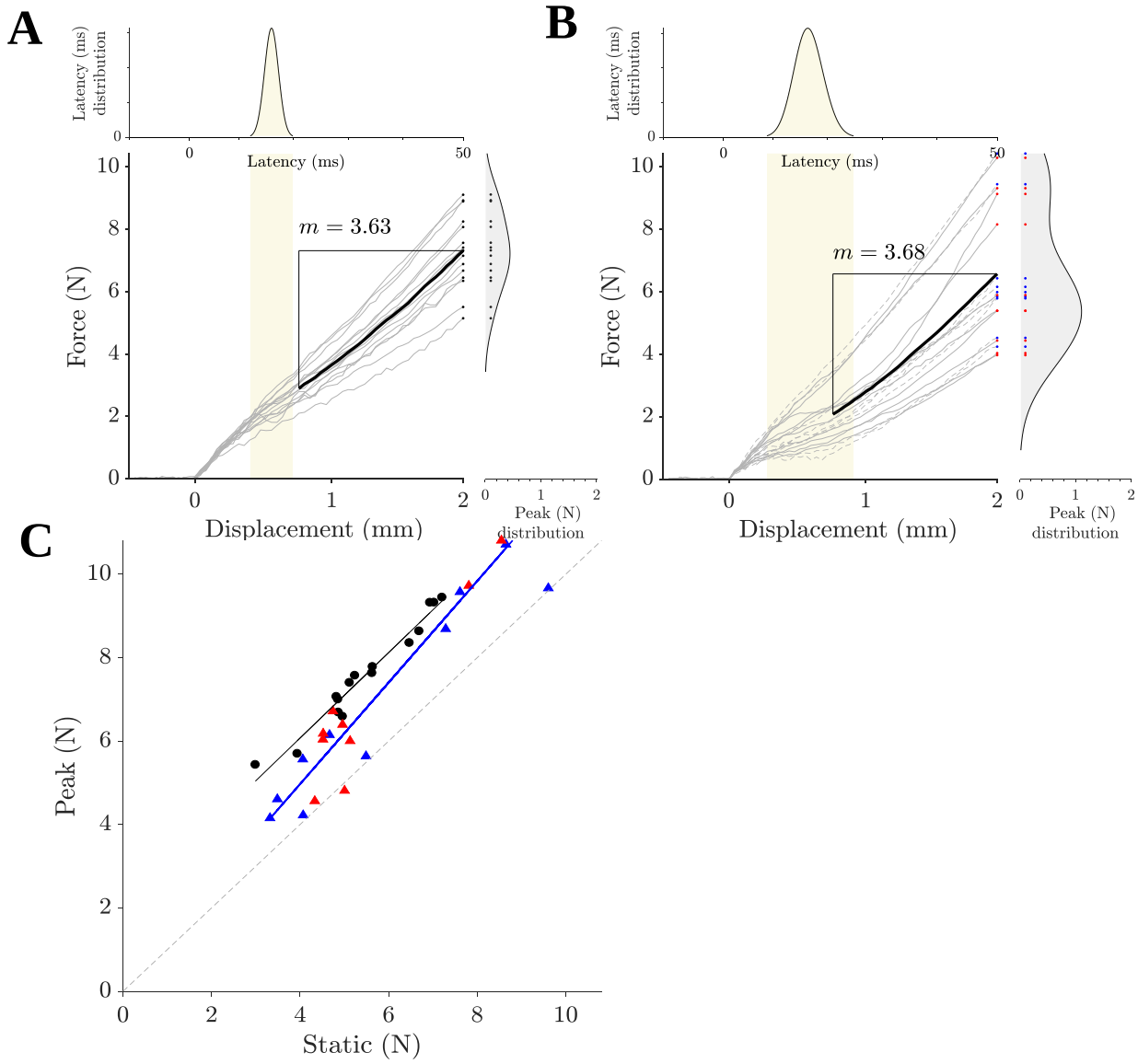

Figure 2-4: PLANT. Subtle and physiologically negligible differences between CNT (*A*) and LHS (*B*) groups, thoroughly explained in text. Notable is the slope of LHS fit (*C*), as it shows larger adaptations at high peak forces for LHS group. Legend details are described in Figure 2-2.

2.3.5 The stiffness of SOL does not significantly change following lateral hemisection

The SOL is a simple, uniform muscle, that has the third largest maximal extensor moment at the ankle joint. The SOL stiffness shows a positive, but not significant trend immediately after the injury (Figure 2-5: A & B; Table 2-1: column 4, (iii)). The substantial adaptations to hold were observed in both spinally-intact cats and following LHS, and there were not significantly different (Figure 2-5: C; Table 2-1: column 4, (iv)).

Latency estimate for this muscle is unreliable, as it did not have a clear transition from mechanical to neural response, as other extensors did. However, estimated latency values were reported in Table 2-1: column 4, (v).

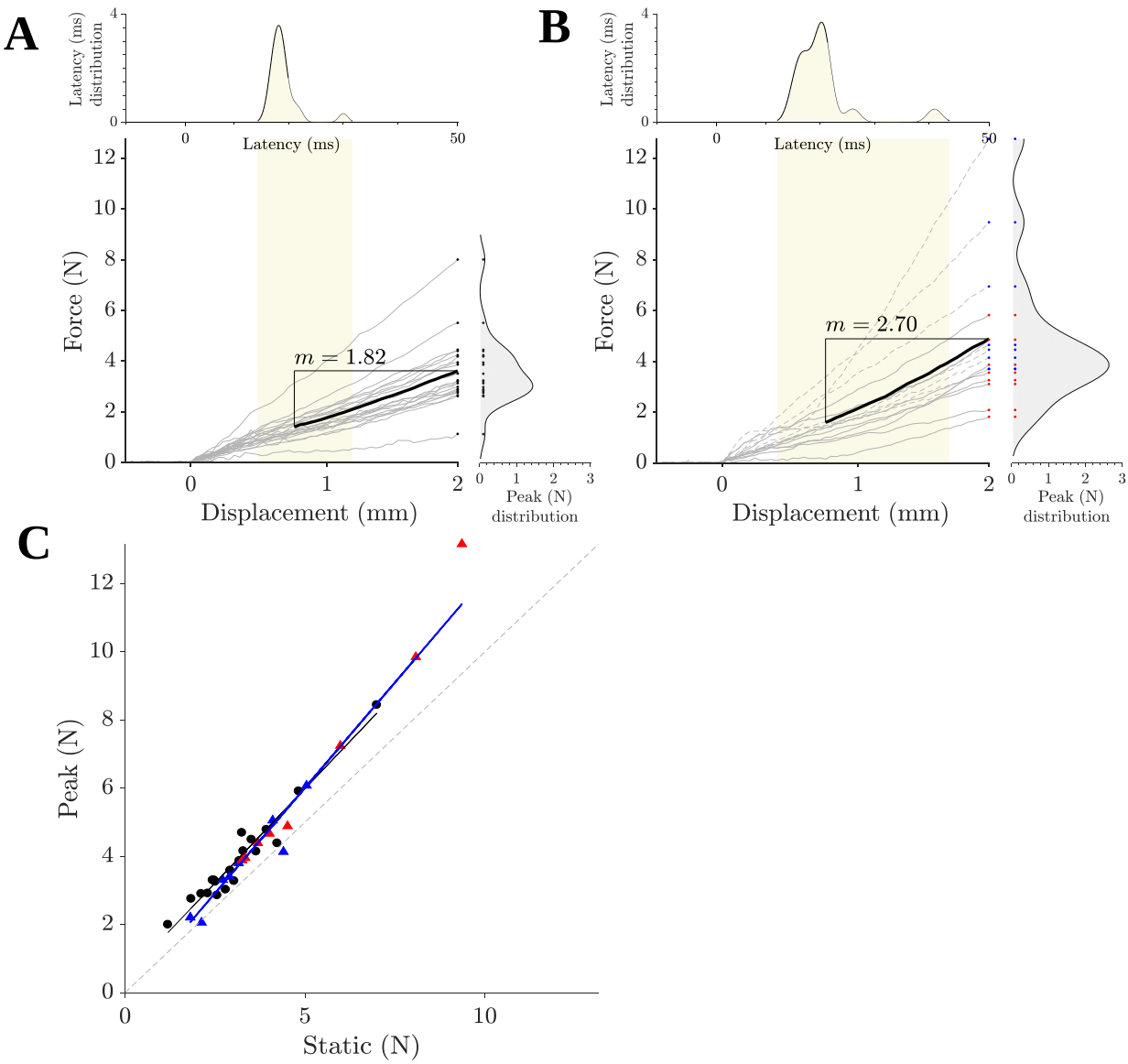

Figure 2-5: SOL. Subtle slope increase is evident in LHS (*B*), compared to CNT (*A*) group, and details are explained in the text. The slopes of CNT (black line) and LHS (blue line) group fits in the *C* panel are virtually indistinguishable, as these two groups do not exhibit any differences in the dynamic index. Legend details are described in Figure 2-2.

2.3.6 The FHL is the least affected muscle by the lesion in this study

The FHL is the most distal ankle extensor (and toe flexor) that we evaluated in this study. Following lateral hemisection, there is very little net change in stiffness of this muscle compared to the CNT group (Figure 2-6: A & B, Table 2-1: column 5, (iii)). Recovery course follows that of other muscles, where after an initial increase, it subsides, just to increase again at the last tested recovery-point (Figure 2-6: A & B; Table 2-1: column 5, (iii)). Again, this observation might be cats-specific responses and not have underlying physiological mechanism attributed to the recovery. Change in the dynamic index is neither physiologically nor statistically different from CNT values (Figure 2-6: C; Table 2-1: column 5, (iv)). Same holds true for the latency of its reflex (Table 2-1: column 5, (v)).

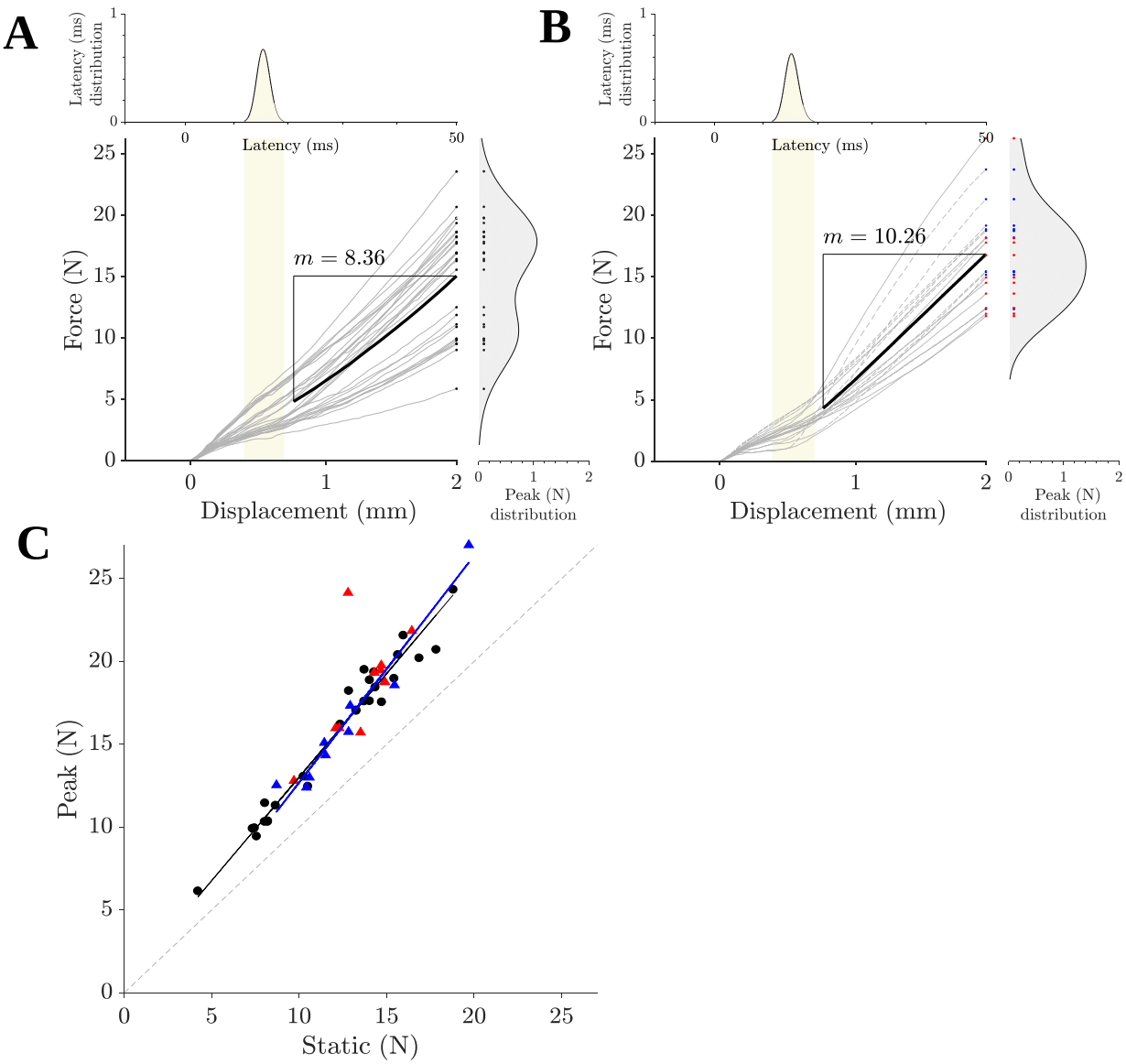

Figure 2-6: FHL. This muscle was least affected by lateral hemisection, as force response parameters showed very subtle and physiologically irrelevant changes. In *A* and *B* figures are CNT and LHS force response parameters supporting that claim. In *C*, slopes of CNT (black line) and LHS (blue line) fits are virtually identical. Legend details are described in Figure 2-2.

2.3.7 The effect of lateral hemisection on TA was not significant, although it shows the opposite trend from those observed in extensor muscles

The TA muscle is the only flexor muscle evaluated in this study. Lateral hemisection had no significant impact on this muscle. Although the gain of its stretch reflex decreased and varied across post-LSH time-periods, these changes are subtle and not significant (Figure 2-7: A & B; Table 2-1: column 6, (iii)). Its dynamic index was more negative compared to CNT group, meaning that adaptations became more pronounced after the injury and through recovery time points (Figure 2-7: C; Table 2-1: column 6, (iv), $p < 0.05$). The latency of the length feedback increased, peaking at week seven, and subsiding in week 12 (Figure 2-7: A & B distributions at the top of the figure; Table 2-1: column 6, (v)). However, very few TA responses were recorded in the CNT group, thus making statistical comparison unavailing.

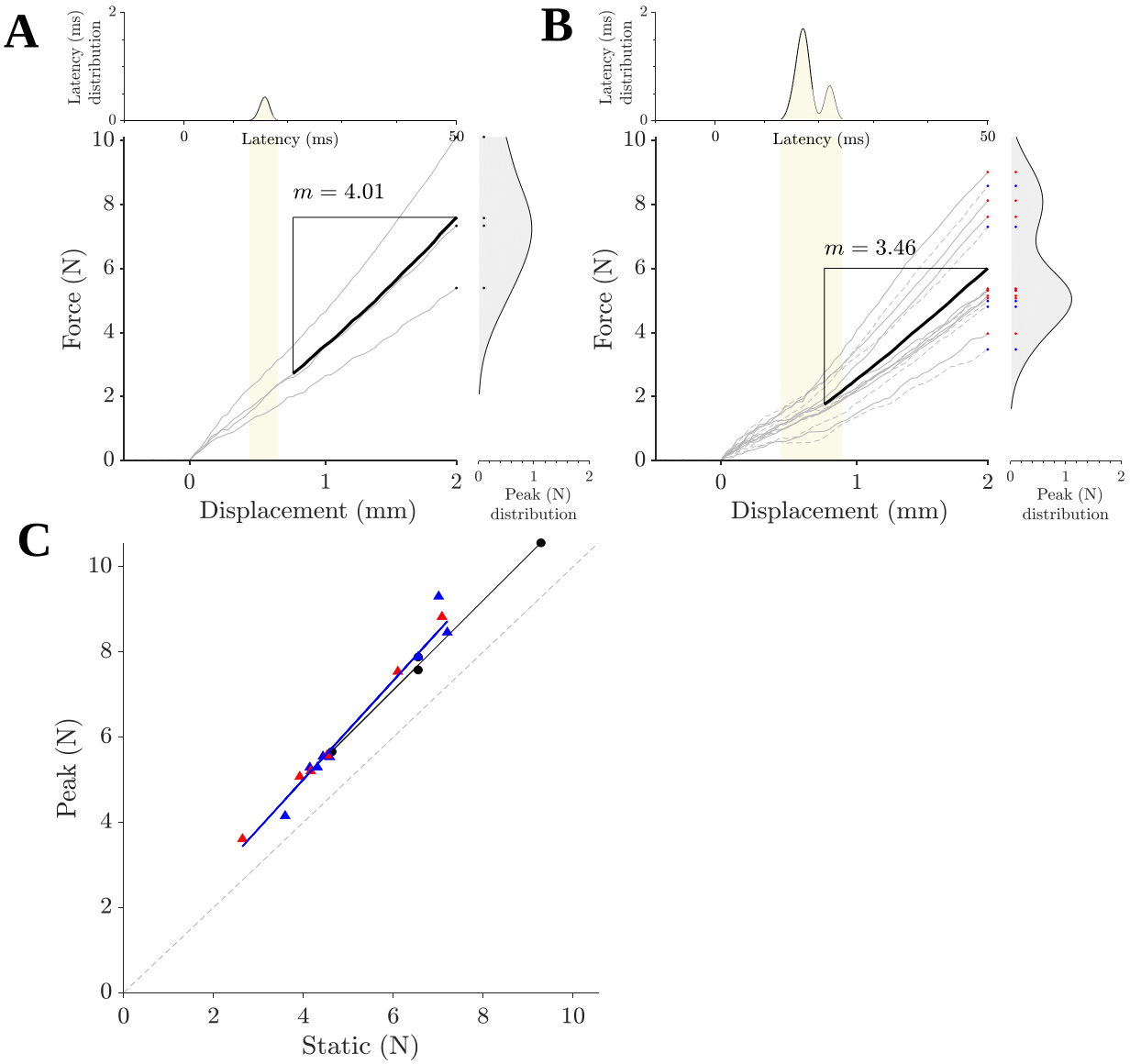

Figure 2-7: TA. The lateral lesion had no statistically significant effect on TA muscle, however the trend was opposite to that it had on extensor muscles. The TA slope of force response, i.e., its stiffness, and peak decreased, while latency increased (*A* & *B*, upper distributions), although physiologically not significant. In *C*, although CNT and LHS fits are identical, the LHS group was shifted forward as it had smaller peak. Legend details are described in Figure 2-2.

2.4 Discussion

Crouched gait that accompanies locomotor recovery following incomplete spinal cord injury is often attributed to low limb strength (Jayaraman, Thompson et al. 2013). In this chapter, we investigated the force-generating capabilities of selected muscles in cats following lateral hemisection. The primary finding is that the stretch evoked stiffness of VASTI and GAS muscle groups is increased significantly, while there seems to be little net change in stiffness for PLANT, SOL, FHL, and TA, although positive trends were observed for extensors, and negative for TA. There is a little doubt that a number of factors could potentially contribute to these results.

The muscle atrophy following inactivity due to spinal cord injury is very well documented (Beattie, Farooqui et al. 2000, Thomas and Zijdewind 2006). Changes in intrinsic muscle properties have been implicated in spastic hypertonia (Dietz and Berger 1983), as some studies reported that an increase in EMG activity did not accompany high tension in the muscles. However, this “intrinsic muscle hypothesis” does not account for many well-established observations such as enhanced monosynaptic Ia EPSP (Hochman and McCrea 1994), and is not considered a leading contributor to spasticity by some (Katz and Rymer 1989). Nonetheless, recent studies report that increase in both intrinsic and reflex components contribute to increased overall joint stiffness, but the primary mechanical abnormality arose from increased reflex activity (Mirbagheri, Barbeau et al. 2001). Unfortunately, one of the limitations of results presented in this chapter is the inability to unequivocally distinguish mechanical and neural contribution to the force output. It remains unknown to what extent intrinsic properties of these muscles change following lateral hemisection and contribute to overall stiffness.

The evidence for motoneuronal hyperexcitability in spastic muscles is substantial (Matthews 1966), as small afferent input is sufficient (Wierzbicka, Wiegner et al. 1991, Wiegner, Wierzbicka et al. 1993) to activate overly depolarized motoneuron pools following an injury (Murray, Nakae et al. 2010). However, persistent inward currents in motoneurons recover, (Johnson, Kajtaz et al. 2013), just as intrinsic resistance and electrotonic length, although membrane time constant is diminished (Hochman and McCrea 1994). This implies that changes in motoneuron properties are unable to account for the increase in EPSP amplitude noted in chronic spinal cats (Hochman and McCrea 1994). However, we were not able to determine the excitability of motoneuronal pool of muscles tested in this study.

The exaggerated response to stretch might arise either from an increase in i.) γ-motoneuron bias, or ii.) gain in the afferent input. Gamma spasticity has once been considered to contribute to spasticity. However, numerous studies have failed to show excessive fusimotor activity in spastic muscles (Burke, Gillies et al. 1970, Hagbarth, Wallin et al. 1973, Hagbarth 1979). This leaves a gain in stretch reflex as a primary contributor to the spasticity. Two types of plastic changes might be occurring after spinal cord injury that may result in gain in stretch reflex; i.) amplification of the afferent signal, or ii.) disinhibition of the afferent signal (or both).

The anatomical changes, such as afferent sprouting, or physiological changes, such as increase of neurotransmitter release, might underlie amplification of the afferent signal. Afferent fibers might undergo sprouting of their terminal branches to compensate for the loss of descending synapses (McCouch, Austin et al. 1958, Helgren and Goldberger 1993). Although signal amplification through afferent sprouting has been observed in the spinal

cord (Bishop 1977), it has not been regarded as an essential process in reorganization following injury by some (Rodin, Sampogna et al. 1983). However, primary afferent fibers have been reported to sprout, providing new input to partially denervated spinal interneurons, but not motoneurons directly (Krenz and Weaver 1998). Nonetheless, this still may cause hyperreflexia by increasing inputs to interneurons. This anatomical reorganizational process might take a longer time to develop. However, we have observed an increase in stretch reflex as early as three weeks post-injury, which might implicate faster physiological processes. Immediately following spinal cord injury, the motoneurons are unresponsive, muscles are flaccid, and limbs are immobile. As a consequence, the proprioceptive network is rarely engaged. Inactivity-induced monosynaptic and heteronymous EPSP increase, although counterintuitive (Hebb 1949), have been reported (Webb and Cope 1992, Mendelsohn, Simon et al. 2015) and might be behind observed increases in stretch reflex gain. It is possible that both of these mechanisms, sprouting and EPSP amplification, are concurrently happening in the spinal cord and contributing to spasticity to a varying extent, as they are both consequences of the removal of excitatory supraspinal input. Finally, an increased gain of stretch reflex could arise from a decrease in baseline presynaptic inhibition of afferent information due to injury to descending tracts.

Regardless of the mechanism, it is evident that severing supraspinal tracts in the lateral column results in a significant increase in gain of stretch reflex only in VASTI and GAS muscles. The selective increase in stretch reflex in ankle extensor muscles has been reported previously. Intracellular recordings of four motoneuron pools revealed a significant rise in an Ia EPSP amplitude in lateral gastrocnemius only, but not in medial gastrocnemius, soleus or plantaris (although all of them showed a positive trend) in cats 6

weeks after L1-L2 transection (Hochman and McCrea 1994). This is consistent with our results, as we observed a significant increase in GAS, and subtle, although insignificant increase in PLANT and SOL muscles, at the corresponding recovery time-point (Table 2-1: columns 2-4, (iii)).

Which muscles undergo these changes, might be contingent on their dependence on the stretch reflex during the activities. As mentioned in the results section, following self-reinnervation and motor recovery, the VASTI and GAS force outputs are significantly decreased, and kinematic consequences are a profound yield of knee and ankle, respectfully. On the other hand, the reinnervation of FHL did not have any apparent walking deficit (Lyle, Kajtaz et al. 2016). In the days following the injury, removal of excitatory command from supraspinal structures renders motoneurons unresponsive. Cats' hindlimbs require larger anti-gravity muscle forces to maintain the relative extension against the flexing forces due to gravity. It is not unreasonable to propose that stretch reflex, as an adaptive evolutionary mechanism, now unregulated, attempts to maintain an extended limb by increasing gain to main extensor muscles, and not changing or attenuating it to flexor muscles, suggesting that spasticity is an adaptive mechanism.

2.4.1 Potential biomechanical consequences of unregulated length feedback

The question arises how these changes affect the stiffness of the whole limb. Unregulated and exuberant length feedback makes some muscles stiffer, while not affecting others, thus affecting one joint preferentially over the other. This inevitably has consequences during locomotion, as moments in specific direction increase, while decreasing in different directions.

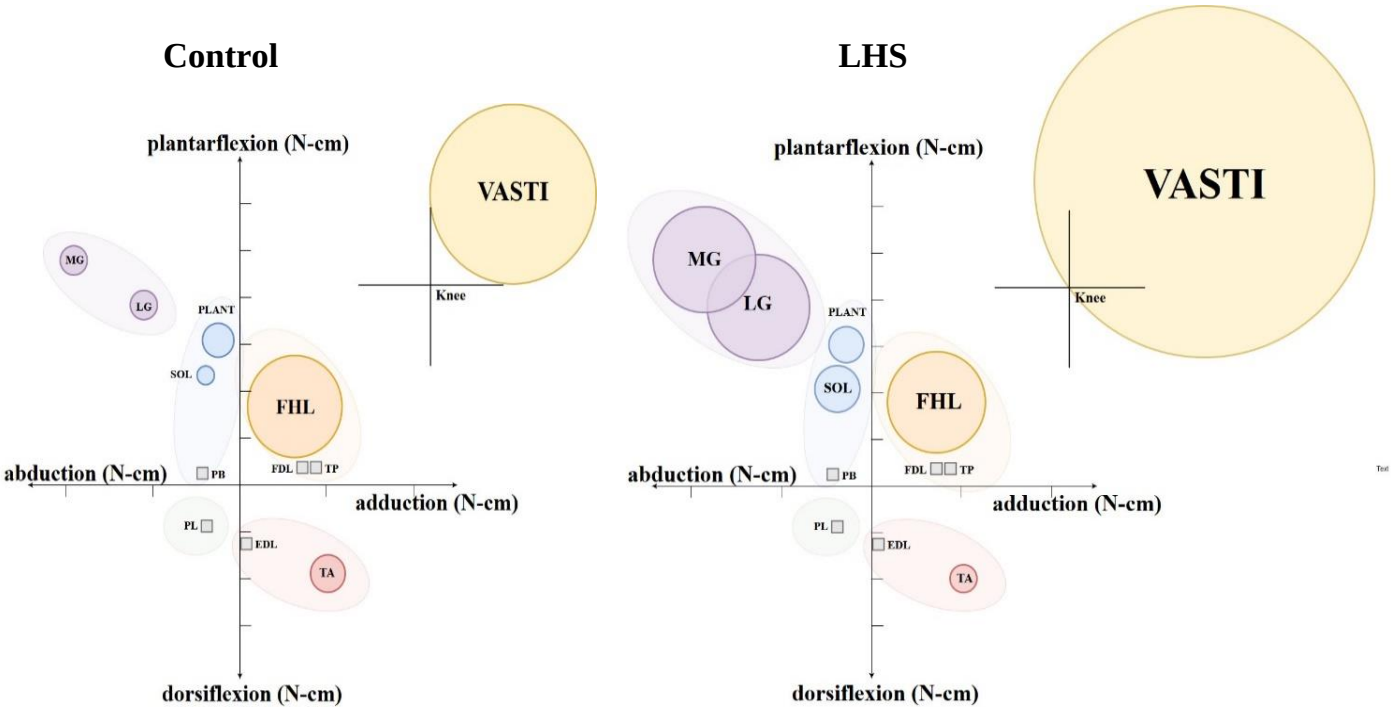

Figure 2-8: Potential moment changes following lateral hemisection. The moments that each muscle can develop are plotted in the sagittal (y-axis) and frontal planes (x-axis). Visual comparison of the stiffness of muscles from averaged CNT (*left*) responses to stiffness of muscles of an LHS cat from 3-wks recovery group (*right*) was accomplished by normalizing the diameter of circles to that of VASTI from LHS group (the largest stiffness). The LHS cat's ankle is, potentially, excessively abducted and extended, as GAS stiffness is significantly larger than in CNT. The stiffness of LHS VASTI is also increased, and this can be manifested as overly extended and stiff knee joint.

In a typical control cat (Figure 2-8: left), an ankle abduction and adduction are nicely balanced by stiffnesses of GAS, PLANT and SOL (on abduction side), and FHL,

and TA (on adduction side). The TA and gravity play a flexor role, which is balanced by ankle extensor activity (by GAS, PLANT, SOL, FHL in decreasing order of their stance moment arms (Burkholder and Nichols 2004)). Following an injury, this balance is disrupted. In the frontal plane, increased stiffness of GAS is not opposed by FHL (unchanged), or TA (unchanged, but decreasing trend). In the sagittal plane, an increase in GAS stiffness is not balanced by an equal TA gain. In behaving cat with lateral hemisection, this should be manifested as excessively extended and abducted ankle (Figure 2-8: right). Increase in VASTI slope and decrease in its dynamic index would translate into more, unsustainably extended knee.

There is a substantial recovery of locomotor function following lateral hemisection in cats and gain in stretch reflex might be a positive contributor to that recovery by maintaining muscle tone and driving activity of motoneurons. However, following the injury, there is a significant deficit in walking cats (Barbeau and Rossignol 1987, Rossignol, Drew et al. 1999). Specifically, their gait is accompanied by more flexed limb and difficulty at the weight-acceptance phase of the step cycle. Findings reported in this chapter could not explain those deficits. On the contrary, these data suggest overly extended and stiff ankle and knee joints. This necessitates the existence of one or more (inhibitory) proprioceptive inputs with distinct circuits in the spinal cord, that also undergo changes following injury. The best candidate is force-dependent feedback from Golgi tendon organs in muscles (described in detail in Chapter III), which has been shown to be inhibitory (Eccles, Eccles et al. 1957) and widely distributed (Bonasera and Nichols 1994, Wilmink and Nichols 2003, Lyle and Nichols 2018). These two circuits, localized length, and distributed force pathways engage in a tug-of-war over motoneurons in a complex and

dynamic manner, whereby determining overall limb mechanics in spinally-intact cats and, to a greater extent, following an injury. We investigated force-feedback changes following the injury in the next chapter.

Table 2-1: Summary of relevant features; (i) weight (g), (ii) impulse (Ns), (iii) stiffness (N/mm), (iv) dynamic index (n.u.), and (v) reflex latency (ms).

			VASTI	GAS	PLANT	SOL	FHL	TA
CNT			(i) 37.31 ± 9.0, *(10)* (ii) 33.93 ± 10.96, *(20)* (iii) 19.15 ± 6.23, *(20)* (iv) 5.40 ± 13.18, *(20)* (v) 18.5 ± 2.8, *(20)*	(i) 27.91 ± 4.08, *(10)* (ii) 5.56 ± 2.92, *(32)* (iii) 3.13 ± 1.67, *(32)* (iv) -22.06 ± 15.15, *(32)* (v) 15.84 ± 0.68, *(32)*	(i) 8.50 ± 1.20, *(7)* (ii) 5.61 ± 1.76, *(15)* (iii) 3.63 ± 0.65, *(15)* (iv) -28.36 ± 5.42, *(15)* (v) 16.00 ± 0.38, *(15)*	(i) 4.43 ± 0.26, *(7)* (ii) 3.5 ± 2.03, *(20)* (iii) 1.82 ± 0.68, *(20)* (iv) -20.21 ± 8.93, *(20)* (v) 19.00 ± 2.96, *(20)*	(i) 6.42 ± 0.80, *(7)* (ii) 12.38 ± 4.11, *(28)* (iii) 8.38 ± 2.6, *(28)* (iv) -22.81 ± 4.31, *(28)* (v) 15.43 ± 0.6, *(28)*	(i) 6.96 ± 1.69, *(2)* (ii) 8.89 ± 1.45, *(4)* (iii) 4.01 ± 0.91, *(4)* (iv) -14.97 ± 2.40, *(4)* (v) 15.75 ± 0.5, *(4)*
SHT	3	I	(i) 39.52 ± 1.15, *(2)* (ii) 60.67 ± 16.35, *(2)* (iii) 30.68 ± 7.03, *(2)* (iv) -4.00 ± 13.8, *(2)* (v) 16.00 ± 0.00, *(2)*	(i) 23.31 ± 2.01, *(2)* (ii) 14.57 ± 6.47, *(2)* (iii) 7.56 ± 3.92, *(2)* (iv) -9.89 ± 11.83, *(2)* (v) 15.5 ± 0.70, *(2)*	(i) 7.10 ± 1.35, *(2)* (ii) 6.48 ± 0.81, *(2)* (iii) 3.46 ± 0.43, *(2)* (iv) -12.72 ± 16.71, *(2)* (v) 17.5 ± 2.12, *(2)*	(i) 3.80 ± 0.2, *(2)* (ii) 8.13 ± 3.39, *(2)* (iii) 3.41 ± 1.58, *(2)* (iv) -16.71 ± 1.21, *(2)* (v) 16.5 ± 0.70, *(2)*	(i) 5.85 ± 0.76, *(2)* (ii) 21.15 ± 3.39, *(2)* (iii) 12.64 ± 1.77, *(2)* (iv) -25.23 ± 0.46, *(2)* (v) 15.00 ± 0.00, *(2)*	(i) 8.03 ± 0.7, *(2)* (ii) 9.98 ± 1.78, *(2)* (iii) 3.51 ± 0.45, *(2)* (iv) -18.94 ± 0.13, *(2)* (v) 17.00 ± 1.41, *(2)*
		C	(i) 43.43 ± 0.03, *(2)* (ii) 52.34 ±15.67, *(2)* (iii) 28.14 ± 5.81, *(2)* (iv) 2.77 ± 9.01, *(2)* (v) 15.5 ± 2.12, *(2)*	(i) 25.05 ± 0.55, *(2)* (ii) 14.36 ± 3.59, *(2)* (iii) 6.54 ± 1.33, *(2)* (iv) -8.23 ± 8.93, *(2)* (v) 15.00 ± 0.00, *(2)*	(i) 7.7 ± 0.38, *(2)* (ii) 5.74 ± 1.07, *(2)* (iii) 3.82 ± 0.99, *(2)* (iv) -23.77 ± 3.24, *(2)* (v) 15.00 ± 0.00, *(2)*	(i) 4.92 ± 0.54, *(2)* (ii) 5.74 ± 0.12, *(2)* (iii) 2.46 ± 0.02, *(2)* (iv) -6.17 ± 12.67, *(2)* (v) 21 ± 7.10, *(2)*	(i) 5.90 ± 0.79, *(2)* (ii) 21.93 ± 0.81, *(2)* (iii) 10.68 ± 0.6, *(2)* (iv) -21.15 ± 4.33, *(2)* (v) 15.00 ± 0.00, *(2)*	(i) 7.59 ± 0.71, *(2)* (ii) 7.8 ± 1.50, *(2)* (iii) 2.96 ± 0.16, *(2)* (iv) -19.28 ± 0.75, *(2)* (v) 18.5 ± 2.12, *(2)*
	7	I	(i) 37.99 ± 7.37, *(3)* (ii) 36.91 ± 14.95, *(3)* (iii) 24.77 ±1.61, *(3)* (iv) -0.51 ± 2.26, *(3)* (v) 16.00 ± 0.0, *(3)*	(i) 23.54 ± 2.58, *(3)* (ii) 7.74 ± 2.42, *(3)* (iii) 4.15 ± 1.38, *(3)* (iv) -4.41 ± 9.04, *(3)* (v) 15.7 ± 0.58, *(3)*	(i) 6.77 ± 1.20, *(3)* (ii) 7.03 ± 3.35, *(3)* (iii) 3.83 ± 1.15, *(3)* (iv) -13.52 ± 6.51, *(3)* (v) 17.00 ± 2.00, *(3)*	(i) 3.55 ± 0.48, *(3)* (ii) 7.45 ± 2.33, *(2)* (iii) 2.64 ± 0.83, *(2)* (iv) -16.90 ± 0.53, *(2)* (v) 17.00 ± 1.41, *(2)*	(i) 5.44 ± 0.7, *(3)* (ii) 15.85 ±3.41, *(3)* (iii) 9.43 ± 1.55, *(3)* (iv) -24.48 ± 1.23, *(3)* (v) 15.33 ± 0.58, *(3)*	(i) 7.13 ± 1.76, *(3)* (ii) 7.47 ± 2.42, *(2)* (iii) 3.71 ± 1.46, *(2)* (iv) -23.22 ± 3.47, *(2)* (v) 24.00 ± 9.90, *(2)*
		C	(i) 38.4 ± 7.72, *(3)* (ii) 42.09 ± 10.98, *(3)* (iii) 24.24 ± 4.15, *(3)* (iv) 0.19 ± 2.27, *(3)* (v) 14.00 ± 0.00, *(3)*	(i) 23.48 ± 2.68, *(3)* (ii) 7.34 ± 1.366, *(3)* (iii) 4.00 ± 1.59, *(3)* (iv) -6.59 ± 12.43, *(3)* (v) 15.00 ± 1.00, *(3)*	(i) 6.77 ± 1.25, *(3)* (ii) 9.24 ± 3.4, *(3)* (iii) 4.8 ± 1.2, *(3)* (iv) -7.52 ± 8.36, *(3)* (v) 16.33 ± 0.58, *(3)*	(i) 3.60 ± 0.46, *(3)* (ii) 3.72 ± 1.35, *(2)* (iii) 2.01 ± 0.97, *(2)* (iv) -17.47 ± 0.48, *(2)* (v) 17.00 ± 2.8, *(2)*	(i) 5.36 ± 0.69, *(3)* (ii) 16.02 ± 1.26, *(3)* (iii) 7.73 ± 0.69, *(3)* (iv) -20.00 ± 3.38, *(3)* (v) 14.3 ± 0.58, *(3)*	(i) 7.15 ± 1.76, *(3)* (ii) 7.74 ± 2.28, *(3)* (iii) 3.34 ± 0.94, *(3)* (iv) -15.81 ± 1.69, *(3)* (v) 17.7 ± 2.89, *(3)*
	12	I	(i) 37.53 ± 6.76, *(5)* (ii) 37.86 ± 6.12, *(3)* (iii) 23.87 ± 1.5, *(3)* (iv) -21.31 ± 9.92, *(3)* (v) 16.67 ± 1.15, *(3)*	(i) 23.27 ± 2.88, *(5)* (ii) 11.18 ± 2.79, *(5)* (iii) 7.62 ± 2.83, *(5)* (iv) -23.19 ± 11.4, *(5)* (v) 15.4 ± 0.55, *(5)*	(i) 6.76 ± 1.29, *(5)* (ii) 6.72 ± 1.32, *(4)* (iii) 3.69 ± 0.84, *(4)* (iv) -23.55 ± 2.72, *(4)* (v) 16.25 ± 0.5, *(4)*	(i) 3.62 ± 0.78, *(5)* (ii) 6.67 ± 3.34, *(4)* (iii) 3.9 ± 2.54, *(4)* (iv) -16.60 ± 7.73, *(4)* (v) 18.75 ± 2.63, *(4)*	(i) 5.47 ± 0.67, *(5)* (ii) 18.27 ± 3.38, *(5)* (iii) 11.29 ± 2.31, *(5)* (iv) -26.17 ± 11.12, *(5)* (v) 15.00 ± 0.00, *(5)*	(i) 7.18 ± 1.10, *(3)* (ii) 5.69 ± 1.86, *(2)* (iii) 2.85 ± 0.09, *(2)* (iv) -21.35 ± 1.39, *(2)* (v) 18.5 ± 3.54, *(2)*
		C	(i) 39.23 ± 6.38, *(5)* (ii) 37.89 ± 18.47, *(4)* (iii) 22.9 ± 7.83, *(4)* (iv) -18.32 ± 18.22, *(4)* (v) 14.5 ± 1.00, *(4)*	(i) 23.59 ± 2.84, *(5)* (ii) 11.68 ± 3.77, *(4)* (iii) 7.34 ± 2.63, *(4)* (iv) -19.08 ± 10.7, *(4)* (v) 15.3 ± 0.96, *(4)*	(i) 6.67 ± 1.83, *(5)* (ii) 5.74 ± 1.73, *(5)* (iii) 2.95 ± 0.93, *(5)* (iv) -17.67 ± 7.64, *(5)* (v) 16.4 ± 0.90, *(5)*	(i) 3.81 ± 0.74, *(5)* (ii) 3.74 ± 1.33, *(4)* (iii) 1.64 ± 0.19, *(4)* (iv) -11.67 ± 8.68, *(4)* (v) 23.25 ± 9.88, *(4)*	(i) 5.20 ± 0.63, *(5)* (ii) 17.47 ± 4.44, *(5)* (iii) 10.11 ± 3.43, *(5)* (iv) -23.12 ± 4.90, *(5)* (v) 15.40 ± 0.89, *(5)*	(i) 7.19 ± 1.8, *(3)* (ii) 8.55 ± 1.26, *(3)* (iii) 4.21 ± 0.96, *(3)* (iv) -20.40 ± 4.09, *(3)* (v) 15.33 ± 0.58, *(3)*

Table 2-1 (cont.): The values presented are the average ± standard deviation, with sample size italicized in the parenthesis.The table is organized with individual muscles in columns (VASTI, GAS, PLANT, SOL, FHL and TA) and the spinal cord condition (data from control (spinally-intact) cats and cats with lateral hemisection) in rows. The lateral hemisection group is broken further into recovery time-points (3, 7, 12) representing weeks since survival (LHS) surgery (see Methods). Each of these is further broken into data from ipsilateral (I) limb (a limb on the same side as the lesion site), and contralateral (C) limb (a limb on an uninjured side).

CHAPTER 3. REDUCTION OF DEGREES OF FREEDOM IN CONTROL OF FORCE FEEDBACK PATHWAY AFTER PARTIAL SPINAL CORD INJURY: IMPLICATIONS FOR THE REGULATION OF LIMB STIFFNESS

3.1 Introduction

The stability during standing and locomotion is maintained and restored by an effective neural control of stiffness at the ankle, knee and hip joints. Joints possess inherent stability which arises from stiff structures surrounding it (ligaments, tendons, muscles, fascia, cartilage, joint capsule, skin) (Lew, Lewis et al. 1993). Except for muscles, the other structures provide a passive, relatively constant, and modest stiffness that is, by itself, insufficient for stability (Loram and Lakie 2002). Furthermore, physiologically and behaviorally, the concept of constant mechanical stiffness may not be beneficial for different motor tasks (Rapoport, Mizrahi et al. 2003), as different tasks may require variable and/or joint-specific compliance (Simon, Ingraham et al. 2014). For instance, walking may require greater compliance of the ankle joint than standing. The mechanism that the nervous system utilizes to meet these task requirements is by modulation of muscle stiffness traversing different limb joints.

Muscle stiffness is described as the ratio of change in its force per change in its length (Johansson and Sjolander 1993). It is a function of intrinsic properties of the muscle (tendon, fascia, and passive contractile structures), and, to a greater extent, a neural activation (Nichols and Houk 1976). The level of neural activation of a muscle at a given

instant is the result of an integration of descending (efferent) inputs and segmental proprioceptive (afferent) feedback in its motoneurons (Riemann and Lephart 2002, Riemann and Lephart 2002). It continually undergoes revisions and adjustments based on resultant movement, movement of other body parts, unexpected obstacles, etc.. Thus an accurate and timely sensory information about internal or external body conditions is critical for effective motor control and appropriate muscle stiffness. Although the source of this modulation is associated with visual perception (Sasaki, Usami et al. 2002), the vestibular system (Paloski, Wood et al. 2006), and tactile receptors (Kavounoudias, Roll et al. 2001), oftentimes proprioceptive feedback is the fastest and the most accurate (Ghez 1991). Furthermore, patients with impaired vision or vestibular function can maintain balance and posture quite well, but not without proprioceptive feedback (Sainburg, Ghilardi et al. 1995).

The proprioceptive feedback from a muscle provides continuous information about mechanical states of the muscle – its length and force - to its motoneuron pool (homonymous afferent feedback) and motoneuron pools of other muscles (heteronymous afferent feedback), either directly (via monosynaptic connections) or indirectly via excitatory or inhibitory interneurons (polysynaptic connections). Specific and unique roles can be assigned to two main muscle mechanoreceptors: muscle spindles have been, almost universally, described as sensors of muscle length and change in its length (Sherrington 1961, Cope, Bonasera et al. 1994), whereas the activity of Golgi tendon organs (GTO) is a function of muscle active (Houk and Henneman 1967, Houk, Singer et al. 1971) and to some extent passive (Jansen and Rudjord 1964, Schafer, Berkelmann et al. 1999) force. The respective connectivity of these two pathways in the spinal cord forms a neural

network of asymmetrically distributed sensory inputs that strongly implies their specific functional roles during motor tasks. Each motoneuron pool receives an excitatory length feedback from its homonymous muscle (Eccles, Eccles et al. 1957, Eccles and Lundberg 1957, Eccles and Lundberg 1958), its synergists (Fritz, Illert et al. 1989, Nichols 1999) and, in rare instances, from heteronymous non-synergist muscles (Edgley, Jankowska et al. 1986), while antagonists receive appropriate reciprocal length-dependent inhibition (Kandel, Schwartz et al. 2000). This focused connectivity to homonymous motoneurons, suggests regulation of individual muscles' resistance to stretch, localized joint stiffness, and joints coupling via biarticular muscles (Nichols 2002, Lyle, Prilutsky et al. 2016). In contrast to length feedback, force-dependent input onto homonymous muscle is not pronounced (Eccles, Eccles et al. 1957). Instead, this feedback seems to converge mainly onto heteronomous motoneuron pools, in most cases onto those of muscles with different biomechanical actions (Bonasera and Nichols 1996, Wilmink and Nichols 2003) decreasing their stiffness. This nonhomogeneous and widespread distribution throughout the limb suggests that inhibitory force feedback helps regulate whole limb and joint-specific compliance (Gottschall and Nichols 2007, Ross and Nichols 2009, Gottschall and Nichols 2011, Nichols, Gottschall et al. 2014), while excitatory force feedback heightens joint coupling during locomotion (Pearson and Collins 1993, Prochazka, Gillard et al. 1997, Donelan and Pearson 2004). Taken together, at the limb-level, it is postulated that excitatory length feedback increases joint stiffness locally, while inhibitory force feedback decreases stiffness selectively, and in a task-dependent manner, throughout the limb.

Integration of proprioceptive input in the spinal cord entails summation, gating or modulation of its activity by descending tracts. This way supraspinal centers 'filter' and

modulate sensory input that is to be conveyed to motoneurons (Riemann and Lephart 2002). The loss of excitatory input from one or more supraspinal tracts, such as in a partial spinal cord injury (SCI), inevitably affects spinal cord circuitry. Although spinally-lesioned cats can recover the ability to stand (Fung and Macpherson 1999) and step (Barbeau and Rossignol 1987, Basso, Murray et al. 1994, Kuhtz-Buschbeck, Boczek-Funcke et al. 1996), the postural balance and adequate response to perturbation remains impaired (Rossignol, Drew et al. 1999, Lyalka, Orlovsky et al. 2009). These cats adapted a crouched gait with increased flexion during the swing and stance phase (Rossignol, Drew et al. 1999) and diminished stability (Macpherson and Fung 1999). This permanent loss of balance, despite the locomotor recovery, suggests that spared spinal circuitry caudal to injury undergoes a reorganization that is detrimental to the limb stability.

In Chapter II, we have reported an increase in gain of stretch reflex in the primary knee and ankle extensors, and negligible and transient changes in other agonists, following T9-10 level lateral hemisection (LHS), results that agree with the literature (Hochman and McCrea 1994, Taylor, Friedman et al. 1997). Much less attention has been focused on changes in the force-dependent pathway, despite it showing a remarkable task-dependent modulation by descending tracts (Gottschall and Nichols 2007, Nichols, Gottschall et al. 2014). Previous attempt to identify these changes was based on a very limited number of ankle extensors (Niazi 2015). Here, we present evidence that inhibitory force feedback assumes directional organization following lateral hemisection targeting main ankle extensors. Specifically, the magnitude of force feedback amplifies selectively from knee extensors and toe flexors onto ankle extensors, while diminishes in the other direction, resulting in a strong, chronic, consistent and bilateral convergence of inhibitory bias onto

ankle extensors. Furthermore, we propose that descending tract(s) in ventral cord, such as vestibulospinal (Nichols, Gottschall et al. 2014) and/or reticulospinal (Stapley and Drew 2009) might be potential regulators of force feedback, as they are involved in postural control. A lateral, but not dorsal spinal lesion (described in detail in Chapter IV), results in a singular force feedback organizational pattern. The preliminary results have been presented elsewhere (Kajtaz, Lyle et al. 2017).

3.2 Methods

3.2.1 Animals

The experiments were performed on ten purpose-bred female cats ranging from 3.3 - 4.1 kg. All data presented in this chapter were acquired during terminal experiments. Before the terminal experiment, cats received lateral hemisections and were allowed to recover for different time periods at the University of Louisville; 3 weeks (n = 2), 7 - 8 weeks (n = 3) and 12 - 13 weeks (n = 5). For comparison purposes only, data from 25 spinally-intact cats were opportunistically used to highlight any changes following the lateral spinal lesion. Data from a subset of these spinally-intact cats have been previously described (Lyle and Nichols 2018). These animals were used in accordance with guidelines from the National Institute of Health and protocols approved by the Institutional Animal Care and Use Committee of Georgia Institute of Technology and the University of Louisville.

3.2.2 Survival surgery

The lateral hemisections were performed on ten cats by Dr. Dena Howland at the University of Louisville. During the surgery, cats were initially anesthetized with isoflurane (5%) and oxygen mix in an induction chamber, then intubated and maintained on a mix of oxygen and isoflurane (1 - 4%) throughout the survival surgery. Blood pressure, EKG, heart rate, respiration rate, temperature, SpO_2 and expired CO_2 were all monitored throughout surgery to assure surgical depth of anesthesia. Laminectomies for lateral hemisections exposed spinal T9-10, the dura was slit, dorsal columns & dorsal root entry zones visualized to identify the midline. The intended area of the cord was cut with iridectomy scissors. Fibers adhering to dura were gently lifted with suction and cut. Dura was then sutured, durafilm and gelfoam placed on top of the dural sutures, and the back closed in layers. Cats were allowed to recover for different periods before being transported to Georgia Institute of Technology where the terminal experiments were conducted.

3.2.3 Terminal experiments

In the terminal experiments, cats were anesthetized with isoflurane gas (5%), tracheal intubation was performed, and 2 - 4% isoflurane was used to maintain deep anesthesia thereafter. An intravenous line was inserted into an external jugular vein to administer saline and medication during the experiment. Adequate deep anesthesia was confirmed during the experiment by the absence of withdrawal reflexes. Heart rate, EKG, respiratory rate, oxygen saturation, expired carbon dioxide, blood pressure, and core body temperature were monitored during all experiments. The core body temperature was maintained at 37º C with a heating pad. The animal's head was fixed in a stereotaxic frame,

and the abdomen was supported by a sling. The hindlimbs were rigidly secured using threaded rods inserted into the proximal (just distal to the greater trochanter) and distal femur (femoral condyle). The rods were connected by a bar and rigidly fixed to the frame. The proximal tibia was stabilized by a separate threaded rod, while the distal tibia was supported with an ankle clamp.

The vasti muscles group (VASTI), gastrocnemius (GAS), plantaris (PLANT), soleus (SOL), and flexor hallicus longus (FHL) were dissected in both hindlimbs. The VASTI and FHL are the most proximal and the most distal muscles, respectively, evaluated in this study. In order to minimize any mechanical coupling, all muscles were separated from adjacent tissues and neighboring muscles carefully, while trying to preserve their nerve and vascular supply. The PLANT tendons were severed from the GAS, released from its connection to the calcaneus, and cut distally near its insertion to the flexor digitorum brevis muscle. The GAS tendons were carefully separated from the SOL at their common insertion onto the calcaneus with small bone chips preserved. The tendon of FHL was cut where it merges with the flexor digitorum longus tendon. The freed tendons were connected to strain gauge myographs (which recorded forces) in series with linear motors (which displaced the muscles), via custom-made tendon clamps. The VASTI was carefully isolated by first releasing the sartorius muscle from its broad distal insertion since the sartorius completely covers the quadriceps group. Then, blunt dissection was used to separate the VASTI from adjacent tissue along the medial and lateral femur, and the retinaculum was transected proximally (i.e., iliotibial band) and distally around the patella. Next, blunt dissection was used to separate the vastus muscle group from the rectus femoris (RF). The RF was then either transected using electrocautery mid-belly. The transaction

was done to eliminate the need to stabilize the pelvis as RF has an action on it. The VASTI insertion was freed by cutting the patellar tendon. Next, a small hole was drilled in the patella, and the steel cable (0.9 mm diameter) was threaded through the hole. The steel cable was next connected to a tendon clamp in series with a myograph and linear motor via a pulley system.

The standard precollicular decerebration involved a vertical transection at the anterior margin of the superior colliculus (Silverman, Garnett et al. 2005). All brain tissue rostral to the transection was removed. Following the decerebration, anesthesia was titrated down over approximately 5 - 30 minutes and then withdrawn. At the end of the experiment, heparin was injected in preparation for perfusion, and the animal was re-anesthetized using isoflurane. Euthanasia was accomplished by perfusing the animal through the heart first with saline and then paraformaldehyde. Hindlimb muscles were harvested following euthanasia.

3.2.4 Data acquisition

The intermuscular spinal pathways were evaluated using a ramp-hold-release muscle stretch protocol. The details of the software and hardware used have been described previously (Nichols 1987, Ross and Nichols 2009). Briefly, the protocol involved 2-mm muscle stretches with a 50 ms ramp, 100 ms hold and 50 ms release with a velocity of 0.04 m/s. The stretch of muscle results in the opposing force response. The muscle stretches were applied in a two-state alternating pattern with a 0.7 Hz stretch repetition frequency (Figure 3-1: top left and right). Each trial had on average 20 – 40 stretch repetitions. In state 1 (S1), a single muscle denoted as the recipient was stretched alone. In state 2 (S2),

the recipient muscle was stretched simultaneously with another muscle referred to as the donor muscle. Muscle stretch repetitions were applied over a constant (a condition termed quiescent) (Figure 3-1: top left) and varying range of background forces (a condition termed active) (Figure 3-1: top right) by eliciting a crossed extension reflex as in earlier work (Bonasera and Nichols 1994, Wilmink and Nichols 2003, Ross and Nichols 2009). The crossed-extension reflex was elicited by stimulating the contralateral tibial nerve with a hook electrode (0.1 ms pulse width, 40 Hz) just proximal to the medial malleolus. Typically, the force in the contralateral extensor muscles increased rapidly and slowly decayed toward the 1 - 3 N background force over a 20 - 40 s (Figure 3-1: top right).

3.2.5 Data analysis

The intermuscular interactions were evaluated under quiescent and active conditions (as described above) between knee and ankle extensors. We employed three levels of analysis; (i) processing of quiescent (Figure 3-1: top left) and active trials (Figure 3-1: top right), (ii) within cat analysis of individual trials from which we obtained averages and standard deviations (quiescent condition) (Figure 3-1: middle left), and the least square quadratic polynomial fits along with 95% confidence intervals (active condition) (Figure 3-1: middle right), and (iii) across cats analysis of pooled quiescent (Figure 3-1: bottom left) and active condition data (Figure 3-1: bottom right). At each level, each data point represents one muscle pair interaction from each limb, which are treated independently.

At the processing level, the varying and constant background forces were subtracted from the raw force profiles prior to the analysis of both quiescent and active condition trials. The vectors used to remove the background force offset were determined

using linear interpolation from a stretch onset to 900 ms after stretch onset, similar to the previously described method (Ross and Nichols 2009). The sudden and unaccounted changes in background forces that precluded an accurate baseline subtraction, as well as spontaneous force response unrelated to muscle stretch or tibial nerve stimulation, were eliminated prior to the analysis. The intermuscular effects caused by mechanical interactions between muscles, although rare, were detected by the apparent heterogenic interaction that occurs within 10 ms from the stretch onset (Bonasera and Nichols 1996). These trials were rejected.

Under the quiescent condition, both recipient and donor muscles were held at constant background force of 1 to 3 N, just enough to make them taut. Under the active condition, intermuscular interactions were evaluated across varying background forces. In both quiescent and active trials, the S1 stretch is dominated solely by homonymous, whereas the S2 stretch by homonymous and heteronymous, length- and force-dependent feedback. Homonymous feedback has been described in Chapter II. The difference between the force responses of S1 and S2 is considered to be a heteronymous effect of donor muscle onto the recipient. Previously, it has been shown that late (or statis) epoch (110-150 ms after stretch onset, i.e., last 40 ms of hold phase) illustrates well intermuscular sensory feedback effects from a donor muscle onto the recipient muscle (Nichols 1999). Thus, we used this late epoch in quiescent and active trials to evaluate all hypotheses in this chapter. Qualitative differences between quiescent and active conditions mandate a different analysis approach.

For statistical analysis, all pooled data are presented as a normalized percentage difference to simplify across-cats comparison. Analysis was blinded in order to eliminate

any potential bias. Unless otherwise stated, we report results of quiescent data as a mean ± standard deviation. Data analysis, statistical tests, and visualization were accomplished using custom programs written in MATLAB 2016b (MathWorks, Natick, MA). To ease the comprehension of the results, we have consistently used pink-red coloring to denote interactions arising from distal to proximal muscles, and blue-light blue coloring represents proximal to distal interactions in all figures presented in this chapter.

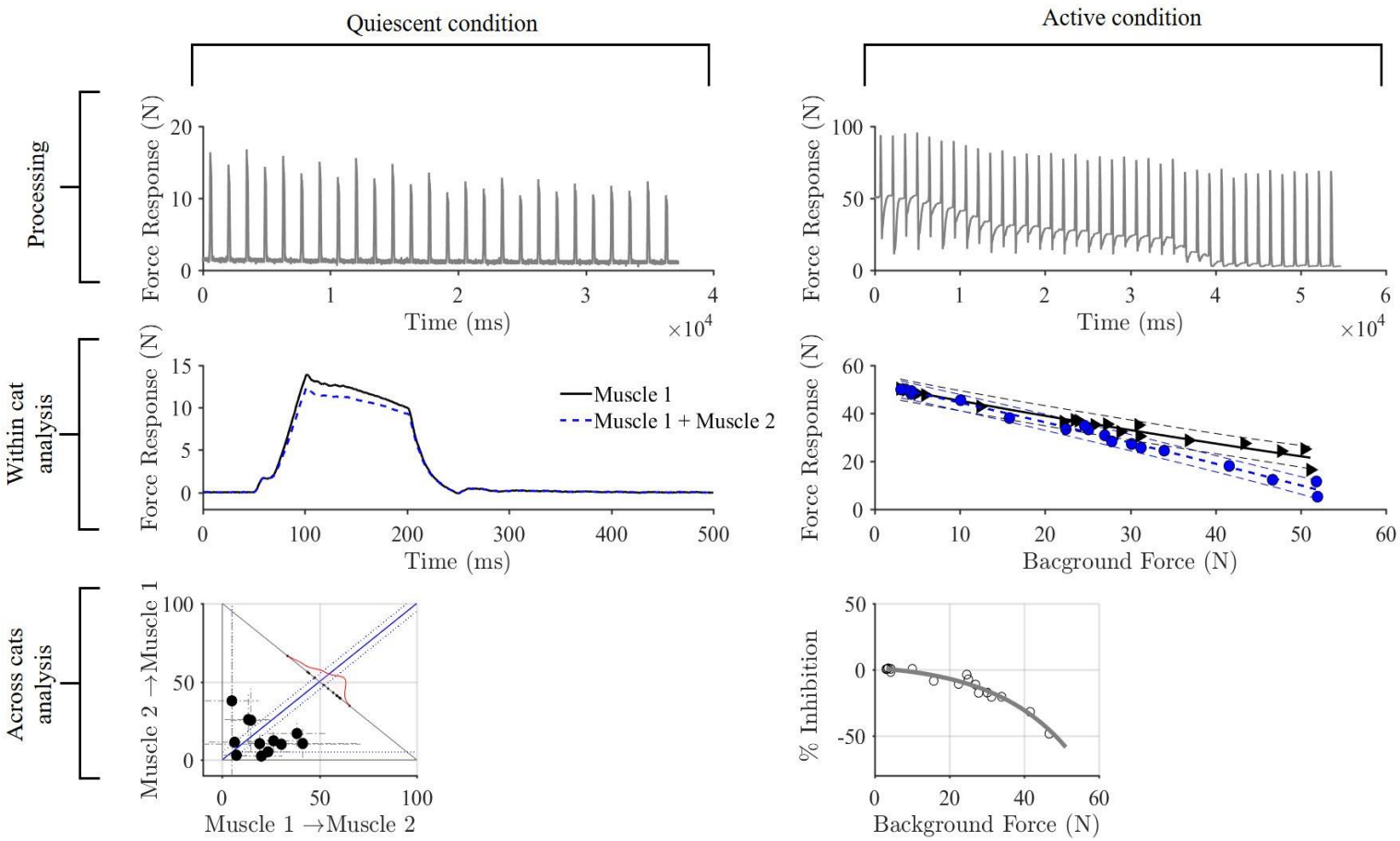

Figure 3-1: Three levels of data analysis. Recorded raw data are first processed and outliers are eliminated (*top*). Next, both quiescent (*left middle*) and active (*right middle*) data are analyzed within cat. In quiescent trials, the force response of lone stretch is compared to the stretch in tandem with another muscle (*left*). Under active conditions, the same comparison is accomplished across varying background forces (*right*). The next step in analysis of active trials is fitting the state 1 and state 2 responses with polynomial fits, separately. Following within cat analysis, under quiescent conditions, the data are pooled together as individual magnitudes in one direction plotted against magnitudes in the other direction within the pair of the muscles (*left bottom*). For active trials, the difference between polynomial curves are plotted against the common background force (*right bottom*). More detailed explanation can be found under quiescent and active condition sections.

3.2.5.1 Quiescent condition

In the quiescent condition, all muscles evaluated were kept taut up to 3 N of background force (which was subtracted prior to the analysis). This enabled us to compare two features of intermuscular interactions across cats; (i) magnitude of interaction, and (ii) directional bias. Magnitude is operationally defined as a sign and an amount of unidirectional interaction and was computed as the normalized difference between S1 and S2 static (late) epochs (Figure 3-1: left middle)

$$\mu_{M12} = \frac{\mu_{S1} - \mu_{S2}}{\mu_{S1}} 100 \quad (\%) \qquad 3.1$$

μ_{M12} is a relative percent difference between recipient force responses obtained in the S1 and S2, calculated in an effort to facilitate across limbs and cats comparisons. In general, μ that is less than 5% in magnitude is considered physiologically negligible.

The standard deviation of the magnitude was obtained by calculating its derivative with respect to the S1 and S2 static (late) epochs and covariance between those two states (Taylor 1997), per individual trial:

$$\sigma_{M12} = \frac{\partial \mu_{M12}^2}{\partial S1} \cdot \sigma_{S1} + \frac{\partial \mu_{M12}^2}{\partial S2} \cdot \sigma_{S2} + 2 \cdot \frac{\partial \mu_{M12}}{\partial S1} \cdot \frac{\partial \mu_{M12}}{\partial S2} \cdot S1 \cdot S2 \qquad 3.2$$

If an experiment had more than one trial of the same muscle pair interaction, the averages of μ_{M12} and σ_{M12} of those trials are used as a representative of an interaction magnitude and its standard deviation for that experiment. The Wilcoxon rank-sum test was

used to determine whether the recipient muscle forces recorded when stretched alone (S1) were different from that when stretched pairwise with the donor muscle (S2), in the within-cat analysis.

The *directional bias* is a difference of unidirectional interaction magnitudes between muscles in a pair that exchanges feedback. The sign of the bias is arbitrarily defined based on muscles' anatomical origins as positive to denote distal to proximal bias (when more distal muscle inhibits more proximal one more so than the other way around), balanced (when muscles exchange the same ± 5% of inhibition), or negative to denote proximal to distal bias (when more proximal muscle inhibits more distal one more so than the other way around):

$$B_{12-21} = \mu_{M12} - \mu_{M21} \qquad 3.3$$

To compare the effect of the lesion across cats, and to gain insight into main changes following LHS, all quiescent data were pooled together in the form of individual interaction results plotted against each other (Figure 3-1: bottom left). Specifically, each data point was obtained from one muscle pair in a limb. The individual data points were positioned in a coordinate system based on average magnitude values (μ_{M12}, μ_{M21}), presented as black circles with standard deviation plotted as grey dashed lines (calculated using equation 3.1 and 3.2, respectively). The x-axis represents averaged interactions from muscle 1 to muscle 2 (μ_{M12}), and the y-axis represents averaged interactions from muscle 2 to muscle 1 (μ_{M21}). The distributions opposite of x- and y-axis represent kernel density

estimates of μ_{M12} (Figure 3-3: A, pink colored distribution) and μ_{M21} (Figure 3-3: A, blue colored distribution), respectively. The blue line represents the balanced interaction between μ_{M12}, and μ_{M21}, and deviation from this line in either direction suggests a biased interaction. The direction of the bias was calculated using equation 3.3 and visualized by the projection of data onto the grey line that is orthogonal to the balance line. If the projections lie above the balance line, the directional bias is proximal to distal (P→D), while below the balance line projections have a distal to proximal (D→P) bias. Data clustered close to the balance line are considered to be balanced (B) interactions. A dark grey trace on the grey line is a distribution fit of the projected data points and represents the said bias.

3.2.5.2 Active conditions

The force responses for each state were plotted separately as a function of recipient background forces. The averages of background force 15 ms prior to each stretch of recipient muscle were used as values of background forces in the regression plots. However, if the background force did not change, despite tibial nerve stimulation, i.e., background force was constant and less than 3 N, the trial is considered quiescent and analyzed accordingly. The plotted force responses of S1 and S2 stretches were fit with least squares quadratic polynomial curves and 95% confidence intervals (Figure 3-1: middle left). The intermuscular effects were detected by significant differences between the polynomials corresponding to S1 and S2 responses. In a case when the confidence intervals for a pair of polynomials were overlapping, the two polynomials were considered statistically nonsignificant for the range over which they overlapped. To ease comparison

across cats, the relative magnitude of any difference between the polynomial curve fit vectors from S1 and S2 were expressed as a percent difference and represent a magnitude of interaction across varying background forces of recipients.

Next, these magnitudes in both directions were pooled together across common recipient background forces (Figure 3-1: bottom right, example Figure 3-3: B). Magnitudes of interaction from more distal to more proximal muscles were colored red, while proximal to distal interactions were colored blue (example Figure 3-3: B). It was attempted to distinguish different recovery time points as a gradient from lighter (early recovery time-points) to darker (late recovery time-points), but this was not always accomplished due to the lack of data.

3.3 Results

The purpose of this study was to determine the organization of the force-dependent feedback following lateral hemisection (LHS). This was accomplished by comparing i.) interactions between a pair of muscles in ipsilateral and contralateral limb under both quiescent and active condition in a representative cat, ii.) magnitudes and resultant bias of quiescent interactions across all cats with LHS to those without injury, iii.) magnitudes of interactions in a muscle pair across varying background forces throughout three recovery time points post-injury. The data for each muscle interaction from each limb were pooled together. The representative cat (7 wks post-LHS) was chosen based on subjectively determined typical response and a large number of muscle interactions evaluated. The organizational patterns of force feedback across knee and ankle joints in the decerebrate and spinally-intact cat have been determined recently (Lyle, 2018). Hence the patterns

observed in this study will be compared to those characterized by Drs. T. Richard Nichols and Mark Lyle. Additionally, the spectrum of interactions across all cats and each muscle pair interactions was determined at the end of the Results section. Quiescent data from cats, spinally-intact (CNT) and those with LHS were fit with least squares quadratic polynomial curves and two standard deviations as confidence intervals in order to estimate changes in interactions across the spectrum.

3.3.1 The VASTI, a knee extensor muscles, strongly, consistently and chronically inhibits all distal muscles, following lateral hemisection, resulting in a strong proximal to distal bias in interactions involving VASTI

The intermuscular feedback arising from VASTI is selectively amplified, while feedback onto VASTI is depressed following lateral hemisection, compared to spinally-intact cats. This generalization is bilateral, chronic and consistent across all cats. Homonymous feedback arising from this muscle undergoes changes as well, described in detail in Chapter II.

3.3.1.1 <u>The VASTI strongly inhibits GAS, while GAS only weakly inhibits VASTI, resulting in a strong proximal to distal bias</u>

Previously, Wilmink and Nichols (Wilmink and Nichols 2003) found that interactions between VASTI and GAS in the decerebrate and spinally-intact cats are inhibitory. Later, Lyle and Nichols (Lyle, 2018) have confirmed that interaction magnitudes between VASTI and GAS were indeed inhibitory, but variable. In pattern 1, VASTI and GAS do not exchange significant interaction, in pattern 2, VASTI strongly inhibits GAS, and in pattern 3, VASTI and GAS exchange balanced inhibition (Lyle and

Nichols 2018). In this study, following lateral hemisection in cats, we have consistently observed a strong VASTI onto GAS inhibition, and weak or non-existent interaction vice versa (Figure 3-2, Figure 3-3), a pattern that most resembles pattern 2 in the control condition (Lyle and Nichols 2018).

Common to all cats is consistency in this profile in both ipsilateral and contralateral limb (Figure 3-2) and in both quiescent and active conditions across cats (Figure 3-3). Compared to spinally-intact cats, under quiescent conditions inhibition from VASTI to GAS was on average significantly larger ($p < 0.05$), in both ipsilateral and contralateral limb (Figure 3-2), and across recovery time-points (Table 3-1).

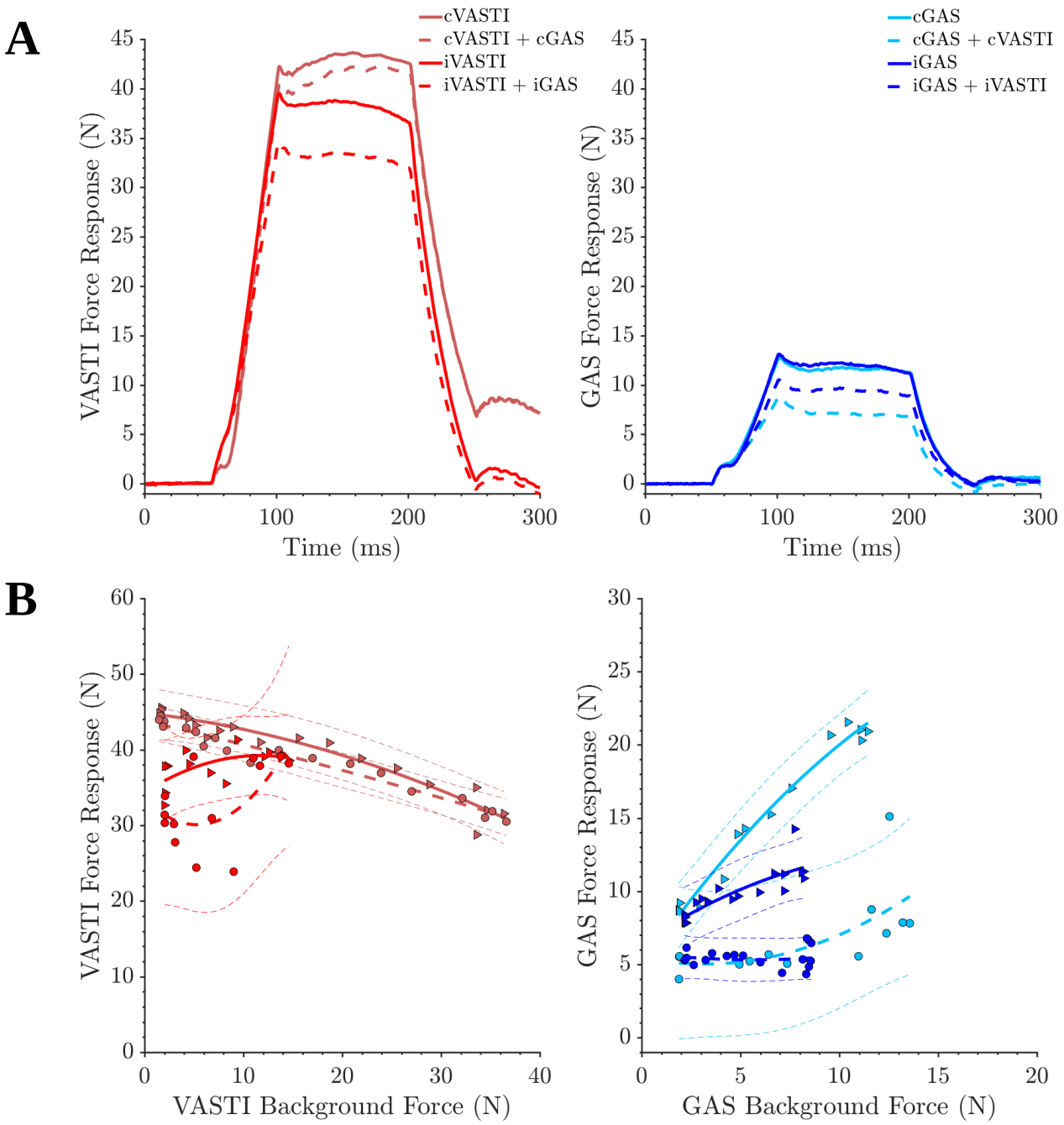

Figure 3-2: VASTI ↔ GAS interactions in a representative cat. In *A*, quiescent GAS→VASTI interactions (*left*) from ipsilateral (dark red) and contralateral (light red) limb, and quiescent VASTI→GAS interaction (*right*) from ipsilateral (dark blue) and contralateral (light blue) were presented to show bilateral effect of unilateral lesion. In *B*, same interactions were presented across varying background forces. On the left, interaction from GAS to VASTI in ipsilateral (dark red) and contralateral (light red) limb, and on the right are interactions from VASTI to GAS from ipsilateral (dark blue) and contralateral (light blue) limb. Note: in the legend, *i* in front of the muscle name stands for ipsilateral, and *c* stands for contralateral.

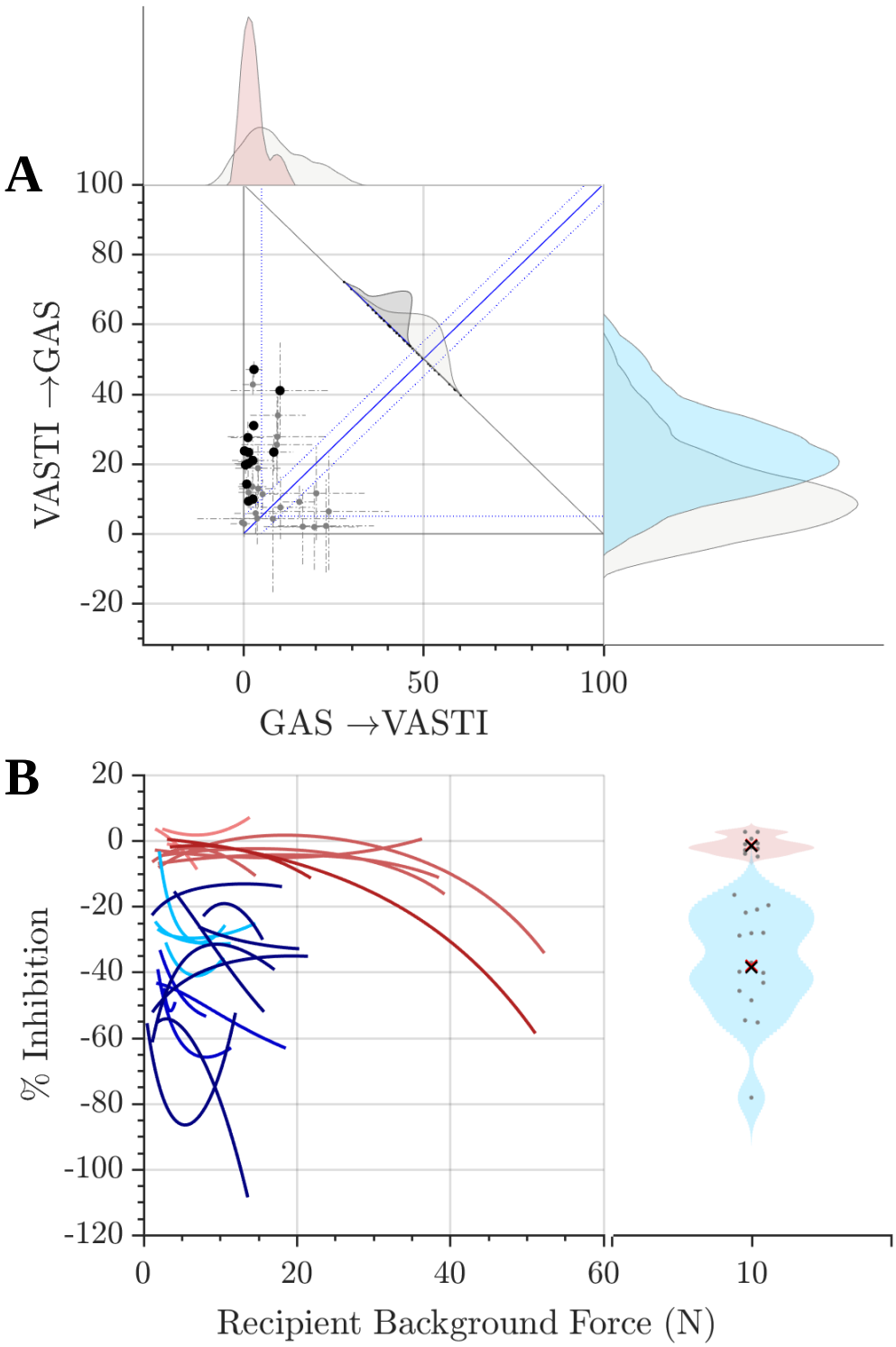

Figure 3-3: VASTI ↔ GAS interactions across all cats. In *A* are quiescent data pooled across all cats. The averages of interaction from GAS to VASTI are plotted against the averages of interaction from VASTI to GAS across LHS (black markers) and CNT cats (grey markers). The pink filled trace is the distribution of GAS→VASTI magnitudes, and blue filled trace is the distribution of VASTI→GAS magnitudes, both from LHS cats. In the background are light grey filled distributions of magnitudes from CNT cats. In *B* are pooled active data magnitudes across LHS cats. The GAS→VASTI interactions are in red-pink color, while interaction VASTI→GAS interactions are blue-light blue color. The intensity of coloring corresponds to recovery time-points. The longer recovery period the darker the color. On the right, is a snapshot of interaction magnitudes at 10 N of recipient background force where each point is interaction from one limb.

Table 3-1: VASTI↔GAS quiescent interactions across recovery time-points and limbs. Values of this interaction are presented as the mean ± standard deviation, for all three-recovery time-points, in both limbs, ipsilateral and contralateral to the lesion. For comparison purposes, presented are the mean ± standard deviation from CNT cats. Additionally, the number of muscle pairs evaluated and the net bias is given in the last column. ND means no data.

			GAS→VASTI	**VASTI→GAS**	**GAS↔VASTI**
			Magnitude *M ± SD (%)*	*Magnitude* *M ± SD (%)*	*N, Bias*
Control			8.7 ± 8.1	12.7 ± 8.4	10/22, P→D 6/22, B 6/22, D→P
Lateral Hemisection	3 wks	contralateral	1.3 ± 3.8	20.1 ± 17.7	13/13, P→D
		ipsilateral	0.5 ± 2.5	19.7 ± 14.7	
	7 wks	contralateral	2.8 ± 1.6	30.9 ± 17	
		ipsilateral	1.2 ± 4.7	27.5 ± 11.1	
	12 wks	contralateral	2.5 ± 3.5	14.2 ± 4.7	
		ipsilateral	0.8 ± 2.0	ND	

Interaction from GAS onto VASTI diminished, but not significantly when all recovery time-points were pooled together ($p = 0.09$), and it did not recover through 12-weeks post-LHS (Table 3-1). In the active condition, inhibition from VASTI onto GAS was significantly larger than inhibition vice versa across all recipient background forces evaluated. At background force of 10 N, inhibition of GAS by VASTI was 40 ± 20%, while interaction onto VASTI from GAS was physiologically negligible (–) 2 ± 3% (Figure 3-3). Consequently, the directional bias of this interaction was uniformly proximal to distal bias in all LHS cats studied (Figure 3-3: A, dark grey bias trace). Furthermore, this held true across all time points post-injury (Table 3-1), although the bias seems to increase and peaks at seven weeks post-LHS, likely due to an increase and subsequent subsiding of inhibition from VASTI onto GAS.

3.3.1.2 The VASTI inhibits PLANT more strongly than vice versa, resulting in proximal to distal bias

Previously, Lyle observed weak inhibitory interactions between VASTI and PLANT categorized into three patterns: weak proximal to distal bias, weak distal to proximal bias, and balanced, but not significant interactions (Lyle and Nichols 2018).

In the current study, all LHS cats exhibited consistent proximal to distal physiologically significant inhibition from VASTI onto PLANT in both quiescent ($p < 0.05$, Figure 3-5: A) and active condition (Figure 3-5: B), while vice versa interactions were not significant (Figure 3-5: A & B). Specifically, interaction from VASTI to PLANT displayed a medium magnitude of inhibition in a quiescent state across both limbs and recovery time-periods, that was larger than in CNT cats ($p < 0.05$) (Figure 3-4: A & B, Figure 3-5: A & B, Table 3-2). In the active state, at 5 N BGF, the inhibition from VASTI onto PLANT averaged 31 ± 19% (Figure 3-5: B). The challenge in evaluating this interaction was manipulating background forces in PLANT muscle, as PLANT poorly responded to crossed-extension. Thus, only a limited range of BGF was recorded. On the other hand, interactions onto VASTI were evaluated across a wide range of background forces, with no significant heteronymous effect from PLANT. At 5 N background force of VASTI, inhibition was not significant (2 ± 5%) and did not vary across background forces (Figure 3-5: B).

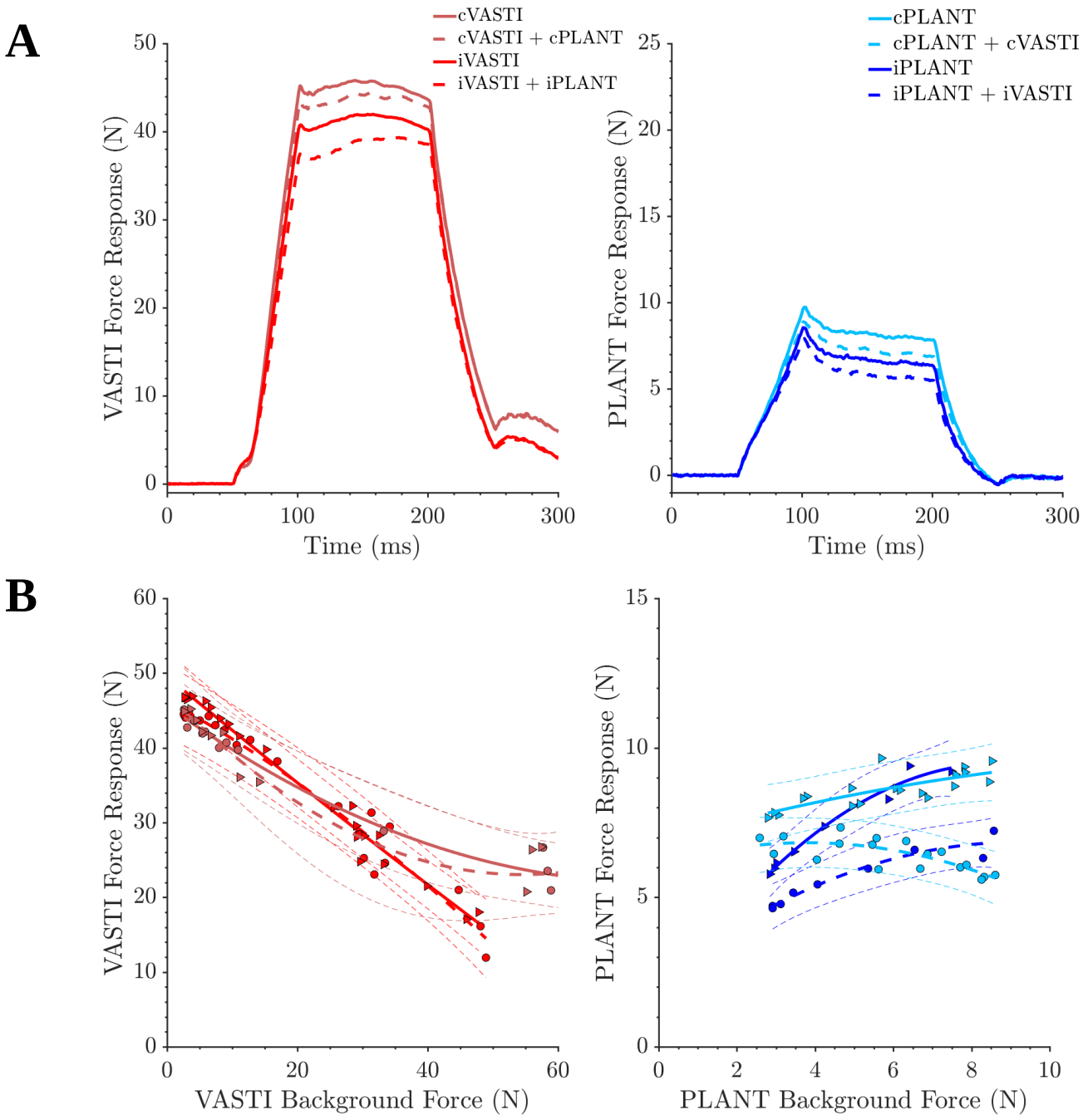

Figure 3-4: VASTI ↔ PLANT interaction in representative cat. In *A*, quiescent PLANT→VASTI interactions (*left*) from ipsilateral (dark red) and contralateral (light red) limb, and quiescent VASTI→PLANT interaction (*right*) from ipsilateral (dark blue) and contralateral (light blue) were presented to show bilateral effect of unilateral lesion. In *B*, same interactions were presented across varying background forces. Left, interaction from PLANT to VASTI in ipsilateral (dark red) and contralateral (light red) limb, and on the right are interactions from VASTI to PLANT from ipsilateral (dark blue) and contralateral (light blue) limb.

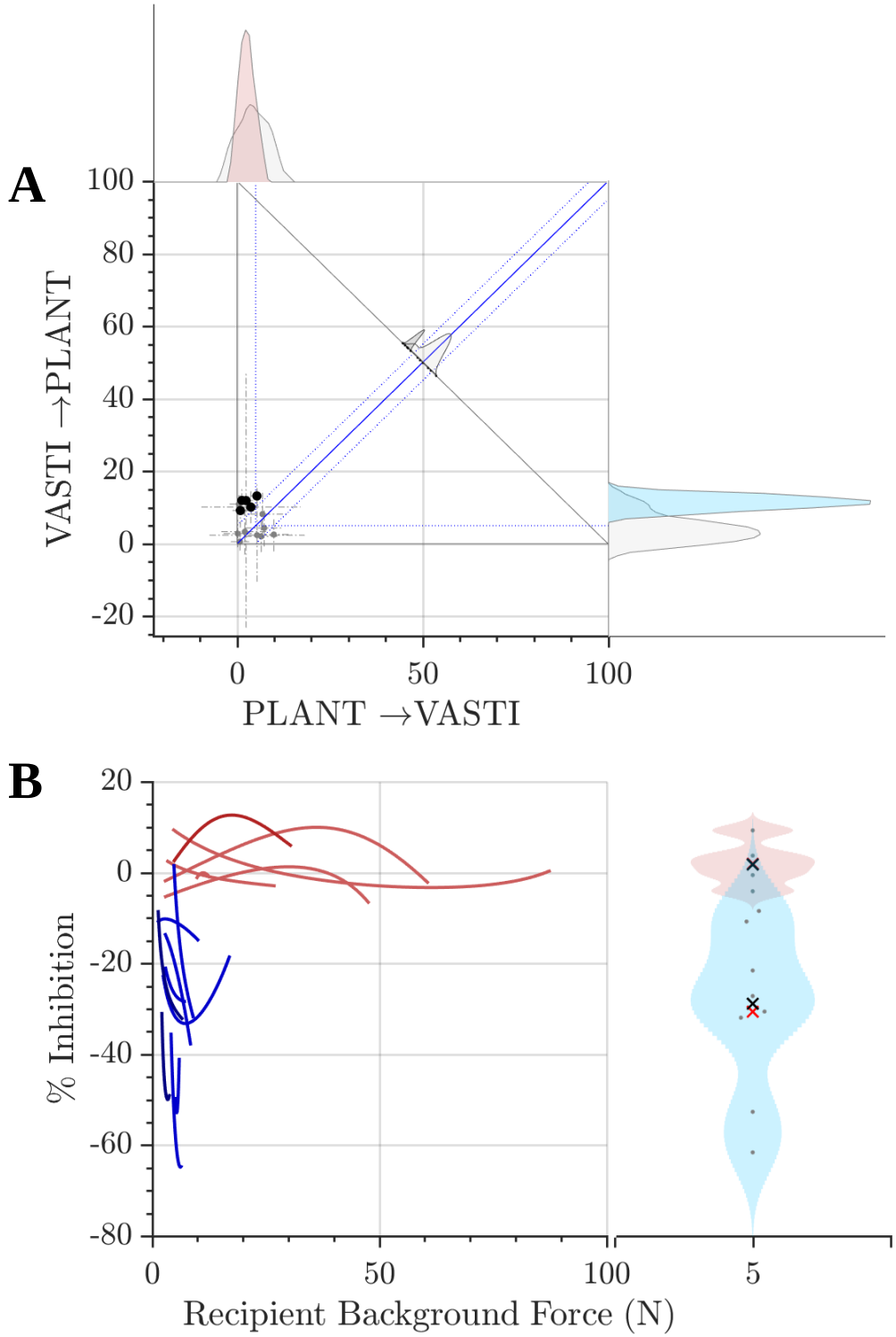

Figure 3-5: VASTI ↔ PLANT interaction across all cats. In *A* are quiescent data pooled across all cats. The averages of interaction from PLANT to VASTI are plotted against the averages of interaction from VASTI to PLANT across LHS (black markers) and CNT cats (grey markers). The pink filled trace is the distribution of PLANT→VASTI magnitudes, and blue filled trace is the distribution of VASTI→PLANT magnitudes from LHS cats. In the background are light grey filled distributions of magnitudes from CNT cats. In *B* are pooled active data across LHS cats. The PLANT→VASTI interactions are in red-pink color, while interaction VASTI→PLANT interactions are blue-light blue. The intensity of coloring corresponds to recovery time-points. The longer recovery period the darker the color. On the right, is a snapshot of interaction magnitude at 5 N of recipient background force.

Table 3-2: VASTI↔PLANT quiescent interactions across recovery time-points and limbs. Values of this interaction are presented as the mean ± standard deviation, for all three-recovery time-points, in both limbs, ipsilateral and contralateral to the lesion. For comparison purposes, presented are the mean ± standard deviation from CNT cats. Additionally, the number of muscle pairs evaluated and the net bias are given in the last column. ND means no data.

			PLANT→VASTI	**VASTI→PLANT**	**PLANT↔VASTI**
			Magnitude *M ± SD (%)*	*Magnitude* *M ± SD (%)*	*N, BIAS*
Control			5.38 ± 12.8	2.38 ± 3.2	1/9 P→D 7/9 B 1/9 D→P
Lateral Hemisection	3 wks	contralateral	ND	ND	5/5, PD
		ipsilateral	ND	ND	
	7 wks	contralateral	2.49 ± 1.8	11.91 ± 35	
		ipsilateral	5.33 ± 1.5	13.21 ± 3.2	
	12 wks	contralateral	1.29 ± 1.1	11.96 ± 3.3	
		ipsilateral	2.30 ± 7.7	9.66 ± 4.6	

The same profile and similar magnitudes were observed across both limbs (Figure 3-4: A & B), and recovery time-points (Table 3-2).

3.3.1.3 The VASTI strongly inhibits FHL, while FHL inhibits VASTI only weakly, resulting in a strong proximal to distal bias

In spinally-intact cats, the interaction between VASTI and FHL are inhibitory but, due to variability, categorized into three profiles: strong proximal to distal bias (pattern 1), balanced (pattern 2) or strong distal to proximal bias (pattern 3) (Lyle and Nichols 2018).

Following LHS, VASTI and FHL interactions remain inhibitory. Interactions from VASTI onto FHL amplified compared to CNT group, significantly ($p < 0.05$, Figure 3-7: A) while physiologically nonsignificant interaction was observed vice versa (Figure 3-7: A). In the active condition, interactions from FHL onto VASTI seem to have a force-

dependent component (Figure 3-7: B), as an increase in VASTI background force increased relative inhibition, especially in later recovery time-points (Figure 3-7: B). At 10 N of recipients BGF, inhibition from VASTI onto FHL averaged 20 ± 3%, while inhibition from FHL onto VASTI was 2 ± 2% (Figure 3-7: B).

Proximal to distal gradient of inhibition in this interaction was consistent in both ipsilateral and contralateral limb (Figure 3-6: A & B), and across recovery time-points (Table 3-3). With time this bias seems to increase, as inhibition from VASTI increases, while inhibition from FHL remains non-significant.

Table 3-3: VASTI ↔FHL quiescent interactions across recovery time-points and limbs. Values of this interaction are presented as the mean ± standard deviation, for all three-recovery time-points, in both limbs, ipsilateral and contralateral to the lesion. For comparison purposes, presented are the mean ± standard deviation from CNT cats. Additionally, the number of muscle pairs evaluated and the net bias are given in the last column. ND means no data.

			FHL→VASTI	**VASTI→FHL**	**FHL↔VASTI**
			Magnitude *M ± SD (%)*	*Magnitude* *M ± SD (%)*	*N, BIAS*
Control			9.8 ± 3.7	7.3 ± 6.1	5/16, P→D 9/16, B 2/16, D→P
Lateral Hemisection	3 wks	contralateral	0.31 ± 2.3	11.83 ± 3.2	12/12, P→D
		ipsilateral	ND	12.88 ± 4.2	
	7 wks	contralateral	2.67 ± 2.1	25.53 ± 7.1	
		ipsilateral	4.42 ± 1.9	18.77 ± 19.7	
	12 wks	contralateral	2.27 ± 3.0	27.84 ± 8.7	
		ipsilateral	1.56 ± 2.5	17.7 ± 5.9	

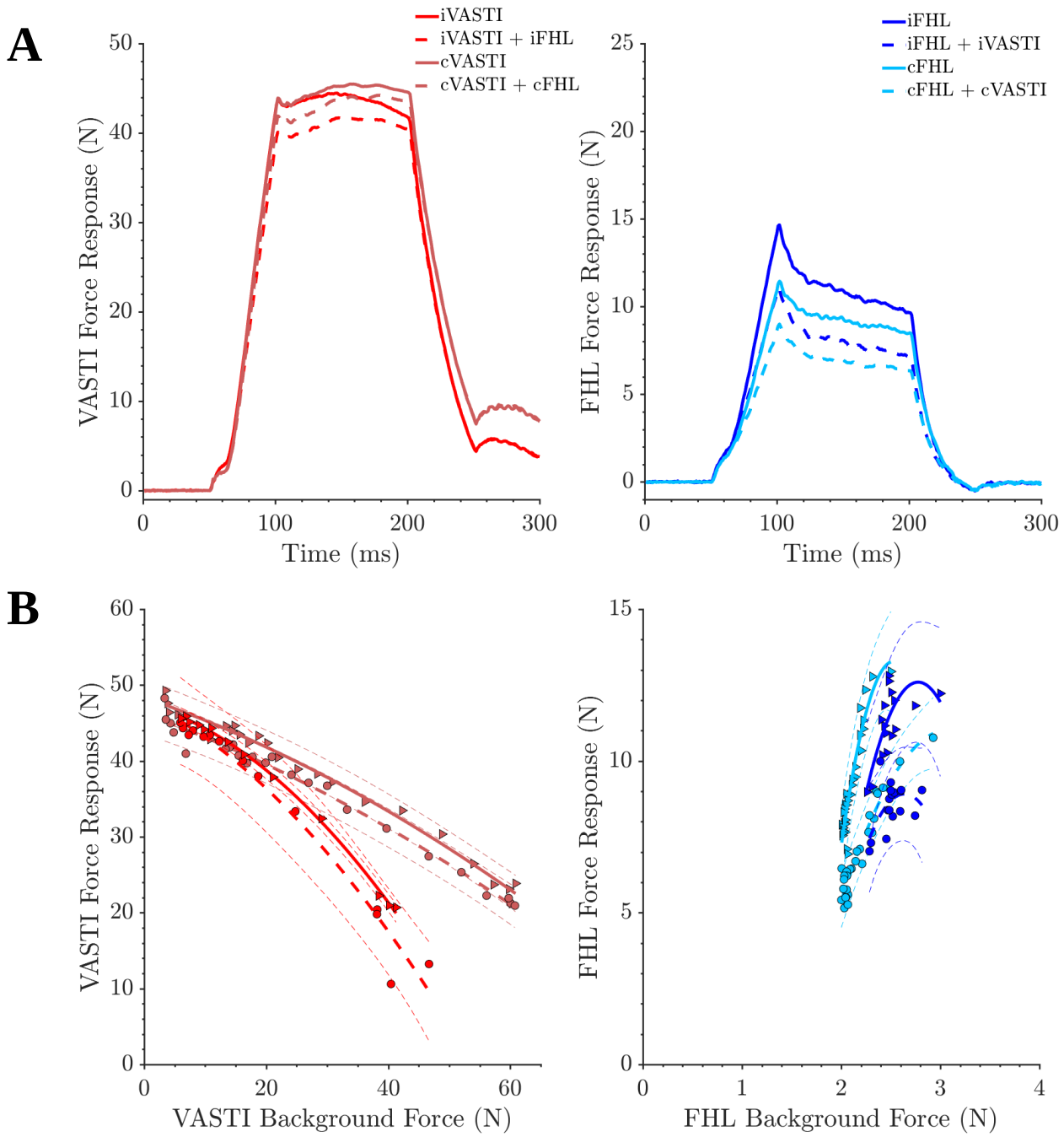

Figure 3-6: VASTI ↔ FHL interaction in a representative cat. In *A*, quiescent FHL→VASTI interactions (left) from ipsilateral (dark red) and contralateral (light red) limb, and quiescent VASTI→FHL interaction (right) from ipsilateral (dark blue) and contralateral (light blue) were presented to show bilateral effect of unilateral lesion. In *B*, same interactions were presented across varying background forces. Left, interaction from FHL to VASTI in ipsilateral (dark red) and contralateral (light red) limb, and on the right are interactions from VASTI to FHL from ipsilateral (dark blue) and contralateral (light blue) limb.

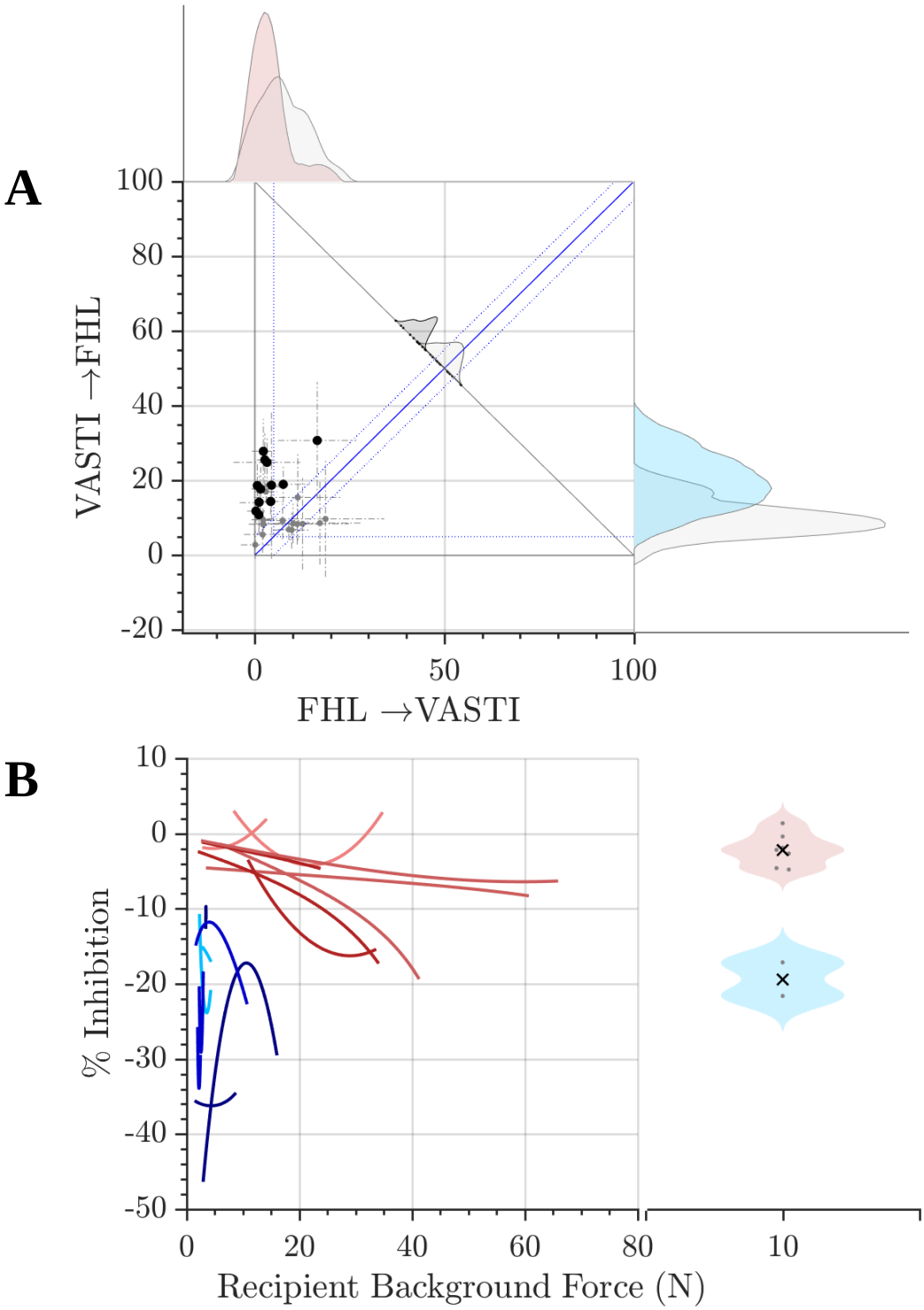

Figure 3-7: VASTI ↔ FHL interaction across all cats. In *A* are quiescent data pooled across all cats. The averages of interaction from FHL to VASTI are plotted against the averages of interaction from VASTI to FHL across LHS (black markers) and CNT cats (grey markers). The pink filled trace is the distribution of FHL→VASTI magnitudes, and blue filled trace is the distribution of VASTI→FHL magnitudes from LHS cats. In the background are light grey filled distributions of magnitudes from CNT cats. In *B* are pooled active data across LHS cats. The FHL→VASTI interactions are in red-pink color, while interaction VASTI→FHL interactions are blue-light blue. The intensity of coloring corresponds to recovery time-points. The longer recovery period the darker the color. On the right, is a snapshot of interaction magnitude at 10 N of recipient background force.

3.3.2 The FHL, which is primarily a toe flexor and ankle extensor, consistently and strongly inhibits all other ankle extensors, but not knee extensor, following lateral hemisection, resulting in a strong distal to proximal bias in interactions involving ankle extensors

It has been previously recognized that interneurons mediating FHL force feedback are under tight supraspinal control (Eccles and Lundberg 1959)[4]. In this study, we have shown that removal of this control results in amplified inhibition from FHL onto other ankle extensors, but not knee extensors. Inhibition onto FHL from other ankle extensor muscles is slightly increased or unchanged. Homonymous feedback arising from FHL does not undergo significant change following lateral hemisection (described in detail in Chapter II).

3.3.2.1 <u>FHL inhibits GAS more strongly than vice versa, resulting in distal to proximal bias</u>

Bonasera was first to report sizeable bidirectional inhibition linking FHL and GAS (Bonasera and Nichols 1994). Lyle confirmed the inhibitory nature of this interaction and found variability in this interaction. In one case, FHL inhibited GAS very strongly, while inhibition in the other way was mediocre. This type of interaction was associated with patterns 2 and 3. Another case observed was mutual medium inhibition, as in pattern 1 (Lyle and Nichols 2018). Preliminary (Niazi 2015) and the current study are in agreement that the interactions between GAS and FHL remain purely inhibitory in quiescent and

[4] Eccles and Lundberg (1957) reported that FDL was a powerful source of inhibition to other muscles, but more recent results indicate that this inhibition emerges from FHL, while FDL provides relatively little force feedback (Bonasera and Nichols 1994). The studies of Eccles and coworkers depended upon electrical stimulation of muscle nerves, it may have been difficult to distinguish contributions of these two synergists.

active conditions in LHS cats. Inhibition magnitude from FHL onto GAS was larger than the other way around ($p < 0.05$, Figure 3-9: A), and although magnitudes varied, they were stronger than in spinally-intact cat ($p < 0.05$, evident as a positive shift in probability density distributions in Figure 3-9: A, and Table 3-4). Inhibition from GAS onto FHL did not differ significantly between LHS and CNT groups ($p = 0.08$, Figure 3-9: A). The FHL dominated this interaction in the active conditions across all background forces (Figure 3-9: B), and although interaction onto GAS was quite variable (Figure 3-9: B), it was consistently stronger than the other way around. At 10 N of GAS background force, inhibition by FHL was 45 ± 18%, whereas at the same background force, GAS inhibited FHL by only 8 ± 7% (Figure 3-9: B).

Table 3-4: FHL ↔ GAS quiescent interactions across recovery time-points and limbs. Details of this interaction are presented as the mean ± standard deviation, for all three-recovery time-points, in both limbs, ipsilateral and contralateral to the lesion. For comparison purposes, presented are the mean ± standard deviation from CNT cats. Additionally, the number of muscle pairs evaluated and the net bias are given in the last column.

			FHL→GAS	**GAS→FHL**	**FHL↔GAS**
			Magnitude M ± SD (%)	*Magnitude M ± SD (%)*	*N, BIAS*
Control			17.8 ± 10.2	5.9 ± 3.8	1/22, P→D 7/22, B 14/22, D→P
Lateral Hemisection	3 wks	contralateral	15.31 ± 17.8	1.45 ± 2.3	2/16, B 14/16, D→P
		ipsilateral	10.61 ± 11.3	3.92 ± 3.11	
	7 wks	contralateral	27.17 ± 18.5	6.91 ± 2.7	
		ipsilateral	43.37 ± 15.7	5.25 ± 2.3	
	12 wks	contralateral	9.2 ± 4.9	8.4 ± 1.7	
		ipsilateral	17.41 ± 7.6	7.99 ± 2.6	

The inhibition from FHL onto GAS increased throughout the recovery time points, peaking at week seven and subsequently subsiding (Table 3-4). On the other hand, inhibition from GAS onto FHL, after initial suppression slowly surpassed control values (Table 3-4). As such, GAS↔FHL bias is more balanced in week 12 compared to immediately after the injury. There was noticeable variability between ipsilateral and contralateral limbs, specifically at seven weeks after the injury, inhibitory force-feedback from FHL onto GAS is twice as strong in the ipsilateral limb, compared to contralateral, while interaction the other way does not differ across limbs. Consequently, distal to proximal directional bias is stronger on the ipsilateral than on contralateral side (Figure 3-8: A & B, Table 3-4).

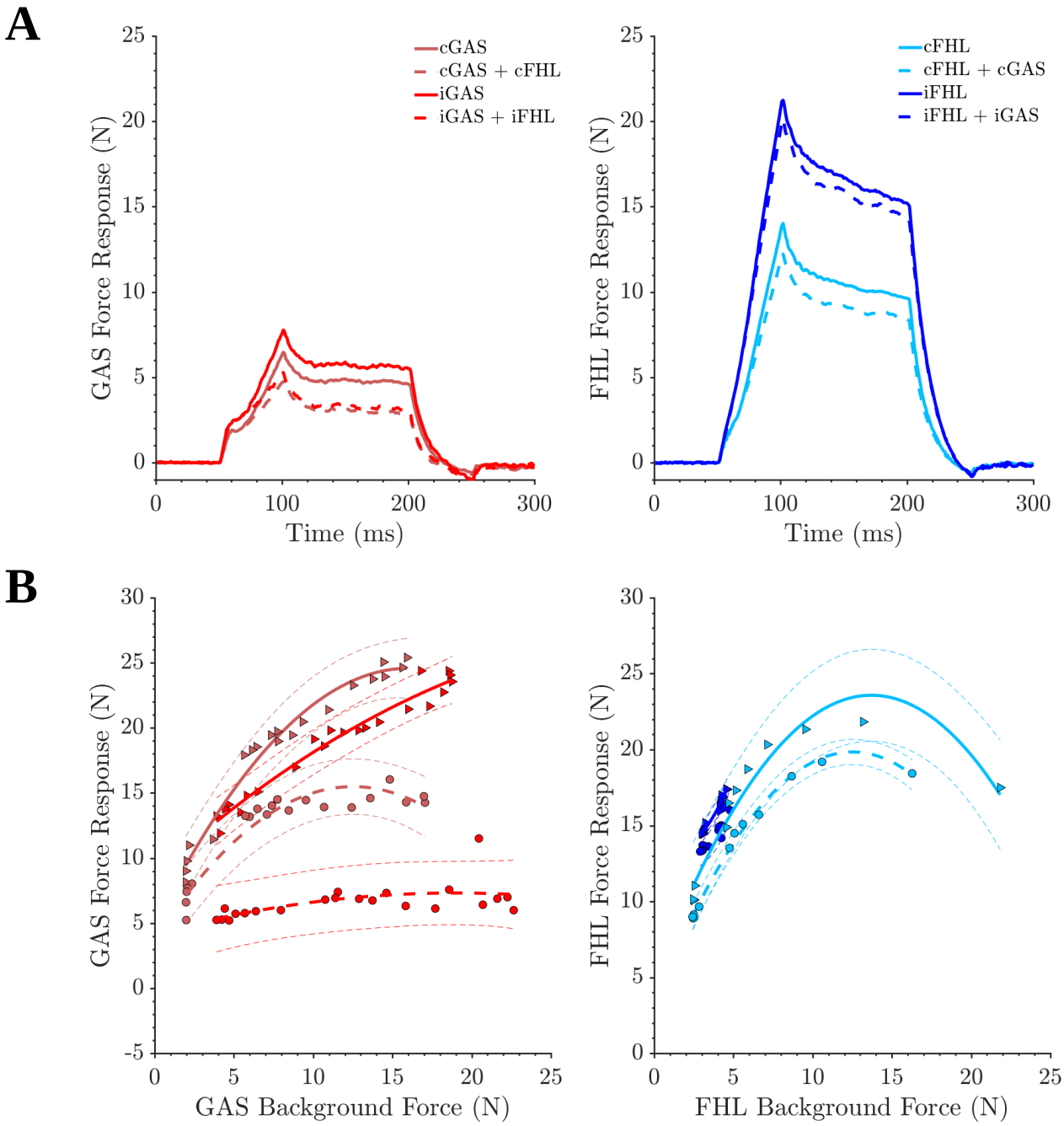

Figure 3-8: FHL ↔ GAS interaction in a representative cat. In *A*, quiescent FHL→GAS interactions (*left*) from ipsilateral (dark red) and contralateral (light red) limb, and quiescent GAS→FHL interaction (*right*) from ipsilateral (dark blue) and contralateral (light blue) were presented to show bilateral effect of unilateral lesion. In *B*, same interactions were presented across varying background forces. Left, interaction from FHL to GAS in ipsilateral (dark red) and contralateral (light red) limb, and on the right are interactions from GAS to FHL from ipsilateral (dark blue) and contralateral (light blue) limb. Only poor GAS response to crossed-extension was obtained (left, dark blue) in this cat, but in order to show bilateral effect of LHS, we decided to present this trial.

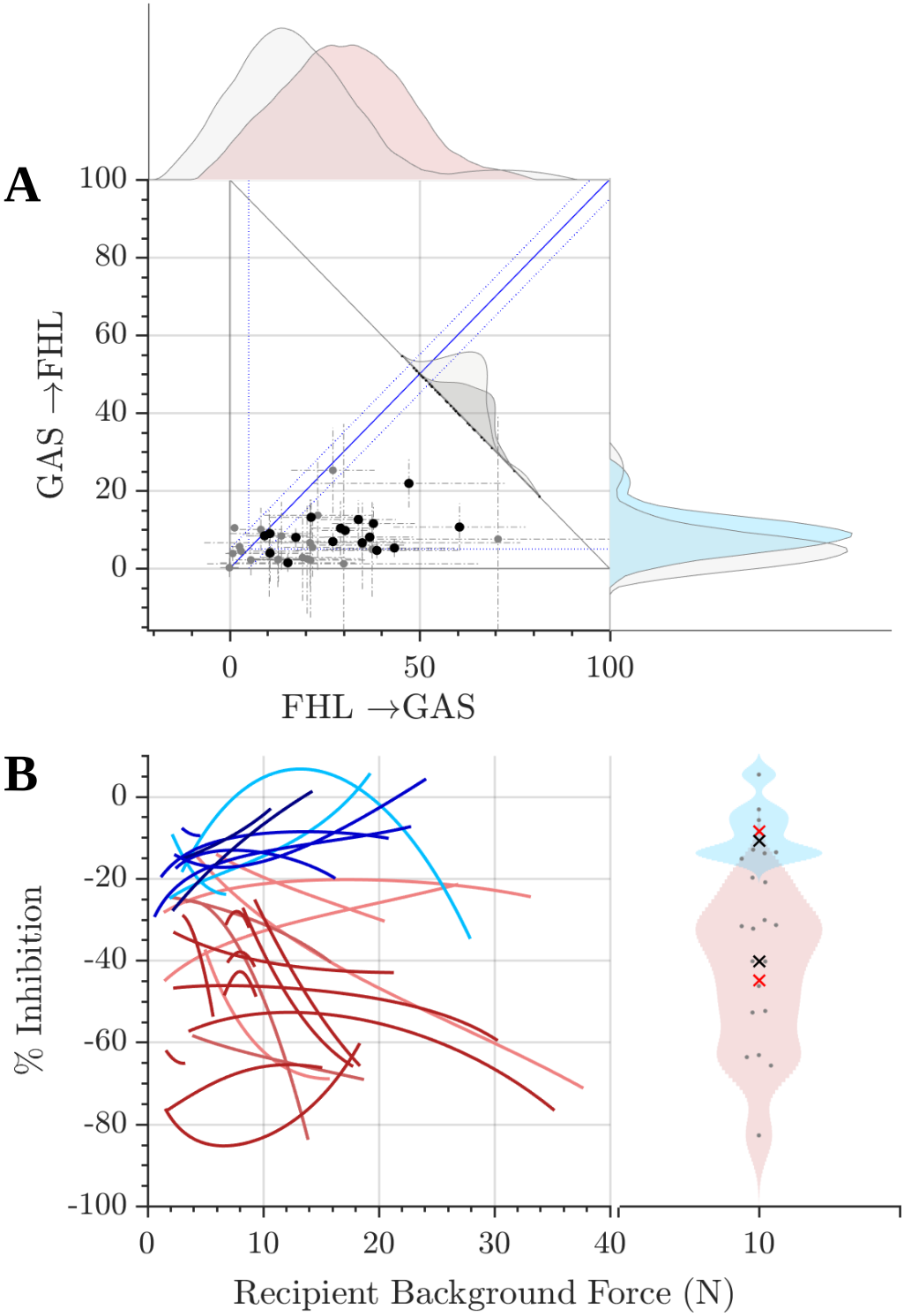

Figure 3-9: FHL ↔ GAS interaction across all cats. In *A* are quiescent data pooled across all cats. The averages of interaction from FHL to GAS are plotted against the averages of interaction from GAS to FHL across LHS (black markers) and CNT cats (grey markers). The pink filled trace is the distribution of FHL→GAS magnitudes, and blue filled trace is the distribution of GAS→FHL magnitudes from LHS cats. In the background are light grey filled distributions of magnitudes from CNT cats. In *B* are pooled active data across LHS cats. The FHL→GAS interactions are in red-pink color, while interaction GAS→FHL interactions are blue-light blue. The intensity of coloring corresponds to recovery time-points. The longer recovery period the darker the color. On the right, is a snapshot of interaction magnitude at 10 N of recipient background force.

3.3.2.2 The FHL inhibits PLANT strongly, while PLANT does not inhibit FHL, resulting in a strong distal to proximal bias

The interactions between FHL and PLANT in spinally-intact cats were inhibitory with strong FHL onto PLANT inhibitory bias and weak or not significant PLANT to FHL interaction (pattern 2 and 3), or they were balanced (pattern 1) (Lyle and Nichols 2018). In cats with LHS, it was predominantly strong inhibition from FHL onto PLANT in both quiescent (Figure 3-11: A) and active conditions (Figure 3-11: B). Compared to spinally-intact cats, the magnitude of this inhibition was larger in LHS cats ($p < 0.05$), despite considerable variability (Figure 3-11: A).

Under the active condition, the inhibition from FHL onto PLANT is apparent and pronounced (Figure 3-11: B). While PLANT does not physiologically interact with FHL across its varying background forces, FHL inhibits PLANT strongly, and that inhibition seems to be strongly dependent on PLANT background force, as an increase in force increases the amount of inhibition (Figure 3-11: B). At 10 N of background force, FHL inhibits PLANT 93 ± 40%, while PLANT inhibits FHL about 0.7 ± 4%, making it the most biased distal to proximal interaction observed in this study.

The recovery time-course of this interaction was similar to that of FHL and GAS interaction; the increase in inhibition magnitudes from FHL onto PLANT peaks in week seven post-LHS (Table 3-5). On the other hand, inhibitory interactions from PLANT to FHL slowly increases through recovery time-points. The oddity is consistently stronger FHL onto PLANT inhibition in the contralateral limb, while PLANT to FHL was stronger

in the ipsilateral limb (Figure 3-10: A). Consequently, distal to proximal bias was stronger in a contralateral side (Table 3-5).

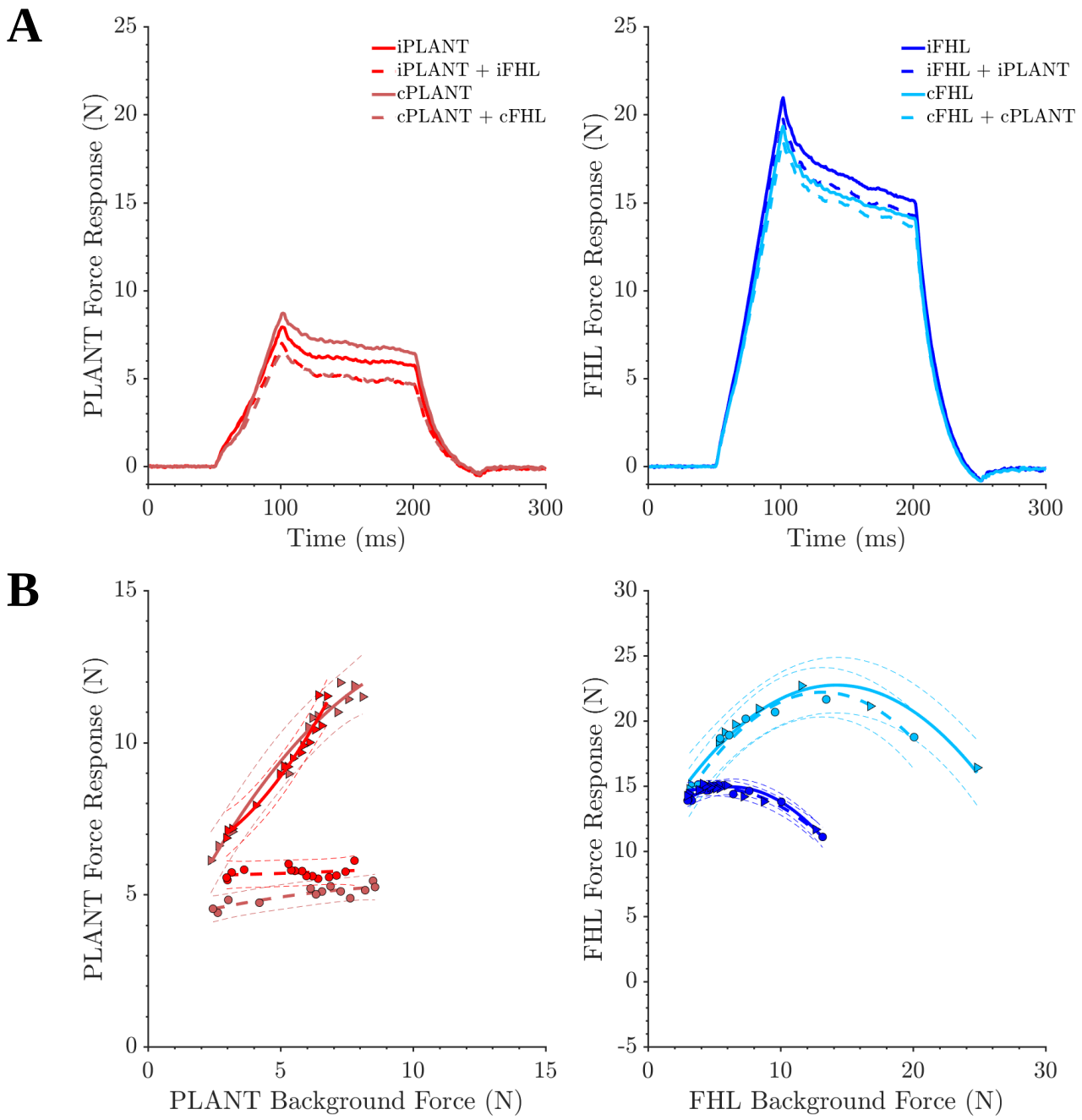

Figure 3-10: FHL ↔ PLANT interaction in a representative cat. In *A*, quiescent FHL→PLANT interactions (left) from ipsilateral (dark red) and contralateral (light red) limb, and quiescent PLANT→FHL interaction (right) from ipsilateral (dark blue) and contralateral (light blue) were presented to show bilateral effect of unilateral lesion. In *B*, same interactions were presented across varying background forces. Left, interaction from FHL to PLANT in ipsilateral (dark red) and contralateral (light red) limb, and on the right are interactions from PLANT to FHL from ipsilateral (dark blue) and contralateral (light blue) limb.

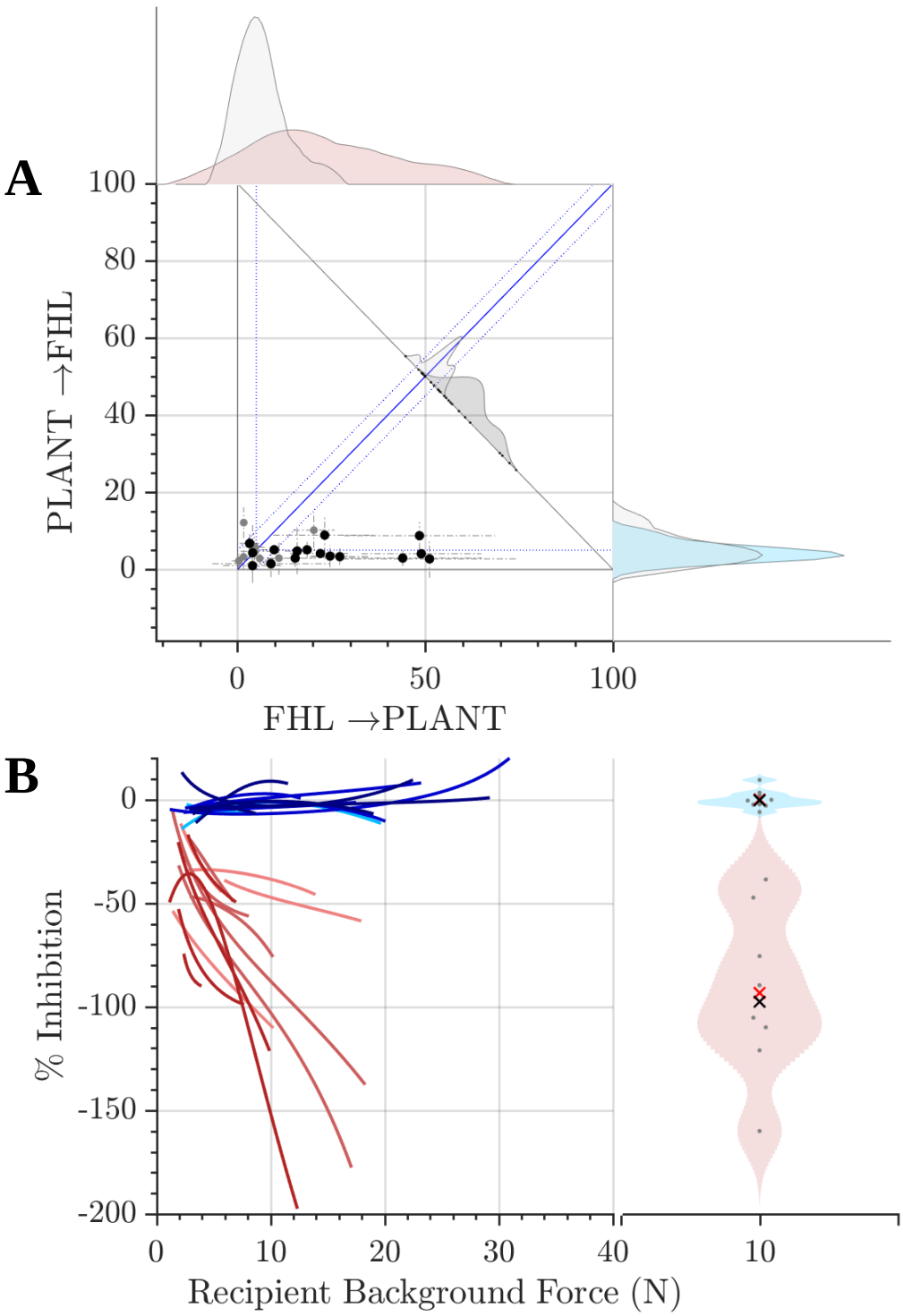

Figure 3-11: FHL ↔ PLANT interactions across all cats. In *A* are quiescent data pooled across all cats. The averages of interaction from FHL to PLANT are plotted against the averages of interaction from PLANT to FHL across LHS (black markers) and CNT cats (grey markers). The pink filled trace is the distribution of FHL→PLANT magnitudes, and blue filled trace is the distribution of PLANT→FHL magnitudes from LHS cats. In the background are light grey filled distributions of magnitudes from CNT cats. In *B* are pooled active data across LHS cats. The FHL→PLANT interactions are in red-pink color, while interaction PLANT→FHL interactions are blue-light blue. The intensity of coloring corresponds to recovery time-points. The longer recovery period the darker the color. On the right, is a snapshot of interaction magnitude at 10 N of recipient background force.

Table 3-5: FHL ↔ PLANT quiescent interactions across recovery time-points and limbs. Details of this interaction are presented as the mean ± standard deviation, for all three-recovery time-points, in both limbs, ipsilateral and contralateral to the lesion. For comparison purposes, presented are the mean ± standard deviation from CNT cats. Additionally, the number of muscle pairs and the net bias are given in the last column.
.

			FHL→PLANT	**PLANT→FHL**	**FHL↔PLANT**
			Magnitude M ± SD (%)	*Magnitude M ± SD (%)*	*N, BIAS*
Control			0.33 ± 1.8	2.18 ± 1.8	1/10, D→P 6/10, B 3/10, P→D
Lateral Hemisection	3 wks	contralateral	8.91 ± 15.6	1.46 ± 3.5	4/16, B 12/16, D→P
		ipsilateral	3.99 ± 7.9	0.99 ± 2.8	
	7 wks	contralateral	27.23 ± 7.6	3.33 ± 2.2	
		ipsilateral	18.53 ± 4.1	5.1 ± 2.1	
	12 wks	contralateral	22.1 ± 8.0	4.12 ± 0.8	
		ipsilateral	3.22 ± 2.6	6.76 ± 2.6	

3.3.3 The close ankle extensor synergists, GAS and PLANT, either exchange balanced strong inhibition or directional distal to proximal inhibition, resembling varying patterns observed in spinally-intact cats.

In spinally-intact cats, the interaction between GAS and PLANT was either strong and balanced, or biased toward GAS (Lyle and Nichols 2018). It is this latter pattern that we see most commonly after lateral hemisection, although, in week 12, these two directions seem to equalize resulting in a balanced, but strong interaction. The distal to proximal bias was observed bilaterally (Figure 3-12: A & B, Table 3-6).

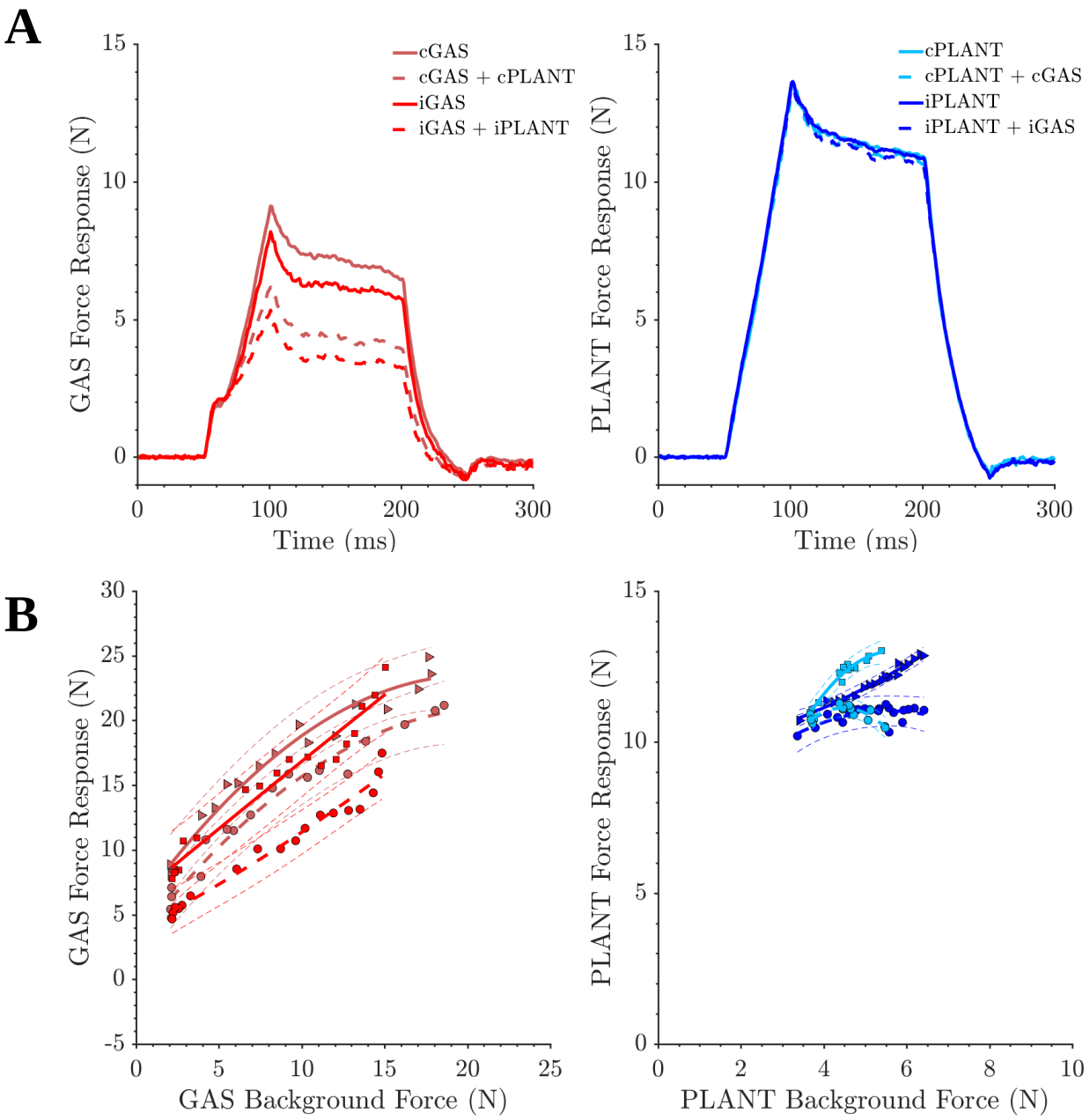

Figure 3-12: PLANT ↔ GAS interaction in a representative cat. In *A*, quiescent PLANT→GAS interactions (left) from ipsilateral (dark red) and contralateral (light red) limb, and quiescent GAS→PLANT interaction (right) from ipsilateral (dark blue) and contralateral (light blue) were presented to show bilateral effect of unilateral lesion. In *B*, same interactions were presented across varying background forces. Left, interaction from PLANT to GAS in ipsilateral (dark red) and contralateral (light red) limb, and on the right are interactions from GAS to PLANT from ipsilateral (dark blue) and contralateral (light blue) limb.

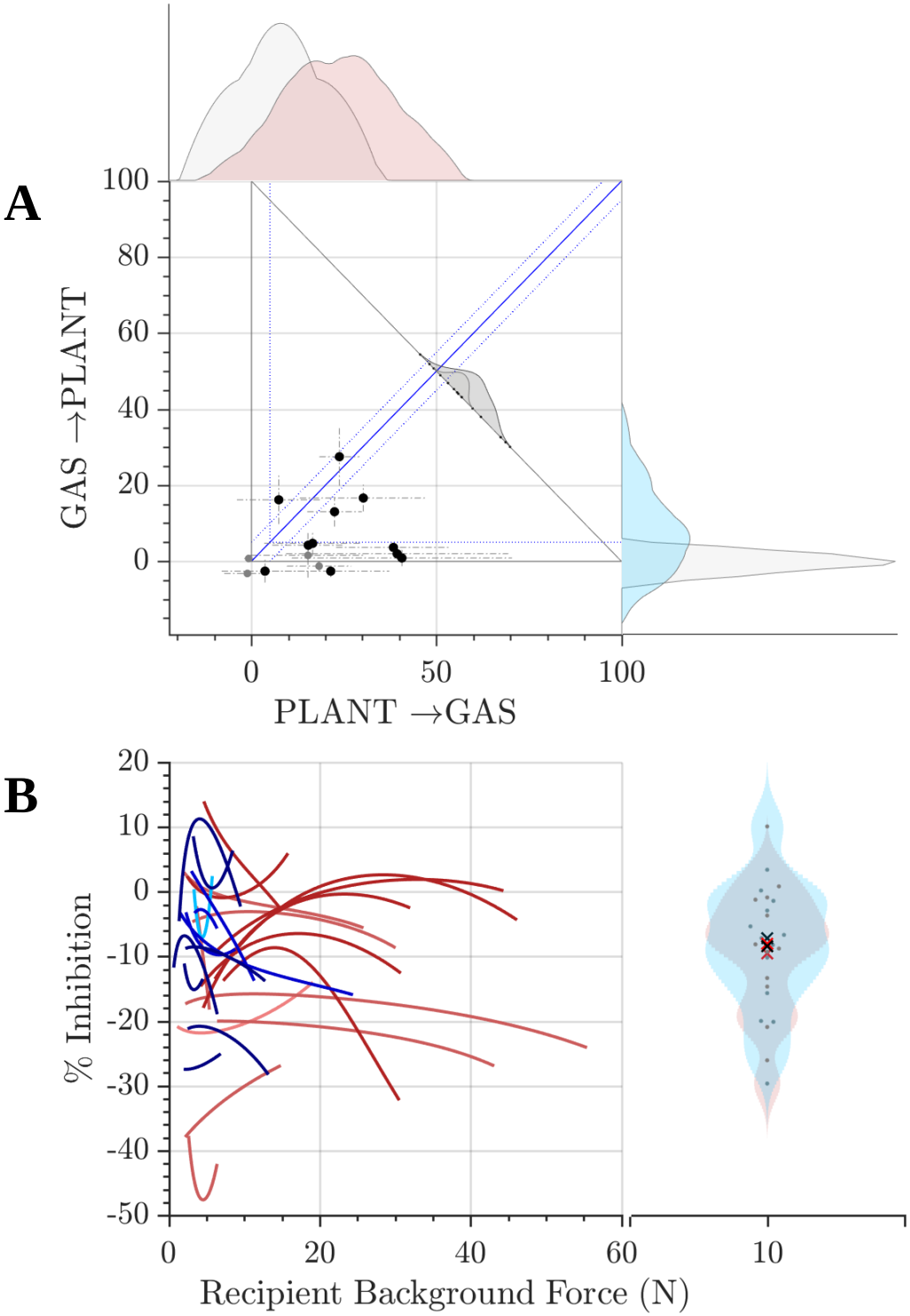

Figure 3-13: PLANT ↔ GAS interaction across all cats. In *A* are quiescent data pooled across all cats. The averages of interaction from PLANT to GAS are plotted against the averages of interaction from GAS to PLANT across LHS (black markers) and CNT cats (grey markers). The pink filled trace is the distribution of PLANT→GAS magnitudes, and blue filled trace is the distribution of GAS→PLANT magnitudes from LHS cats. In the background are light grey filled distributions of magnitudes from CNT cats. In *B* are pooled active data across LHS cats. The PLANT→GAS interactions are in red-pink color, while interaction GAS→PLANT interactions are blue-light blue. The intensity of coloring corresponds to recovery time-points. The longer recovery period the darker the color. On the right, is a snapshot of interaction magnitude at 10 N of recipient background force (for GAS) and 5 N (for PLANT).

Table 3-6: PLANT ↔ GAS quiescent interactions across recovery time-points and limbs. Details of this interaction are presented as the mean ± standard deviation, for all three-recovery time-points, in both limbs, ipsilateral and contralateral to the lesion. For comparison purposes, presented are the mean ± standard deviation from CNT cats. Additionally, the number of muscle pairs evaluated and the net bias are given in the last column.ND denotes no data.

			PLANT→GAS	**GAS→PLANT**	**PLANT↔GAS**
			Magnitude M ± SD (%)	*Magnitude M ± SD (%)*	*N, BIAS*
Control			-1.09 ± 6.3	-3.22 ± 0.79	2/4 B 2/4 P→D
Lateral Hemisection	3 wks	contralateral	3.67 ± 11.7	-2.6 ± 3.0	1/11 D→P 1/11 B 9/11 P→D
		ipsilateral	21.44 ± 15.8	-2.6 ± 1.6	
	7 wks	contralateral	39.37 ± 30.0	2.00 ± 1.5	
		ipsilateral	38.39 ± 15.5	3.63 ± 0.9	
	12 wks	contralateral	23.78 ± 5.4	27.50 ± 7.6	
		ipsilateral	19.78 ± 5.8	ND	

3.3.4 Interactions involving SOL muscle were more variable likely due to common excitatory length dependent linkage this muscle shares with other muscles

The quiescent interactions between VASTI and SOL were either not significant bidirectionally (6/9), weakly inhibitory from VASTI onto SOL (11.46 ± 7.00%) and negligible in other direction (1/9), and weakly excitatory from SOL onto VASTI (5 - 10% excitation in 2/9), and negligible in the other direction.

The GAS and SOL muscle share both excitatory length and inhibitory force feedback (Nichols 1989). In this study, GAS excited SOL in 3/3 cases by 4, 41, and 67%, while SOL either did not have a significant effect (in 2/3) or it inhibited GAS in 1/3 cases (by 13%). Under the active conditions, inhibition was frequently observed at high forces, while excitation is dominant at low forces.

We have also evaluated the interaction between FHL and SOL and confirmed the previous conclusion that these interactions remain inhibitory following LHS (Niazi 2015). The averaged magnitudes of FHL onto SOL quiescent interactions were larger than the other way around ($p < 0.05$), 15% vs. 4% respectively. In 3 out of 8 interactions evaluated, the interaction was insignificant and balanced in both directions. In the active condition, inhibition from FHL onto SOL amplified, while it was unchanged and negligible in the other direction.

3.3.5 The magnitude of inhibition each muscle receives and donates suggests convergent force feedback bias

Examining the total inhibition that muscle receives and donates, reveals convergent directional bias onto ankle extensors (Figure 3-14, Figure 3-16). Since all cats exhibited the same directional bias across both limbs, it was acceptable to pool the data together and present averaged values of incoming and outgoing inhibition (Figure 3-14). The VASTI muscle donates the most inhibition onto other muscles and receives the least. The GAS muscle recieves the most inhibition while donates the least. Other muscles lie on a spectrum between these two extremes (Figure 3-14). The magnitudes of individual interactions were presented in Figure 3-16.

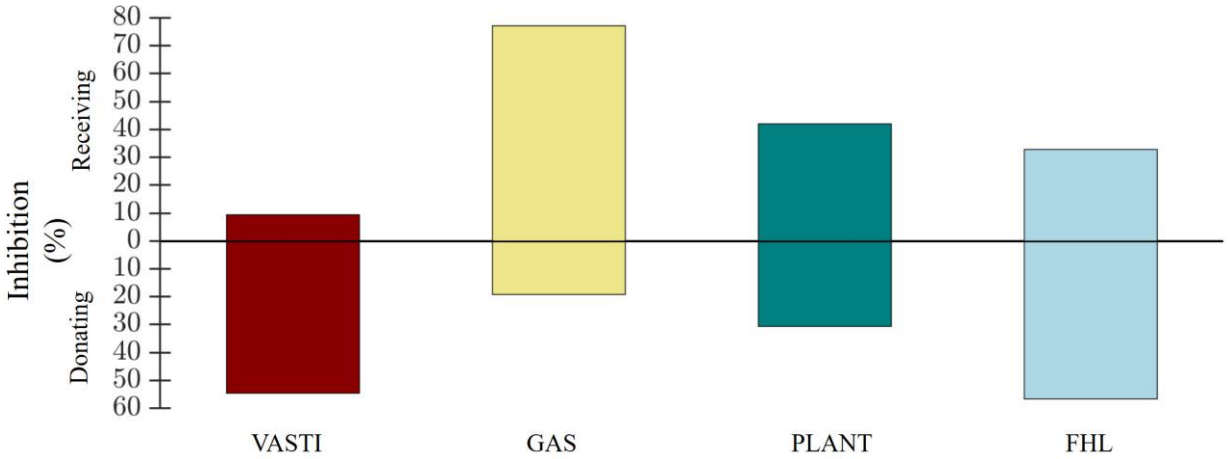

Figure 3-14: Average amount of inhibition each muscle receives and donates. As is evident VASTI and FHL donate the most inhibition, while GAS and PLANT receive the most of inhibition. This results in a convergent inhibitory force feedback bias targeting the main ankle extensors.

3.3.6 Reduction in degrees of freedom in regulation of force feedback following LHS, as potential explanation of consistently observed convergent bias

The variability in magnitudes of individual interactions, despite the consistency of directional bias, suggests that force dependent interactions of lesioned cats lie on a spectrum, as a continuation of the spectrum we observed in spinally-intact cats. That is why we evaluated every single interaction within a cat with LHS and spinally-intact cat against arbitrarily chosen bias. Specifically, we determined the bias based on a directionality of VASTI↔FHL interaction of each cat in the same way as described in methods (Figure 3-1, equation 3.3). This arbitrarily chosen bias serves as a surrogate for stiff knee and compliant ankle (when VASTI→FHL inhibition is stronger than FHL→VASTI) on one side, and compliant knee and stiff ankle (when VASTI→FHL inhibition is weaker than FHL→VASTI) on the other side of the spectrum. The bias on the x-axis in Figure 3-15 ranged from proximal→distal on the left side to distal→proximal on

the right side of the figure. Next, we plotted each quiescent muscle interaction against that bias in separate subplots. This way we were able to compare magnitudes of interactions against the bias across all cats, where vertically aligned data points belong to individual cats. We found that data from LHS (Figure 3-15, filled marker) and CNT (Figure 3-15, open marker) cats lie on a spectrum of proximal→distal to distal→proximal bias. An interaction from more distal muscle onto more proximal in a pair has been colored in pink, whereas the interaction from more proximal muscle onto more distal one has a blue coloring in each subplot. Next, we fitted a least squares quadratic polynomial curves ± 2 standard deviations (linear regression for GAS↔PLANT interaction) to each individual muscle pair interaction with respect to the bias (solid lines, colored according to the direction of interaction). As the inhibition from VASTI onto ankle extensors subsides, interaction from the same ankle extensors onto VASTI increases. Along the spectrum, the switch from proximal→distal to distal→proximal bias happens across all muscle interactions involving VASTI. The inhibitory interactions from FHL onto other ankle extensors subsided as well as bias moves to distal→proximal, and in the middle of the spectrum, we observe balanced interaction and bias switch. Linear regression was a better fit for GAS↔PLANT interaction (judged by the lack-of-fit sum of squares). This may be due to a much smaller data sample of this muscle pair interaction, compared to other muscle pairs. On one end of the spectrum, at more substantial inhibition from VASTI onto FHL than vice versa, we observe clustered data (filled markers) from cats with lateral hemisection (a consistent directional bias). Observed individual interactions between muscle pairs of LHS cats were depicted on the far left of Figure 3-15. Going along the spectrum toward the distal→proximal bias we observed scattered data (open markers) from

spinally-intact decerebrate cats (justifying three patterns of force feedback organization). Using coefficients obtained from fitting data from LHS and CNT cats, we were able to project and propose what interactions could be at very strong distal→proximal bias (broken lines). At this far right, we observed, coupled with strong inhibition of VASTI by ankle extensors, an emergence of excitation amongst ankle extensors (possible bias of intermuscular interactions were depicted to the far right of the Figure 3-15). This potential pattern would render knee compliant and ankle stiff. The excitation of ankle extensors by other ankle extensors was observed in quietly standing cat previously (Pratt 1995). It might be proposed that decerebration disables these excitatory interactions in non-locomoting cats, just as spinalization disables other possible patterns, progressively reducing degrees of freedom in the regulation of the force feedback.

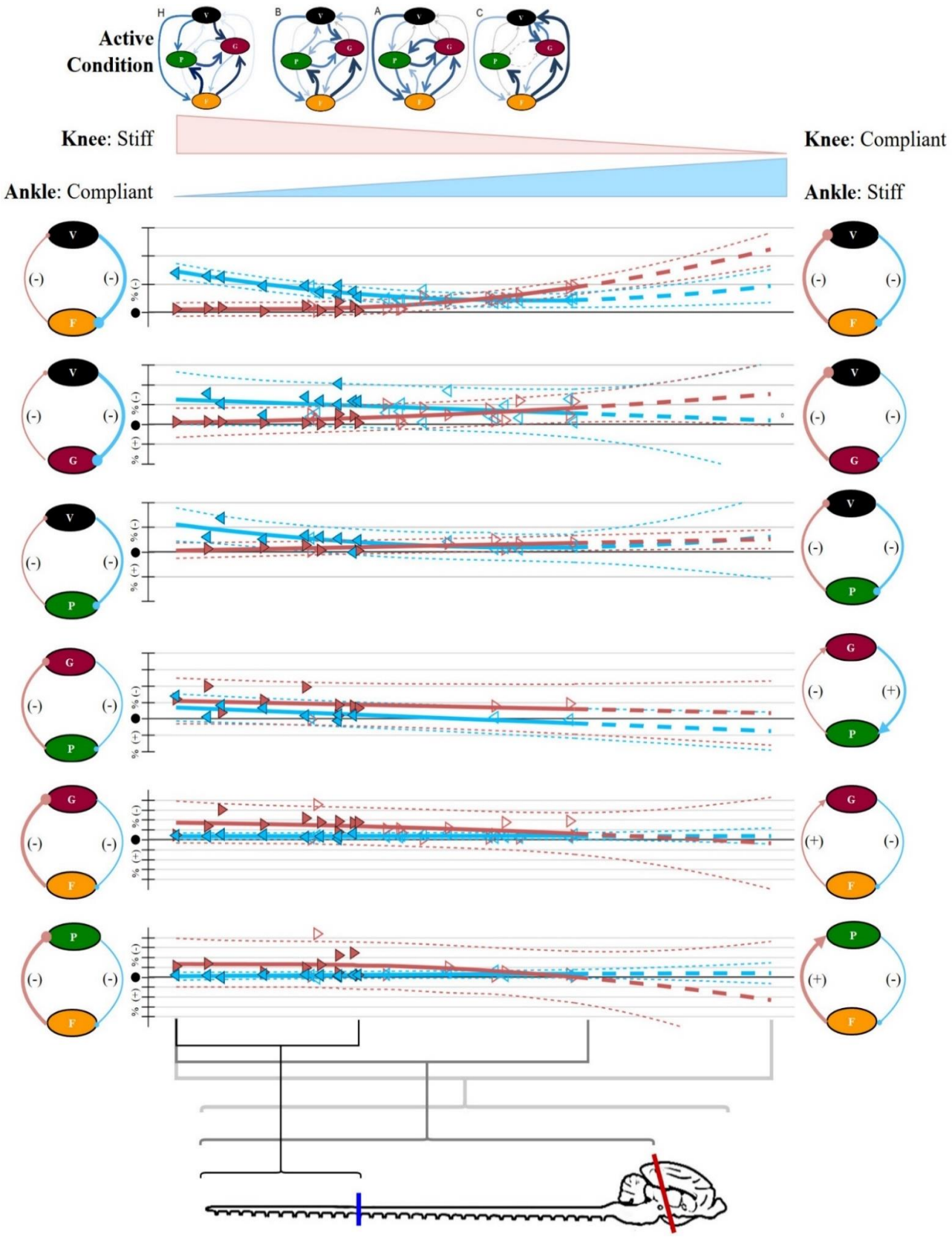

Figure 3-15: Reduction of degrees of freedom as potential explanation of observed data. All data lies on spectrum of proximal→distal to distal→proximal bias. However, data from LHS cats are limited to only one side of the spectrum, while CNT data are scattered and can assume several directional bias patterns.Detailed explanation is in text.

3.4 Discussion

In this chapter, we presented data that suggest that spinal cord circuitry can support only one type of force feedback organization. Consistently and chronically directed (i.e., selectively amplified) inhibition was observed only onto ankle extensors, while other muscles, most proximal (VASTI) and most distal (FHL), receive negligible inhibition (Figure 3-14, Figure 3-16). At the same time, the most proximal and most distal muscles were donors of inhibition directed onto ankle extensors. The interactions between GAS and PLANT seem to be the least affected by lateral hemisection as both magnitude and varied bias resemble variety observed in spinally-intact cats. At the limb-level, these individual intermuscular interactions assemble into a consistent and bilaterally observed pattern resembling selectively amplified and depressed interactions of pattern 2 in spinally-intact cats (Lyle and Nichols 2018).

Previously, in the spinal decerebrate cat, the electrophysiological studies reported indiscriminate amplification of inhibition among ankle extensor muscles (Eccles and Lundberg 1959). It was suggested that supraspinal centers exert a tonic inhibition onto interneurons that relay impulses from these afferents, thus severing supraspinal pathways releases inhibitory effect. Using a stretch evoked force feedback mechanographic method, we found a selective amplification and suppression of inhibitory force feedback magnitudes following lateral hemisection. The inhibition from proximal (VASTI) and distal (FHL) muscles was amplified but, suppressed from ankle extensors, such as GAS. It had been shown that interneurons mediating Ib inhibitory actions from FHL (Note: footnote 4, page 94) are more tightly controlled compared to those mediating Ib actions from other ankle extensors (Eccles and Lundberg 1959). We can provide support for this

finding as, following the lateral hemisection, inhibition from FHL onto other ankle extensors amplified significantly (but not the other way around). Additionally, Ib actions from VASTI onto all ankle extensors tested amplified while interaction in the other direction diminished. We propose that interneurons mediating Ib actions form VASTI undergo similar tonic inhibition by supraspinal tracts (in spinally-intact cats), as FHL interneurons do.

In this study, the consistent convergent bias is observed bilaterally despite the unilateral lesion. It is possible that uninjured contralateral pyramidal fibers make connections onto interneurons on the lesion side caudal to the lesion. Similarly, removal of crossed supraspinal fibers connections from the uninjured side has the same effect as on lesion side, thus indirectly impairing undamaged side. This could potentially decrease a deficit gap between the injured and undamaged side and produce strong directional bias in both limbs.

All intermuscular interactions examined via the mechanographic method in the decerebrate cat are inhibitory, with the exception of SOL interactions that shares excitatory Ia pathways with other muscles. Previously, in locomoting decerebrate cat, the autogenic excitatory force feedback was observed only in specific muscles (Ross 2006), while interactions between extensor muscles remain inhibitory (Ross and Nichols 2009) exhibiting proximal to distal bias of inhibition resembling pattern 1 in the decerebrate non-locomoting cat (Lyle and Nichols 2018). Intermuscular stimulation studies in intact and quietly standing cat have suggested that twitch evoked feedback, presumably GTO feedback, in awake and stationary cat, is indeed widespread, but excitatory (Pratt 1995). The evidence for excitatory GTO feedback is stronger for a locomoting cat. Studies that

employed electrical nerve stimulation and natural stimulation to evoke muscle feedback during locomotion have all shown excitatory (Pearson and Collins 1993, Prochazka, Gillard et al. 1997, Donelan and Pearson 2004) and widespread feedback (Guertin, Angel et al. 1995). These studies suggest that during locomotion excitatory force feedback contributes significantly to propulsion and stance during walking, as well as interjoint coupling. This apparent discrepancy in results regarding the sign of force feedback was reconciled as the coexistence of both excitatory and inhibitory components (Ross 2006), in various combinations, that are selectively employed or disengaged depending on a particular motor task.

The decrease in degrees of freedom in increasingly reduced preparations results in a reduction of available force feedback organizational patterns that the system is capable. In decerebrate, but the spinally-intact non-locomoting cat, force feedback organization, can take three distinct patterns as points on a biased spectrum. In decerebrate, spinally-lesioned cat, force feedback organization takes only one strongly directed pattern. It is plausible that all of these patterns, along with excitatory interactions that emerged from projections, are at the disposal of an intact nervous system in a control of joint stiffness (Figure 3-15).

3.4.1 Potential functional consequences of convergence of inhibition onto ankle extensors

The idea that supraspinal centers can selectively engage and depress reflex pathways in a task-dependent manner was proposed a long time ago (Lundberg 1979). Severing these modulatory tracts reduces the available selection to those that are grounded-in the spared circuitry caudal to spinal cord lesion. Nonetheless, disconnected spinal cord circuits can

sustain stepping (Barbeau and Rossignol 1987, Basso, Murray et al. 1994, Kuhtz-Buschbeck, Boczek-Funcke et al. 1996), and maintain stance (Fung and Macpherson 1999) in the spinal cat. These cats adapt a crouched gait with increased flexion during swing and stance (Rossignol, Drew et al. 1999) and exhibit diminished vertical and lateral stability (Macpherson and Fung 1999). Extrapolating findings from decerebrate and lesioned non-locomoting cat to freely walking cat with spinal lesion is difficult and mandates an assumption that intermuscular interactions among extensors are inhibitory. However, strongly biased inhibition onto ankle extensors could potentially explain flexed gait and difficulty with weight-acceptance phase observed by others (Barbeau and Rossignol 1987).

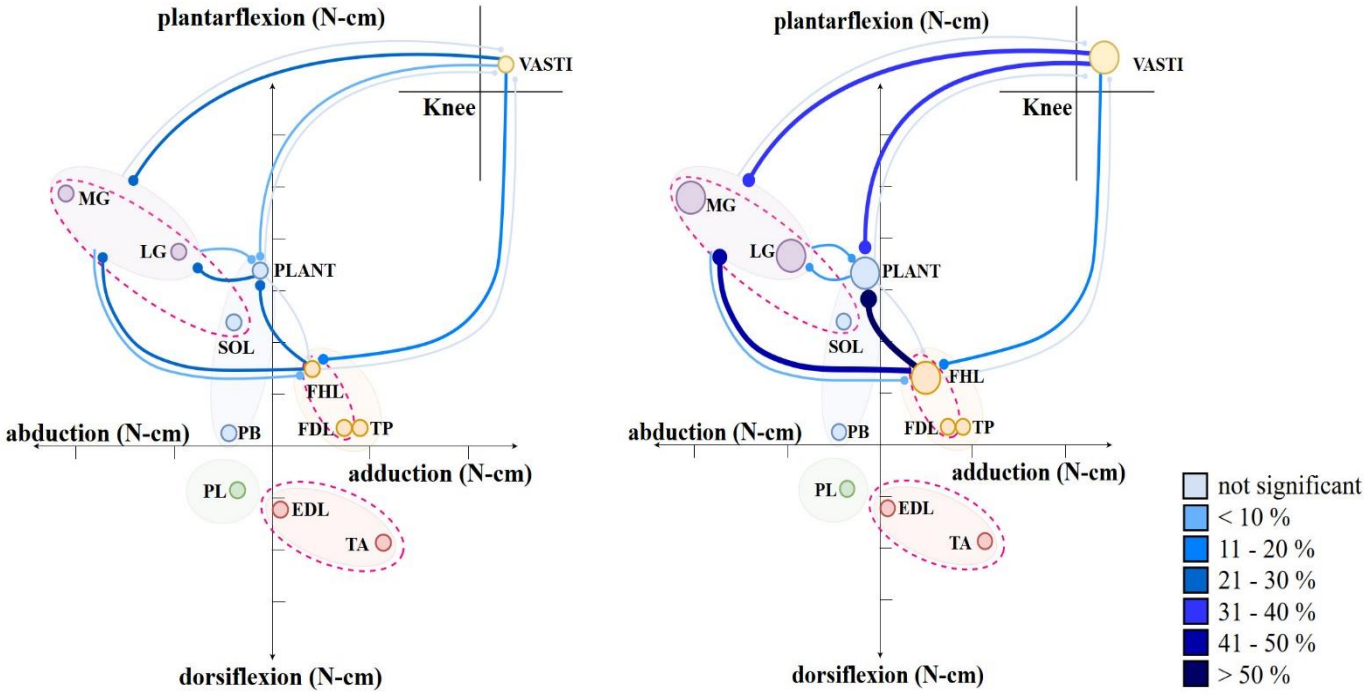

Figure 3-16: Potential functional consequences of convergence of inhibition onto ankle extensors. Observed interactions in quiescent (*left*) and active (*right*) conditions were plotted between established maximal torques of ankle extensors in the frontal (x-axis) and the sagittal (y-axis) plane.

During the stance phase, when all anti-gravity extensor muscles are active, strong inhibition onto ankle extensors would render ankle joint overly compliant and the weakest link in a limb. During level walking these cats probably exhibit ankle yield in the sagittal plane and adduct their ankles medially in the frontal plane as GAS (a significant ankle extensor and abductor (Lawrence, Nichols et al. 1993)) is significantly inhibited, while FHL (ankle extensor with 1/3 of the GAS extensor moment, and slight ankle adductor (Lawrence, Nichols et al. 1993)) is spared from this inhibition. Although muscles acting at the hip likely play a significant role in the maintenance of vertical posture, there is insufficient data describing interactions from and onto these muscles to draw conclusions regarding compliance of the hip joint, or impact of these muscles on knee or ankle compliance. It was reported previously, that rectus femoris (hip flexor and knee extensor) exchanges inhibitory force feedback with VASTI and GAS (Wilmink and Nichols 2003), but we have not evaluated directionality of this inhibition in lesioned cats. However, we presume that force feedback arising from muscles crossing hip (and potentially even trunk muscles) influence knee and ankle joint stiffness. Based on current data, ankle extensors do not significantly influence knee compliance. Therefore, the main conclusion of this chapter is that unregulated force feedback focused on ankle extensors may make the ankle excessively compliant and adducted during the stance phase of walking, thus contributing to vertical instability and difficulty at the weight-acceptance phase.

3.4.2 Potential modulatory supraspinal tracts

In this project, we also have sought to localize the supraspinal tract(s) responsible for modulating force feedback circuitry. The brainstem has been shown to play an active role in balance control (Schepens, Stapley et al. 2008, Stapley and Drew 2009), as

disrupting the connection between the brainstem and spinal cord disrupts balance and response to perturbations (Deliagina, Beloozerova et al. 2008, Honeycutt, Gottschall et al. 2009). Disinhibition of spinal interneurons following spinal lesions has been proposed to modulate stretch reflex gains (Jordan, Brownstone et al. 1992, Jankowska, Riddell et al. 1993), and the same mechanism might be involved in the change of force feedback gain. The dorsal reticulospinal tract has been indicated in control of clasp-knife inhibition but considering that amplification of force feedback was not accompanied with the presence of clasp-knife inhibition we consider this tract to be an unlikely regulator of force feedback. However, these cats exhibited selectively and transiently increase in gain of the stretch reflex, which has been discussed in detail in Chapter II, as is characteristic of lateral hemisection. As suggested in the introduction, a potential modulator of force feedback, that would also affect length feedback gain, may lay in ventral cord. In particular, tracts that mediate postural responses such as vestibulospinal (Nichols, Gottschall et al. 2014) and/or pontomedullary reticulospinal (Deliagina, Beloozerova et al. 2008, Stapley and Drew 2009) might be potential regulators of force feedback. In identifying the location of the regulatory tract(s), we have evaluated force feedback in cats with bilateral dorsal hemisection, and the findings were presented in Chapter V. Briefly, we observed all bias patterns found in spinally-intact cats and a sporadic clasp-knife inhibition. Thus, we suspect that the regulatory tract is indeed located in the ventral spinal white matter. However, future work is warranted to identify and characterize how descending systems influence the magnitude and bias of intermuscular force feedback.

CHAPTER 4. USING COMPUTATIONAL METHODS TO GENERATE FORWARD DYNAMIC SIMULATION OF STANCE PERTURBATION FROM MECHANOGRAPHIC DATA

4.1 Introduction

Stiffness has been extensively studied for single muscle/joint, and our understanding of control of posture and movement arises from those studies. Although it is clear that the nervous system modulates stiffness of a particular muscle, stiffness of the limb is more than a simple sum of stiffnesses of individual muscles. Indeed, many muscles span more than one joint, inherently linking the joints together. Furthermore, many joints are linked neutrally via heterogenic, i.e., intermuscular feedback exchanged between muscles. Observed changes in intermuscular feedback inevitably impact limb stiffness and therefore stability, but much less is known about the significance of this impact.

The mechanographic data from Chapter II and III suggest that amplified gain of excitatory length feedback from knee and ankle extensors and strong inhibitory convergent force feedback bias would render knee stiff and ankle compliant, following lateral hemisection (LHS). It follows that the ankle joint would be overly flexed during the weight acceptance phase and yield under cats' weight, which could potentially explain the crouched gait and flexed limbs frequently noted during locomotion of spinal cats (Barbeau and Rossignol 1987, Rossignol, Drew et al. 1999). On the other hand, the knee, based on Chapter III findings, would be overly extended partially due to its extensor muscles being spared the inhibitory effect and considerable inhibition directed onto its flexor muscles

(two-joint GAS and PLANT muscles). However, mechanographic data remain several steps removed from kinematics and kinetics data. In order to bridge the gap between these two types of data, we estimated joint angles and moments based on the stiffness of knee and ankle muscles and their intermuscular interactions in two LHS cats using a forward kinematics approach.

In preceding chapters, the data presented were based on an evaluation of individual muscles and their isolated interactions. Although the individual muscles are actuators of the motor system, the integration of length (Chapter II) and force feedback (Chapter III), and therefore the regulation of stiffness occurs at the level of proprioceptive networks that regulate whole-limb mechanics, rather than the level of individual muscles. How these two feedback systems, when integrated, govern the kinetics and kinematics of individual joints is not clear from data presented. Previous research has pointed to the role of length feedback in transforming the mechanical properties of individual muscles into more spring-like actuators, while the purpose of force feedback is to regulate compliance of joints throughout the limb.

To show that directed inhibitory force feedback can be significant contributor to the pronounced joint yield at the weight-acceptance phase, we estimated joint angles and moments in two states, autogenic and heterogenic state, and then subjected them to vertical perturbations. The autogenic state is result of an individual muscles' stretch responses, and heterogenic state is the sum of the inhibitory influence from all donor muscles onto stiffness of a recipient muscle. Additionally, two magnitudes of the heterogenic feedback were compared. One from a limb with a strong autogenic and strong inhibitory heterogenic (AH) feedback and another from a limb with a strong autogenic and weak inhibitory

heterogenic (Ah) feedback (Table 4-1). Any difference between autogenic and heterogenic state is due to the influence of inhibitory force feedback, and any difference between AH and Ah heterogenic states is due to the strength of inhibitory feedback.

Should estimates from heterogenic state predict more flexed joint angles under perturbations compared to autogenic state, that would suggest that unregulated force feedback could contribute to the crouched gait deficit following LHS. Furthermore, this suggestion would be bolstered in case if larger magnitudes of inhibitory feedback (as in AH limb) resulted in more flexed limb under perturbations compared to weaker inhibitory magnitudes (Ah limb).

4.2 Methods

The aim of this chapter was to estimate the effect of inhibitory force feedback onto joints during the maintenance of postural equilibrium. This was accomplished by predicting joint moments and joint angles from muscle stiffness and intermuscular interactions data recorded using a mechanographic method, and then impose vertical perturbations to an assembled geometric limb model. This is a four-step process that involved determining (i) slack muscle lengths and joint angles, (ii) initial (BGF) muscle

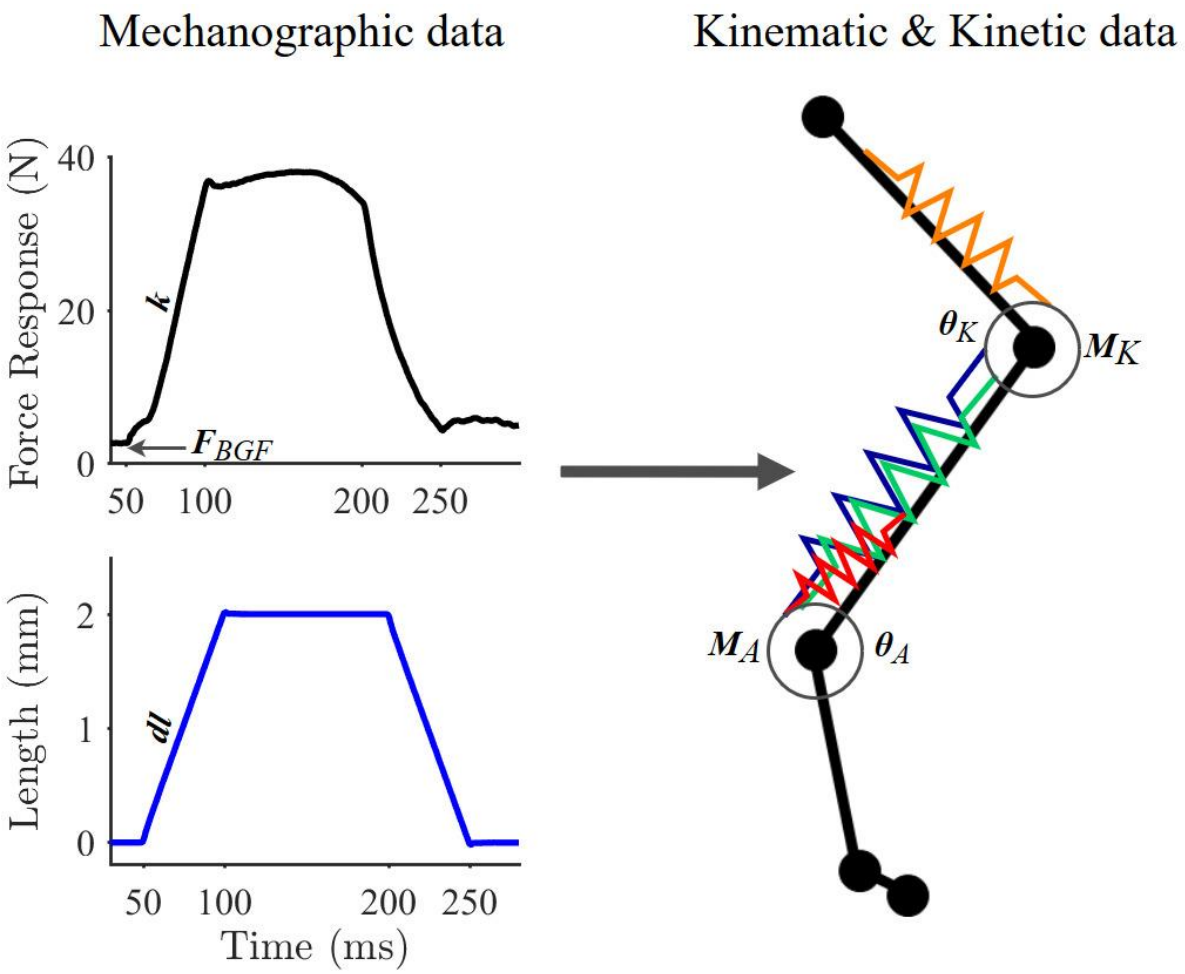

Figure 4-1: The goal of this chapter is to estimate the kinematic and kinematic data (*right*) (joint angles and moments) from mechanographic data (*left*) (initial force, stiffness and length change). Data from VASTI (yellow), GAS (blue), PLANT (green) and FHL (red) was used for this purpose, because of their strong force-feedback interactions.

lengths and joint angles, (iii) unloaded stance configuration and corresponding muscle forces and joint moments (Figure 4-1, left), and lastly (iv) imposing vertical perturbations in the form of cat's mass onto assembled limb and subsequent increase of the perturbation amplitude (Figure 4-2).

4.2.1 Muscles and their feedback features

Four extensors that exchange inhibitory feedback were chosen for this project. A knee extensor, VASTI is a one-joint muscle that extends the knee (moment arm is d = 9.7 mm/rad). Following LHS, it exhibited a strong amplification of the gain of stretch reflex (Chapter II) and donated a profound inhibition onto all ankle extensors (Chapter III). The GAS and PLANT are two joint muscles with flexion action at the knee (d = -8.7 mm/rad and d = -9.4 mm/rad, respectively) and extension action at the ankle (d = 15.35 mm/rad and d = 15.5 mm/rad, respectively) (Burkholder and Nichols 2004). The GAS stiffness also significantly increased following LHS (Chapter II) and inhibition onto this muscle increased from all sources (Chapter III). The PLANT stiffness did not undergo significant change (Chapter II), although inhibition onto this muscle increased (Chapter III). The FHL is also biarticular muscle, and it generates an extensor moment at the ankle (d = 2.3 mm/rad). The LHS does not impact its stiffness significantly (Chapter II), although following the LHS inhibition from FHL muscle onto other ankle extensors is greatly amplified (Chapter III).

The magnitudes of the stretch reflex gain (autogenic feedback/state) and the bias of inhibitory force feedback (heterogenic feedback/state) varied across LHS cats. In order to answer the question whether or not force-dependent inhibition has a significant effect on

the maintenance of postural equilibrium, two cases were compared; i.) strong autogenic feedback and weak heterogenic feedback (Ah limb) (Table 4-1, *left*), and ii.) strong autogenic feedback and strong heterogenic feedback (AH limb) (Table 4-1, *right*). Labeling an Ah limb as a representative of weak heterogenic feedback is not entirely correct since significant inhibition is still exchanged between VAST and GAS. However, it is weaker in comparison to AH limb in all interactions. Although there was an attempt to match the gain of the stretch reflex, i.e., muscular stiffness across AH and Ah muscles, that was not possible. The VASTI and GAS of Ah limb are stiffer than in AH limb, while PLANT and FHL were less stiff.

Table 4-2: Autogenic and heterogenic interactions in LHS cats' Ah (*left*) and AH (*right*) limbs. For presentation purposes only, autogenic feedback is a diagonal of the matrix, while heterogenic interactions are presented from donor (rows) to recipients (columns) off diagonally.

d: \ r:	V	G	P	F	V	G	P	F
V	**37.7 N/mm**	19.7 %	3.2 %	12.9 %	**29.6 N/mm**	31.0 %	11.9 %	25.5 %
G	0.53 %	**11.5 N/mm**	2.61 %	3.92 %	2.79 %	**6.2 N/mm**	1.99 %	6.91 %
P	1.02 %	21.4 %	**3.9 N/mm**	0.99 %	2.43 %	39.4 %	**5.7 N/mm**	3.33 %
F	0.56 %	10.6 %	3.99 %	**10.9 N/mm**	2.68 %	27.2 %	27.2 %	**8.3 N/mm**

The autogenic feedback data (in Table 4-1 shown diagonally (yellow cells), only for presentation purposes) were presented in Chapter II. Briefly, they were obtained as the slope of force rise during the muscle stretch using equation 2.2 (i.e., muscular stiffness). Interaction magnitudes from a donor (Table 4-1: rows) to the recipient (Table 4-1:

columns) were presented in Chapter III. Briefly, the magnitude of interaction is defined as normalized difference between autogenic and heterogenic state during the hold of a muscle (late epoch) obtained using equation 3.1.

4.2.2 From mechanographic measurements to joint angles and moments

The first step in estimating the joint moments and angles was to determine the joint angles that correspond to recorded background forces (BGF) of muscles VASTI, GAS, PLANT, and FHL muscles ($F_{INITIAL}$). Since initial muscle displacement used to make these muscles taut (Figure 4-1, also see Methods of Chapters II or III) is not recorded, estimation of initial joint angles relied on information acquired from the literature.

Table 4-3: Table showing muscles and joints characteristics when joints are in a configuration that makes muscles (in rows) slack.

	L_{MUSCLE} *(mm)*	L_F *(mm)*	L_T *(mm)*	L_{MTU} *(mm)*	A_T *(mm^2)*	Θ_K *(deg)*	Θ_A *(deg)*
VASTI	86.4 (1)	25.6 (1)	11 (1)	97.4 (2a)		160 (3a)	NA
GAS	92.9 (3b)	21.57 (3b)	98.36 (3b)	191.26 (2a)	5.67 (3b)	30 (3a)	170 (3a)
PLANT	97.7 (3b)	20.19 (3b)	96.06 (3b)	193.76 (2a)	5.06 (3b)	30 (3a)	170 (3a)
FHL	92.0 (3b)	13.5 (3b)	57.4 (3b)	149.4 (2a)	2.85 (3b)	NA	170 (3a)
Notes:	The values in this table are either 1.) measured, 2a.) calculated as $L_{MTU} = L_{MUSCLE} + L_{TENDON}$, 2b.) calculated as $A_T = \frac{W_T}{L_T \cdot \rho_T}$ (W_T is measured, and ρ_T is $1.12 g \cdot 10^{-3}/mm^3$ (Ker 1981), or taken from literature 3a.) (Goslow, Reinking et al. 1973), 3b.) (Cui, Perreault et al. 2008).						

The joint angles that render these muscles slack are taken from Goslow, 1973 (Table 4-3). The assumption is that at these joint angles (Table 4-3: θ_K and θ_A), the muscles are slack and do not produce any force. Flexing these joint angles, changes muscles'

lengths which, in turn, generate the force according to the initial stiffness. The step-by-step method follows:

The initial stiffness was estimated using background forces and anatomical parameters of selected muscles. The assumption here is that, when a muscle is held isometrically at background force of 2 - 3 N ($F_{INITIAL}$), the force is generated mostly by short-range stiffness, with a minor neural contribution. Thus, we used anatomical parameters of muscles to estimate the initial stiffness of individual muscles and their tendons (Table 4-3):

$$K_M^i = \gamma \frac{F_{INITIAL}^i}{L_F^i} \qquad 4.1$$

where K_M is stiffness of muscle fibers at recorded background force ($F_{INITIAL}$), and L_F is the length of muscle fibers for selected muscles (for *i* = VASTI, GAS, PLANT, FHL). The value of the scaling parameter γ is 23.4, and it is taken from literature (Cui, Perreault et al. 2008). The tendon stiffness was assumed to be a function of the tendon length L_T, cross-sectional area A_T, and elastic modulus E (the value 522 MPa is the same for all muscles and acquired from literature (Cui, Perreault et al. 2008)).

$$K_T^i = \frac{EA_T^i}{L_T^i} \qquad 4.2$$

It is assumed that stiffness of a muscle arises from the serial linkage of muscle fiber stiffness (K_M) and tendon stiffness (K_T):

$$K_{MTU}^{i} = \frac{K_{M}^{i} K_{T}^{i}}{K_{M}^{i} + K_{T}^{i}} \qquad 4.3$$

With estimated initial stiffness of the muscle-tendon unit (K_{MTU}) of each individual muscle (*i* = VASTI, GAS, PLANT, FHL), it was possible to determine the change in length of the muscle-tendon unit (MTU) required to produce recorded background forces:

$$dL_{MTU}^{i} = -\frac{F_{INITIAL}^{i} - F_{SLACK}}{K_{MTU}^{i}} \qquad 4.4$$

where F_{SLACK} is the force of the muscle when it is slack (presumed to be 0 N), and $F_{INITIAL}$ are the recorded background forces of *i* muscles. The MTU displacement (i.e., elongation) is a negative value (Prilutsky 2000). Knowing length changes of MTU (from now on, dL_{MTU} is denoted as dL), it was possible to estimate changes in joint angles required to change muscle lengths to produce background forces of individual muscles. This was accomplished using their known moment arms (Zatsiorsky and Prilutsky 2012). The moment arms ($d^{j,i}$) were arranged as:

$$d = \begin{bmatrix} d_{kv} & d_{kg} & d_{kp} & d_{kf} \\ d_{av} & d_{ag} & d_{ap} & d_{af} \end{bmatrix} \qquad 4.5a$$

where elements of $d^{j,i}$ are transformations of small muscle length changes (dL) of *i* muscles into small changes in joint angles (dθ) of *j* joints (j = knee, ankle). In 4.5a, subscripts *k* and *a* denote the knee and ankle joints, respectively, and *v*, *g*, *p*, and *f* denote the VASTI, GAS, PLANT and FHL muscles. The values of $d^{j,i}$ were taken from the literature (Burkholder and Nichols 2004) and assumed to be constant throughout the joint angle changes:

$$d = \begin{bmatrix} 9.7 & -8.7 & -9.4 & 0 \\ 0 & 15.35 & 15.5 & 2.3 \end{bmatrix} \qquad 4.5b$$

The moment arms were then transformed into units mm/deg using an element-wise multiplication by 180/π. The changes in joint angles:

$$d\theta^j = \sum_{i=1}^{4} \frac{dL^i}{d^{j,i}} \qquad 4.6$$

were then added to the known slack joint angles (Table 4-3) to acquire values for initial joint angles ($\theta_{INITIAL}$) when muscles produce initial force ($F_{INITIAL}$):

$$\theta^j_{INITIAL} = \theta^j_{SLACK} + d\theta^j \qquad 4.7$$

With the conclusion of this section, the joint angles that correspond to recorded background forces ($F_{INITIAL}$) were established as $\theta_{INITIAL}$.

4.2.3 Geometric limb model of an unloaded, standing limb configuration

The joint angles 60º, 110º, and 100º (degrees) of MTP, ankle, and knee joints respectively correspond to the general stance configuration of cat hindlimb (Goslow, Reinking et al. 1973).

Rearranging initial joint angles to the corresponding stance configuration angles:

$$d\theta^j = \theta^j_{STANCE} - \theta^j_{INITIAL} \qquad 4.8$$

where $\theta_{INITIAL}$ are joint angles determined in the previous step when the force of the muscle is the initial background force. The change in joint angles, in turn, changes the lengths of selected muscles according to their respective moment arms:

$$dL^i = \sum_{j=1}^{2} d^{j,i} d\theta^j \qquad 4.9$$

Lengthening muscles will change their force responses reflexively based on autogenic stiffness data (K_A) recorded during the terminal experiments (Table 4-1: diagonal):

$$dF^i = -K^i_A dL^i \qquad 4.10$$

Thus, the force responses of muscles at stance are:

$$F^i_{STANCE} = F^i_{INITIAL} + dF^i \qquad 4.11$$

Translating individual muscle forces to moments around corresponding joints via $d^{j,i}$:

$$M^j = \sum_{i=1}^{4} F^i_{STANCE} d^{j,i} \qquad 4.12$$

The net moment at knee joint (M^k) is a function of extensor activity by VASTI and flexor activity by GAS and PLANT muscles in this model (neglecting the contribution of other anatomical and physiological agonists and antagonists, and other structures contributing passive forces). The moment at ankle joint (M^a) is a function of extensor

activity of GAS, PLANT and FHL (neglecting the contribution of other anatomical and physiological agonists and antagonists).

Based on measured limb segments and joint angles at the stance, we can predict joint positions in 2D space. Lengths of limb segments were taken from a cat with comparable mass, and they are: L_{THIGH} = 9.8 cm, L_{SHANK} = 11.1, and L_{FOOT} = 6 cm (Figure 4-2). The MTP joint is anchored at (0, 0) position, and MTP joint angle fixed at a 60º angle:

$$\begin{aligned}
M_X &= 0 \\
M_Y &= 0 \\
A_X &= L_{FOOT}\cos(\theta_{MTP}) \\
A_Y &= L_{FOOT}\sin(\theta_{MTP}) \\
K_X &= A_X + (L_{SHANK}\cos(\theta_{MTP} + (180 - \theta_A))) \\
K_Y &= A_Y + (L_{SHANK}\sin(\theta_{MTP} + (180 - \theta_A))) \\
H_X &= K_X + (L_{THIGH}\cos(\theta_K + \theta_{MTP} - (180 - (180 - \theta_A)))) \\
H_Y &= K_Y + (L_{THIGH}\sin(\theta_K + \theta_{MTP} - (180 - (180 - \theta_A))))
\end{aligned} \qquad 4.13$$

where subscript X corresponds with horizontal position and subscript Y corresponds with vertical position of individual joints (Figure 4-2).

Because the vertical perturbation vector is set to go through the MTP joint, it was easy to estimate the orthogonal distance (i.e., r^j) from knee and ankle joint position to that vector, as an absolute values of K_x and A_x, respectively (Figure 4-2). Furthermore, it was possible to estimate the position of the hip joint, however, since muscles crossing the hip were not evaluated in preceding chapters the hip position, angle and moment were ignored.

A cat carries approximately 40% of its mass (m_{CAT}) on a hindlimb during the stance phase of the step cycle (Fowler, Gregor et al. 1993). Thus, the initial force imposed onto a

limb was 40% of cat's mass (recorded weights of AH and Ah cats were 4.1 and 3.75 kg, respectively).

$$F_{APP} = 0.4 m_{CAT} \qquad 4.14$$

The moments (M_{REQ}) at the knee and ankle joints required to resist this initial force and maintain the limb in a static equilibrium are determined by the absolute orthogonal distance to the force vector from the particular joint (r^j).

$$M^j_{REQ} = F_{APP} r^j \qquad 4.15$$

If the current moment (M^j) at a joint is insufficient to resist the cat's mass, there is going to be a reconfiguration of the limb in terms of joint angle changes, per individual joint stiffness (K^j). Individual joint stiffness is determined from muscle stiffness acting at that joint:

$$K^j = \frac{dM^j}{d\theta^j} = \sum_{i=1}^{m} \frac{dF^i d^{j,i}}{\frac{dL^i}{d^{j,i}}} = \sum_{i=1}^{m} K^i_A (d^{j,i})^2 \qquad 4.16$$

The change in joint angle is:

$$d\theta^j = -\frac{dM^j}{K^j} \qquad 4.17$$

where dM^j is the difference between moment required to withstand the imposed force by the cat's mass (equation 4.15) and moment developed by muscles at those joints (equation 4.12).

With the conclusion of this section, joint angles and moments of knee and ankle joint of a limb loaded with 40% of cat's mass are known.

4.2.4 Imposing vertical perturbations onto the limb with autogenic and the limb with autogenic and heterogenic feedback

The perturbations were applied in an increasing order of 1% of the initial force i.e., cat's mass. Response to perturbations was evaluated in the autogenic state (with autogenic feedback only) and heterogenic state (combined autogenic responses with heterogenic feedback). The autogenic responses are recorded stiffnesses of a muscle when stretched alone at initial background force (Table 4-1):

$$\vec{K}_A = (K_A^V \quad K_A^G \quad K_A^P \quad K_A^F) \qquad 4.18$$

where K_A is recorded dF/dL of individual muscles, with units of N/mm. These data were acquired under the quiescent conditions when a muscle is stretched alone (presented in Chapter II).

The resultant change in force (dF_A) of selected muscles due to the change in length:

$$dF_A^i = -dL^i \vec{K}_A \qquad 4.19$$

and the force of individual muscles due to autogenic feedback:

$$F_A^i = F_{STANCE}^i + dF_A^i \qquad 4.20$$

The force change due to the autogenic feedback is modulated by the heterogenic feedback matrix. Heterogenic matrix is composed of interactions a donor muscle elicits onto the recipient (as% effect) (Table 4-1: off diagonal). These data were also acquired during the quiescent trial and presented in Chapter III. Although force dependent feedback (as its name implies) depends on a donor muscle force, in this chapter, the heterogenic interactions were triggered by the change in length of a donor. The justification for using length instead of force to elicit heterogenic feedback is that these data were acquired from quiescent trials where the heterogenic effect is initiated by the change in length of a donor (Chapter III: Figure 3-1, left panel)

$$I^i = d\vec{L} \cdot H \qquad 4.21a$$

or expanded:

$$I^i = \begin{bmatrix} dL^V & dL^G & dL^P & dL^F \end{bmatrix} \cdot \begin{bmatrix} 0 & V \to G & V \to P & V \to F \\ G \to V & 0 & G \to P & G \to F \\ P \to V & P \to G & 0 & P \to F \\ F \to V & F \to G & F \to P & 0 \end{bmatrix} \qquad 4.21b$$

As it can be seen in 4.21b, the I vector of heterogenic interactions is organized as a linear sumation of all interactions from all donors onto each recipient. dL is a vector with individual muscle length changes. The change in force response to perturbation was due to both autogenic and heterogenic input:

$$dF^i_{A+H} = dF^i_A I^i \qquad 4.22$$

and the resultant force of a muscle incorporating its own autogenic feedback and all heterogenic feedback from other muscles that are stretched:

$$F^i_{A+H} = F^i_{STANCE} + dF^i_{A+H} \qquad 4.23$$

The moments at joints that result from forces F_A or F_{A+H} developed by spanning muscles were calculated using equation 4.12. The expected changes in joint angles were dictated by the stiffness of those joints calculated according to equation 4.16, in the autogenic and heterogenic state (i.e., dF_A or dF_{A+H}). The perturbations were increased by 1% of cat's mass until the failure of one of the joints. The failure, i.e., joint collapse is defined as joint angle being 0 degrees.

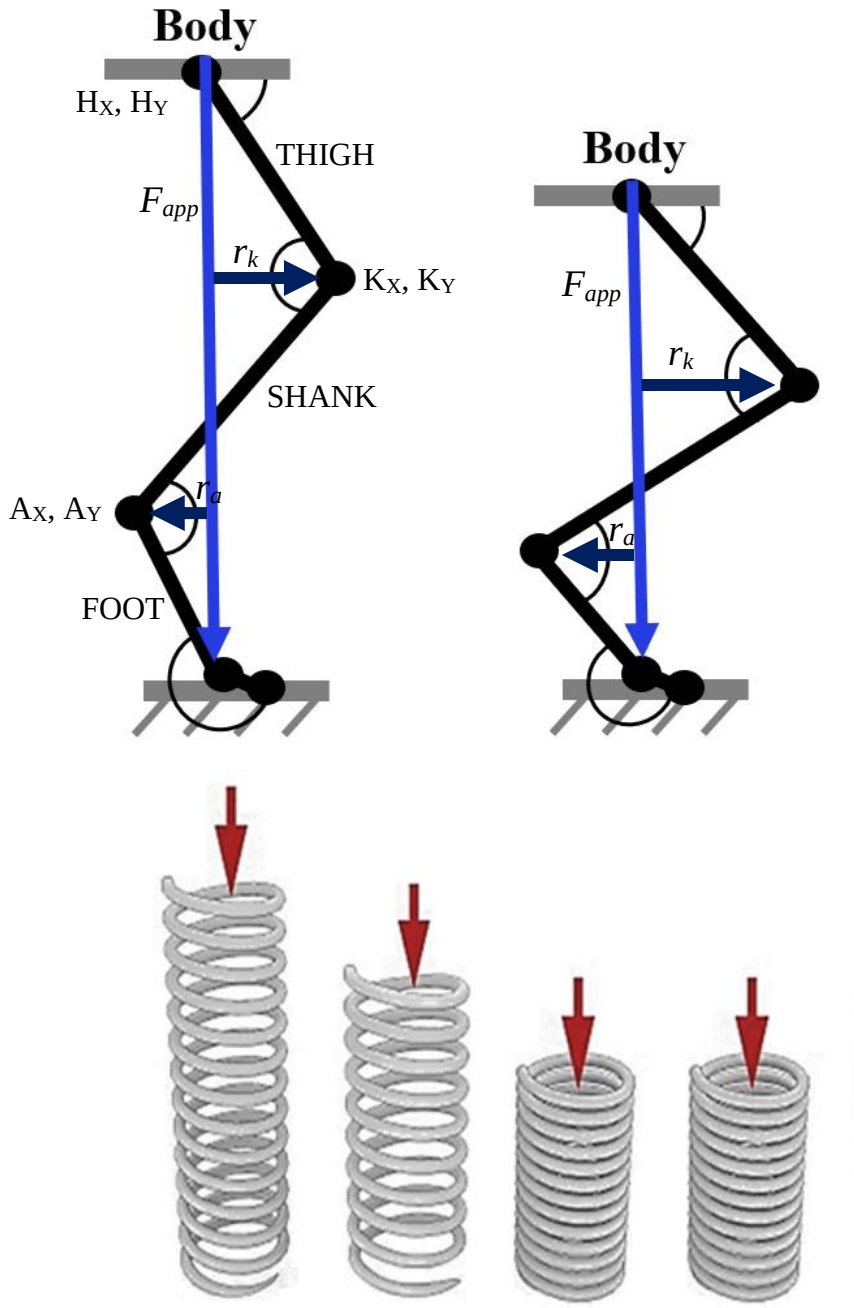

Figure 4-2: Limb configuration at initial load (left) and subsequent increased load (right). Limb is loaded with 40% of individual cat's mass. The vector of this force is set to go through MTP joint (blue downward arrow), as to make moment produced at MTP joint zero (r_{MTP} = 0). Resisting ground reaction force is equal in amplitude but in the opposite direction. Moment required at knee and ankle joints to resist cat's mass will depend on the distance of force vector to position of those joints (i.e., rk and ra, respectively). If the moment at those joints does not match required moment imposed by perturbation, the limb will go through reconfiguration based on stiffness of those joints. Since the stiffness of a joint is dependent on stiffness of all muscles crossing that joint, autogenic and heterogenic state will greatly impact the stiffness developed at those joints. This is equivalent to having a thicker or thinner coils of the spring.

4.3 Results

The primary goal of this chapter was to establish the role of heterogenic feedback in the maintenance of static equilibrium. This was accomplished by estimating joint moments and joint angles from muscle stiffness recorded using a mechanographic method first, and then predicting responses to vertical perturbation in autogenic (stiffness of a muscle due to its autogenic feedback) and heterogenic (stiffness of a muscle due to its autogenic feedback and heterogenic feedback elicited by the length change of donors) state. Furthermore, we compared the data from two cats' limbs; i.) one that exhibited strong autogenic and strong heterogenic feedback (AH limb), and ii.) the other that displayed strong autogenic feedback and (relatively) weak heterogenic feedback (Ah limb). An attempt was made to match the autogenic stiffness of the muscles and cats' mass, while varying magnitudes of heterogenic feedback. However, that was challenging to accomplish perfectly.

As perturbation force increased, the joints became more flexed (joint angle decreased). The point of failure was defined as the joint angle being 0 degrees. The main question was whether heterogenic feedback contributes to failure of the joint. Which joint and under which force amplitude failed first were also estimated.

4.3.1 Responses to perturbation

To maintain static equilibrium, joints needed to develop moments that match required moments imposed by vertical perturbations. This requirement is a significant burden on the knee joint since its position sets it farther away from the vector of force than the ankle (because of longer lengths of femur and tibia, compared to tarsals) in this stance

configuration. Furthermore, the VASTI is the only muscle that contributes to the extensor moment around the knee, while GAS and PLANT develop flexor moment at the knee.

The knee of AH limb collapses before ankle joint under the perturbations in the autogenic state in (Figure 4-3: left & right, blue trace). Strong heterogenic inhibition in AH limb made both ankle and knee joints more flexed throughout the perturbations, and both AH ankle and knee joints failed together (Figure 4-3: left & right, pink trace). However, heterogenic inhibition directed toward GAS and PLANT (both have flexor moment at the knee), actually improved knee response to perturbation as the perturbations increased. Specifically, as perturbations made ankle joint more flexed, it resulted in activation of heterogenic feedback from FHL muscle and a further stretch of GAS and PLANT (that exchange inhibition), which together decreased GAS and PLANT flexor moment at the knee. However, the knee was still more flexed in heterogenic compared to autogenic state.

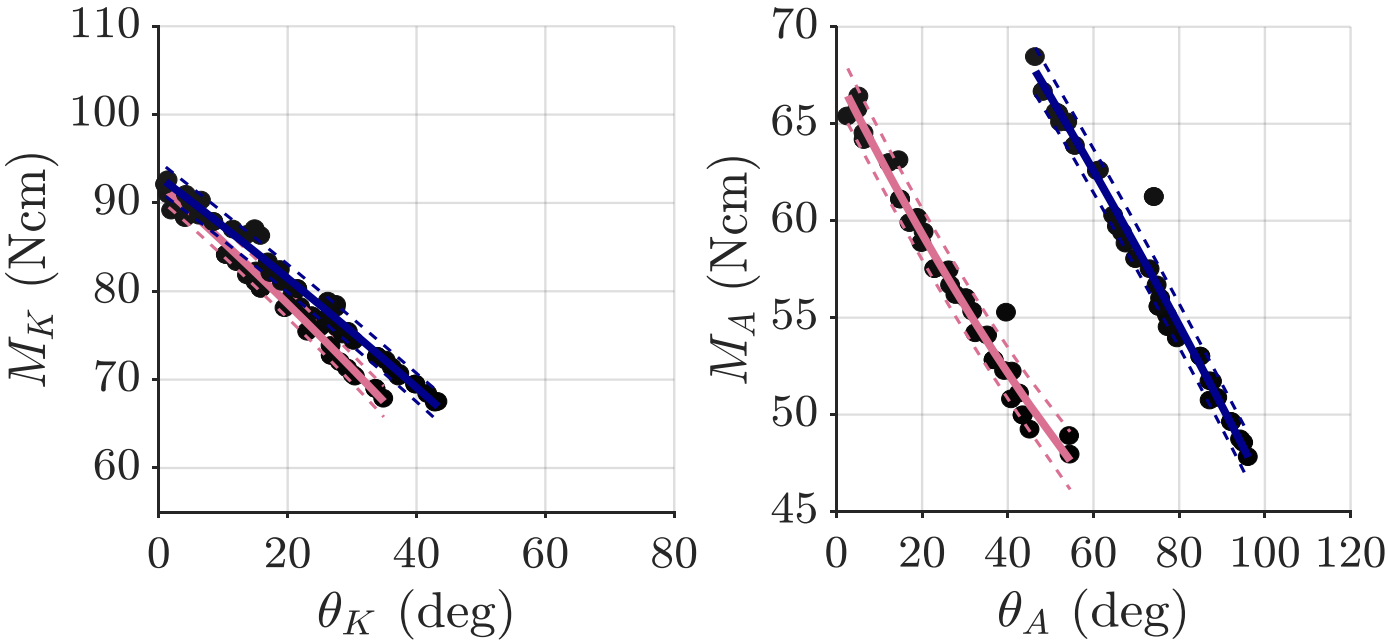

Figure 4-3: Responses of knee (*left*) and ankle (*right*) joints of AH limb in autogenic (blue) and heterogenic (pink) state. Heterogenic state renders both joints more flexed.

Comparing AH limb to Ah limb, it is evident that stronger heterogenic inhibition makes both knee and ankle joints more flexed in AH than in Ah. In Ah limb, the knee in both autogenic and heterogenic state fails before the ankle (Figure 4-4: left & right panels). The Ah ankle is, however, more flexed in the heterogenic state (Figure 4-4: right, blue vs pink trace). Negligible inhibition form ankle extensors to the VASTI (0.53 – 1.02%) obviously had no effect onto the Ah knee. Furthermore, relatively weak inhibition from FHL onto GAS and PLANT did not impact their flexor moment at knee joint to make it different from the autogenic state (Figure 4-4: left, blue and pink traces overlap).

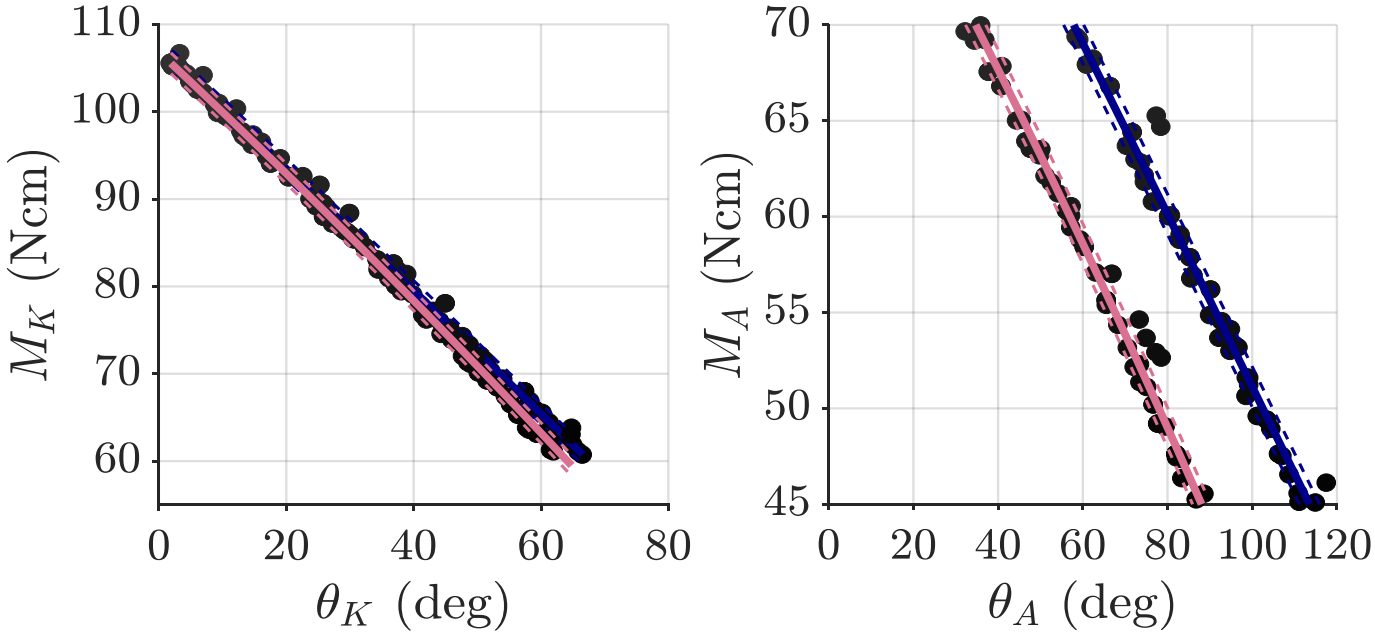

Figure 4-4: Responses of knee (*left*) and ankle (*right*) joints of Ah limb in autogenic (blue) and heterogenic (pink) state**.** Heterogenic state makes both joints more flexed, however this depends on the strength of heterogenic feedback as weaker feedback had lesser effect onto joints.

4.3.1.1 Which joint collapses first?

The conclusion of Chapter III was that inhibition directed toward ankle extensors would render knee stiff (by sparing the knee extensors (VASTI) and inhibiting knee flexors (PLANT and GAS)), and ankle compliant (by directing inhibition onto all ankle extensors). Whether or not this is the case in freely behaving cat is not known at the moment, as analysis of biomechanics data prior and after LHS injury is still underway. However, estimated joint angles and moments from mechanographic data in this chapter suggest that strong heterogenic inhibition directed toward ankle extensors could indeed make both joints more flexed.

Comparing estimated joint angles of the knee and ankle in the autogenic and heterogenic state in limbs with strong and weak heterogenic inhibition (Figure 4-5: left & right, blue (autogenic) vs pink (heterogenic)) suggest that the stronger inhibition directed

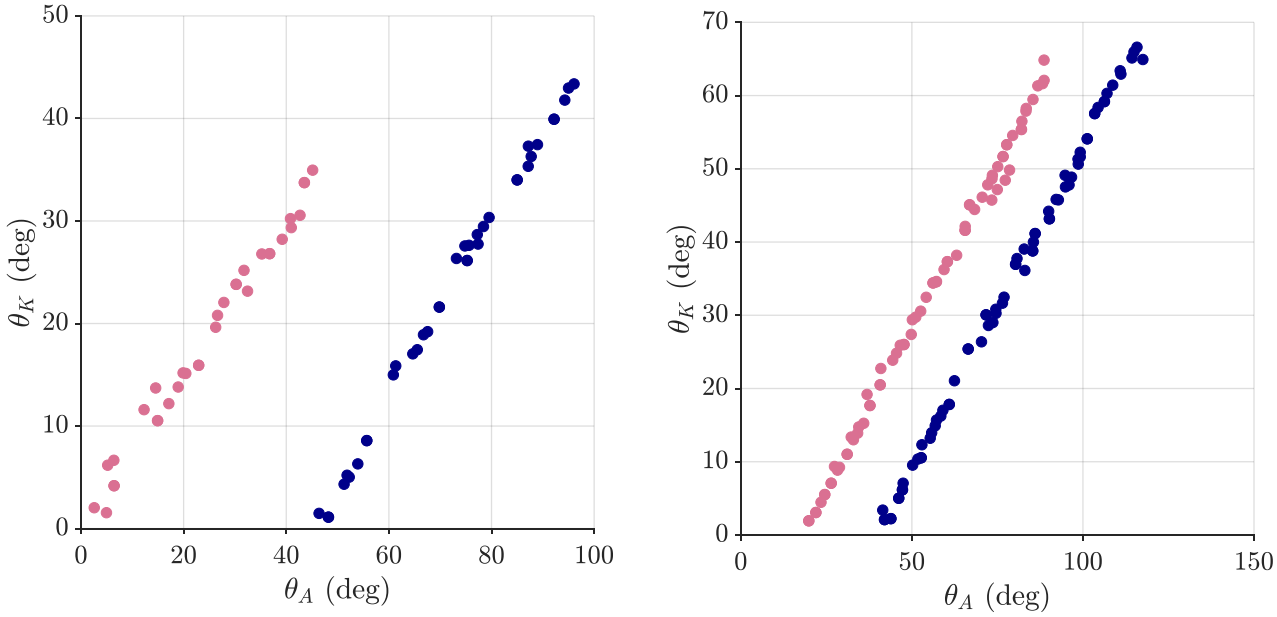

Figure 4-5: Join angles of ankle and knee of AH (left) and Ah (right) limb in autogenic (blue) and heterogenic (pink) states. Inhibitory feedback had detrimental impact onto the ankle joint, and this impact was magnitude dependent.

toward ankle extensors the more likely the ankle will collapse. The ankle of AH limb is significantly more flexed than the ankle of Ah limb (Figure 4-5: left & right, pink trace), although they were both more flexed than their corresponding autogenic states.

4.3.1.2 When do joints collapse?

To show that strong inhibitory heterogenic feedback can be detrimental to joint stability, we have evaluated what amount of force applied vertically can cause joint failure. In AH limb, strong heterogenic inhibition toward and exchanged amongst ankle extensors had a profound effect and made ankle joint more flexed throughout perturbation amplitudes compared to the autogenic state.

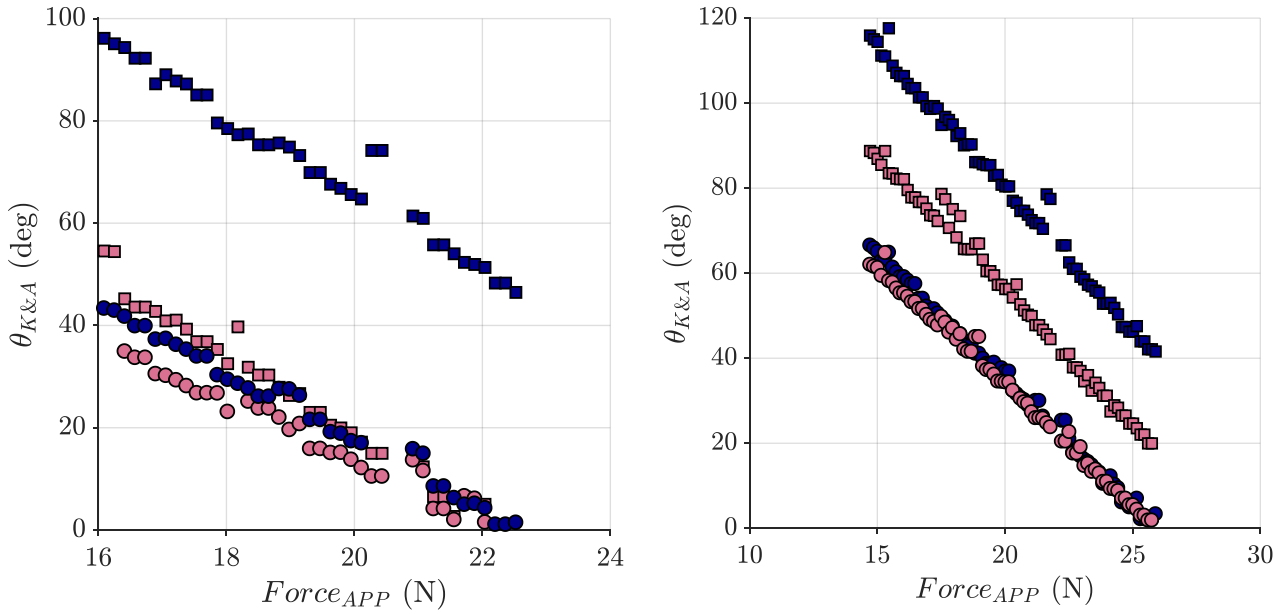

Figure 4-6: Joint angles of knee (circle) and ankle (square) in autogenic (blue) and heterogenic (pink) state of AH (left) and Ah (right limb) across perturbation amplitudes.

Both knee and ankle joints failed at the same imposed forces (22 N). In the autogenic state, AH ankle resisted perturbation significantly better than the knee, which failed at 22.5 N of the applied force (Figure 4-6: left). In Ah limb, both joints in both autogenic and heterogenic states were less flexed throughout the forces applied due to stiffer muscles and weaker heterogenic interactions (Table 4-1) compared to AH cat (Figure 4-6: left & right). However, the knee joint fails at 25.2 N in both autogenic and heterogenic state (heterogenic interactions onto VASTI are negligible, thus responses of this joint are the same in both states). The ankle in the heterogenic state is more flexed throughout the perturbations compared to the autogenic state. At the point of knee failure, the ankle is at 20 degrees in the heterogenic state, and 40 degrees in the autogenic state (Figure 4-6: right).

4.4 Discussion

In this short, but important chapter we predicted joint moments and angles at quiet stance from mechanographic data. Moreover, we evaluated the integration of autogenic and heterogenic feedback under perturbations. The primary goal was to compare responses to perturbations in autogenic and strong and weak heterogenic conditions. The main conclusion was that joint angles of both knee and ankle were more flexed in the heterogenic state, compared to the autogenic state. The magnitude of flexion was dependent on the strength of inhibitory heterogenic feedback, as knee and ankle of AH limb were flexed more than Ah limb in the heterogenic state.

Additionally, we evaluated which joint fails first. A failure is defined as the joint angle being 0 degrees. Due to the fact that the knee extensor moment is generated by one

extensor muscle group (VASTI) in this model and is opposed by flexor moment produced by GAS and PLANT, the knee failed prior to the ankle joint, in both autogenic and heterogenic state, despite large inhibition directed toward GAS and PLANT. The convergent inhibitions onto GAS and PLANT are supposed to enhance extensor activity at the knee. Indeed, in AH limb the inhibition of GAS and PLANT by both VASTI and FHL in heterogenic state improve the knee resistance to perturbations at smaller joint angles (flexed joints). Striking is the effect of heterogenic feedback onto ankle joint. In both AH and Ah limbs, the ankle is more flexed compared to the autogenic state. In AH limb, both knee and ankle joints fail simultaneously. Despite heterogenic inhibition, Ah ankle joint did not fail, although it was more flexed compared to autogenic state, presumably due to significant GAS muscle stiffness that maintains it in more extended position.

The range of imposed perturbations depended on cat's mass. The Ah cat (smaller cat, 3.75 kg) withstood larger amplitude of perturbations, presumably due to stiffer VASTI and GAS muscles. However, heterogenic feedback, integrated with autogenic feedback had decreased the perturbation amplitude an AH limb (4.1 kg) could withstand, but only slightly.

In the literature, most studies examining the control of the limb stiffness involve or assume constrained limb posture, such as in this chapter. At a fixed postural limb configuration, stiffness can be regulated primarily through control of muscle activation via integration of descending and sensory neural input (or integration of autogenic and heterogenic inputs as presented in this chapter). However, the changes in limb posture have a profound effect on limb stiffness and stability (Mussa-Ivaldi, Hogan et al. 1985, Flash and Mussa-Ivaldi 1990). The muscle forces (and stiffness) are subject to change due to

their moment arms as the join angles change. As a consequence, the contribution of an individual muscle to the total stiffness of the limb is significantly different for different limb positions. Additionally, since the neural input to the muscles changes their spring constants (Rack and Westbury 1969, Nichols and Houk 1976) the stiffness of muscles may be result of different levels of neural activation associated with different postures.

The results from this chapter suggest that inhibitory force feedback could contribute to crouched gait and difficulty in weight-acceptance phase of a step cycle significantly. However, several significant, although necessary simplifications were assumed that might influence the responses of the limb and conductions of this chapter. The suggestions were contingent on force feedback remaining inhibitory in walking cat with a spinal lesion. Furthermore, it is assumed, and probably incorrectly, that inhibitory force feedback onto recipient sums up linearly. It is, however, more likely that in a behaving cat there are numerous ways these inputs are gated, occluded or canceled within the spinal cord interneurons. Additionally, it is assumed that stiffness of a muscle is constant throughout the length changes for which there is support in literature (Cui, Perreault et al. 2008). Significant limitation of this model is that its moment arms are considered constant, despite nonlinearity at joint angle extremes (Fowler, Gregor et al. 1993).This simplification was necessary, as to map changes in muscle lengths to changes in joint angles.

CHAPTER 5. DORSAL LESION OF THE SPINAL CORD RELEASES CLASP-KNIFE INHIBITION BUT DOES NOT AFFECT FORCE-DEPENDENT FEEDBACK

5.1 Introduction

Spinal cord injury (SCI) causes profound changes in virtually all physical systems and significantly diminishes functional motor abilities. Many spinal cord injuries are partial or incomplete having some descending tracts preserved. These types of injuries, termed incomplete spinal cord injuries, have varying clinical manifestations contingent on location and the extent of the lesion. Patients with incomplete spinal cord injuries can regain some sensory and motor functions caudal to the injury, and even recover walking, although it is accompanied by gait deficits. These deficits often include spasticity (Barbeau, Ladouceur et al. 1999) and gait with flexed limbs, as if semi-crouching (Barbeau, Ladouceur et al. 1999, Pepin, Norman et al. 2003). Spasticity is an umbrella term used to describe a series of diverse clinical symptoms and includes hypertonia, flexor or adductor spasms, clonus, clasp-knife phenomena, etc. (Mirbagheri, Barbeau et al. 2001).

Some individuals with spasticity have increased overall joint stiffness (Mirbagheri, Barbeau et al. 2001). However, this initial stiffness abruptly plummets as the joint is moved beyond some threshold angle (Burke, Gillies et al. 1970). This phenomenon is called clasp-knife inhibition (CKI). At the muscle level, CKI is characterized by 'catch-and-give' phases, where the catch is due to resistance to elongation, and the give is due to a

subsequent abrupt decline in force as muscle yields (Pierrot-Deseiligny and Burke 2012). The essential feature here is the abolition of resistance during the lengthening.

Previously, the CKI was attributed to inhibitory Golgi tendon organ (GTO) pathway (Ballif, Fulton et al. 1925, Fulton and Pi-Suner 1927), as it was mistakenly thought that GTO's respond vigorously only to large stretches and have a protective role to its homonymous muscle (Matthews 1933). However, subsequent research had shown that the adequate stimulus for GTO's is not a passive stretch, but rather an active muscle force and that GTO's are active throughout the normal range of force gradation (Houk and Henneman 1967). Next, it was believed that the CKI must be mediated by secondary spindle afferents (Burke 1980), which sense the length of the muscle, after electrophysiological studies pointed to their inhibitory effect on extensor muscles (Holmqvist and Lundberg 1961), and because of the CKI's dependence on joint angle (and therefore on muscle length) (Burke, Gillies et al. 1970). This led researchers to assign group II afferents to a broad class of flexor-reflex afferents (Holmqvist and Lundberg 1961) which exerted strong inhibition onto extensors, and excitation onto flexors. However, later studies have shown that the actions of group II are not as uniform as previously thought. Specifically, evidence has accumulated that suggests group II afferents can have an excitatory influence on motoneurons (Kanda and Rymer 1977). Moreover, excitatory monosynaptic connections onto motoneurons have been found (Kirkwood and Sears 1974, Kirkwood and Sears 1975). Subsequent studies have implicated muscle high threshold free nerve endings from group III and IV mechanoreceptors (Rymer, Houk et al. 1979, Cleland, Hayward et al. 1990, Cleland and Rymer 1990) as they also have inhibitory input to motoneurons. These low-sensitive receptors are innervated by the long-latency group III and IV afferents and

respond to a variety of noxious, chemical, thermal or mechanical stimuli (Kumazawa and Mizumura 1977). As such, they serve a protective role, once attributed to the GTO's, and can inhibit muscles strongly, causing the limb to collapse. The dorsal reticulospinal descending system has a modulatory role over group III and IV pathways, as a disruption in this system disinhibits the segmental interneurons that mediate the inhibitory effect of this pathway, thus releasing the CKI (Engberg, Lundberg et al. 1968).

The tonic influence of the reticulospinal tract is involved in regulation of gait and posture. It inhibits numerous spinal interneurons involved in the transmission of reflexes to motoneurons (Baldissera, Hultborn et al. 1981, Jankowska 1992). The goal of this project was to determine if and to what extent inhibitory force feedback (iFFB) from GTO's is modulated by this tract and other tracts passing through the dorsal column. To investigate this, we compared the distribution of force feedback in cats with dorsal or lateral hemisection. Previously, Lyle and Nichols established three patterns of force feedback organization (Lyle and Nichols 2018). In Chapter III, we have shown that only one pattern of strong inhibitory and directional bias can be found in cats with lateral hemisection. Observation of the three patterns (i.e., the preserved variability of iFFB bias) after dorsal hemisection would indicate that force feedback is regulated by pathways other than those that control CKI. This finding would add yet another distinction between these two pathways to the scientific knowledge.

Both dorsal (Heckman 1994) and lateral (Hultborn and Malmsten 1983, Malmsten 1983) hemisections have been used as an experimental model of reflex pathology, as they both exhibit exaggerated stretch reflex. However, there are notable differences between these two preparations regarding the influence on force feedback organization. We have

shown in Chapter III that lateral hemisection is characterized by a directionally amplified iFFB, selectively exaggerated stretch reflex and lack of CKI. In this chapter, we will show that dorsal hemisection does not affect the force feedback, but exhibits the CKI autogenically in vasti muscle group and, more prevalent, heterogenic CKI between knee and ankle extensors. The preliminary results have been presented elsewhere (Kajtaz, Lyle et al. 2018).

5.2 Methods

5.2.1 Animals

The experiments were performed on nine purpose-breed female cats ranging from 2.9 - 3.6 kg. All data presented in this paper were acquired during terminal experiments. Before the terminal experiment, cats received a dorsal hemisection and were allowed to recover for different time periods; 3 weeks (n = 2), 7 - 8 weeks (n = 4) and 12 weeks (n = 3). All procedures presented in this chapter were completed in accordance with guidelines from the National Institute of Health and protocols approved by the Institutional Animal Care and Use Committee of the Georgia Institute of Technology and the University of Louisville.

5.2.2 Survival surgery

Dr. Dena Howland performed the dorsal hemisections on nine cats at the University of Louisville. During the surgery, cats were initially anesthetized with isoflurane (5%) and oxygen mix in an induction chamber, then intubated and maintained on a mix of oxygen and isoflurane (1 - 4%) throughout the survival surgery. Blood pressure, EKG, heart rate,

respiration rate, temperature, SpO_2 and expired CO_2 were monitored throughout surgery to assure surgical depth of anesthesia. Laminectomies for dorsal hemisections exposed spinal T9-10, the dura was slit, dorsal columns and dorsal root entry zones were visualized to identify the midline. The intended area of the spinal cord was cut with iridectomy scissors. The fibers adhering to dura were gently lifted with suction and cut. Dura was then sutured, durafilm and gelfoam placed on top of the dural sutures, and the back closed in layers.

5.2.3 Terminal experiments

In the terminal experiments, cats were initially anesthetized with 5% isoflurane gas, tracheal intubation was performed, and 2 - 4% isoflurane was used to maintain deep anesthesia. An IV was inserted into an external jugular vein for hydration and drug delivery. Adequate deep anesthesia was confirmed during the experiment by the absence of withdrawal reflexes. Heart rate, EKG, respiratory rate, oxygen saturation, expired carbon dioxide, blood pressure, and core body temperature were monitored during all experiments. The head and the hindlimbs were rigidly fixed in a stereotaxic frame, while a sling supported the abdomen. The hindlimbs were secured by threaded rods inserted into the proximal (just distal to the greater trochanter) and distal femur (femoral condyle). The rods were connected by a bar and rigidly fixed to the supporting frame. The proximal tibia was stabilized by a separate threaded rod, while the distal tibia was stabilized with a custom-made ankle clamp (Figure 1: A).

The gastrocnemius (GAS), plantaris (PLANT), soleus (SOL), flexor hallicus longus (FHL), and the vastus muscle group (VASTI) were dissected in both hindlimbs. The muscle dissection was described in detail in Chapters II and III. Briefly, all muscles were separated

free from adjacent tissues and neighboring muscles to minimize mechanical coupling while preserving their nerve and vascular supply. The tendons of all muscles were attached to custom-made tendon clamps which were then connected to the myographs in series with linear motors.

All cats underwent a standard precollicular decerebration (Silverman, Garnett et al. 2005) that rendered them comatose and insensate. This procedure involved a vertical transection at the anterior margin of the superior colliculus, and removal of all brain matter rostral to the transection. After the decerebration, isoflurane anesthesia was titrated down and eventually withdrawn. At the end of the experiment, heparin was injected in preparation for perfusion, and the animal was re-anesthetized using isoflurane. Euthanasia was accomplished by perfusing the animal through the heart first with saline and then paraformaldehyde. Hindlimb muscles were harvested following euthanasia.

5.2.4 Data acquisition

The autogenic and intermuscular spinal reflex pathways were examined using a ramp-hold-release muscle stretch protocol. The details of the software and hardware used have been described previously (Nichols 1987, Ross and Nichols 2009). Briefly, the protocol involved 2-mm muscle stretches with a 50 ms ramp, 100 ms hold and 50 ms release with a velocity of 0.04 m/s. The muscle stretches were applied in a two-state alternating pattern with a stretch repetition frequency of 0.7 Hz (Figure 5-1: B). Each trial had on average 20 – 40 stretch repetitions. In state 1 (S1), a single muscle denoted as the recipient was stretched alone. In state 2 (S2), the recipient muscle was stretched simultaneously with another muscle referred to as the donor muscle (Figure 5-1: B).

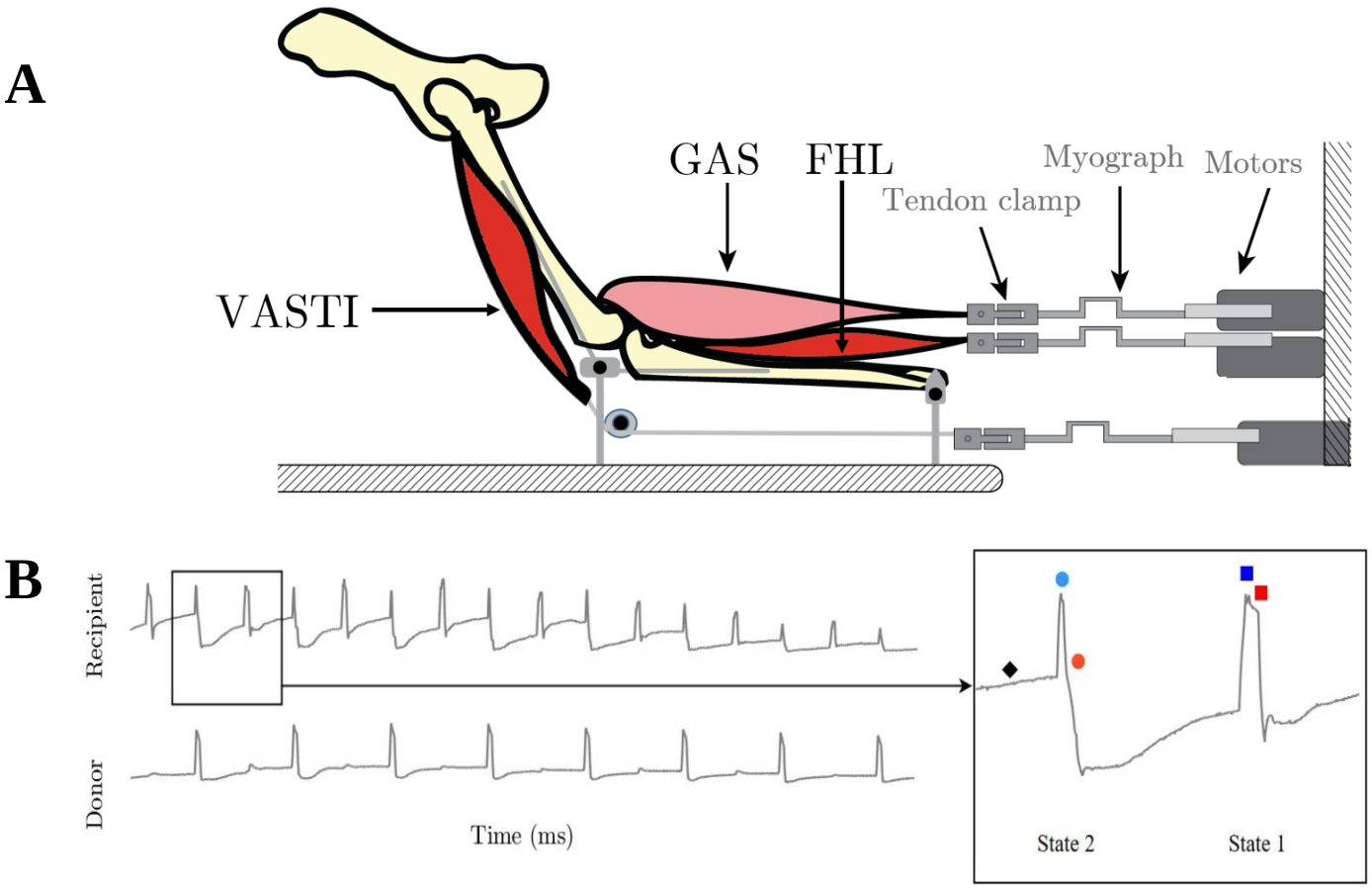

Figure 5-1: Showing experimental set up (*A*) and raw force traces (*B*). The raw data (*B - left*) showing force responses of recipient (GAS) and donor (FHL) across varying background forces (active condition). The force responses show a strong CKI heteronymously exchanged from FHL onto GAS, and no apparent autogenic CKI in GAS. The pair of recipient stretches (*right*) stretched in tandem with donor (state 2 - circle) and alone (state 1 - square). The stretch is broken down into an early (30-70 ms after the stretch onset - blue) and late epoch (110-150 ms after the stretch onset – red). Background force is marked with a black diamond.

We relied on the known latencies of group I and group III/IV pathways in distinguishing iFFB and CKI pathways, respectively. Thus, the S1 and S2 stretches were broken down into an early epoch (the average of muscle force between 30 to 70 ms after the stretch onset) (Figure 5-1: B, blue filled markers) and late epoch (the average of muscle force between 110 to 150 ms after the stretch onset) (Figure 5-1: B, red filled markers). The comparison of the early and late epochs in S1 (Figure 5-1: B, square markers), and S2

(Figure 5-1: B, circle markers) reveal autogenic and heterogenic CKI, whereas the comparison of late epochs of S1 and S2 stretches (Figure 5-1: red circle and square) reveals heterogenic iFFB (also in Table 5-1). In subsequent figures, S1 is marked with full line or trace, while S2 with dashed line or trace.

Table 5-1: Table showing epochs and states of force response used to distinguish autogenic and heterogenic iFFB and CKI. The line and marker denote state and epoch (for example, the early epoch of state 2 is marked by blue circle marker and broken blue line in subsequent figures).

Epoch/State	**State 1** (autogenic)	**State 2** (heterogenic)
Early Epoch (30 – 70 ms)	No iFFB or CKI	Heterogenic iFFB
Late Epoch (110 – 150 ms)	Autogenic CKI	Heterogenic CKI & Heterogenic iFFB

The muscle stretch repetitions were applied over a constant (a condition termed quiescent) and varying range of background forces (a condition termed active) (Figure 5-1: B) by eliciting a crossed extension reflex as in earlier work (Bonasera and Nichols 1994, Wilmink and Nichols 2003, Ross and Nichols 2009). The crossed-extension reflex was elicited by stimulating the contralateral tibial nerve just proximal to the medial malleolus with a hook electrode (0.1 ms pulse width, 40 Hz, 20-40 s duration). Typically, this reflex naturally habituates over 20-40 s and forces in the contralateral extensor muscles slowly decay toward the 1-3 N background force (Figure 5-1: B, black diamond).

5.2.5 Data analysis

Due to qualitative differences between quiescent and active conditions different approaches to analysis were applied. All data were analyzed using custom programs written in MATLAB 2016b (MathWorks, Natick, MA). Analysis was blinded in order to eliminate any potential bias.

5.2.5.1 Quiescent condition

In the quiescent condition, all muscles evaluated were kept taut up to 3 N of background force. This enabled us to evaluate two features of intermuscular interactions (i) magnitude of interaction, and (ii) directional bias in the same fashion as in Chapter III. The *magnitude* is operationally defined as a sign and an amount of unidirectional interaction and was computed as the normalized difference between S1 and S2 early and late epochs, using equation 3.1. The magnitude of interaction from muscle 1 to 2 (μ_{M12}) is a relative percent difference between recipient muscle forces obtained in S1 and S2. The standard deviation of the magnitude was obtained by computing its derivative with respect to the S1 and S2 late epochs and covariance between those two terms (Taylor 1997), per individual trial. It was computed using equation 3.2. If an experiment had more than one trial of the same muscle pair interaction, the averages of μ_{M12} and σ_{M12} of those trials were used as a representative of an interaction magnitude and its standard deviation for that experiment.

The *directional bias* is a difference of unidirectional interaction magnitudes between muscles in a pair that exchanges feedback. The sign of the bias is arbitrarily

defined based on muscles' anatomical origins and insertions. It can be positive or distal to proximal bias (when more distal muscle inhibits more proximal one more so than the other way around), balanced (when muscles exchange the same ± 5% of inhibition), and negative or proximal to distal (when more proximal muscle inhibits more distal one more so than the other way around). It was computed using equation 3.3.

The *stiffness* of homonymous force response, i.e., the gain of length feedback, was computed using equation 2.2 (described in Chapter II).

Wilcoxon rank-sum tests were used to determine whether the recipient muscle force recorded when stretched alone (S1) was different from that when stretched pairwise with the donor muscle (S2). Reported values are mean difference between S1 and S2 in either absolute values (N) or percentage (%, a difference normalized to S1 according to equation 3.1) and result of a statistical test with p-value set to 0.05.

5.2.5.2 Active conditions

The baseline force vector for each stretch repetition in a trial was subtracted from the raw force profiles before the analyses (Figure 5-1: B, raw force responses). The baseline force vectors used to remove the background force offset (Figure 5-1: B, black diamond) were determined using linear interpolation from stretch onset to a point 900 ms after stretch onset similar to that previously described (Ross and Nichols 2009).

The epochs of force responses for each state were plotted separately as a function of recipient background forces (Figure 5-1: B, black diamond marks background force, blue marks an early epoch, red marks late epoch). The background force values used in the

regression plots were the recipient muscle force means for the 15 ms period before the stretch onset for each stretch repetition. However, if the recipient muscle background force did not change during the tibial nerve stimulation, i.e., background force was constant and less than 3 N, the trial is considered quiescent and analyzed with the quiescent approach. The plotted force responses of early and late epochs of the S1 and S2 stretches were fit with least squares quadratic polynomial curves and 95% confidence intervals. Heterogenic effects were detected by significant differences between the polynomials corresponding to early and late epochs of S1 and S2 responses (Table 5-1). In a case when the confidence intervals for a pair of polynomials were overlapping, the two polynomials were considered statistically indistinguishable for the range over which they overlapped.

Stretches that had a sudden background force change and spontaneous force responses unrelated to muscle stretch or tibial nerve stimulation were eliminated from the analysis. Mechanical artifacts caused by mechanical interactions between muscles, although rare, were detected by apparent heterogenic effects that were observed 10 ms after the initiation of a stretch (Bonasera and Nichols 1996). These trials were rejected.

5.3 Results

The goal of this project was to determine if and to what extent inhibitory force feedback (iFFB) between knee and ankle extensors is affected by dorsal hemisection. This task was made difficult by the presence of autogenic and heterogenic clasp-knife inhibition (CKI) that was released following this type of lesion. Rymer and colleagues provided evidence that CKI in animals is autogenically based, but non-autogenous CKI sources can contribute to an overall inhibition (Rymer, Houk et al. 1979, Cleland and Rymer 1990). The autogenic and heterogenic CKI is entangled with iFFB making it challenging to evaluate changes in the iFFB pathway.

We have confirmed that surgically inflicted dorsal lesion released the CKI pathway by squeezing FHL tendon during varying GAS background forces, as suggested by Dr. Timothy Cope. The squeeze had a strong inhibitory effect on GAS, abolishing background forces to zero (data not shown). In order to minimize evoking the CKI pathway, we used 2-mm stretches as previous studies reported that CKI was elicited by 5-mm (Rymer, Houk et al. 1979) or 4-mm (Nichols and Cope 2001) muscle stretch. However, we observed both autogenic and heterogenic CKI even with small amplitude stretches. In distinguishing CKI form iFFB, we mainly relied on the magnitude and latency of the interactions.

5.3.1 The VASTI exhibited significant autogenic CKI and exchanged heteronymous iFFB and CKI with ankle extensors.

In this study, employing 2-mm muscle stretch, we observed an autogenic CKI only in VASTI muscle in both quiescent and active conditions. While VASTI muscles in cats with lateral hemisection often exhibit significant adaptation during the hold phase of a

stretch (compared to spinally-intact cats), the presence of the CKI in cats with dorsal hemisection can be distinguished from an adaptation by magnitude and latency, as the CKI is a large magnitude and long latency reflex pathway. Thus, in the following figures, we present early and late epochs of S1 and S2 force responses from quiescent and active trials.

5.3.1.1 VASTI↔GAS

The heterogenic iFFB effect onto VASTI was challenging to determine considering that autogenic CKI was frequent and abolished force response of the S1 VASTI stretch (Figure 5-2: A). To circumvent this, we compared regression lines from S1 and S2 during the early epoch (Figure 5-2: C, blue full vs dashed line) of stretch and observed weak and not significant (mean percent difference in late quiescent condition was 1.8%) iFFB from GAS onto VASTI. However, the iFFB takes a while to develop and is most notable in the late epoch, so we sought examples where the VASTI does not exhibit autogenic CKI. In those cases, the magnitude of iFFB onto VASTI varied and resembled that of spinally-intact cats. On the other hand, the VASTI donated moderate and significant iFFB (with mean percent difference in late epoch under quiescent condition of 26% and $p < 0.05$, Figure 5-2: B & D) and large CKI onto GAS, as two distinct inhibitory phases could be discerned from traces where GAS is held isometrically (Figure 5-12). The GAS muscle did not exhibit autogenic CKI, either in quiescent (Figure 5-2: B, S1 – full black trace) or active trials, as regression of early and late epoch in S1 overlapped (Figure 5-2: D, full blue and red line overlap). The VASTI inhibited GAS most strongly in late epoch under active conditions (Figure 5-2: D, separate red full (S1) and dashed (S2) lines with mean percent difference of 60%, $p < 0.05$), presumably due to compounded iFFB and CKI.

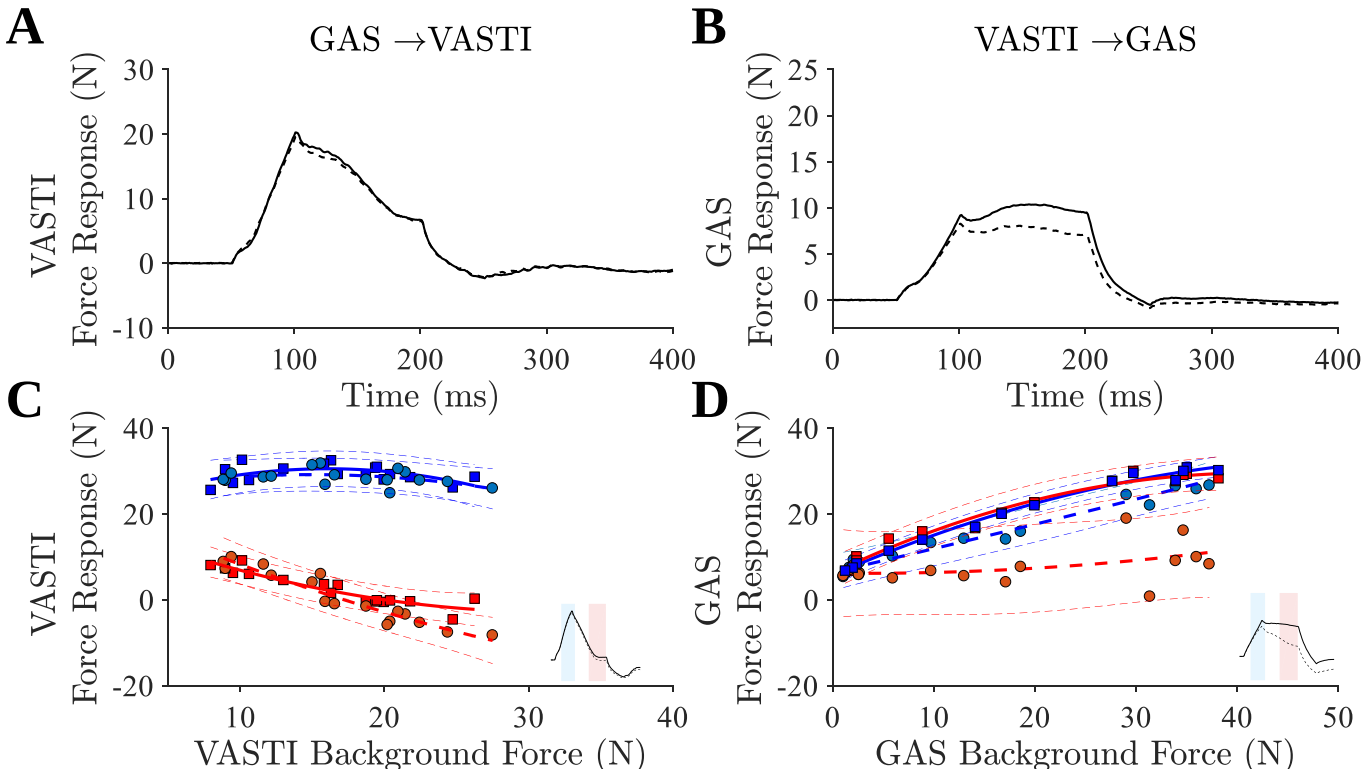

Figure 5-2: VASTI↔GAS interaction in a representative cat. The VASTI muscle showed significant autogenic CKI in quiescent (*A*) and active (*C*) condition (separate early (blue) and late (red) regression lines in both S1 (full line) and S2 (dashed line). The force feedback arising from GAS to VASTI was insignificant. On the other hand, VASTI inhibited GAS strongly in both quiescent (*B*) and active (*D*) conditions. In active trials (*D*) there was insignificant CKI inhibition autogenically in GAS (red and blue full lines are overlapping). In state 2, there was medium force feedback inhibition in early epoch (blue full vs. blue dashed line), that strengthens in late epoch (red full vs red dashed line), presumably as a result of entangled CKI and iFFB.

In cats with lateral hemisection, the VASTI inhibited GAS more strongly than the other way around in all cases, while in dorsal hemisection we observed a varied bias in the quiescent condition. Specifically, comparing this interaction across cats, we found a proximal to distal bias in 2/6, balanced bias in 3/6, and one non-significant interaction in both directions (Figure 5-3)[5].

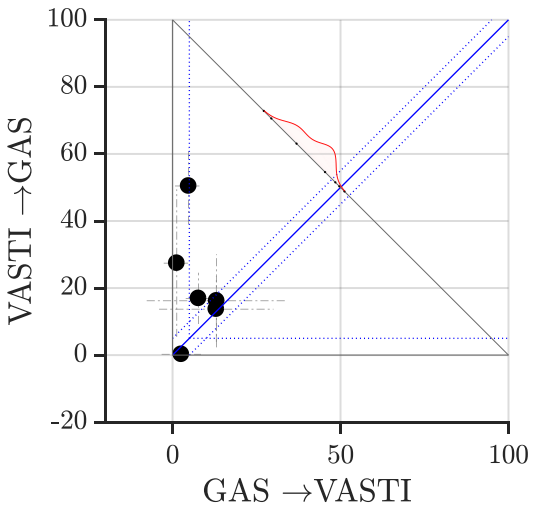

Figure 5-3: VASTI↔GAS quiescent interactions across cats with dorsal hemisection. The magnitudes of interaction from GAS to VASTI were plotted against the magnitudes of interactions from VASTI to GAS (as described in detail in the Methods section). Overall, proximal to distal bias (red trace distribution) is prominent, presumably due to autogenic CKI that abolishes VASTI S1 force response, thus occluding the effect of heterogenic iFFB from GAS.

[5] Note: Figures presenting data pooled across all cats in this chapter were obtained in the same manner as Figure 3.1, bottom left.

5.3.1.2 VASTI↔FHL

The interaction from FHL onto VASTI was difficult to evaluate due to autogenic CKI expressed in VASTI (Figure 5-4: A). By comparing interaction in the early epoch of the active trail (Figure 5-4: C, blue full line (S1) and blue dashed line (S2)), it can be discerned that iFFB from FHL onto VASTI is negligible. The late epoch is characterized by modest inhibition from FHL (absolute difference of 2.5 N or 43%), presumably only due to iFFB (supported by latency data in Figure 5-12). More precisely, comparing conditions where VASTI or FHL were held isometrically, while the other was being stretched (Figure 5-12), it can be observed that these two muscles exchange iFFB and unidirectional CKI (from VASTI to FHL). The VASTI donates a modest, but significant inhibition onto FHL in quiescent (in early epoch 19% and in late epoch 26% mean difference, both significant $p < 0.05$, Figure 5-4: B) and active (in early epoch 24% that is not significant, Figure 5-4: D) conditions, that gets stronger in late epoch (26% mean difference, significant, $p < 0.05$, Figure 5-4: D, red full vs. red dashed line), presumably due to compounded iFFB and CKI. The FHL does not exhibit autogenic CKI in either quiescent (Figure 5-4: B, absent force drop in full black trace) or active trials (Figure 5-4: D, early (blue) and late (red) regression lines of S1 (full) do not differ significantly).

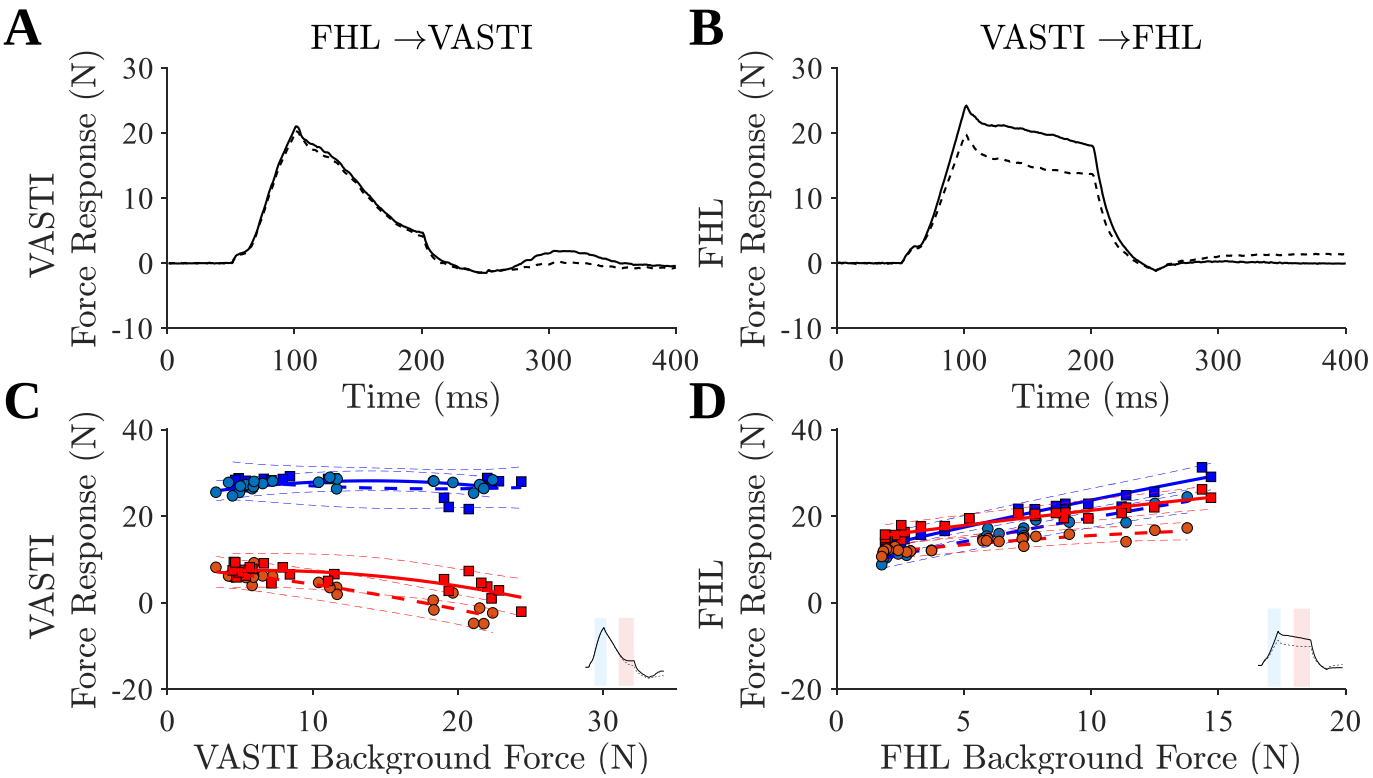

Figure 5-4: VASTI↔FHL interactions. The VASTI exhibits autogenic CKI in both quiescent (*A*), and active (*C*) trials (separate early (blue) and late (red) epoch S1 regression lines. Negligible force dependent inhibition was observed from FHL onto VASTI. On the other hand, VASTI donates medium force dependent inhibition onto FHL in quiescent (*B*) and active (*D*) trials, while FHL does not show signs of autogenic CKI in either conditions.

Comparison of quiescent data across all cats (Figure 5-5) reveals that VASTI inhibited FHL more strongly than the other way around in 4/5 cases, most likely as a result of an autogenic CKI that ablates VASTI force response (Figure 5-4: A). However, the magnitude of iFFB in isometric condition shows stronger iFFB from FHL onto VASTI (Figure 5-12).

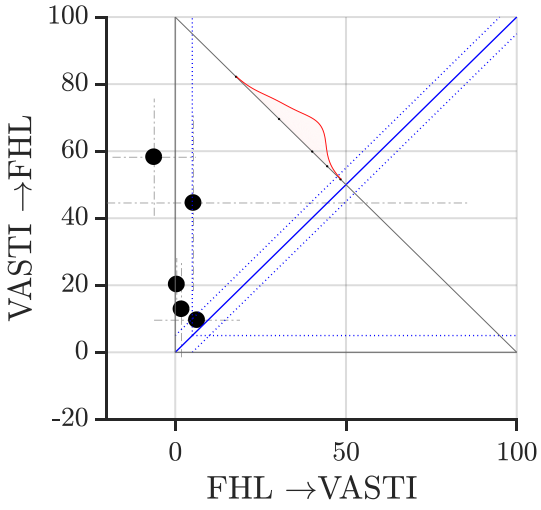

Figure 5-5: VASTI↔FHL quiescent interactions across cats with dorsal hemisection. The magnitudes of interaction from FHL onto VASTI were plotted against the magnitudes of interactions from VASTI onto FHL (as described in detail in Methods section). Overall, the prominent is proximal to distal bias (red trace distribution), presumably due to autogenic CKI that abolishes VASTI S1 force response, occluding the effect of heterogenic iFFB from FHL.

5.3.2 The FHL donates the CKI and iFFB to other ankle extensors, but receives the CKI only from GAS, and varying magnitudes of iFFB from other muscles

IFFB interactions between FHL and other ankle extensors were obscured by the presence of heterogenic CKI. Inhibition onto isometrically held muscles shows that GAS and FHL exchange balanced iFFB, and a very strong CKI (stronger from FHL to GAS) (Figure 5-12).

5.3.2.1 <u>FHL↔GAS</u>

Under quiescent conditions, FHL and GAS often exchanged a balanced and physiologically significant interaction but no autogenic CKI is apparent in either muscles (Figure 5-6: A & B, no significant force decrease in either GAS or FHL S1 (black full lines)). However, force dependent inhibition was stronger from FHL onto GAS in early epoch (Figure 5-6; C, early epoch S1 (blue full) vs. S2 (blue dashed line)) had mean difference of 28%, compared to the same epoch in interaction from GAS onto FHL which was only 12% (Figure 5-6: D, early epoch S1 (blue full) vs. S2 (blue dashed line)). While

interaction from GAS to FHL in the late epoch remained insignificant (Figure 5-6: D late S1 (red full) vs. S2 (red dashed line)), inhibition from FHL onto GAS in late epoch significantly increased (Figure 5-6: C, late epoch S1 (red full) and S2 (red dashed) line are considerably separated with mean difference of 120%, $p < 0.05$). This late inhibition is probably due to the compounded effect of iFFB and CKI.

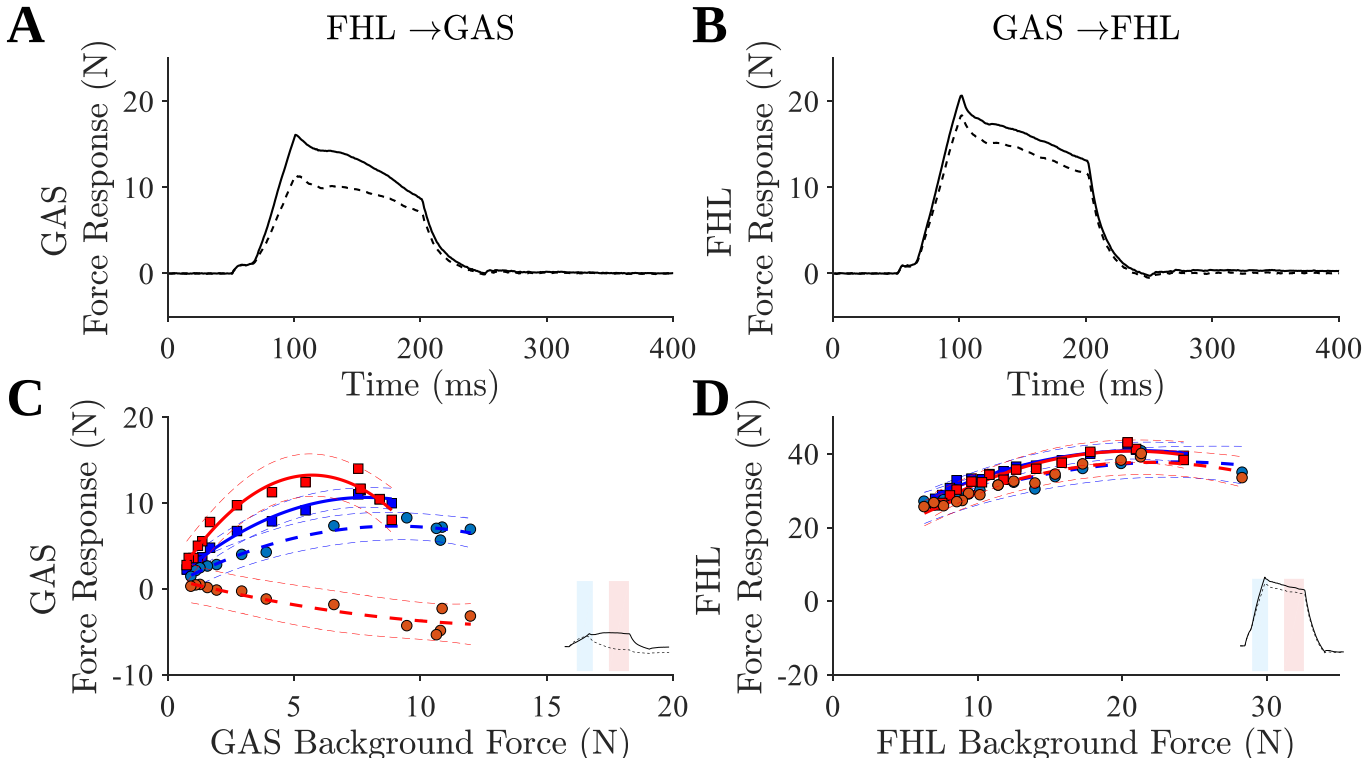

Figure 5-6: FHL↔GAS interaction. Balanced force feedback inhibition was exchanged between GAS and FHL and neither of them shows signs of autogenic CKI under quiescent conditions (*A* & *B*). Under active conditions, FHL inhibits GAS more strongly than the other way around in both epochs (*C* & *D*), especially in the late epoch where inhibition is presumably arising from both iFFB and CKI pathways

The hallmark of lateral hemisection is the release of the iFFB from FHL onto other ankle extensors, and decreased magnitude of iFFB onto FHL, resulting in a convergence of inhibition onto the main ankle extensors. Following the dorsal hemisection, we commonly observed varied bias as in spinally-intact cats. Specifically, we observed

proximal to distal bias in 3/12, balanced in 2/12 and distal to proximal bias in 7/12 interactions examined (Figure 5-7). The balanced interaction is evident in the quiescent condition (Figure 5-6: A & B), and early epoch of active condition (Figure 5-6: blue markers and fits in lower panels), while an iFFB and, superimposed on it, a CKI are prevalent in the late epoch of GAS, but not FHL (Figure 5-6: red markers and fits in the lower panels).

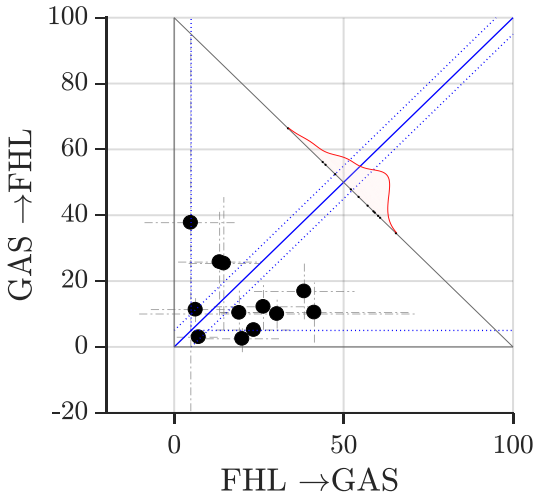

Figure 5-7: FHL↔GAS quiescent interactions across cats with dorsal hemisection. The magnitudes of interaction from FHL onto GAS were plotted against the magnitudes of interactions from GAS onto FHL (as described in detail in Methods section). The bias varied from proximal to distal to distal to proximal (explained in text in detail), and magnitudes of FHL→GAS interactions were on average smaller compared to cats with lateral hemisection (Chapter II). Noteworthy is that these interactions probably include entangled iFFB and CKI in both directions.

5.3.2.2 FHL↔PLANT

A similar bias distribution was observed in FHL and PLANT interaction in a quiescent condition (Figure 5-8: A & B). In a quiescent condition, two distinct inhibitions could be detected in interaction from FHL onto PLANT, an early iFFB (mean difference of 11%, not significant), and late iFFB and CKI combined (mean difference of 62%, $p < 0.05$, Figure 5-8: A). An iFFB from FHL onto PLANT is substantial under active conditions, as attested by separate early epoch S1 (full line) and S2 (dashed line) regression lines with mean difference of 55%, $p < 0.05$, Figure 5-8: C). In late epoch, this inhibition

becomes even stronger (mean difference of 98%, $p < 0.05$, Figure 5-8: C), as the contribution from CKI pathway superimposes onto iFFB. In quiescent conditions, PLANT donates a considerable and significant inhibition onto FHL (the mean difference in early epoch is 20% and in late 14%, both $p < 0.05$, Figure 5-8: B), that wanes in an active condition (not significant, Figure 5-8: D), and no apparent heterogenic CKI (Figure 5-8: B). Neither FHL nor PLANT displayed signs of autogenic CKI in either condition.

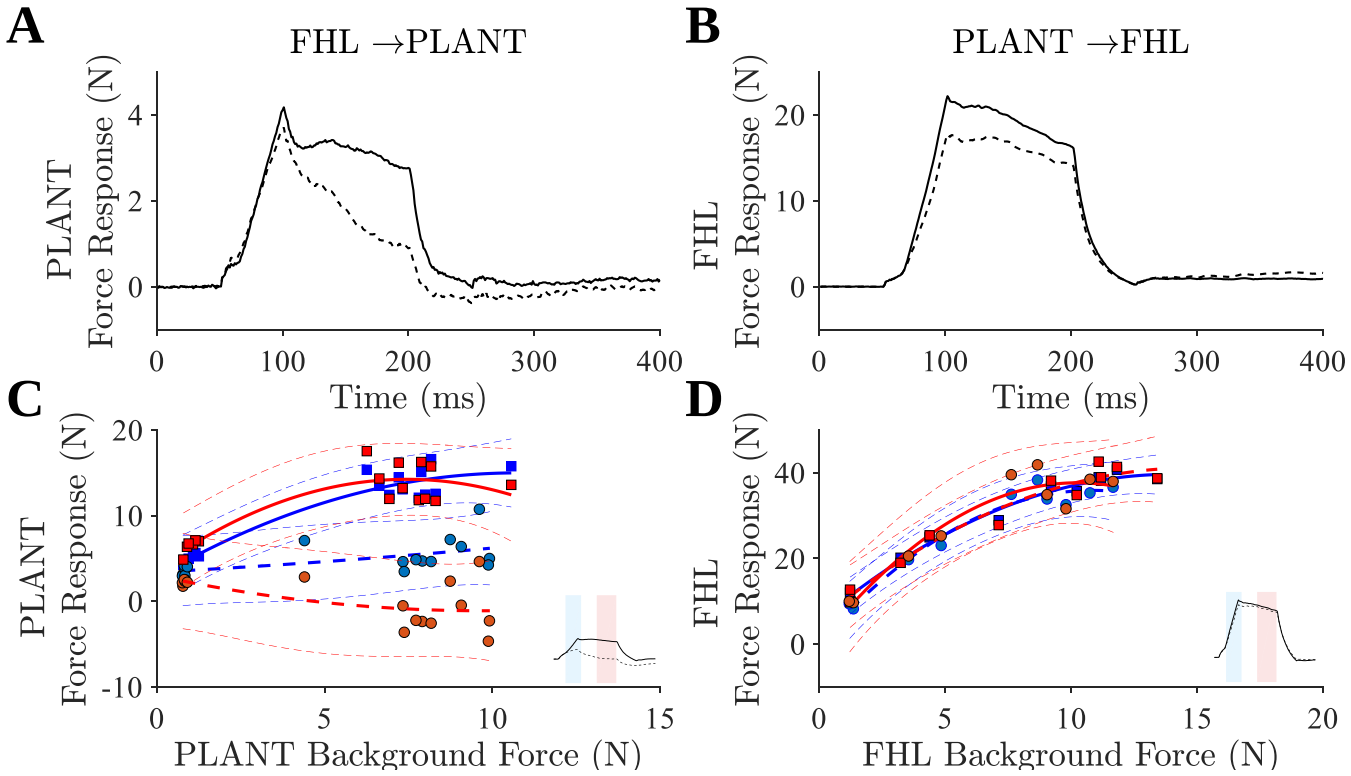

Figure 5-8: FHL↔PLANT interaction. The most noticeable heterogenic effect is separation of two epochs of inhibition from FHL onto PLANT (*A*). Specifically, an early force dependent inhibition and superimposed on it, a clasp-knife inhibition in a late epoch. Similar heterogenic effect is observed in active trials (*C*). In early epoch we detect a strong force feedback inhibition (separated blue full and dashed regression line), and in late epoch in S2 we observed a clasp-knife inhibition superimposed onto force feedback inhibition, all resulting in a strong inhibitory heterogenic effect from FHL onto PLANT. Interaction from PLANT to FHL is characterized by a moderate force dependent inhibition in quiescent condition (*B*), and lack of clasp-knife inhibition in either condition or states (*B* & *D*).

Across all cats, the dominant bias was distal to proximal. However, we observed proximal to distal bias in 1/8 cases, balanced in 3/8 and distal to proximal in 4/8 cases (Figure 5-9).

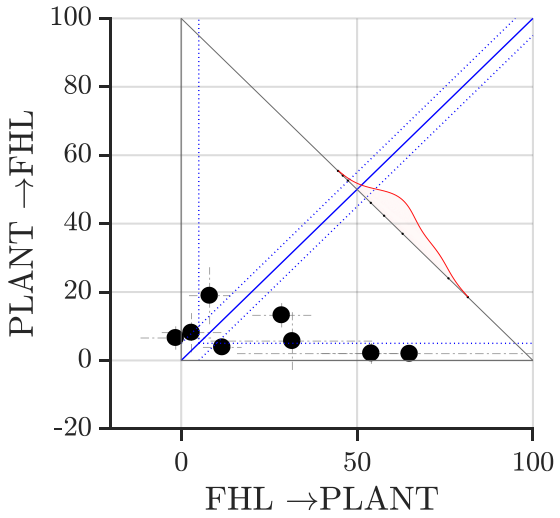

Figure 5-9: FHL↔PLANT quiescent interaction across cats with dorsal hemisection. The magnitudes of interaction from FHL onto PLANT were plotted against the magnitudes of interactions from PLANT onto FHL (as described in detail in Methods section). The bias was distal to proximal, however, there were cases of proximal to distal bias (described in text). Noteworthy, interactions from FHL onto PLANT probably includes a compounded effect of iFFB and CKI, while interactions from PLANT onto FHL are presumably due to iFFB only.

5.3.2.3 FHL↔SOL

The FHL had similar effect onto SOL, as two groups of inhibition can be distinguished by magnitude and latency; sizeable early iFFB (mean difference of 25%., $p < 0.05$), and even larger late (mean difference of 60%, $p < 0.05$), presumably CKI superimposed over iFFB (Figure 5-10: A). A similar effect was observed in the active condition, with modest iFFB in early epoch (mean difference between blue full (S1) and dashed (S2) lines is 27%, not significant, Figure 5-10: C), and heterogenic CKI superimposed onto iFFB in S2 in late epoch (mean difference between red full (S1) and dashed (S2) lines is 85%, $p < 0.05$, Figure 5-10: C). The SOL, on the other hand, did not significantly interact with FHL in either early quiescent (Figure 5-10: B) or active (Figure 5-10: D) trials.

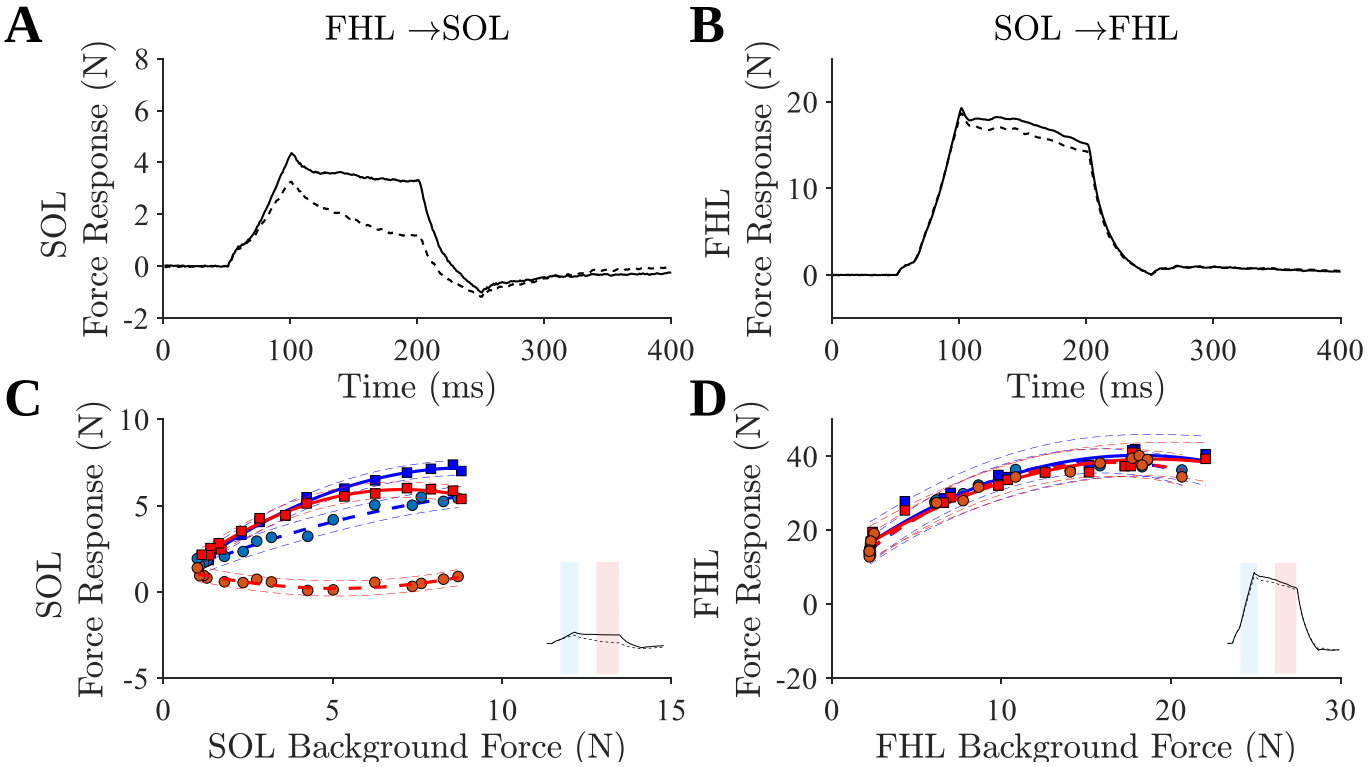

Figure 5-10: FHL↔SOL interaction. The interaction from FHL onto SOL resembled those onto PLANT. In quiescent condition, one can discern two distinguished epochs of inhibition; early force dependent inhibition and late clasp-knife inhibition superimposed onto force dependent inhibition (*A*). Similar distinction between two kinds of inhibition can be made in active trials (*C*), as early (blue full (S1) vs dashed (S2)) regression lines are separate. These lines are even further apart in late epoch (red full (S1) and dashed (S2)). SOL did not significantly interact with FHL in either quiescent (B) or active (D) trials. Neither FHL nor SOL showed autogenic clasp-knife inhibition in either conditions.

Neither SOL nor FHL showed autogenic CKI, in either quiescent nor active conditions (Figure 5-10: C & D: as blue and red full lines overlap across varying background forces). However, under active conditions, in the early epoch, FHL inhibits SOL more strongly than the other way around (Figure 5-10: blue full and dashed lines). In late epoch, superimposed onto iFFB is a very strong CKI from FHL onto SOL (Figure 5-10: lower left figure red dashed line).

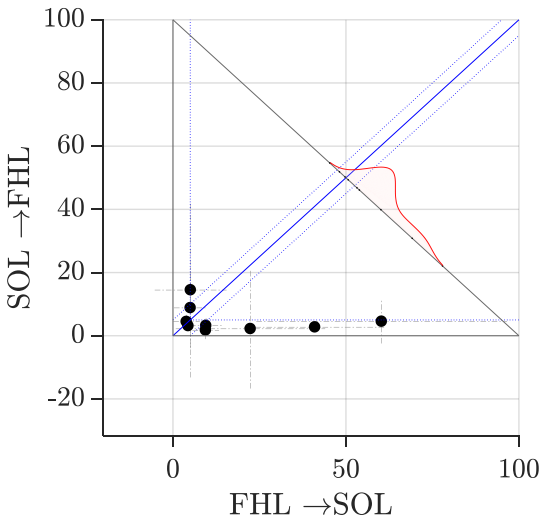

Figure 5-11: FHL↔SOL quiescent interactions across cats with dorsal hemisection. The magnitudes of interaction from FHL onto SOL were plotted against the magnitudes of interactions from SOL onto FHL (as described in detail in Methods section). The overall bias was distal to proximal and, in addition to iFFB, probably incorporated the strong heterogenic CKI from FHL onto SOL.

Although SOL did not have any effect on isometrically held FHL (Figure 5-12), in the quiescent condition (Figure 5-11) it more strongly inhibited FHL in 1/9 interactions evaluated. Under the same condition, the SOL and FHL exchanged balanced inhibition in 3/9 cases, and FHL inhibited SOL more strongly in 5/9 cases.

5.3.3 A note on increased and decreased gain of the stretch reflex following dorsal hemisection

In cats with a lateral hemisection, we observed a substantial increase in gain of stretch reflex in VASTI and GAS, and negligible or no change in other ankle extensors (described in detail in Chapter II). Following dorsal hemisection, we observed that stretch reflex is transiently depressed in VASTI (Table 5-2), while it transiently increases in GAS, PLANT, SOL, and FHL compared to spinally-intact cats. By week 12, stretch reflex magnitudes have settled back to the control values (except for FHL which is diminished).

Table 5-2: Showing stiffness (N/mm) of knee and ankle extensors following dorsal hemisection. Values presented are an average ± standard deviation. These data were collected using the same approach described in Chapter II. Briefly, the slope of force rise during the last 1 mm of muscle elongation is assumed to be representative of muscular stiffness (equation 2.2).

	VASTI	**GAS**	**PLANT**	**SOL**	**FHL**
3 wks (n = 2)	16.66 ± 3.6	6.11 ± 3.2	4.83 ± 0.65	2.57 ± 0.3	9.1 ± 1.25
7 wks (n = 4)	17.86 ± 1	3.98 ± 1.6	4.33 ± 0.3	2.54 ± 1.2	9.5 ±3.6
12 wks (n = 3)	23.74 ± 1.45	4.42 ± 1.8	2.59 ± 0.5	1.83 ± 0.11	5.94 ± 0.7

5.3.4 The latency of CKI and iFFB pathways

In order to distinguish between heterogenic inhibitions originating either from GTO's or free nerve endings, we used their distinct conduction velocities, 70 - 120 m/s, and 3 – 30 m/s, respectively (Kandel, Schwartz et al. 2000).

Based on the conduction velocities, we then determined the presence or absence of CKI in every single heterogenic interaction recorded in cats with dorsal hemisection. This involved a subjective evaluation of responses of isometrically held recipient muscles at high background forces, while the donor is being stretched. Exemplar traces are presented in Figure 5-12. The effects of a stretch of individual donors (columns) were detected as responses with different latencies in the recipient muscles (rows). The y-axis represents force responses of recipient muscles with background forces were subtracted, and the x-axis marks time. The black vertical line marks the onset of donor stretches, the blue vertical line marks the earliest possible appearance of group I feedback (18 ms), and the red vertical

line marks the earliest possible appearance of group III feedback. The presence of interaction beyond the red line would indicate the presence of CKI. This method was used to map the directionality of CKI interactions among knee and ankle extensors (Figure 5-13).

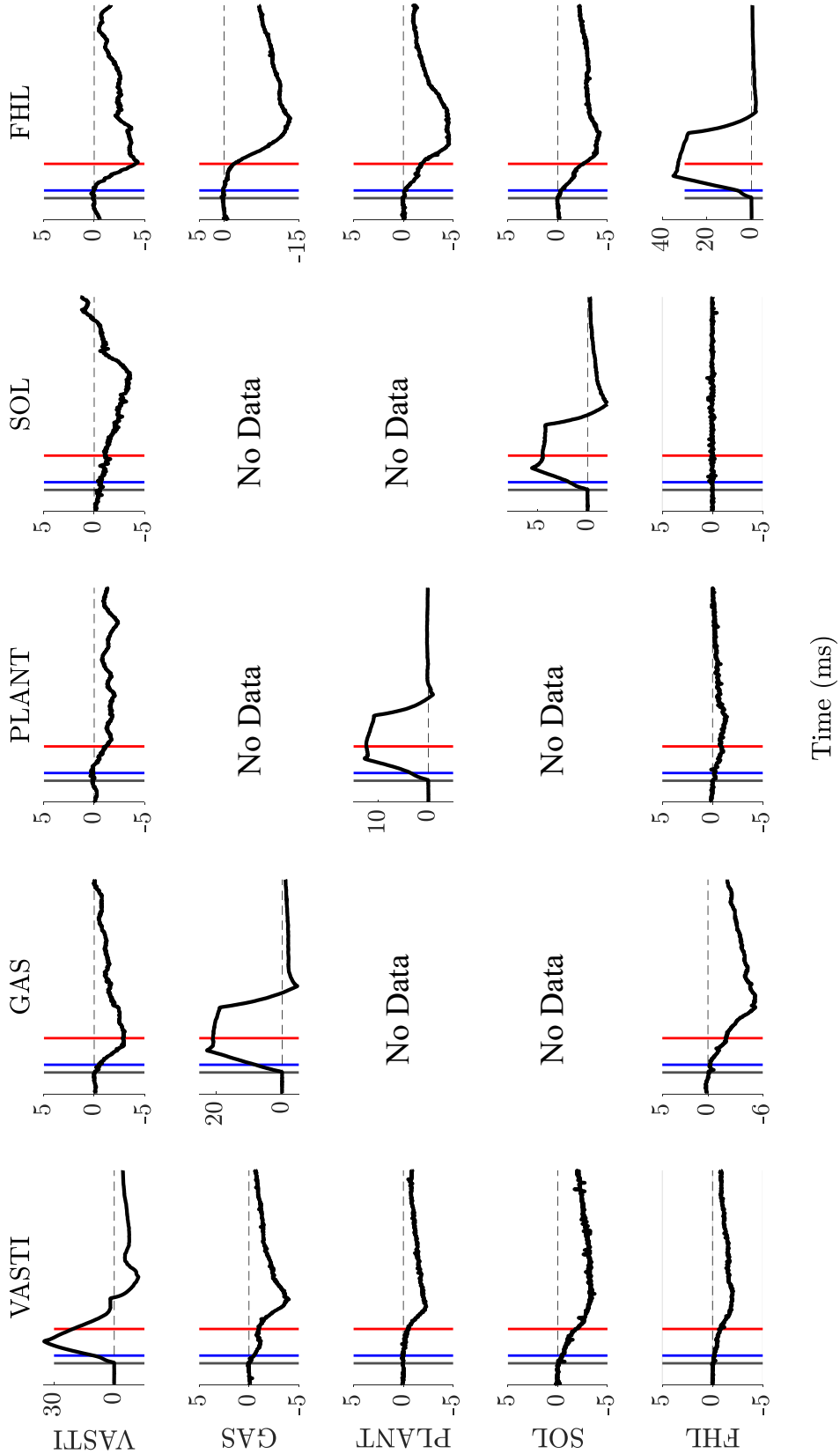

Figure 5-12: Latencies of heterogenic interactions between donor (column) and recipient (rows). Recipient muscles were held isometrically at high background forces, while donors were stretched. The black vertical line marks the stretch onset. The blue vertical lines mark earliest possible appearance of group I feedback (18 ms), and red lines mark the first possible appearance of group III feedback (80 ms).

5.4 Discussion

Following spinal cord injury, a variety of additional reflex pathways become apparent, as the removal of supraspinal inhibition disinhibits them (Burke, Knowles et al. 1972). The goal of this project was to evaluate if and to what extent inhibitory force feedback from the GTO's is affected by dorsal hemisection. The primary challenge in accomplishing this goal was the coexistence of autogenic and heterogenic CKI that either occluded autogenic force responses of recipient muscles or was superimposed onto heterogenic iFFB interactions. Thus, we sought to characterize both the CKI and iFFB pathways in order to be able to distinguish them.

5.4.1 The CKI is apparent after dorsal lesions; sporadic autogenic, but abundant heterogenic CKI among knee and ankle extensors

The CKI is distributed within (autogenically) and between antigravity muscles (heterogenically), and actively targets single joint muscles (such as VASTI in this study) (Nichols and Cope 2001). However, it is not found in ankle stabilizing muscles that exert moment in the transverse plane or muscles linked by reciprocal inhibition that maintain ankle lateral stability (Nichols and Cope 2001). The main effect of the CKI pathway is widespread strong inhibition of major limb extensors, causing the collapse of the limb along the extension-flexion axis while preserving lateral stability. On the other hand, iFFB is not manifested autogenically but rather converges mainly onto heteronomous motoneuron pools, most often onto those of muscles with different biomechanical actions (Eccles, Eccles et al. 1957, Wilmink and Nichols 2003). However, inhibitory interactions

were also found between close synergists, such as PLANT and GAS (Lyle and Nichols 2018).

The lack of abundant autogenic CKI in this study might be explained by the use of 2-mm muscle stretch that probably does not sufficiently activate free nerve endings in the muscle. Previous research has evoked these responses with 5-mm (Chen, Theiss et al. 2001) and 4-mm muscle stretch (Nichols and Cope 2001). However, Nichols and Cope have noted that even stretches of 2-mm should induce the CKI response in the completely spinalized cat. The lack of ubiquitous autogenic CKI response might imply that CKI circuitry is not released sufficiently after dorsal hemisection to be sensitive to 2-mm stretches. However, a more likely explanation is the possibility that the CKI subsided as a part of the recovery process (Nichols and Cope 2001), as data presented in this chapter were collected on chronically lesioned cats. It was challenging to discern the existence of heterogenic CKI from a stretch evoked force response as it is superimposed onto iFFB. Furthermore, muscles adapt to hold independent of the state of the spinal cord (described in detail in Chapter II).

The S2 force responses frequently did not have two distinct inhibition epochs (early iFFB and late iFFB + CKI). Thus, we sought to detect them from force traces when a recipient muscle is held isometrically (Figure 5-12). This approach is helpful in distinguishing short-latency iFFB inhibition (with an onset at about 18 ms) and a long latency, greater magnitude CKI (with an onset of 80 ms (Nichols and Cope 2001)). With this approach, we concluded that heterogenic CKI was prevalent and bidirectional between SOL and VASTI (targeting the single joint muscles, as expected) and GAS and FHL. It was also unidirectional from VASTI and FHL onto PLANT (Figure 5-12).

5.4.2 Varied directional bias observed in cats with dorsal hemisection suggests that the organization of iFFB is not affected by dorsal hemisection

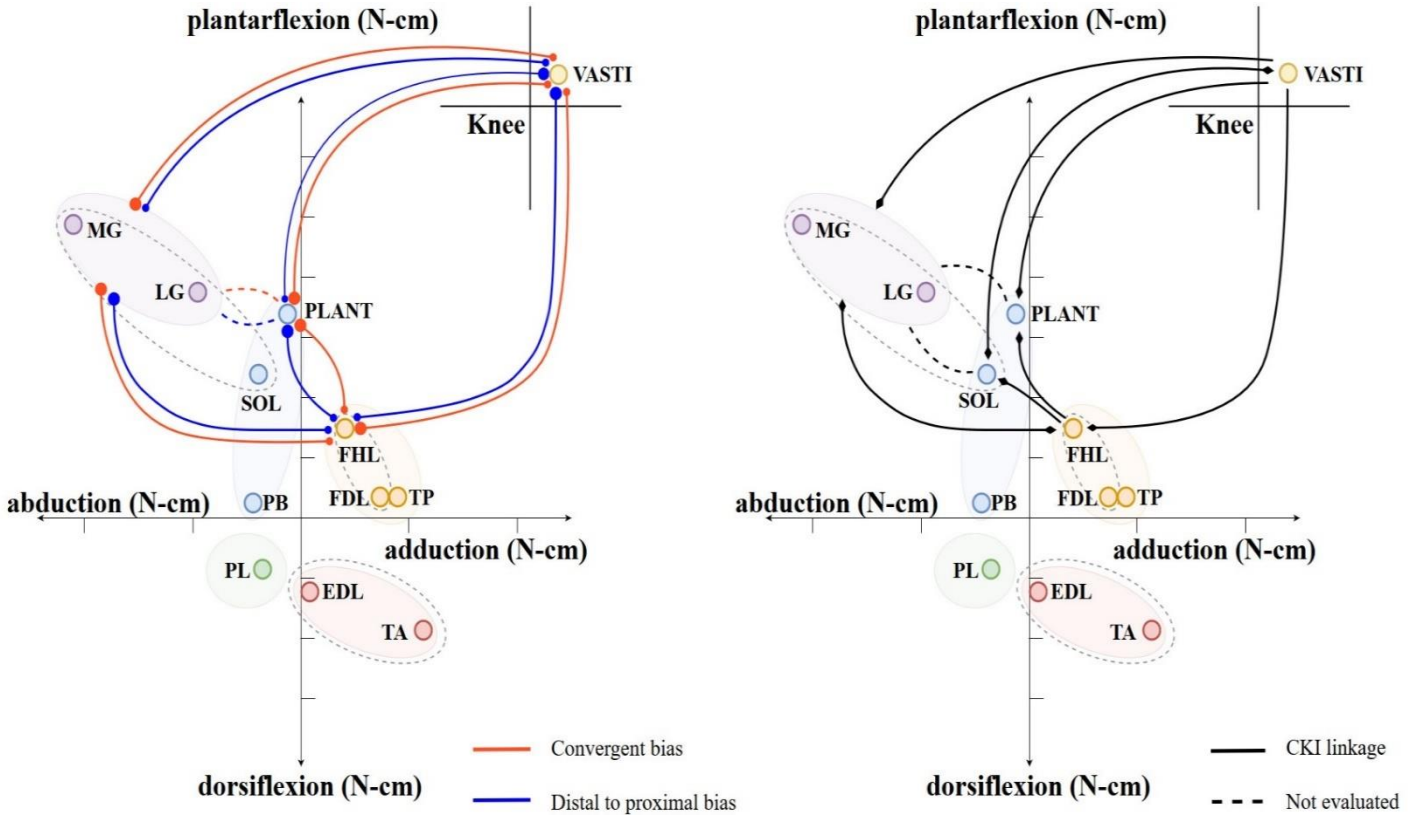

Figure 5-13: Organization of the iFFB (*left*) and the CKI (*right*) following dorsal hemisection. In this chapter we presented data that points to varied inhibitory bias originating from the iFFB pathway. On the left, we presented two of three observed patterns of iFFB organization. On the right, we show organization of CKI compiled based on presence or absence of CKI in isometrically held recipient muscles

Previously, we have shown that following lateral hemisection, iFFB becomes selectively amplified and diminished among extensor muscles, resulting in a convergence of inhibition onto ankle extensors (described in detail in Chapter III). Although iFFB is appreciable in spinally-intact decerebrate cat, its directionality is subject to modulation by supraspinal tracts, and thus it can take three directional patterns; proximal to distal, convergent and distal to proximal (Lyle and Nichols 2018). The reduction of these options to only the convergent pattern consistently observed following lateral hemisection suggests

that iFFB bias is a controlled variable. To more precisely locate a modulatory tract, it was essential to determine if similar reduction happens following lesions of dorsal hemisection. Evaluating early inhibition arising from GTO's enabled us to draw conclusions regarding an organization of iFFB in cats with dorsal hemisection.

The results presented in this chapter suggest that the bias of the iFFB is not affected by dorsal hemisection since a spectrum of magnitudes of iFFB was observed and can be classified into the three established patterns found in the spinally-intact cat (Lyle and Nichols 2018). Two of those patterns are presented in Figure 5-14 (left panel). Taken together with results from lateral hemisection, this suggests that tract(s) that regulate iFFB bias are located in the ventral cord. Confirmation of this suggestion would come from outcomes of ventral cord lesions. It is expected that ventral cord lesions would result in a consistent pattern of iFFB resembling the pattern introduced by the lateral cord lesion, and, unlike the findings in this study, no apparent CKI. This would add to the accumulating knowledge of the differences between iFFB and CKI pathways.

5.4.3 The supraspinal tracts affected by dorsal hemisection are unlikely to be modulators of the force-dependent pathway

The short latency stretch reflex is also changed in dorsal hemisection, but differently than following lateral hemisection. Although the gain of the stretch reflex increases in ankle extensor muscles following dorsal hemisection, a finding that is consistent with the literature (Taylor, Friedman et al. 1997), this amplification is not as substantial as the amplification found following lateral hemisection (described in detail in Chapter II). Furthermore, following dorsal hemisection, the VASTI stretch reflex is

suppressed and recovers to the control values through the 12-week period, whereas it is transiently amplified and subsides below control values after 12 weeks post-lesion, following lateral hemisection. This might suggest that two supraspinal tracts control stretch reflex gain, one located ventrally and the other located more dorsally, potentially the ventral and dorsal reticulospinal tracts.

The dorsal hemisection severs not only tracts that transmit specific voluntary motor commands, such as the corticospinal and rubrospinal, but also those that exert tonic influence related to arousal and posture, such as the dorsal reticulospinal tract. Although tonically active in the decerebrate cat preparation (Baldissera, Hultborn et al. 1981), removal of dorsal reticulospinal influence preferentially disinhibits interneurons with the weak group I input, while interneurons with the strong group I input tend to be inhibited (Chen, Theiss et al. 2001). Considering that the reticular formation and the brainstem affect proximal muscles more than distal muscles (Hall and McCloskey 1983, Buford and Davidson 2004), it is not surprising that the VASTI exhibited both attenuated stretch reflex and a strong autogenic and heterogenic CKI.

The influence of the reticulospinal tract onto iFFB is unknown, although neurons in the pontomedullary reticular formation have been strongly implicated in postural control (Schepens, Stapley et al. 2008). The dorsal reticulospinal tract was severed in both dorsal and lateral hemisection, but no reorganization of iFFB was found following a dorsal hemisection. Thus, this tract is an unlikely modulator of the iFFB. The spared pathways on the ventral side, such as medial (pontine) reticulospinal and vestibulospinal tracts might modulate segmental circuitry mediating force feedback. There is accumulating evidence that the vestibulospinal tract modulates iFFB (Nichols, Gottschall et al. 2014), although

this does not exclude influence from the medial reticulospinal tract. There is evidence for and against the existence of interneurons co-modulated by both reticulospinal and vestibulospinal fibers (Davies and Edgley 1994). Interneurons coexcited by both reticulospinal and vestibulospinal tracts have been found in lamprey (Rovainen 1979). However, inhibitory actions of these tracts have been shown to be mediated by different populations of inhibitory interneurons. The inhibitory effect from the vestibulospinal tracts is mediated by Ia inhibitory interneurons mediating inhibition from extensors to flexors (Grillner and Hongo 1972), whereas inhibition by medullary reticulospinal tract is mediated by pathways of Ia/Ib nonreciprocal inhibition (Takakusaki, Kohyama et al. 2001). A ventral hemisection would eliminate the signal from both of these tracts, and more precise lesions would be required to rule out one of them.

5.4.4 The potential clinical implications of results presented in this chapter

Despite similarities between intermuscular distributions of iFFB and CKI, their release following ventral or dorsal hemisection would be manifested as specific and distinct clinical symptoms. This is important from a clinical perspective as the location and extent of a lesion can be discerned from clinical symptoms. The CKI pathway release, as observed in dorsal hemisection, has a characteristic motor deficit defined by resistance to stretch followed by an abrupt yield. On the other hand, an inability to modulate iFFB, due to lesions of the ventral tract(s), can manifest itself as an inadequate stiffness during upslope or downslope walking, as those situations require joint-specific stiffness (Simon, Ingraham et al. 2014). Furthermore, since the CKI is not found in ankle stabilizers, lateral stability should be conserved following dorsal hemisection, but impaired after ventral hemisection. This speculation is supported by Lyalka's research that points to the importance of the

ventral column in postural stability, as T12 ventral hemisection drastically reduced postural response in rabbits, while rabbits with dorsal and lateral hemisection regained the postural response (Lyalka, Orlovsky et al. 2009). However, further work is warranted to support the use of CKI and iFFB bias as diagnostic clinical symptoms.

CHAPTER 6. DISCUSSION

The primary focus of this dissertation was the contribution of proprioceptive feedback to postural instability following an incomplete spinal cord injury. In preceding Chapters, I have provided a comprehensive overview of changes in autogenic and heterogenic feedback arising from muscle spindles, Golgi tendon organs, and free nerve endings, following different spinal lesions. Furthermore, I characterized the magnitude, bias, and distribution of these feedbacks among knee, ankle, and toe extensors and flexors. In addition, I have addressed the potential mechanisms underlying the changes in these pathways. However, questions remain regarding the role, the integration, and relative contribution of these pathways to the postural stability of walking cat. In this chapter, I will discuss results and their importance for postural control from both neural and biomechanical perspective.

When evaluating the organization of these pathways and their functional implications for postural control and locomotion, it is important to first consider the state of the overall motor functions following injury. Following immediate flaccid paresis after spinal cord injury (SCI), cats recovered the ability to stand (Fung and Macpherson 1999) and step (Barbeau and Rossignol 1987, Basso, Murray et al. 1994, Kuhtz-Buschbeck, Boczek-Funcke et al. 1996), although gait was accompanied by a deficit. After SCI, cats adapted a crouched gait with increased flexion during swing and stance phase (Rossignol, Drew et al. 1999) and diminished vertical and lateral stability (Macpherson and Fung 1999). Similarly, a subpopulation of individuals with partial SCI can regain some ability to walk (Burns, Golding et al. 1997, Scivoletto and Di Donna 2009). However, walking is

often is accomplished using flexed lower extremities as if semi-crouching. Elucidating the underlying causes of this deficit can provide us with an insight into default organization of spinal cord circuitry (when not modulated by supraspinal tract(s)) and propose a link between unregulated spinal circuitries and postural instability.

6.1 Modulation of limb stiffness via integration of length and force feedback

The emerging idea is that SCI limits the capacity of humans and animals to develop adequate limb stiffness[6], required by various motor tasks. In an intact organism, overall limb stiffness is determined by the properties of the musculoskeletal system, such as the stiffness of bones, joints, cartilage, muscle, and tendons (Latash and Zatsiorsky 1993) and neural control. Meanwhile, muscle stiffness is determined by intrinsic mechanical properties and integration of supraspinal drive and proprioceptive feedback. It follows that, after SCI, muscle stiffness relies mainly on proprioceptive feedback, an integration of length and force feedback. Houk (Houk 1979) initially proposed the idea that proprioceptive feedback regulates muscular stiffness. He reasoned that the combined feedback from muscle spindle receptors and Golgi tendon organs (GTO) should result in the regulation of muscular stiffness, with the balance between excitatory length feedback and inhibitory force feedback determining stiffness magnitude. The stiffness of the soleus muscle does appear regulated in the decerebrate cat (Nichols and Houk 1976). However, this regulation was solely attributed to length feedback (Houk, Rymer et al. 1981) as the

[6] The mechanical properties of limbs can be summarized by the property of impedance that includes components related to elasticity, viscosity and inertia. The terms corresponding to elasticity and viscosity are generally nonlinearly related to position and velocity (Houk et al 2000), respectively, and frequently lumped together in the motor control literature as “stiffness” despite the fact that the term “stiffness” properly refers to the static mechanical properties of a system (Latash and Zatsiorsky 1993).

autogenic, inhibitory force feedback was found to be rather negligible (Rymer and Hasan 1980).

The length feedback is a negative feedback loop that increases the muscular force to resist stretching. Ever since its discovery (Sherrington 1910), its role has been a matter of intense debate. Merton proposed that the primary action of this reflex is to compensate for changes in the external mechanical load (Merton 1953). It follows that the length of a muscle should be a controlled variable via single-input, single-output servo-mechanism (SISO). This matter was subsequently pursued by Nichols (Nichols and Houk 1976), who proposed that individual muscle stiffness may be the regulatory variable. The length feedback augments the intrinsic properties of a muscle in a way to compensate for their inherent non-linearity, maintaining the stiffness of a muscle constant across physiological length changes (Nichols and Houk 1976). This relationship between displacement and force is what gives the muscle a spring-like property (Hogan 1985), where the spring constant is determined by the gain of the length feedback (evaluated in spinal cats in Chapters I and V). The synergists and antagonists are linked by a network of heterogenic length feedback consisting of primarily mutual excitation between the synergists and reciprocal inhibition of muscles with opposing action (Eccles, Eccles et al. 1957, Eccles, Eccles et al. 1957). On this account, the autogenic and heterogenic length feedback has been implicated in coordinating anatomical and physiological synergists to generate a unified and localized joint stiffness (Nichols 1999). This very property is an attractive mechanism a motor control system might manipulate to meet environmental demands, maintain posture and resist perturbation.

However, the actions of inhibitory force feedback would decrease the spring constant of a muscle in a task-dependent manner. The electrophysiological studies conducted by Eccles and colleagues have shown that feedback from GTO is heterogenic, inhibitory and widespread across extensor motoneurons (Eccles, Eccles et al. 1957). Mechanographic method employing stretch evoked GTO feedback yielded findings that independent of motor task, the interaction between extensor muscles are generally inhibitory in decerebrate cats (Nichols 2002, Ross and Nichols 2009, Lyle and Nichols 2018), force-dependent and widely distributed (Bonasera and Nichols 1994, Wilmink and Nichols 2003, Lyle and Nichols 2018). However, the magnitudes of these inhibitions exist on a spectrum resulting in a directional bias that is state-dependent. Discernable patterns of force feedback organization can be viewed as distinct points on that spectrum. For instance, a locomoting decerebrate cat exhibits inhibition directed to the most distal muscles (Ross and Nichols 2009). In Chapter II, we showed that cats with lateral hemisection display directional bias toward ankle joint muscles (Kajtaz, Lyle et al. 2017). Both of these states lie on a spectrum of possible force feedback directional organizations. Thus, it was reasonable to expect that spinally-intact and quiescent (non-locomoting) decerebrate cats would exhibit a variable directional bias across the spectrum (Lyle and Nichols 2018). This directionality does not seem random, but rather organized in a way to allow a flexible reconfiguration of the limb to meet unexpected environmental challenges. On one end of the spectrum, the inhibitory bias of control cat was directed toward distal toe flexors and ankle extensors; a pattern termed proximal→distal bias. On the other end, the inhibitory bias targets more proximal muscles, such as ankle and knee extensors, resulting in a pattern called distal→proximal bias. At the center of the spectrum is a most

commonly observed pattern of inhibitory convergence onto ankle extensors from both more proximal and distal muscles (Lyle and Nichols 2018). These findings are consistent with previous studies that evaluated the interactions segmentally between a small number of muscles (Bonasera and Nichols 1994, Bonasera and Nichols 1996, Wilmink and Nichols 2003).

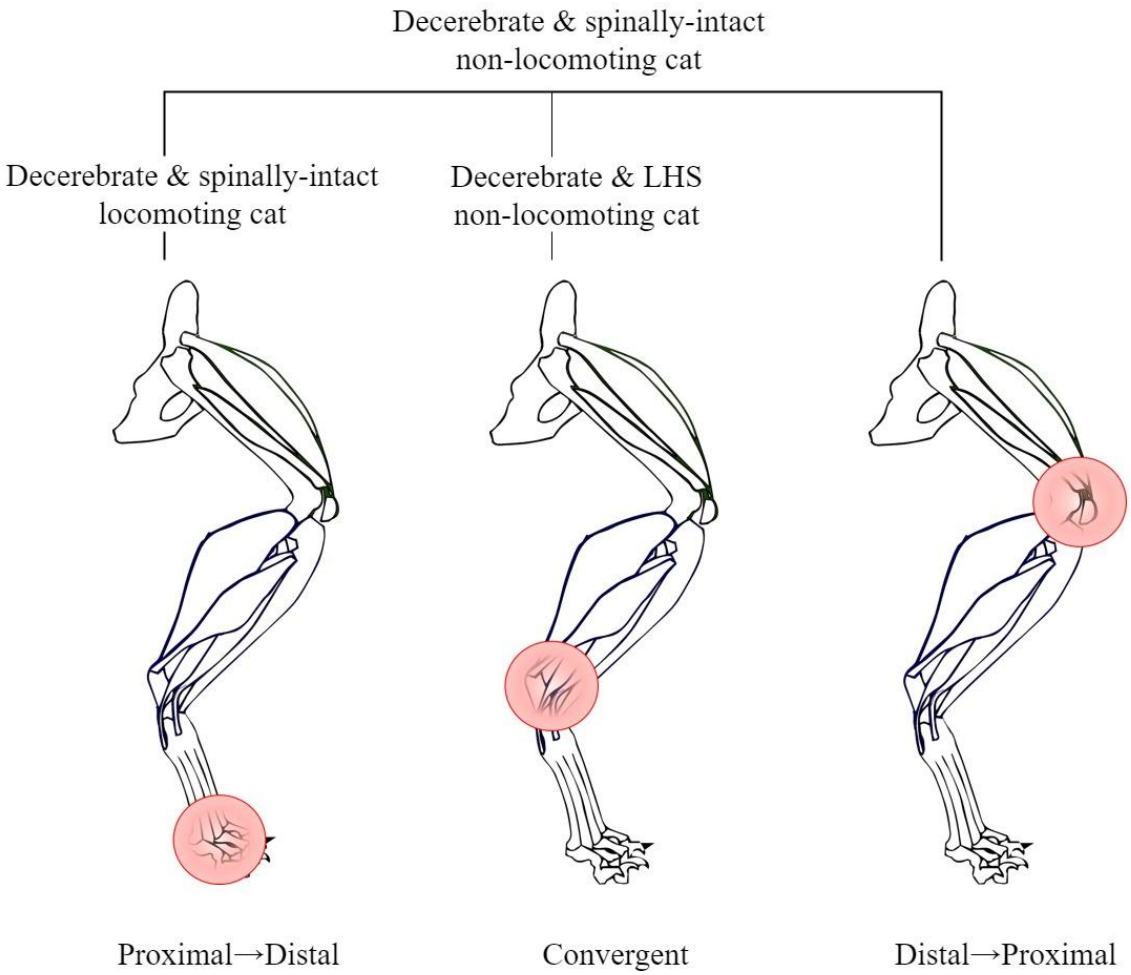

Figure 6-1: The ability of the nervous system to direct inhibitory bias toward the most distal joints (as in walking or running activity), an ankle (quiescent state following lateral hemisection) and to all limb joints (i.e., MTP, ankle and knee) in a quiescent and non-locomoting intact cat.

These results indicate the capability of the nervous system to modulate intermuscular force feedback bias according to the state of an animal. Such variability may reflect a constant tuning of magnitude and distribution of compliance of the limb through a change in the gain of length feedback (adjusting a localized joint stiffness) and modification of the bias of force feedback (adjusting compliance of multiple joints throughout a limb). Although stiffness adjustments happen in a muscle, the benefit of this tuning is not apparent at the level of a muscle. The integration of widely distributed and heterogenic force feedback and locally focused length feedback networks occurs at the limb level in a manner to allow for flexible adjustment of joint-specific stiffness. Although the individual muscles are actuators of the motor system, they are constituents of strongly integrated mechanical structures and are never activated in isolation. Furthermore, this limb-centric view recognizes a robust mechanical coupling due to dynamic (such as inertial coupling), and structural properties (such as coupling by biarticular or triarticular muscles) between all skeletal segments. Thus, a limb, with its constituent joints, muscles and their neural linkages, is a uniform ensemble and as such the basic unit for movement.

A limb is frequently modeled as a simple linear spring (Farley and Gonzalez 1996, Farley and Morgenroth 1999), where the resultant force is equal to the product of the spring constant (k_{leg}) and linear displacement ($F = k_{limb}\, dL$). Translated into angular dynamics, the joint stiffness can be defined because the resultant moment at a joint is equal to the product of the torsional spring constant and angular displacement of the joint ($M = k_{joint}\, d\theta$) (Farley and Morgenroth 1999, Brughelli and Cronin 2008). For instance, during stereotyped behaviors, such as running, hopping, or trotting, humans bounce on the ground in a spring-like manner (Cavagna, Saibene et al. 1964, Cavagna, Heglund et al. 1977, Cavagna and

Kaneko 1977, Blickhan 1989, McMahon and Cheng 1990). A considerable amount of energy is stored and released by joints, depending on joint angles and motion frequency. Accordingly, the leg is modeled as a single linear spring, or, in terms of joints, as a constant torsional spring with no damping. However, this view often does not account for a powerful and extended force feedback network where the sign, magnitude, and bias render k_{joint} variable in a task-dependent manner. Physiologically, the concept of constant stiffness is a simplification. For example, muscular stiffness is not constant throughout the stance phase of hopping, mainly due to the heterogenic effect of activation of numerous muscles. Thus, it can be expected that the joint stiffness is nonlinear in nature and that damping may be employed selectively and in a task-dependent manner.

6.2 Potential benefits of variable joint stiffness

This imposes a question, why would it ever be beneficial to have a variable k_{joint}? In other words, what are the advantages of targeted joint compliance? The answer might be in work done by individual joints. Individual joints generate or absorb energy during walking in a way that the net limb work depends on the energy balance among the joints. The mechanical role of the hip is not much affected by the limb loading, whereas the ankle and MTP can assume a role of a spring or dampener depending on limb configuration at touchdown. The limb postural configuration is determined by an initial knee joint angle that alters the balance of work among the joints (Daley, Usherwood et al. 2006), although the knee contributes little work itself. This results in posture-dependent changes in work performance of the limb, which allow an animal to rapidly absorb or generate energy in response to the perturbation. Since physiology is inherently linked with anatomy (muscle anatomy overview in Chapter I), this, in turn, has an anatomical basis. The distal hindlimb

muscles tend to have a distinct muscle–tendon architecture with short muscle fibers and long tendons (Crouch 1969, Biewener 1998). The architecture of distal muscles promotes economical force generation and elastic energy savings, whereas long-fibered proximal muscles modulate limb and body work (Biewener and Roberts 2000). During walking, the distal limb joints are the first to interact with the ground which imposes mechanical changes onto distal limb muscles which receive rapid proprioceptive feedback. The received feedback can turn an ankle and/or MTP joints into either spring or a dampener, depending on knee joint angles. It is not surprising that in running guinea fowl (Daley, Usherwood et al. 2006) and locomoting decerebrate cat (Ross 2006, Ross and Nichols 2009), the prominent bias is proximal→distal inhibitory bias as it can enhance stability during running by allowing rapid adjustment of the distal foot over rough terrain (Daley, Usherwood et al. 2006).

However, the patterns of muscle activation during the level walking are significantly different from those observed during upslope or downslope walking (Smith, Carlson-Kuhta et al. 1998, Gregor, Smith et al. 2006) with different behavior from distal joints. The configuration of the body is such that muscle activity is shifted to the hindlimbs, particularly extensors, during upslope walking and to the forelimbs during downslope walking. Previous research indicates that hindlimb extensors undergo significant length changes during downslope rather than upslope walking (Gregor, Smith et al. 2006), and upslope walking might be a motor task in which positive force feedback would become more critical (Gregor, Smith et al. 2006). During upslope walking in the cats, strong activation of gastrocnemius is driven by excitatory force-, and not length-, dependent feedback (Donelan, McVea et al. 2009). Contrarily, in the downslope walking magnitude

of excitatory force feedback diminishes and length feedback takes over as the primary modulator of eccentric contraction, as gastrocnemius self-reinnervation results in ankle yield during the downslope walking (Maas, Prilutsky et al. 2007). It should be apparent that the proximal→distal bias can be upregulated or downregulated depending on the slope of the surface in order to increase or reduce the impedance of the distal joints.

6.3 Potential gait deficit in cats that cannot modulate force feedback bias

What does it mean when an animal cannot modulate the force feedback bias and thus k_{joint}? In Chapter II, the main conclusions are that the directional bias is the controlled variable and that inhibitory bias is directed toward ankle extensors following lateral hemisection, rendering the ankle overly compliant and the weak link in the joint chain. The developed postural tone in ankle extensors of those cats might not supply sufficient ankle moment to maintain static equilibrium against the gravity. Furthermore, ankle muscles that receive strong heterogenic inhibition fail to develop appropriate postural restorative forces to resist postural perturbations (Chapter IV). However, it is during locomotion that the balance is the most challenged. Assuming intermuscular interactions remain inhibitory in a walking cat following lateral hemisection, the potential gait deficit would be best estimated in a biomechanical and anatomical context.

The main donors of inhibition in LHS cats are the most proximal, vasti muscle group (VASTI), and the most distal muscle, flexor hallucis longus (FHL). The FHL acts as ankle extensor with the smallest moment arm out of other ankle extensors examined. It also adducts the ankle, flexes the toes and contributes to the protrusion of the claws (Goslow, Reinking et al. 1973, Lawrence, Nichols et al. 1993). It very strongly inhibits the

anatomically similar muscle, the plantaris (PLANT), a more powerful ankle extensor and abductor. Both FHL and PLANT affect toes through their insertion into flexor digitorum longus and flexor digitorum brevis, respectively. This way, they both contribute to proper foot placement and clearance, which is vital for proper postural control. The inhibition emanating from FHL is not limited to multiarticular muscles such as PLANT since it strongly inhibits soleus (SOL). The SOL is significant antigravity muscle that is active throughout the stance, and with a minor abductor role at this ankle joint. The coupling between ankle and knee joints is mainly accomplished by actions of gastrocnemius (GAS), due to its prominent moment arms at both joints. The GAS is also the most significant abductor out of all ankle extensor muscles mentioned (Lawrence, Nichols et al. 1993). The FHL is the only muscle among these that generates an adduction moment. It is noteworthy that inhibition from FHL, an adductor, is directed toward all other ankle abductors. All ankle extensors are inhibited by VASTI, that provides a knee extension via patellar tendon. Previously, it has been often observed that feedback between VASTI and GAS is bi-directionally strong (Wilmink and Nichols 2003, Lyle and Nichols 2018), while in locomoting cat these interactions were relatively weak in comparison (Ross 2006). The bi-directional interactions might suggest some sort of impedance matching during the stance between knee and ankle joints. The weak inhibition during locomotion, coupled with excitatory force feedback arising from medial gastrocnemius (Ross 2006), might enhance coupling between knee and ankle joint. However, potent inhibition of biarticular GAS and PLANT (among other ankle extensors) by VASTI suggests decoupling of these two joints in cats with lateral hemisection.

During locomotion, the muscular activation in both spinally-intact and lesioned cats is primarily orchestrated by the activity of the central pattern generator (CPG). Thus, it is important to view these interactions in a time-domain as muscles become active at different time points during the step cycle. The activity of knee and ankle extensors starts at the E1 swing phase. Activated, these muscles extend the knee and ankle joints and prepare the limb for the ground contact. The activation of VASTI in LHS cats would inhibit or delay the activation of the ankle extensors during this critical phase, and the ankle would be overly flexed during the swing phase and unprepared for a touchdown. Once on the ground, at the beginning of the E2 phase, the ankle would yield under the cats' weight. The activation of SOL would bolster ankle extensor moment by virtue of its activation and excitatory length feedback it shares with GAS. However, CPG activated FHL, enhanced by the stretch evoked by an exaggerated ankle yield, emits substantial inhibition onto all ankle extensors causing a further yield of an ankle. Furthermore, this inhibition by FHL decreases abductor moment. This results in an adducted ankle which decreases the base of support and thus further reduces limb stability. Relatively unaffected FHL (which receives inhibition only from VASTI), could maintain MTP and distal interphalangeal (IP) joints stable. Additionally, the unaffected VASTI would maintain relatively stiff knee. As the step progresses onto E3 phase, the ankle muscles would not be able to develop adequate propulsive forces to propel the body forward. Considering that we did not observe excitatory force feedback in quiescent cat, irrespective of SCI, I hesitate to speculate about its existence in freely walking cat with a spinal lesion. Furthermore, we did not evaluate the interactions between and across the muscles acting at the hip, which could aid or impede the propulsion via heterogenic pathways to ankle extensors and flexors. However, the

activation of hip muscles is also driven by the CPG. During the E3 phase, and progressing into the initial stages of swing, there is coactivation of rectus femoris (RF), biceps femoris posterior (BFP), semitendinosus (ST), and tibialis anterior (TA) (Rossignol 1996). The hamstrings muscles may aid in propulsion through the crural fascia during the E3 phase (Stahl 2010) and then continue with knee flexion as swing progresses. Their activity would also reinforce the action of TA to flex the ankle during the subsequent swing phase (Rossignol 1996), which unopposed by ankle extensor activity would make the ankle flexed throughout the swing phase. Walking on different slope surfaces requires joint specific stiffness/compliance (Simon, Ingraham et al. 2014), and as cats with lateral hemisection are unable to modulate joint stiffness, the gait deficit would be more pronounced. During upslope walking, these cats would not be able to develop required propulsion forces at the ankle necessary to propel the body forward (assuming no emergent excitatory force feedback) and would rely on knee stiffness, and inherent ankle joint stiffness. During downslope walking, relatively unaffected distal FHL muscle would make MTP joint overly extended. In contrast, the ankle joint would be excessively compliant, potentially resulting in plantigrade locomotion, with an ankle yield. The analysis of biomechanical deficits during level and slope walking of these cats is underway in Dr. Dena Howland's laboratory.

In Chapters II and III, the consistent convergent inhibitory force feedback bias and amplified length feedback were observed bilaterally, despite the unilateral lesion. It is possible that uninjured contralateral supraspinal tract fibers make connections onto interneurons on the lesion side caudal to the lesion. Similarly, removal of crossed supraspinal fibers connections from the uninjured side has the same effect as on lesion side,

thus indirectly impairing undamaged side. This could potentially decrease a deficit gap between the injured and undamaged side and produce strong directional bias in both limbs. An alternative explanation might be that the bilaterally projecting interneurons attempt inter-limb coordination to match global limb parameters across the limbs, and thus impairing the uninjured limb.

If inhibitory force feedback exchanged between the ankle and knee extensors were bi-directional (balanced bias), that would result in simple scaling of the stiffness of those joints by the magnitude of the feedback exchanged. If inhibitory force feedback were proportional only to the force of the recipient (dependent on recipient's motoneuronal pool activity), that would result in stiffness matching between ankle and knee joints. If the inhibitory force feedback were proportional only to the force of donors (dependent on GTO's recruited from donor muscles), that would result in stiffer donor joint, and more compliant recipient joint, probably preserving some global limb parameter, such as a limb length. However, force feedback is dependent on both GTO's recruited in a donor muscle, and an available motoneuronal pool of the recipient muscle (Bonasera and Nichols 1994, Bonasera and Nichols 1996). Since it can be selectively directed toward most distal joints (as in locomotion) or ankle joint (after lateral hemisection) or assume directionality toward any joint (as observed in a control cat), it strongly implies that this peripheral dependence on donor GTO's and recipient motoneurons is heavily modulated by supraspinal centers.

6.4 Potential modulatory supraspinal tract(s)

Sensory convergence is a common property of the spinal cord and higher levels of the central nervous system. It is not surprising that sensory feedback throughout the body

contributes to the moments at any single joint (Speers, Kuo et al. 2002). Each of limb-extrinsic sensors (such as vestibular and visual systems) provide a fraction of information necessary for adequate postural control, which, when integrated with the proprioception, enables the central nervous system to generate an appropriate motor command. It follows that there might be a minimal set of information necessary to stabilize the body during different motor tasks. For instance, it is well documented that integrated sensory information from the otolith organs and muscle spindle receptors in the neck muscles, representing a body-orientation signal (Brink, Suzuki et al. 1985, Marchand, Manzoni et al. 1987), regulates muscular activity patterns during slope walking compared to level walking (Smith and Carlson-Kuhta 1995, Gottschall and Nichols 2007). These findings suggest that, during downslope walking, the body orientation signal reduces activity in the gastrocnemius muscles, ablates or significantly reduces the activity of muscles of propulsion, and activates hip flexors (Gottschall and Nichols 2007, Gottschall and Nichols 2011). These actions contribute to the braking effect of the limbs required for controlled downslope locomotion. In this fashion, supraspinal tracts modulate the CPG and, therefore, muscular activation, depending on environmental circumstances.

Similarly, the supraspinal centers can selectively engage and depress reflex pathways in a task-dependent manner (Lundberg 1979). This selective engagement presumably happens by changing the gain of length feedback, affecting local joint stiffness and/or modulating a bias of force feedback, thus modulating compliance throughout the limb. How exactly is this accomplished is unclear. It is possible that the referential gain change is achieved by predetermining the gain of specific interneuronal pools serving a particular muscle, by decreasing or increasing their thresholds selectively. Which

descending tract(s) accomplish this is also unknown. In this project, we sought to localize the supraspinal tract(s) responsible for modulating force feedback circuitry. Selectively severing the potential modulatory tracts enables us to eliminate pathways that do not contribute to modulation of force feedback bias or gain of length feedback.

The dorsal hemisection severs not only tracts that transmit specific voluntary motor commands, such as corticospinal and rubrospinal, but also those that exert tonic influence related to arousal and posture, such as dorsal reticulospinal tract. The dorsal reticulospinal tract was severed in both dorsal and lateral hemisection, but no effect on force feedback bias was found following a dorsal hemisection. Thus this tract is an unlikely modulator of the force feedback bias. The dorsal reticulospinal tract has been indicated in control of clasp-knife inhibition (Rymer, Houk et al. 1979), and we observed both autogenic and heterogenic clasp-knife inhibition following dorsal hemisection (described in detail in Chapter V). The spared pathways on the ventral side, such as medial (pontine) reticulospinal and vestibulospinal tracts might modulate segmental circuitry mediating force feedback. Recently, accumulating evidence has suggested that the vestibulospinal tract modulates force feedback (Nichols, Gottschall et al. 2014), although the medial reticulospinal tract influence cannot be excluded. There is evidence for and against the existence of interneurons co-modulated by both reticulospinal and vestibulospinal fibers (Davies and Edgley 1994). Interneurons coexcited by both reticulospinal and vestibulospinal tracts have been found in lamprey (Rovainen 1979). However, different populations of inhibitory interneurons may mediate the inhibitory actions of these tracts. The inhibitory effect from vestibulospinal tracts is mediated by Ia inhibitory interneurons mediating inhibition from extensors to flexors (Grillner and Hongo 1972), whereas

inhibition by medullary reticulospinal tract is mediated by pathways of Ia/Ib nonreciprocal inhibition (Takakusaki, Kohyama et al. 2001). The ventral hemisections would sever influence from both of these tracts, and more precise lesions would be required to rule out one of them.

The short latency stretch reflex is also affected in dorsal hemisection, but differently than following lateral hemisection. Although the gain of stretch reflex increases in ankle extensor muscles following dorsal hemisection (described in Chapter V), the finding that is consistent with the literature (Taylor, Friedman et al. 1997), this amplification is not as substantial as the amplification found following lateral hemisection (described in detail in Chapter II). Furthermore, the gain of length feedback from VASTI is suppressed and amplified before returning to control values following dorsal and lateral hemisection, respectively. This might suggest that two supraspinal tracts control stretch reflex gain, one located ventrally and the other located more dorsally, potentially ventral and dorsal reticulospinal tracts. As the convergent action of supraspinal tracts onto spinal interneurons is documented, it is conceivable that more than one tract modulates force feedback bias, one located laterally (affected by lateral hemisection) and the other located ventrally. In particular, tracts that mediate postural responses such as vestibulospinal (Nichols, Gottschall et al. 2014) and/or pontomedullary reticulospinal (Deliagina, Beloozerova et al. 2008, Stapley and Drew 2009) might be potential regulators of force feedback. However, at this point, this is just speculation, and future work is warranted to identify and characterize how descending systems affect the bias of intermuscular force feedback.

6.5 Implications for rehabilitation

It is well documented that locomotor training can bolster recovery of stepping after spinal cord injury in mice (Fong, Cai et al. 2005), rats (Timoszyk, Nessler et al. 2005), cats (Barbeau and Rossignol 1987, de Leon, Hodgson et al. 1998) and even in humans (Edgerton, Leon et al. 2001, Dietz and Harkema 2004, Harkema, Behrman et al. 2012). The spinal cord circutry is highly sensitive to proprioceptive feedback. Engaging the spinal circutry caudal to injury with approptiate proprioceptive input enables spinal cord to 'prune' many abberant connections that formed as a consequence of injury, while strengthening those circuits that are relavent for locomotion (Ahn, Lee et al. 2006). Which locomotor training is the most effective is a long-winded discussion that has been reviewed plenty (Fong, Roy et al. 2009). Briefly, repetitive and consistent weight-bearing training with appropriate and timely sensory stimulus that matches normal conditions and engages and challenges both length and force-dependent feedback, seems to be essential for maximizing recovery (Edgerton, Roy et al. 1991).

6.6 Methodological and prognostic limitations

Stereotyped behaviors, such as locomotion or patterns of muscle recruitment, are usually quite consistent between animals, even across many surgical reductions such as hemisections or peripheral nerve reinnervations. Variability in reflex research, in contrast, has been well documented in the cat (Loeb 1993). Furthermore, different muscles have more variable reflex responses within a cat, and reflex responses of the same muscle are variable across cats with a similar physiognomy (Loeb 1993). The variation within and across cats may reflect a randomly distributed fluctuation in the expression of the optimal

pattern that is achieved through trial and error (Cullins, Gill et al. 2015). This intra- and inter-animal variability is an inevitable part of the reflex research, and as such, inherited limitation of conclusions in preceding chapters.

Extent and location of spinal cord lesions in Chapters II, III and V have not been determined yet. Following the euthanasia, all cats were perfused, and their spinal cords dissected for staining and determination of the lesion extent. However, as of writing of this chapter, the extent of the lesion has not been determined. The cats with spinal lesions in corresponding chapters have been regarded as dorsal or lateral hemisection cats based on intended hemisection inflicted during the survival surgery (and prior to the terminal experiments).

The surgical dissections of muscles of interest during the terminal experiment have been carried out by trained lab personnel. However, variations in surgical approach that different lab members employ during the muscle dissection may have added additional variability to the presented data. Additionally, among decerebrate preparations, the specific level of transection might have also influenced the data obtained in the current study. It has been documented, although not extensively, that patterns of heterogenic feedback are not affected by the level of decerebration significantly (Ross 2006). However, the overall gain of the system is slightly depressed in the premammillary compared to intercollicular decerebrate preparation (Nichols 1989). In particular, the higher background forces and the more substantial muscle stiffness have been reported in intercollicular animals when compared to premammillary decerebrate animals (Nichols and Steeves 1986). Even though all cats in this project underwent precollicular decerebration by the same person, variations

in the level of decerebration between the animals are inevitable and might have added additional variability to the observations.

Extending these findings onto the freely locomoting cat, or awake stationary cat for that manner is challenging for three main reasons. First, a stretch was used as an input to the system. A lone stretch elicited homonymous length feedback, while stretch in tandem with another muscle elicited heteronymous force feedback from that muscle. This mechanographic technique has traditionally been the method to evaluate force feedback network using a natural stimulus (Nichols 1987). However, in behaving cat muscles rarely are activated in isolation. Although the stretch amplitude is within the physiological range of muscle length change during locomotion (Goslow, Reinking et al. 1973), in a walking cat the feedback from individual muscles compete over the available interneuronal and motoneuronal pools. Thus, incoming feedback undergoes an integration which can involve summation, gating, cancelation or occlusion of proprioceptive input in an extent that is not discernable from the protocol using isolated muscle pair stretches. Because of this reason, we have recorded simultaneous stretches of multiple muscles which we will use in the future project to evaluate how heterogenic feedback from multiple sources summates onto individual recipient muscles.

Second, muscles acting at the hip likely play a significant role in the maintenance of vertical posture. However, there is insufficient data describing interactions from and onto these muscles to draw conclusions regarding compliance of the hip joint. It was reported previously that RF (hip flexor and knee extensor) exchanges inhibitory force feedback with VASTI group and GAS (Wilmink and Nichols 2003), but we have not evaluated directionality of this inhibition in lesioned cats. However, it is safe to presume

that force feedback arising from muscles crossing the hip (and potentially even trunk muscles) influence the knee and ankle stiffness, and future work extending to hip extensors and flexors is warranted.

Lastly, the main limitation to extrapolation of mechanographic findings from decerebrate non-locomoting cat to the biomechanics of freely walking and awake cat is that those two states are diagonally different. In reduced preparation, such as decerebrate cat, many higher motor structures and sensory input from sources, such as from visual system, are eliminated. Furthermore, in the stationary cat with rigidly fixed limbs, inertial forces, movement of other body parts (such as tail or head), cutaneous feedback from paw as the limb touches the ground, joint receptors, etc., that complement and modulate dynamics of walking cat, are eliminated. All of these inevitably contribute to the mechanics of the limb during walking; however, it was impossible to account for them in this type of project.

6.7 Conclusion

Despite these limitations, the mechanographic method is currently the best tool at our disposal in evaluating homonymous and heteronymous interactions among muscles, as it employs natural input into the system, a stretch. With this method, we mapped changes in gain of length feedback, the bias of force feedback and distribution of clasp-knife inhibition following lateral and dorsal hemisections. Relating these changes to the biomechanical deficit during walking will require supplementing mechanographic data with the analysis of biomechanical recordings, which is underway in our collaborator's laboratory.

Table 6-1: Summary of main findings from Aims I-IV.

	Aim I	**Aim II**	**Aim III**	**Aim IV**
Intellectual merit	The autogenic stiffness of knee and ankle joints is overall increased following lateral hemisection, however no CKI is apparent.	Lateral hemisection results in a bilateral and chronic convergence of strong inhibition onto ankle extensors.	Unregulated inhibitory force feedback can have a detrimental effect on walking gait and impair weight acceptance phase.	The supraspinal tract(s) that control inhibitory force feedback organization are likely located in ventral spinal cord. Dorsal tracts control CKI.
Broader impact	The detrimental effect of an unregulated force feedback onto walking gait might be mitigated by combination of • conditioning, • training, • medication			Determining lesion location and extent based on presence or absence of CKI and/or inadequate joint stiffness

We propose that inhibitory force feedback can be significant contributor to the crouched gain deficit often observed in spinal cats following locomotor recovery. Although future work is warranted, we gained significant insight into changes that proprioceptive pathways undergo following spinal lesions, that will, hopefully, incite development of new rehabilitation methods and further future research.

REFERENCES

Abelew, T. A., C. Huyghues-Despointes and T. R. Nichols (1996). Three dimensional knee torques produced by the quadriceps and hamstrings muscles in the cat. Society of Neuroscience. Washington, D.C.

Abelew, T. A., M. D. Miller, T. C. Cope and T. R. Nichols (2000). "Local loss of proprioception results in disruption of interjoint coordination during locomotion in the cat." J Neurophysiol **84**(5): 2709-2714.

Abu-Hijleh, M. F. and P. F. Harris (2007). "Deep fascia on the dorsum of the ankle and foot: extensor retinacula revisited." Clin Anat **20**(2): 186-195.

Aggelopoulos, N. C., P. Bawa and S. A. Edgley (1996). "Activation of midlumbar neurones by afferents from anterior hindlimb muscles in the cat." J Physiol **497 (Pt 3)**: 795-802.

Aggelopoulos, N. C., S. Chakrabarty and S. A. Edgley (2008). "Presynaptic control of transmission through group II muscle afferents in the midlumbar and sacral segments of the spinal cord is independent of corticospinal control." Exp Brain Res **187**(1): 61-70.

Ahn, Y. H., G. Lee and S. K. Kang (2006). "Molecular insights of the injured lesions of rat spinal cords: Inflammation, apoptosis, and cell survival." Biochem Biophys Res Commun **348**(2): 560-570.

Akazawa, K., J. W. Aldridge, J. D. Steeves and R. B. Stein (1982). "Modulation of stretch reflexes during locomotion in the mesencephalic cat." J Physiol **329**: 553-567.

Alexander, R. M. and H. C. Bennet-Clark (1977). "Storage of elastic strain energy in muscle and other tissues." Nature **265**(5590): 114-117.

Allum, J. H., K. H. Mauritz and H. Vogele (1982). "The mechanical effectiveness of short latency reflexes in human triceps surae muscles revealed by ischaemia and vibration." Exp Brain Res **48**(1): 153-156.

Ariano, M. A., R. B. Armstrong and V. R. Edgerton (1973). "Hindlimb muscle fiber populations of five mammals." J Histochem Cytochem **21**(1): 51-55.

Baldissera, F., H. Hultborn and M. Illert (1981). Integration in spinal neuronal systems. Handbook of Physiology. The Nervous System. Motor Control. Bethesda, American Physiological Society**:** 509-595.

Ballif, L., J. F. Fulton and E. G. T. Liddell (1925). "Observations on spinal and decerebrate knee jerks with special reference to their inhibition by single break shocks." Proc. R. Soc. London Ser. B **98**: 589-607.

Banks, R. W., D. Barker and M. J. Stacey (1979). "Sensory innervation of cat hind-limb muscle spindles [proceedings]." J Physiol **293**: 40P-41P.

Banks, R. W., M. Hulliger, H. H. Saed and M. J. Stacey (2009). "A comparative analysis of the encapsulated end-organs of mammalian skeletal muscles and of their sensory nerve endings." J Anat **214**(6): 859-887.

Banks, R. Y. and M. J. Stacey (1988). Quantitative studies on mammalian muscle spindles and their sensory innervation. Mechanoreceptors – Development, Structure, and Function. P. Hnik, T. Soukup, R. Vejsada and J. Zelená. New York, NY, Plenum Press**:** 263-269.

Bannatyne, B. A., T. T. Liu, I. Hammar, K. Stecina, E. Jankowska and D. J. Maxwell (2009). "Excitatory and inhibitory intermediate zone interneurons in pathways from feline group I and II afferents: differences in axonal projections and input." J Physiol **587**(2): 379-399.

Barbeau, H., M. Ladouceur, K. E. Norman, A. Pepin and A. Leroux (1999). "Walking after spinal cord injury: evaluation, treatment, and functional recovery." Arch Phys Med Rehabil **80**(2): 225-235.

Barbeau, H. and S. Rossignol (1987). "Recovery of locomotion after chronic spinalization in the adult cat." Brain Res **412**(1): 84-95.

Barker, D. (1967). The innervation of mammalian skeletal muscle. Myostatic, kinesthetic and vestibular mechanisms. A. V. S. De Reuck and J. Knight. Boston, MA, Little Brown2-19.

Basso, D. M., M. Murray and M. E. Goldberger (1994). "Differential recovery of bipedal and overground locomotion following complete spinal cord hemisection in cats." Restor Neurol Neurosci **7**(2): 95-110.

Beattie, M. S., A. A. Farooqui and J. C. Bresnahan (2000). "Review of current evidence for apoptosis after spinal cord injury." J Neurotrauma **17**(10): 915-925.

Bergman, R. A. and M. P. D'Alessandro. (2018, January 1, 2018). "Anatomy Atlases. An anatomy digital library - Curated by Ronald A. Bergman, Ph.D.", 2018.

Bergmark, A. (1989). "Stability of the lumbar spine. A study in mechanical engineering." Acta Orthop Scand Suppl **230**: 1-54.

Bernstein, N. (1967). The coordination and regulation of movements. New York, NY, Pergamon Press.

Biewener, A. A. (1998). "Muscle-tendon stresses and elastic energy storage during locomotion in the horse." Comp Biochem Physiol B Biochem Mol Biol **120**(1): 73-87.

Biewener, A. A. and T. J. Roberts (2000). "Muscle and tendon contributions to force, work, and elastic energy savings: a comparative perspective." Exerc Sport Sci Rev **28**(3): 99-107.

Bishop, B. (1977). "Spasticity: its physiology and management. Part III. Identifying and assessing the mechanisms underlying spasticity." Phys Ther **57**(4): 385-395.

Blickhan, R. (1989). "The spring-mass model for running and hopping." J Biomech **22**(11-12): 1217-1227.

Blum, K. P., B. Lamotte D'Incamps, D. Zytnicki and L. H. Ting (2017). "Force encoding in muscle spindles during stretch of passive muscle." PLoS Comput Biol **13**(9): e1005767.

Bonasera, S. J. and T. R. Nichols (1994). "Mechanical actions of heterogenic reflexes linking long toe flexors with ankle and knee extensors of the cat hindlimb." J Neurophysiol **71**(3): 1096-1110.

Bonasera, S. J. and T. R. Nichols (1996). "Mechanical actions of heterogenic reflexes among ankle stabilizers and their interactions with plantarflexors of the cat hindlimb." Journal of Neurophysiology **75**: 2050-2070.

Bonnot, A., D. Morin and D. Viala (1998). "Genesis of spontaneous rhythmic motor patterns in the lumbosacral spinal cord of neonate mouse." Brain Res Dev Brain Res **108**(1-2): 89-99.

Bonnot, A., P. J. Whelan, G. Z. Mentis and M. J. O'Donovan (2002). "Locomotor-like activity generated by the neonatal mouse spinal cord." Brain Res Brain Res Rev **40**(1-3): 141-151.

Boyd, I. A. and M. R. Davey (1968). Composition of peripheral nerves. Edinburgh, London,, E. & S. Livingstone.

Brink, E. E., I. Suzuki, S. J. Timerick and V. J. Wilson (1985). "Tonic neck reflex of the decerebrate cat: a role for propriospinal neurons." J Neurophysiol **54**(4): 978-987.

Brouwer, B. and P. Ashby (1992). "Corticospinal projections to lower limb motoneurons in man." Exp Brain Res **89**(3): 649-654.

Brown, P. B. and J. L. Culberson (1981). "Somatotopic organization of hindlimb cutaneous dorsal root projections to cat dorsal horn." J Neurophysiol **45**(1): 137-143.

Brughelli, M. and J. Cronin (2008). "A review of research on the mechanical stiffness in running and jumping: methodology and implications." Scand J Med Sci Sports **18**(4): 417-426.

Buford, J. A. and A. G. Davidson (2004). "Movement-related and preparatory activity in the reticulospinal system of the monkey." Exp Brain Res **159**(3): 284-300.

Burke, D. (1980). Reassessment of muscle spindle contribution to muscle tone in normal and spastic man. Spasticity: Disordered Motor Control. R. G. Feldman, R. R. Young and W. P. Koella. Chicago, IL, Year Book Medical Publishers**:** 261-278.

Burke, D., J. D. Gillies and J. W. Lance (1970). "The quadriceps stretch reflex in human spasticity." J Neurol Neurosurg Psychiatry **33**(2): 216-223.

Burke, D., L. Knowles, C. Andrews and P. Ashby (1972). "Spasticity, decerebrate rigidity and the clasp-knife phenomenon: an experimental study in the cat." Brain **95**(1): 31-48.

Burkholder, T. J. and T. R. Nichols (2004). "Three-dimensional model of the feline hindlimb." J Morphol **261**(1): 118-129.

Burns, S. P., D. G. Golding, W. A. Rolle, Jr., V. Graziani and J. F. Ditunno, Jr. (1997). "Recovery of ambulation in motor-incomplete tetraplegia." Arch Phys Med Rehabil **78**(11): 1169-1172.

Cabaj, A., K. Stecina and E. Jankowska (2006). "Same spinal interneurons mediate reflex actions of group Ib and group II afferents and crossed reticulospinal actions." J Neurophysiol **95**(6): 3911-3922.

Carrasco, D. I., J. Lawrence, 3rd and A. W. English (1999). "Neuromuscular compartments of cat lateral gastrocnemius produce different torques about the ankle joint." Motor Control **3**(4): 436-446.

Castro, M. J., D. F. Apple, Jr., E. A. Hillegass and G. A. Dudley (1999). "Influence of complete spinal cord injury on skeletal muscle cross-sectional area within the first 6 months of injury." Eur J Appl Physiol Occup Physiol **80**(4): 373-378.

Cavagna, G. A., N. C. Heglund and C. R. Taylor (1977). "Mechanical work in terrestrial locomotion: two basic mechanisms for minimizing energy expenditure." Am J Physiol **233**(5): R243-261.

Cavagna, G. A. and M. Kaneko (1977). "Mechanical work and efficiency in level walking and running." J Physiol **268**(2): 467--481.

Cavagna, G. A., F. P. Saibene and R. Margaria (1964). "Mechanical Work in Running." J Appl Physiol **19**: 249-256.

Chen, D., R. D. Theiss, K. Ebersole, J. F. Miller, W. Z. Rymer and C. J. Heckman (2001). "Spinal interneurons that receive input from muscle afferents are differentially modulated by dorsolateral descending systems." J Neurophysiol **85**(2): 1005-1008.

Chin, N. K. (1962). Number and distrbution of spindle capsule in seven hindilinmb muscles of the cat. Symposium on Muscle Receptors, Hong Kong University Press**:** 241-248.

Cleland, C. L., L. Hayward and W. Z. Rymer (1990). "Neural mechanisms underlying the clasp-knife reflex in the cat. II. Stretch-sensitive muscular-free nerve endings." J Neurophysiol **64**(4): 1319-1330.

Cleland, C. L. and W. Z. Rymer (1990). "Neural mechanisms underlying the clasp-knife reflex in the cat. I. Characteristics of the reflex." J Neurophysiol **64**(4): 1303-1318.

Cope, T. C., S. J. Bonasera and T. R. Nichols (1994). "Reinnervated muscles fail to produce stretch reflexes." J Neurophysiol **71**(2): 817-820.

Crouch, J. E. (1969). Text-atlas of cat anatomy. Philadelphia, PA, Lea & Febiger.

Cui, L., E. J. Perreault, H. Maas and T. G. Sandercock (2008). "Modeling short-range stiffness of feline lower hindlimb muscles." J Biomech **41**(9): 1945-1952.

Cullins, M. J., J. P. Gill, J. M. McManus, H. Lu, K. M. Shaw and H. J. Chiel (2015). "Sensory Feedback Reduces Individuality by Increasing Variability within Subjects." Curr Biol **25**(20): 2672-2676.

Cutts, A. (1989). "Sarcomere length changes in muscles of the human thigh during walking." J Anat **166**: 77-84.

Daley, M. A., J. R. Usherwood, G. Felix and A. A. Biewener (2006). "Running over rough terrain: guinea fowl maintain dynamic stability despite a large unexpected change in substrate height." J Exp Biol **209**(Pt 1): 171-187.

Davies, H. E. and S. A. Edgley (1994). "Inputs to group II-activated midlumbar interneurones from descending motor pathways in the cat." J Physiol **479 (Pt 3)**: 463-473.

De Leon, R. D., J. A. Hodgson, R. R. Roy and V. R. Edgerton (1998). "Full weight-bearing hindlimb standing following stand training in the adult spinal cat." J Neurophysiol **80**(1): 83-91.

de Leon, R. D., J. A. Hodgson, R. R. Roy and V. R. Edgerton (1998). "Locomotor capacity attributable to step training versus spontaneous recovery after spinalization in adult cats." J Neurophysiol **79**(3): 1329-1340.

Deliagina, T. G., I. N. Beloozerova, P. V. Zelenin and G. N. Orlovsky (2008). "Spinal and supraspinal postural networks." Brain Res Rev **57**(1): 212-221.

Deliagina, T. G., G. N. Orlovsky, P. V. Zelenin and I. N. Beloozerova (2006). "Neural bases of postural control." Physiology (Bethesda) **21**: 216-225.

Dietz, V. and W. Berger (1983). "Normal and impaired regulation of muscle stiffness in gait: a new hypothesis about muscle hypertonia." Exp Neurol **79**(3): 680-687.

Dietz, V. and S. J. Harkema (2004). "Locomotor activity in spinal cord-injured persons." J Appl Physiol (1985) **96**(5): 1954-1960.

Dietz, V., K. H. Mauritz and J. Dichgans (1980). "Body oscillations in balancing due to segmental stretch reflex activity." Exp Brain Res **40**(1): 89-95.

Donelan, J. M., D. A. McVea and K. G. Pearson (2009). "Force regulation of ankle extensor muscle activity in freely walking cats." J Neurophysiol **101**(1): 360-371.

Donelan, J. M. and K. G. Pearson (2004). "Contribution of force feedback to ankle extensor activity in decerebrate walking cats." J Neurophysiol **92**(4): 2093-2104.

Eccles, J. C., R. M. Eccles and A. Lundberg (1957). "The convergence of monosynaptic excitatory afferents on to many different species of alpha motoneurones." J Physiol **137**(1): 22-50.

Eccles, J. C., R. M. Eccles and A. Lundberg (1957). "Synaptic actions on motoneurones caused by impulses in Golgi tendon organ afferents." J Physiol **138**(2): 227-252.

Eccles, J. C., R. M. Eccles and A. Lundberg (1957). "Synaptic actions on motoneurones in relation to the two components of the group I muscle afferent volley." J Physiol **136**(3): 527-546.

Eccles, R. and A. Lundberg (1957). "Integrative pattern of reflex actions by impulses in large muscle spindle afferents on motoneurones to hip muscles." Experientia **13**(10): 414-415.

Eccles, R. M. and A. Lundberg (1958). "Integrative pattern of Ia synaptic actions on motoneurones of hip and knee muscles." J Physiol **144**(2): 271-298.

Eccles, R. M. and A. Lundberg (1959). "Supraspinal control of interneurones mediating spinal reflexes." J Physiol **147**: 565-584.

Edgerton, V. R., R. D. Leon, S. J. Harkema, J. A. Hodgson, N. London, D. J. Reinkensmeyer, R. R. Roy, R. J. Talmadge, N. J. Tillakaratne, W. Timoszyk and A. Tobin (2001). "Retraining the injured spinal cord." J Physiol **533**(Pt 1): 15-22.

Edgerton, V. R., R. R. Roy, J. A. Hodgson, A. Connections and B. V. Publishers (1991). Recovery of full weight-supporting locomotion of the hindlimbs after complete thoracic spinalization of adult and neonatal cats, Elsevier Science.

Edgley, S., E. Jankowska and D. McCrea (1986). "The heteronymous monosynaptic actions of triceps surae group Ia afferents on hip and knee extensor motoneurones in the cat." Exp Brain Res **61**(2): 443-446.

Edgley, S. A. and E. Jankowska (1987). "An interneuronal relay for group I and II muscle afferents in the midlumbar segments of the cat spinal cord." J Physiol **389**: 647-674.

Edin, B. B. and N. Johansson (1995). "Skin strain patterns provide kinaesthetic information to the human central nervous system." J Physiol **487**(1): 243-251.

Eldred, E., C. F. Bridgman, J. E. Swett and B. Eldred (1962). Quantitative comparisons of muscle receptros of the cat's medial gastrocnemius, soleus, and extensor digirotum brevis muscles. Muscle Receptors. D. Barker, Hong Kong University Press**:** 207-213.

Engberg, I., A. Lundberg and R. W. Ryall (1968). "Reticulospinal inhibition of transmission in reflex pathways." J Physiol **194**(1): 201-223.

English, A. W. and O. I. Weeks (1987). "An anatomical and functional analysis of cat biceps femoris and semitendinosus muscles." J Morphol **191**(2): 161-175.

Farley, C. T. and O. Gonzalez (1996). "Leg stiffness and stride frequency in human running." J Biomech **29**(2): 181-186.

Farley, C. T. and D. C. Morgenroth (1999). "Leg stiffness primarily depends on ankle stiffness during human hopping." J Biomech **32**(3): 267-273.

Feldman, A. G. and G. N. Orlovsky (1972). "The influence of different descending systems on the tonic stretch reflex in the cat." Exp Neurol **37**(3): 481-494.

Fetz, E. E., E. Jankowska, T. Johannisson and J. Lipski (1979). "Autogenetic inhibition of motoneurones by impulses in group Ia muscle spindle afferents." J Physiol **293**: 173-195.

Flash, T. and F. Mussa-Ivaldi (1990). "Human arm stiffness characteristics during the maintenance of posture." Exp Brain Res **82**(2): 315-326.

Fong, A. J., L. L. Cai, C. K. Otoshi, D. J. Reinkensmeyer, J. W. Burdick, R. R. Roy and V. R. Edgerton (2005). "Spinal cord-transected mice learn to step in response to quipazine treatment and robotic training." J Neurosci **25**(50): 11738-11747.

Fong, A. J., R. R. Roy, R. M. Ichiyama, I. Lavrov, G. Courtine, Y. Gerasimenko, Y. C. Tai, J. Burdick and V. R. Edgerton (2009). "Recovery of control of posture and locomotion after a spinal cord injury: solutions staring us in the face." Prog Brain Res **175**: 393-418.

Fowler, E. G., R. J. Gregor, J. A. Hodgson and R. R. Roy (1993). "Relationship between ankle muscle and joint kinetics during the stance phase of locomotion in the cat." J Biomech **26**(4-5): 465-483.

Fritz, N., M. Illert, S. de la Motte, P. Reeh and P. Saggau (1989). "Pattern of monosynaptic Ia connections in the cat forelimb." J Physiol **419**: 321-351.

Fukami, Y. and R. S. Wilkinson (1977). "Responses of isolated Golgi tendon organs of the cat." J Physiol **265**(3): 673-689.

Fulton, J. F. and J. Pi-Suner (1927). "Note concerning probable function of various afferent end organs in skeletal muscle." American Journal of Physiology **83**: 554-562.

Fung, J. and J. M. Macpherson (1999). "Attributes of quiet stance in the chronic spinal cat." J Neurophysiol **82**(6): 3056-3065.

Ghez, C. (1991). The control of movement. Principles of Neural Science. E. R. Kandel, J. H. Scwartz and T. M. Jessell. New York, NY, Elsevier Science**:** 533-547.

Ghez, C. (1991). Voluntary movement. Principles of Neural Science. E. R. Kandel, J. H. Schwartz and T. M. Jessell. New York, NY, Elsevier Science**:** 756-779.

Goslow, G. E., Jr., R. M. Reinking and D. G. Stuart (1973). "The cat step cycle: hind limb joint angles and muscle lengths during unrestrained locomotion." J Morphol **141**(1): 1-41.

Gottschall, J. S. and T. R. Nichols (2007). "Head pitch affects muscle activity in the decerebrate cat hindlimb during walking." Exp Brain Res **182**(1): 131-135.

Gottschall, J. S. and T. R. Nichols (2011). "Neuromuscular strategies for the transitions between level and hill surfaces during walking." Philos Trans R Soc Lond B Biol Sci **366**(1570): 1565-1579.

Grau, J. W., J. A. Salinas, P. A. Illich and M. W. Meagher (1990). "Associative learning and memory for an antinociceptive response in the spinalized rat." Behav Neurosci **104**(3): 489-494.

Gregor, R. J., D. W. Smith and B. I. Prilutsky (2006). "Mechanics of slope walking in the cat: quantification of muscle load, length change, and ankle extensor EMG patterns." J Neurophysiol **95**(3): 1397-1409.

Griffiths, R. I. (1991). "Shortening of muscle fibres during stretch of the active cat medial gastrocnemius muscle: the role of tendon compliance." J Physiol **436**: 219-236.

Grigg, P. (1994). "Peripheral neural mechanisms in proprioception." Journal of Sport Rehabilitation **3**: 2-17.

Grillner, S. (1972). "The role of muscle stiffness in meeting the changing postural and locomotor requirements for force development by the ankle extensors." Acta Physiol Scand **86**(1): 92-108.

Grillner, S. (1975). "Locomotion in vertebrates: Central mechanism and reflex interaction."

Grillner, S. and T. Hongo (1972). "Vestibulospinal effects on motoneurones and interneurones in the lumbosacral cord." Prog Brain Res **37**: 243-262.

Grillner, S., C. Perret and P. Zangger (1976). "Central generation of locomotion in the spinal dogfish." Brain Res **109**(2): 255-269.

Grillner, S. and S. Rossignol (1978). "On the initiation of the swing phase of locomotion in chronic spinal cats." Brain Res **146**(2): 269-277.

Guertin, P., M. J. Angel, M. C. Perreault and D. A. McCrea (1995). "Ankle extensor group I afferents excite extensors throughout the hindlimb during fictive locomotion in the cat." J Physiol **487 (Pt 1)**: 197-209.

Guyton, A. C. and J. E. Hall (2006). Textbook of medical physiology. Philadelphia, Elsevier Saunders.

Hagbarth, K. E. (1979). "Exteroceptive, proprioceptive, and sympathetic activity recorded with microelectrodes from human peripheral nerves." Mayo Clin Proc **54**(6): 353-365.

Hagbarth, K. E., G. Wallin and L. Lofstedt (1973). "Muscle spindle responses to stretch in normal and spastic subjects." Scand J Rehabil Med **5**(4): 156-159.

Hall, L. A. and D. I. McCloskey (1983). "Detections of movements imposed on finger, elbow and shoulder joints." J Physiol **335**: 519-533.

Harkema, S., A. Behrman and H. Barbeau (2012). Evidence-based therapy for recovery of function after spinal cord injury. Handbook of Clinical Neurology, Elsevier**:** 259-274.

Hasan, Z. (2005). "The human motor control system's response to mechanical perturbation: should it, can it, and does it ensure stability?" J Mot Behav **37**(6): 484-493.

Hebb, D. O. (1949). The organization of behavior; a neuropsychological theory. New York, Wiley.

Heckman, C. J. (1994). "Alterations in synaptic input to motoneurons during partial spinal cord injury." Med Sci Sports Exerc **26**(12): 1480-1490.

Helgren, M. E. and M. E. Goldberger (1993). "The recovery of postural reflexes and locomotion following low thoracic hemisection in adult cats involves compensation by undamaged primary afferent pathways." Exp Neurol **123**(1): 17-34.

Henneman, E. (1985). "The size-principle: a deterministic output emerges from a set of probabilistic connections." J Exp Biol **115**: 105-112.

Henneman, E. (1991). "The size principle and its relation to transmission failure in Ia projections to spinal motoneurons." Ann N Y Acad Sci **627**: 165-168.

Hill, J. C. (1968). "Tension due to interaction between sliding filaments in resting striated muscle. The effect of stimlation." Journal of Physiology **199**: 637-684.

Hochman, S. and D. A. McCrea (1994). "Effects of chronic spinalization on ankle extensor motoneurons. I. Composite monosynaptic Ia EPSPs in four motoneuron pools." J Neurophysiol **71**(4): 1452-1467.

Hochman, S. and D. A. McCrea (1994). "Effects of chronic spinalization on ankle extensor motoneurons. II. Motoneuron electrical properties." J Neurophysiol **71**(4): 1468-1479.

Hochman, S. and D. A. McCrea (1994). "Effects of chronic spinalization on ankle extensor motoneurons. III. Composite Ia EPSPs in motoneurons separated into motor unit types." J Neurophysiol **71**(4): 1480-1490.

Hoffer, J. A., A. A. Caputi, I. E. Pose and R. I. Griffiths (1989). "Roles of muscle activity and load on the relationship between muscle spindle length and whole muscle length in the freely walking cat." Prog Brain Res **80**: 75-85; discussion 57-60.

Hogan, N. (1985). "The mechanics of multi-joint posture and movement control." Biol Cybern **52**(5): 315-331.

Holmqvist, B. and A. Lundberg (1961). "Differential supraspinal control of synaptic actions evoked by volleys in the flexion reflex afferents in alpha motoneurones." Acta Physiol Scand Suppl **186**: 1-15.

Honeycutt, C. F., J. S. Gottschall and T. R. Nichols (2009). "Electromyographic responses from the hindlimb muscles of the decerebrate cat to horizontal support surface perturbations." J Neurophysiol **101**(6): 2751-2761.

Honeycutt, C. F. and T. R. Nichols (2014). "The mechanical actions of muscles predict the direction of muscle activation during postural perturbations in the cat hindlimb." J Neurophysiol **111**(5): 900-907.

Houk, J. and E. Henneman (1967). "Responses of Golgi tendon organs to active contractions of the soleus muscle of the cat." J Neurophysiol **30**(3): 466-481.

Houk, J. C. (1979). "Regulation of stiffness by skeletomotor reflexes." Annu Rev Physiol **41**: 99-114.

Houk, J. C., W. Z. Rymer and P. E. Crago (1981). "Dependence of dynamic response of spindle receptors on muscle length and velocity." J Neurophysiol **46**(1): 143-166.

Houk, J. C., J. J. Singer and E. Henneman (1971). "Adequate stimulus for tendon organs with observations on mechanics of ankle joint." J Neurophysiol **34**(6): 1051-1065.

Hoy, K. C., J. R. Huie and J. W. Grau (2013). "AMPA receptor mediated behavioral plasticity in the isolated rat spinal cord." Behav Brain Res **236**(1): 319-326.

Huie, J. R., E. D. Stuck, K. H. Lee, K. A. Irvine, M. S. Beattie, J. C. Bresnahan, J. W. Grau and A. R. Ferguson (2015). "AMPA Receptor Phosphorylation and Synaptic Colocalization on Motor Neurons Drive Maladaptive Plasticity below Complete Spinal Cord Injury." eNeuro **2**(5).

Hultborn, H. and J. Malmsten (1983). "Changes in segmental reflexes following chronic spinal cord hemisection in the cat. I. Increased monosynaptic and polysynaptic ventral root discharges." Acta Physiol Scand **119**(4): 405-422.

Jami, L. (1988). "[Functional properties of the Golgi tendon organs]." Arch Int Physiol Biochim **96**(4): A363-378.

Jami, L. (1992). "Golgi tendon organs in mammalian skeletal muscle: functional properties and central actions." Physiol Rev **72**(3): 623-666.

Jankowska, E. (1992). "Interneuronal relay in spinal pathways from proprioceptors." Prog Neurobiol **38**(4): 335-378.

Jankowska, E. and S. Edgley (1993). "Interactions between pathways controlling posture and gait at the level of spinal interneurones in the cat." Prog Brain Res **97**: 161-171.

Jankowska, E. and S. A. Edgley (2010). "Functional subdivision of feline spinal interneurons in reflex pathways from group Ib and II muscle afferents; an update." Eur J Neurosci **32**(6): 881-893.

Jankowska, E., D. McCrea and R. Mackel (1981). "Pattern of 'non-reciprocal' inhibition of motoneurones by impulses in group Ia muscle spindle afferents in the cat." J Physiol **316**: 393-409.

Jankowska, E., J. S. Riddell, B. Skoog and B. R. Noga (1993). "Gating of transmission to motoneurones by stimuli applied in the locus coeruleus and raphe nuclei of the cat." J Physiol **461**: 705-722.

Jansen, J. K. and T. Rudjord (1964). "On the Silent Period and Golgi Tendon Organs of the Soleus Muscle of the Cat." Acta Physiol Scand **62**: 364-379.

Jayaraman, A., C. K. Thompson, W. Z. Rymer and T. G. Hornby (2013). "Short-term maximal-intensity resistance training increases volitional function and strength in chronic incomplete spinal cord injury: a pilot study." J Neurol Phys Ther **37**(3): 112-117.

Jinks, S. L., J. T. Martin, E. Carstens, S. W. Jung and J. F. Antognini (2003). "Peri-MAC depression of a nociceptive withdrawal reflex is accompanied by reduced dorsal horn activity with halothane but not isoflurane." Anesthesiology **98**(5): 1128-1138.

Johansson, H. and P. Sjolander (1993). The neurophysiology of joints. Mechanics of Joints: Physiology, Pathophysiology and Treatment. V. Wright and E. Radin. New York, NY, Marcel Dekker Inc**:** 243:290.

Johnson, M. D., E. Kajtaz, C. M. Cain and C. J. Heckman (2013). "Motoneuron intrinsic properties, but not their receptive fields, recover in chronic spinal injury." J Neurosci **33**(48): 18806-18813.

Jordan, L. M., R. M. Brownstone and B. R. Noga (1992). "Control of functional systems in the brainstem and spinal cord." Curr Opin Neurobiol **2**(6): 794-801.

Kajtaz, E., M. A. Lyle, K. A. Chaffer, D. R. Howland and T. R. Nichols (2017). Changes in inhibitory force feedback pathways following lateral hemisection in cats. Society of Neuroscience. Washington, DC.

Kajtaz, E., M. A. Lyle, K. A. Cheffer, L. R. Montgomery, D. R. Howland and T. R. Nichols (2018). Evidence for separate descending control of clasp-knife inhibition and force feedback in the feline spinal cord. Society for Neuroscience. San Diego, CA.

Kanda, K. and W. Z. Rymer (1977). "An estimate of the secondary spindle receptor afferent contribution to the stretch reflex in extensor muscles of the decerebrate cat." J Physiol **264**(1): 63-87.

Kandel, E. R., J. H. Schwartz and T. M. Jessell (2000). Principles of neural science. New York, McGraw-Hill, Health Professions Division.

Katz, R. T. and W. Z. Rymer (1989). "Spastic hypertonia: mechanisms and measurement." Arch Phys Med Rehabil **70**(2): 144-155.

Kavounoudias, A., R. Roll and J. P. Roll (2001). "Foot sole and ankle muscle inputs contribute jointly to human erect posture regulation." J Physiol **532**(Pt 3): 869-878.

Ker, R. F. (1981). "Dynamic tensile properties of the plantaris tendon of sheep (Ovis aries)." J Exp Biol **93**: 283-302.

Kim, J. H. and L. D. Partridge (1969). "Observations on types of response to combinations of neck, vestibular, and muscle stretch signals." J Neurophysiol **32**(2): 239-250.

Kingma, H. (2006). "Posture, balance and movement: Role of the vestibular system in balance control during stance and movements." Journal of Cliniccal Neurophysiology **46**(4-5): 238.

Kirkwood, P. A. and T. A. Sears (1974). "Monosynaptic excitation of motoneurones from secondary endings of muscle spindles." Nature **252**(5480): 243-244.

Kirkwood, P. A. and T. A. Sears (1975). "Monosynaptic excitation of motoneurones from muscle spindle secondary endings of intercostal and triceps surae muscles in the cat." J Physiol **245**(2): 64P-66P.

Kistemaker, D. A., A. J. Van Soest, J. D. Wong, I. Kurtzer and P. L. Gribble (2013). "Control of position and movement is simplified by combined muscle spindle and Golgi tendon organ feedback." J Neurophysiol **109**(4): 1126-1139.

Konow, N., E. Azizi and T. J. Roberts (2012). "Muscle power attenuation by tendon during energy dissipation." Proc Biol Sci **279**(1731): 1108-1113.

Krenz, N. R. and L. C. Weaver (1998). "Sprouting of primary afferent fibers after spinal cord transection in the rat." Neuroscience **85**(2): 443-458.

Kuhtz-Buschbeck, J. P., A. Boczek-Funcke, A. Mautes, W. Nacimiento and C. Weinhardt (1996). "Recovery of locomotion after spinal cord hemisection: an X-ray study of the cat hindlimb." Exp Neurol **137**(2): 212-224.

Kumazawa, T. and K. Mizumura (1977). "Thin-fibre receptors responding to mechanical, chemical, and thermal stimulation in the skeletal muscle of the dog." J Physiol **273**(1): 179-194.

Latash, M. L. and V. M. Zatsiorsky (1993). "Joint stiffness: Myth or reality?" Human Movement Science **12**(6): 653-692.

Lawrence, J. H., 3rd, T. R. Nichols and A. W. English (1993). "Cat hindlimb muscles exert substantial torques outside the sagittal plane." J Neurophysiol **69**(1): 282-285.

Lee, K. H., J. D. Turtle, Y. J. Huang, M. M. Strain, K. M. Baumbauer and J. W. Grau (2015). "Learning about time within the spinal cord: evidence that spinal neurons can abstract and store an index of regularity." Front Behav Neurosci **9**: 274.

Lemon, R. and J. Griffiths (2004). "Comparative anatomy of the motor system: differences in the organization of corticospinal control in different species." Handbook of Clinical Neurophysiology **4**: 7-25.

Leonard, C. T. (1998). The Neuroscience of Human Movement. St. Louis, MO, Mosby-Year Book.

Lew, W. D., E. V. Lewis and E. V. Craig (1993). Stabilization by capsule, ligaments and labrum: stability at the extremes of motion. The Shoulder: A Balance of Mobility and Stability. F. A. Matsen, F. H. Fu and R. J. Hawkins. Rosemont, IL, American Academy of Orthopaedic Surgeons**:** 69-89.

Lichtwark, G. A. and A. M. Wilson (2007). "Is Achilles tendon compliance optimised for maximum muscle efficiency during locomotion?" J Biomech **40**(8): 1768-1775.

Loeb, G. E. (1993). "The distal hindlimb musculature of the cat: interanimal variability of locomotor activity and cutaneous reflexes." Exp Brain Res **96**(1): 125-140.

Loram, I. D. and M. Lakie (2002). "Direct measurement of human ankle stiffness during quiet standing: the intrinsic mechanical stiffness is insufficient for stability." J Physiol **545**(Pt 3): 1041-1053.

Lundberg, A. (1979). "Multisensory control of spinal reflex pathways." Prog Brain Res **50**: 11-28.

Lyalka, V. F., G. N. Orlovsky and T. G. Deliagina (2009). "Impairment of postural control in rabbits with extensive spinal lesions." J Neurophysiol **101**(4): 1932-1940.

Lyle, M. A., E. Kajtaz and T. R. Nichols (2016). Toe flexor reinnervation results in nonsagittal plane motor deficits during downslope walking in the cat. Society for Neuroscience. San Diego, CA.

Lyle, M. A. and T. R. Nichols (2018). "Patterns of intermuscular inhibitory force feedback across cat hindlimbs suggest a flexible system for regulating whole limb mechanics." J Neurophysiol **119**(2): 668-678.

Lyle, M. A., B. I. Prilutsky, R. J. Gregor, T. A. Abelew and T. R. Nichols (2016). "Self-reinnervated muscles lose autogenic length feedback, but intermuscular feedback can recover functional connectivity." J Neurophysiol **116**(3): 1055-1067.

Maas, H., R. J. Gregor, E. F. Hodson-Tole, B. J. Farrell and B. I. Prilutsky (2009). "Distinct muscle fascicle length changes in feline medial gastrocnemius and soleus muscles during slope walking." J Appl Physiol (1985) **106**(4): 1169-1180.

Maas, H., H. J. Meijer and P. A. Huijing (2005). "Intermuscular interaction between synergists in rat originates from both intermuscular and extramuscular myofascial force transmission." Cells Tissues Organs **181**(1): 38-50.

Maas, H., B. I. Prilutsky, T. R. Nichols and R. J. Gregor (2007). "The effects of self-reinnervation of cat medial and lateral gastrocnemius muscles on hindlimb kinematics in slope walking." Exp Brain Res **181**(2): 377-393.

Maas, H. and T. G. Sandercock (2010). "Force transmission between synergistic skeletal muscles through connective tissue linkages." J Biomed Biotechnol **2010**: 575672.

Macpherson, J. M. (1988). "Strategies that simplify the control of quadrupedal stance. I. Forces at the ground." J Neurophysiol **60**(1): 204-217.

Macpherson, J. M. (1988). "Strategies that simplify the control of quadrupedal stance. II. Electromyographic activity." J Neurophysiol **60**(1): 218-231.

Macpherson, J. M. and J. Fung (1999). "Weight support and balance during perturbed stance in the chronic spinal cat." J Neurophysiol **82**(6): 3066-3081.

Macpherson, J. M., J. Fung and R. Jacobs (1997). "Postural orientation, equilibrium, and the spinal cord." Adv Neurol **72**: 227-232.

Magnus, R. (1926). "Physiology of posture." Lancet **11**: 531:581.

Malmsten, J. (1983). "Time course of segmental reflex changes after chronic spinal cord hemisection in the rat." Acta Physiol Scand **119**(4): 435-443.

Marchand, A. R., D. Manzoni, O. Pompeiano and G. Stampacchia (1987). "Effects of stimulation of vestibular and neck receptors on Deiters neurons projecting to the lumbosacral cord." Pflugers Arch **409**(1-2): 13-23.

Markin, S. N., M. A. Lemay, B. I. Prilutsky and I. A. Rybak (2012). "Motoneuronal and muscle synergies involved in cat hindlimb control during fictive and real locomotion: a comparison study." J Neurophysiol **107**(8): 2057-2071.

Matthews, B. H. (1933). "Nerve endings in mammalian muscle." J Physiol **78**(1): 1-53.

Matthews, G. G. (1997). Brain motor mechanisms. Neurobiology: Molecules, Cells & Systems. G. G. Matthews. Malden, MA, Blackwell Science Inc.

Matthews, P. B. C. (1972). Mammalian muscle receptors and their central actions. London,, Edward Arnold.

Matthews, W. B. (1966). "Ratio of maximum H reflex to maximum M response as a measure of spasticity." J Neurol Neurosurg Psychiatry **29**(3): 201-204.

McCouch, G. P., G. M. Austin, C. N. Liu and C. Y. Liu (1958). "Sprouting as a cause of spasticity." J Neurophysiol **21**(3): 205-216.

McMahon, T. A. and G. C. Cheng (1990). "The mechanics of running: how does stiffness couple with speed?" J Biomech **23 Suppl 1**: 65-78.

McNair, P. J., G. A. Wood and R. N. Marshall (1992). "Stiffness of the hamstring muscles and its relationship to function in anterior cruciate ligament deficient individuals." Clin Biomech (Bristol, Avon) **7**(3): 131-137.

Mehta, R. (2016). Mechanisms of coordination between one- and two-joint synerfist muscle, Georgia Institute of Technology.

Mendell, L. M. and E. Henneman (1968). "Terminals of single Ia fibers: distribution within a pool of 300 homonymous motor neurons." Science **160**(3823): 96-98.

Mendell, L. M. and E. Henneman (1971). "Terminals of single Ia fibers: location, density, and distribution within a pool of 300 homonymous motoneurons." J Neurophysiol **34**(1): 171-187.

Mendelsohn, A. I., C. M. Simon, L. F. Abbott, G. Z. Mentis and T. M. Jessell (2015). "Activity Regulates the Incidence of Heteronymous Sensory-Motor Connections." Neuron **87**(1): 111-123.

Merton, P. A. (1953). Speculations on the servo control of movement. The Spinal Cord. Boston, MA, Little Brown.

Mihailoff, G. A. (1997). Motor system I: Peripheral sensory, brainstem and spinal influence on ventral horn neurons. Fundamental Neuroscience. D. E. Haines and M. D. Ard. New York, NY, Churchill Livingstone Inc**:** 335-346.

Mihailoff, G. A. and D. E. Hainses (1997). Motor system II: Conrtiofugal systems and the control of movement. Fundamental Neuroscience. D. E. Haines. New York, NY, Churchill Livingstone Inc**:** 360-376.

Mirbagheri, M. M., H. Barbeau, M. Ladouceur and R. E. Kearney (2001). "Intrinsic and reflex stiffness in normal and spastic, spinal cord injured subjects." Exp Brain Res **141**(4): 446-459.

Mori, S. (1987). "Integration of posture and locomotion in acute decerebrate cats and in awake, freely moving cats." Prog Neurobiol **28**(2): 161-195.

Munson, J. B., R. C. Foehring, S. A. Lofton, J. E. Zengel and G. W. Sypert (1986). "Plasticity of medial gastrocnemius motor units following cordotomy in the cat." Journal of Neurophysiology **5**: 619-634.

Murray, K. C., A. Nakae, M. J. Stephens, M. Rank, J. D'Amico, P. J. Harvey, X. Li, R. L. Harris, E. W. Ballou, R. Anelli, C. J. Heckman, T. Mashimo, R. Vavrek, L. Sanelli, M. A. Gorassini, D. J. Bennett and K. Fouad (2010). "Recovery of motoneuron and locomotor function after spinal cord injury depends on constitutive activity in 5-HT2C receptors." Nat Med **16**(6): 694-700.

Mussa-Ivaldi, F. A., N. Hogan and E. Bizzi (1985). "Neural, mechanical, and geometric factors subserving arm posture in humans." J Neurosci **5**(10): 2732-2743.

Nashner, L. M. (1976). "Adapting reflexes controlling the human posture." Exp Brain Res **26**(1): 59-72.

Nelson, S. G. and L. M. Mendell (1979). "Enhancement in Ia-motoneuron synaptic transmission caudal to chronic spinal cord transection." J Neurophysiol **42**(3): 642-654.

Niazi, I. (2015). Altered intermuscular force feedback after spinal cord injury in cat. Atlanta, GA, (unpublished PhD Thesis). Georgia Institute of Technology. School of Applied Physiology**:** 184.

Nichols, T. R. (1987). "A technique for measuring the mechanical actions of heterogenic (intermuscular) reflexes in the decerebrate cat." J Neurosci Methods **21**(2-4): 265-273.

Nichols, T. R. (1989). "The organization of heterogenic reflexes among muscles crossing the ankle joint in the decerebrate cat." J Physiol **410**: 463-477.

Nichols, T. R. (1999). "Receptor mechanisms underlying heterogenic reflexes among the triceps surae muscles of the cat." J Neurophysiol **81**(2): 467-478.

Nichols, T. R. (2002). "The contributions of muscles and reflexes to the regulation of joint and limb mechanics." Clin Orthop Relat Res **403 Suppl**(403 Suppl): S43-50.

Nichols, T. R. and T. C. Cope (2001). "The Organization of Distributed Proprioceptive Feedback in the Chronic Spinal Cat." Motor Neurobiology of the Spinal Cord: 305-327.

Nichols, T. R., J. S. Gottschall and C. Tuthill (2014). "The regulation of limb stiffness in the context of locomotor tasks." Adv Exp Med Biol **826**: 41-54.

Nichols, T. R. and J. C. Houk (1976). "Improvement in Linearity and Regulation of Stiffness that results from actions of stretch reflex."

Nichols, T. R. and J. D. Steeves (1986). "Resetting of resultant stiffness in ankle flexor and extensor muscles in the decerebrate cat." Exp Brain Res **62**(2): 401-410.

Noga, B. R., H. Bras and E. Jankowska (1992). "Transmission from group II muscle afferents is depressed by stimulation of locus coeruleus/subcoeruleus, Kolliker-Fuse and raphe nuclei in the cat." Exp Brain Res **88**(3): 502-516.

Norman L., Strominger R.J. and D. L.B.L. (2012). Reflexes and Muscle Tone. Noback's Human Nervous System, Seventh Edition: Structure and Function, Humana Press.

Paloski, W. H., S. J. Wood, A. H. Feiveson, F. O. Black, E. Y. Hwang and M. F. Reschke (2006). "Destabilization of human balance control by static and dynamic head tilts." Gait Posture **23**(3): 315-323.

Pearson, K. G. and D. F. Collins (1993). "Reversal of the influence of group Ib afferents from plantaris on activity in medial gastrocnemius muscle during locomotor activity." J Neurophysiol **70**(3): 1009-1017.

Pearson, K. G. and S. Rossignol (1991). "Fictive motor patterns in chronic spinal cats." J Neurophysiol **66**(6): 1874-1887.

Pepin, A., K. E. Norman and H. Barbeau (2003). "Treadmill walking in incomplete spinal-cord-injured subjects: 1. Adaptation to changes in speed." Spinal Cord **41**(5): 257-270.

Perreault, E. J., P. E. Crago and R. F. Kirsch (2000). "Estimation of intrinsic and reflex contributions to muscle dynamics: a modeling study." IEEE Trans Biomed Eng **47**(11): 1413-1421.

Pierrot-Deseiligny, E. and D. Burke (2012). The Circuitry of the Human Spinal Cord: Spinal and Corticospinal Mechanisms of Movement. New York, NY, Cambridge University Press.

Potvin, J. R. and S. H. Brown (2005). "An equation to calculate individual muscle contributions to joint stability." J Biomech **38**(5): 973-980.

Pratt, C. A. (1995). "Evidence of positive force feedback among hindlimb extensors in the intact standing cat." J Neurophysiol **73**(6): 2578-2583.

Prilutsky, B. I. (2000). "Coordination of two- and one-joint muscles: functional consequences and implications for motor control." Motor Control **4**(1): 1-44.

Prilutsky, B. I., W. Herzog, T. R. Leonard and T. L. Allinger (1996). "Role of the muscle belly and tendon of soleus, gastrocnemius, and plantaris in mechanical energy absorption and generation during cat locomotion." J Biomech **29**(4): 417-434.

Prochazka, A., D. Gillard and D. J. Bennett (1997). "Positive force feedback control of muscles." J Neurophysiol **77**(6): 3226-3236.

Proske, U. (1981). "The Golgi tendon organ. Properties of the receptor and reflex action of impulses arising from tendon organs." Int Rev Physiol **25**: 127-171.

Rack, P. M. and D. R. Westbury (1969). "The effects of length and stimulus rate on tension in the isometric cat soleus muscle." J Physiol **204**(2): 443-460.

Rack, P. M. and D. R. Westbury (1970). "The response of alpha motoneurones to movement of their muscles." J Physiol **206**(2): 2P.

Rapoport, S., J. Mizrahi, E. Kimmel, O. Verbitsky and E. Isakov (2003). "Constant and variable stiffness and damping of the leg joints in human hopping." J Biomech Eng **125**(4): 507-514.

Riemann, B. L. and S. M. Lephart (2002). "The sensorimotor system, part I: the physiologic basis of functional joint stability." J Athl Train **37**(1): 71-79.

Riemann, B. L. and S. M. Lephart (2002). "The Sensorimotor System, Part II: The Role of Proprioception in Motor Control and Functional Joint Stability." J Athl Train **37**(1): 80-84.

Roberts, T. J. and N. Konow (2013). "How tendons buffer energy dissipation by muscle." Exerc Sport Sci Rev **41**(4): 186-193.

Robinson, G. A. and M. E. Goldberger (1986). "The development and recovery of motor function in spinal cats. I. The infant lesion effect." Exp Brain Res **62**(2): 373-386.

Rodin, B. E., S. L. Sampogna and L. Kruger (1983). "An examination of intraspinal sprouting in dorsal root axons with the tracer horseradish peroxidase." J Comp Neurol **215**(2): 187-198.

Ross, K. T. (2006). Quantitative analysis of feedback during locomotion. Atlanta, GA, (unpublished PhD Thesis). Georgia Institute of Technology. Department of Biomedical Engineering.

Ross, K. T. and T. R. Nichols (2009). "Heterogenic feedback between hindlimb extensors in the spontaneously locomoting premammillary cat." J Neurophysiol **101**(1): 184-197.

Rossignol, S. (1996). Neural control of stereotypic limb movements. Handbook of Physiology, Section 12: Exercise: Regulation and Integration of Multiple Systems. L. B. Rowell and J. T. Shepherd. New york, Oxford. **12**.

Rossignol, S., T. Drew, E. Brustein and W. Jiang (1999). Locomotor preformance and adaptation after partial or complete spinal cord lesions in the cat. Peripheral and spinal mechanisms in the neural control of movement. M. D. Binder. Netherlands, Elsevier Science**:** 349-363.

Rovainen, C. M. (1979). "Electrophysiology of vestibulospinal and vestibuloreticulospinal systems in lampreys." J Neurophysiol **42**(3): 745-766.

Rymer, W. Z. and Z. Hasan (1980). "Absence of force-feedback regulation in soleus muscle of the decerebrate cat." Brain Res **184**(1): 203-209.

Rymer, W. Z., J. C. Houk and P. E. Crago (1979). "Mechanisms of the clasp-knife reflex studied in an animal model." Exp Brain Res **37**(1): 93-113.

Sacks, R. D. and R. R. Roy (1982). "Architecture of the hind limb muscles of cats: functional significance." J Morphol **173**(2): 185-195.

Sainburg, R. L., M. F. Ghilardi, H. Poizner and C. Ghez (1995). "Control of limb dynamics in normal subjects and patients without proprioception." J Neurophysiol **73**(2): 820-835.

Sasaki, O., S. Usami, P. M. Gagey, J. Martinerie, M. Le Van Quyen and P. Arranz (2002). "Role of visual input in nonlinear postural control system." Exp Brain Res **147**(1): 1-7.

Schafer, S. S., B. Berkelmann and K. Schuppan (1999). "Two groups of Golgi tendon organs in cat tibial anterior muscle identified from the discharge frequency recorded under a ramp-and-hold stretch." Brain Res **846**(2): 210-218.

Schepens, B., P. Stapley and T. Drew (2008). "Neurons in the pontomedullary reticular formation signal posture and movement both as an integrated behavior and independently." J Neurophysiol **100**(4): 2235-2253.

Scivoletto, G. and V. Di Donna (2009). "Prediction of walking recovery after spinal cord injury." Brain Res Bull **78**(1): 43-51.

Sherrington, C. S. (1906). The integrative action of the nervous system. New York,, C. Scribner's sons.

Sherrington, C. S. (1910). "Flexion-reflex of the limb, crossed extension-reflex, and reflex stepping and standing." J Physiol **40**(1-2): 28-121.

Sherrington, C. S. (1961). The integrative action of the nervous system. New Haven,, Yale University Press.

Silva, P. L., S. T. Fonseca and M. T. Turvey (2010). "Is tensegrity the functional architecture of the equilibrium point hypothesis?" Motor Control **14**: e35-e40.

Silverman, J., N. L. Garnett, S. F. Giszter, C. J. Heckman, 2nd, J. A. Kulpa-Eddy, M. A. Lemay, C. K. Perry and M. Pinter (2005). "Decerebrate mammalian preparations: unalleviated or fully alleviated pain? A review and opinion." Contemp Top Lab Anim Sci **44**(4): 34-36.

Simon, A. M., K. A. Ingraham, N. P. Fey, S. B. Finucane, R. D. Lipschutz, A. J. Young and L. J. Hargrove (2014). "Configuring a powered knee and ankle prosthesis for transfemoral amputees within five specific ambulation modes." PLoS One **9**(6): e99387.

Sinkjaer, T. and R. Hayashi (1989). "Regulation of wrist stiffness by the stretch reflex." J Biomech **22**(11-12): 1133-1140.

Smith, J. L. and P. Carlson-Kuhta (1995). "Unexpected motor patterns for hindlimb muscles during slope walking in the cat." J Neurophysiol **74**(5): 2211-2215.

Smith, J. L., P. Carlson-Kuhta and T. V. Trank (1998). "Forms of forward quadrupedal locomotion. III. A comparison of posture, hindlimb kinematics, and motor patterns for downslope and level walking." J Neurophysiol **79**(4): 1702-1716.

Speers, R. A., A. D. Kuo and F. B. Horak (2002). "Contributions of altered sensation and feedback responses to changes in coordination of postural control due to aging." Gait Posture **16**(1): 20-30.

Stahl, V. A. (2010). Contributions of fascia to force transmission in the cat hindlimb PhD, Georgia Institute of Technology.

Stapley, P. J. and T. Drew (2009). "The pontomedullary reticular formation contributes to the compensatory postural responses observed following removal of the support surface in the standing cat." J Neurophysiol **101**(3): 1334-1350.

Takakusaki, K., J. Kohyama, K. Matsuyama and S. Mori (2001). "Medullary reticulospinal tract mediating the generalized motor inhibition in cats: parallel inhibitory mechanisms acting on motoneurons and on interneuronal transmission in reflex pathways." Neuroscience **103**(2): 511-527.

Taylor, J. R. (1997). An introduction to error analysis: The study of uncertainties in physical measurements. Sausalito, CA, University Science Books.

Taylor, J. S., R. F. Friedman, J. B. Munson and C. J. Vierck, Jr. (1997). "Stretch hyperreflexia of triceps surae muscles in the conscious cat after dorsolateral spinal lesions." J Neurosci **17**(13): 5004-5015.

Taylor, R. G. and J. R. Gleave (1957). "Incomplete spinal cord injuries; with Brown-Sequard phenomena." J Bone Joint Surg Br **39-B**(3): 438-450.

Thomas, C. K. and I. Zijdewind (2006). "Fatigue of muscles weakened by death of motoneurons." Muscle Nerve **33**(1): 21-41.

Timoszyk, W. K., J. A. Nessler, C. Acosta, R. R. Roy, V. R. Edgerton, D. J. Reinkensmeyer and R. de Leon (2005). "Hindlimb loading determines stepping quantity and quality following spinal cord transection." Brain Res **1050**(1-2): 180-189.

Vincent, J. A., H. M. Gabriel, A. S. Deardorff, P. Nardelli, R. E. W. Fyffe, T. Burkholder and T. C. Cope (2017). "Muscle proprioceptors in adult rat: mechanosensory signaling and synapse distribution in spinal cord." J Neurophysiol **118**(5): 2687-2701.

Voss, H. (1971). "[Tabulation of the absolute and relative muscular spindle numbers in human skeletal musculature]." Anat Anz **129**(5): 562-572.

Webb, C. B. and T. C. Cope (1992). "Modulation of la EPSP amplitude: the effects of chronic synaptic inactivity." J Neurosci **12**(1): 338-344.

Whelan, P., A. Bonnot and M. J. O'Donovan (2000). "Properties of rhythmic activity generated by the isolated spinal cord of the neonatal mouse." J Neurophysiol **84**(6): 2821-2833.

Whelan, P. J. (1996). "Control of locomotion in the decerebrate cat." Prog Neurobiol **49**(5): 481-515.

Wiegner, A. W., M. M. Wierzbicka, L. Davies and R. R. Young (1993). "Discharge properties of single motor units in patients with spinal cord injuries." Muscle Nerve **16**(6): 661-671.

Wierzbicka, M. M., A. W. Wiegner, E. L. Logigian and R. R. Young (1991). "Abnormal most-rapid isometric contractions in patients with Parkinson's disease." J Neurol Neurosurg Psychiatry **54**(3): 210-216.

Wilmink, R. J. and T. R. Nichols (2003). "Distribution of heterogenic reflexes among the quadriceps and triceps surae muscles of the cat hind limb." J Neurophysiol **90**(4): 2310-2324.

Winter, D. A., A. E. Patla, F. Prince, M. Ishac and K. Gielo-Perczak (1998). "Stiffness control of balance in quiet standing." J Neurophysiol **80**(3): 1211-1221.

Wolpaw, J. R. (2010). "What can the spinal cord teach us about learning and memory?" Neuroscientist **16**(5): 532-549.

Wolpaw, J. R. and J. S. Carp (2006). "Plasticity from muscle to brain." Prog Neurobiol **78**(3-5): 233-263.

Young, R. P., S. H. Scott and G. E. Loeb (1993). "The distal hindlimb musculature of the cat: multiaxis moment arms at the ankle joint." Exp Brain Res **96**(1): 141-151.

Zatsiorsky, V. M. and B. I. Prilutsky (2012). Biomechanics of Skeletal Muscles. Champaign, IL, Human Kinetics, Inc.

Zelená, J. (1994). Nerves and Mechanoreceptors: The Role of Innervation in the Development and Maintenance of Mammalian Mechanoreceptors. London, UK, Springer Science & Business Media.

Zhang, L. Q. and W. Z. Rymer (1997). "Simultaneous and nonlinear identification of mechanical and reflex properties of human elbow joint muscles." IEEE Trans Biomed Eng **44**(12): 1192-1209.